Role of galectin-3 in modulating tumor-specific immunity and lung metastasis in mice

By

Aparna Dilip Chaudhari

[LIFE09200904018]

Tata Memorial Centre

Mumbai

A thesis submitted to the

Board of Studies in Life Sciences

In partial fulfillment of requirements

for the Degree of

DOCTOR OF PHILOSOPHY

of

HOMI BHABHA NATIONAL INSTITUTE

October, 2016

Homi Bhabha National Institute

Recommendations of the Viva Voce Committee

As members of the Viva Voce Committee, we certify that we have read the dissertation prepared by Ms. Aparna Dilip Chaudhari entitled **'Role of galectin-3 in modulating tumor-specific immunity and lung metastasis in mice'** and recommend that it may be accepted as fulfilling the thesis requirement for the award of Degree of Doctor of Philosophy.

S.N. Dalal 6/10/16

Chairperson : Dr. Sorab N. Dalal **Date:**

S. Chiplunkar 6/10/16

Guide / Convener : Dr. Shubhada V. Chiplunkar **Date:**

6/10/16

Member 1 : Dr. Sanjay Gupta **Date:**

6.10.16

Member 2 : Dr. Narendra N. Joshi **Date:**

6/10/16

External Examiner : Dr. Prabhudas S. Patel **Date:**

Final approval and acceptance of this thesis is contingent upon the candidate's submission of the final copies of the thesis to HBNI.

I hereby certify that I have read this thesis prepared under my direction and recommend that it may be accepted as fulfilling the thesis requirement.

Date: 6/10/16

Place: Navi Mumbai

S. Chiplunkar

Dr. Shubhada V. Chiplunkar
(Guide)

STATEMENT BY AUTHOR

This dissertation has been submitted in partial fulfillment of requirements for an advanced degree at Homi Bhabha National Institute (HBNI) and is deposited in the Library to be made available to borrowers under rules of the HBNI.

Brief quotations from this dissertation are allowable without special permission, provided that accurate acknowledgement of source is made. Requests for permission for extended quotation from or reproduction of this manuscript in whole or in part may be granted by the Competent Authority of HBNI when in his or her judgment the proposed use of the material is in the interests of scholarship. In all other instances, however, permission must be obtained from the author.

Date: 06/10/2016 Aparna Dilip Chaudhari

Place: Navi Mumbai

DECLARATION

I, hereby declare that the investigation presented in the thesis has been carried out by me. The work is original and has not been submitted earlier as a whole or in part for a degree / diploma at this or any other Institution / University.

Date: 06/10/2016

Aparna Dilip Chaudhari

Place: Navi Mumbai

List of Publications arising from the thesis

Journal

1. 'Endogenous galectin-3 expression levels modulate immune responses in galectin-3 transgenic mice', Aparna D. Chaudhari, Rajiv P. Gude, Rajiv D. Kalraiya and Shubhada V. Chiplunkar, *Molecular Immunology*, **2015**, 68 (2): 300-311.

2. 'Role of endogenous galectin-3 in regulation of anti-tumor immunity during progression of B16F10 lung metastasis in galectin-3 transgenic mice', Aparna D. Chaudhari and Shubhada V. Chiplunkar. (Manuscript under preparation).

Conference Proceedings

1. 'Absence of galectin-3 contributes to immune dysfunction favoring lung metastasis of B16F10 melanoma in mice', Aparna Chaudhari, Rajiv Gude, Rajiv Kalraiya and Shubhada V. Chiplunkar, *Journal of Carcinogenesis,* **2015**, 14, Suppl S1:21-38. (International Conference 'Carcinogenesis 2015 - Molecular Pathways to Therapeutics: Paradigms and Challenges in Oncology', Mumbai, February, 2015).

Date: 06/10/2016

Aparna Dilip Chaudhari

Place: Navi Mumbai

Presentations at conferences

1. **Poster Presentation** titled 'Role of Galectin-3 in modulating tumor specific immunity and lung metastasis in mice' at the '32nd Annual Convention of Indian Association for Cancer Research & International Symposium on 'Infection and Cancer'' held at University of Delhi, North Campus between 13th-16th February, 2013.
   'RAJNIKANT BAXI AWARD' for Best Poster Presentation by Young Scientists

2. **Oral and Poster Presentation** titled 'Role of Galectin-3 in modulating tumor specific immunity and lung metastasis in mice' at the 'National Conference on Glycobiology of Cancer: Lectins as Tools and Targets' held at Karnataka University, Dharwad between 7th -9th November, 2013.

3. **Poster Presentation** titled 'Role of Galectin-3 in regulating tumor immunity in B16F10 lung metastasis model' at the 'IX DAE - BRNS Life Sciences Symposium (LSS - 2013) on 'Current Advances in Immunobiology and Cancer'' held at BARC, Mumbai between 28th -30th November, 2013.

4. **Poster Presentation** titled 'Absence of Galectin-3 contributes to immune dysfunction favoring lung metastasis of B16F10 melanoma in mice' at the International Conference 'Carcinogenesis 2015 - Molecular Pathways to Therapeutics: Paradigms and Challenges in Oncology' held at TMC-ACTREC, Mumbai between 11th-13th February, 2015.

5. **Oral Presentation** titled 'Endogenous galectin-3 expression levels modulate immune responses and B16F10 lung metastasis in mice' at International Conference on 'Promotion of animal research, welfare and harmonization of Laboratory Animal Science - LASA 2015' held at TMC-ACTREC, Mumbai between 15th-16th October, 2015.

Date: 06/10/2016 Aparna Dilip Chaudhari

Place: Navi Mumbai

This thesis is dedicated to

My Parents

ACKNOWLEDGEMENTS

Achieving a Ph.D. degree had always been a dream which I had envisioned with my parents. Today, when I am submitting this Ph.D. thesis, a deep sense of contentment fills my heart. I would like to acknowledge the great deal of help received from all the individuals who have been an indispensable part of this memorable journey.

First of all, I would like to express my sincere gratitude to my Principal Supervisor Prof. Shubhada V. Chiplunkar for giving me the opportunity to pursue a Ph.D. under her able guidance. Her immense support, patience and motivation throughout the course of this study have helped me grow as a researcher. Her zeal for science always inspired me to keep learning new things in different facets of research. She has influenced me in myriad roles, being a terrific group leader, a critical scientific analyzer, a wonderful teacher, a great counselor as well as a caring guardian. I am really thankful to Madam for being extremely understanding and encouraging during the tough phases of the tenure. I could not have imagined having a better advisor and mentor for my Ph.D. study. Thank you Madam, for everything!

It was a really fulfilling experience to work at TMC-ACTREC, my *alma mater*. I would like to thank the Director Prof. Shubhada V. Chiplunkar and Deputy Director Dr. Sudeep Gupta for providing the excellent infrastructure facilities and a great working environment at ACTREC.

I am thankful to all the members of my Doctoral Committee: Prof. K. B. Sainis (Former Chairperson), Late Dr. Rajiv Kalraiya (Former Chairperson), Dr. Sorab Dalal (Current Chairperson), Dr. Sanjay Gupta and Dr. Narendra Joshi, for their insightful comments, suggestions and encouragement during the entire Ph.D. tenure.

It has been a pleasure indeed to work with all the fellow members in Chiplunkar Lab, where I spent these constructive years of my life. I would like to thank Meena madam and Trupti madam for introducing me to different experimental techniques; Shamal madam and Rekha madam for their enormous help during designing as well as analysis of all the flow cytometry based experiments. Special thanks to Dakave sir for his help with all the animal handling techniques. I really appreciate the support by Dakave sir, Desai sir, Sawant sir, Kalpesh and Ram who ensured that our lab work always

ran smoothly. Sincere thanks to Dr. Jyoti Kode madam for all her help and encouragement. I am grateful to all my seniors: Bhairav, Nirmala, Dimpu, Babita; my colleagues and juniors: Pradeep, Alok, Sagar, Jaydeep, Vasanti, Atul, Swati, Gauri, Asif, Rushikesh, Sajad, Shalini, Sachin, Priyanka, Siddhesh, Chinmayee, Neha for all the scientific discussions and fun we have had during this journey together.

I acknowledge the help by Dr. Rajiv P. Gude (Ex-Scientific Officer F, ACTREC) during intravenous B16F10 injections in mice. I would like to thank the Laboratory Animals Facility, Flow Cytometry Facility, Histology department, Imaging Facility, Photography department, Common Instruments Facility, IT department, Bioinformatics facility, Library, SCOPE cell, Steno pool, Administration and Accounts departments of ACTREC for their valuable support. Heartfelt thanks to Maya madam from HBNI Program Office at ACTREC for all her help with HBNI related documentation and submission formalities.

I am also thankful to Chiplunkar Sir and Dr. Chiplunkar Madam for arranging annual picnics at beautiful places as well as all the get-togethers at their place, which were very refreshing and created wonderful memories to cherish.

No words can express my respect and deep sense of gratitude towards my ex-colleague, best friend and now my life partner, Sagar. He has been my pillar of strength and has stood beside me through thick and thin. Without him, it would not have been possible for me to sail through this challenging journey. This thesis belongs as much to him as it does to me. Thank you dear Sagar, we did this together!

I feel blessed to have really amazing parents and family members, their unconditional love and strong faith in me. It gives me immense satisfaction to be able to realize the dream which we had seen through these years. Aai and Pappa, I dedicate this thesis to you! I am where I am today, only because of your determination, sacrifices and hardships. I am really lucky to have a wonderful brother, Ojas, who was there for me always and lifted my spirits, whenever I felt low. I will be forever indebted to my in-laws for their affection and care; and to all my extended Shah family members for their best wishes and blessings!

Lastly, I am grateful to The Almighty for bestowing me with His favors and positive energy to continue with the good work always!

Aparna Dilip Chaudhari

CONTENTS

SYNOPSIS

Homi Bhabha National Institute

SYNOPSIS OF Ph. D. THESIS

1. **Name of the Student:** Aparna Dilip Chaudhari
2. **Name of the Constituent Institution:** Tata Memorial Centre - Advanced Centre for Treatment, Research and Education in Cancer
3. **Enrolment No. :** LIFE09200904018
4. **Title of the Thesis:** 'Role of Galectin-3 in modulating tumor-specific immunity and lung metastasis in mice'
5. **Board of Studies:** Life Sciences

SYNOPSIS

INTRODUCTION

Galectin-3 is a unique chimera-type member of the β-galactoside-binding mammalian galectin family encoded by *LGALS3* gene. It is a 31kDa protein composed of an N-terminal domain, a repetitive collagen-like sequence rich in glycine, proline and tyrosine and a C-terminal carbohydrate recognition domain (CRD) [1]. It is a ubiquitously expressed molecule with diverse physiological functions based on its subcellular and extracellular localization. Galectin-3 is involved in various biological processes such as maintenance of cellular homeostasis, organogenesis, immune responses, angiogenesis, tumor invasion and metastasis [2-4].

Role of galectin-3 in various steps of cancer progression and metastasis has been extensively reported [5-8]. However, how the levels of expression of endogenous galectin-3 in the host influence tumor growth and metastasis remains poorly understood. Galectin-3 is expressed in

highest amounts on majority of the tissue compartments of lung and constitutively on lung vascular endothelium in mice [9,10]. Previous studies using B16F10 murine melanoma model have shown that, interactions between galectin-3 on the mice lung endothelium and its high affinity ligand poly-*N*-acetyl lactosamine (polyLacNAc) on β1,6 branched N-oligosaccharides present on B16F10 melanoma cells facilitates B16F10 colonization in the lungs of the mice [9,11,12]. Studies done using galectin-3 wild-type and null mice have reported contradictory research findings related to primary tumor growth as well as metastasis frequency [12-16]. To resolve the ambiguity in the reported findings, it is important to unveil the possible underlying mechanisms in endogenous galectin-3 mediated regulation of tumorigenic and metastatic events in the host.

Role of immune system in the modulation of tumor progression and metastasis has been widely documented [17,18]. Galectin-3 is expressed in many cells subsets of immune system, including monocytes/macrophages, dendritic cells, eosinophils, neutrophils, mast cells, uterine NK cells, activated T and B cells. Accumulating evidence suggests the importance of galectin-3 in functionally regulating the host immune response [3,19]. However, the role of endogenous galectin-3 in the modulation of anti-tumor immune responses in the host and the mechanisms involved therein need to be further investigated.

Based on the above studies, we hypothesized that endogenous galectin-3 regulates host immune responses in mice thereby modulating lung metastasis of B16F10 murine melanoma cells. To test this hypothesis, we analyzed how different expression levels of endogenous galectin-3 in the host regulate immune responses and what are the possible underlying mechanisms. In the present thesis, *LGALS3* transgenic mice of C57BL/6 background strain, including Gal-$3^{+/+}$ (Wild-type), Gal-$3^{+/-}$ (Hemizygous) and Gal-$3^{-/-}$ (Knockout) genotypes were used and their immune status was thoroughly investigated. The findings provide strong links to understand the crosstalk between

galectin-3 and immune system that may dictate metastatic outcome and would help in designing efficient therapeutic strategies against cancer.

AIMS AND OBJECTIVES

1. To study the immune scenario in Gal-3 wild type (Gal-$3^{+/+}$), Gal-3 hemizygous (Gal-$3^{+/-}$) and Gal-3 null (Gal-$3^{-/-}$) mice.
2. To monitor the immune responses in Gal-3 wild type (Gal-$3^{+/+}$), Gal-3 hemizygous (Gal-$3^{+/-}$) and Gal-3 null (Gal-$3^{-/-}$) mice during progression of B16F10 lung metastasis.
3. To study the mechanisms involved in endogenous galectin-3 mediated regulation of anti-tumor immune responses in *LGALS3* transgenic mice.

RESULTS

<u>Objective 1</u>: To study the immune scenario in Gal-3 wild type (Gal-$3^{+/+}$), Gal-3 hemizygous (Gal-$3^{+/-}$) and Gal-3 null (Gal-$3^{-/-}$) mice

Flow cytometric analysis of immune cell subsets in Gal-$3^{+/+}$, Gal-$3^{+/-}$ and Gal-$3^{-/-}$ mice

To assess whether reduction or total absence of galectin-3 levels in host affects the frequency of major immune cell subtypes, we performed immunophenotyping of splenocytes and thymocytes isolated from Gal-$3^{+/+}$, Gal-$3^{+/-}$ and Gal-$3^{-/-}$ mice. Gal-$3^{-/-}$ mice splenocytes showed significantly lower percentages of NK ($CD3^-NK1.1^+$) cells as compared to Gal-$3^{+/+}$ mice. No significant differences were observed in the percentages of NKT ($CD3^+NK1.1^+$) cells, γδ T ($CD3^+\gamma\delta^+$) cells, macrophages ($CD14^+$), dendritic cells ($CD209^+$), helper ($CD3^+CD4^+$) and cytotoxic ($CD3^+CD8^+$) T cells as well as T_{reg} ($CD4^+CD25^+Foxp3^+$) in splenocytes of Gal-$3^{+/+}$, Gal-$3^{+/-}$ and Gal-$3^{-/-}$ mice. Further it was noted that, there were no significant differences in the percentages of $CD4^+CD8^-$ (CD4 Single positive), $CD4^-CD8^+$ (CD8 Single positive), $CD4^+CD8^+$ (Double positive) and $CD4^-CD8^-$ (Double negative) cell subsets in the thymocytes of Gal-$3^{+/+}$, Gal-$3^{+/-}$ and Gal-$3^{-/-}$ mice.

Proliferative responses upon in vitro stimulation of mice splenocytes

In order to study whether functional immune responses differ with galectin-3 expression levels in the host, we checked the ability of splenocytes isolated from Gal-$3^{+/+}$, Gal-$3^{+/-}$ and Gal-$3^{-/-}$ mice to respond to stimulants *in vitro*. Gal-$3^{+/-}$ and Gal-$3^{-/-}$ mice splenocytes exhibited significantly higher proliferative response than Gal-$3^{+/+}$ mice splenocytes on T cell stimulation as studied by [^{3}H] Thymidine incorporation assay. Results of CFSE proliferation assay supported and confirmed these findings, with CFSE labeled splenic T cells of Gal-$3^{+/-}$ and Gal-$3^{-/-}$ mice exhibiting higher proliferative responses than Gal-$3^{+/+}$ mice upon *in vitro* stimulation with PMA (50 ng/ well) + Ionomycin (50 ng/ well) or plate bound anti-CD3 (0.25 μg/ well) + soluble CD28 mAbs (0.25 μg/ well). It was observed that, splenic T cell proliferative responses showed *LGALS3* gene dosage effects, albeit with an inverse correlation to galectin-3 expression levels. The enhancement of T cell proliferative responses observed in Gal-$3^{+/-}$ and Gal-$3^{-/-}$ mice might be possibly due to abrogation of the previously reported inhibitory effects of galectin-3 on TCR signaling [20].

Intracellular calcium flux and ROS generation in activated mice splenocytes

Calcium ions (Ca^{++}) act as important secondary messengers in T cell activation and signaling cascade leading to various T cell responses. In the present study, upon *in vitro* stimulation of splenocytes (1 x 10^{6} cells) using PMA (100 ng) + Ionomycin (500 ng) or anti-CD3 mAb (1 μg), Gal-$3^{+/-}$ and Gal-$3^{-/-}$ mice showed increased intracellular calcium flux compared to Gal-$3^{+/+}$ mice. On the other hand, *in vitro* stimulated T cells of Gal-$3^{-/-}$ mice showed decreased intracellular calcium flux compared to Gal-$3^{+/+}$ and Gal-$3^{+/-}$ mice. Reactive oxygen species (ROS) play a role in the regulation of cellular signaling and in modulating immune responses in the host. In this study, Gal-$3^{+/-}$ and Gal-$3^{-/-}$ mice splenocytes (1.5 x 10^{6} cells) exhibited significantly lower intracellular ROS generation compared to Gal-$3^{+/+}$ mice upon *in vitro* stimulation using PMA (100 ng) + Ionomycin

(500 ng) or anti-CD3 mAb (1 μg). The increased T cell proliferation with reduced intracellular Ca^{++} flux observed in stimulated splenic T cells of Gal-$3^{-/-}$ mice; as well as decreased ROS generation in stimulated splenocytes indicate possible impairment of functional T cell responses in the absence of endogenous galectin-3 in Gal-$3^{-/-}$ mice.

Frequency of spontaneous apoptosis in freshly isolated mice splenocytes

Extracellular galectin-3 is known to induce apoptosis in human and mouse T cells [21-23]; whereas intracellular galectin-3 has been found to be anti-apoptotic in various cell types including human leukemia T cells [24-26]. In the present study, frequency of spontaneous apoptosis in freshly isolated splenic T cell subsets and B cells was analyzed by Annexin V-PI staining. In splenic T cells ($CD3^+$) and helper T cell subset ($CD3^+CD4^+$), percentages of early apoptotic (Annexin V^+PI^-) cells were found to be significantly higher in Gal-$3^{-/-}$ mice as compared to those in Gal-$3^{+/-}$ mice. No significant differences were found in the frequency of early apoptotic cells in cytotoxic T cell subset ($CD3^+CD8^+$) and B cells amongst splenocytes of the three mice groups. On the other hand, percentages of late apoptotic cells (Annexin V^+PI^+) in splenic B cell subset were significantly lower in Gal-$3^{-/-}$ mice than those in Gal-$3^{+/+}$ and Gal-$3^{-/-}$ mice.

Serum cytokine profile in Gal-$3^{+/+}$, Gal-$3^{+/-}$ and Gal-$3^{-/-}$ mice

Cytokines are the important modulators of immune responses in normal physiological processes as well as during pathological conditions. In the present investigation, Gal-$3^{+/-}$ and Gal-$3^{-/-}$ mice showed reduced serum levels of Th1 (IL-2, IFN-γ, TNF), Th2 (IL-4, IL-6, IL-10) and Th17 (IL-17A) cytokines compared to Gal-$3^{+/+}$ mice as studied by Cytometric Bead Array. It was interesting to note that, serum levels of IL-2 and IFN-γ showed a trend that correlated with endogenous galectin-3 expression levels in Gal-$3^{+/+}$, Gal-$3^{+/-}$ and Gal-$3^{-/-}$ mice. These results indicated that endogenous galectin-3 expression levels are important regulators of serum cytokine production in the host.

<u>Objective 2</u>: To monitor immune responses in Gal-3 wild type (Gal-$3^{+/+}$), Gal-3 hemizygous (Gal-$3^{+/-}$) and Gal-3 null (Gal-$3^{-/-}$) mice during progression of B16F10 lung metastasis

Experimental metastasis assay using B16F10 murine melanoma cells

To establish experimental metastasis, B16F10 murine melanoma cells were intravenously injected at the concentration of 1 x 10^5 cells/ 100 µl plain DMEM/ mouse in the lateral tail vein of Gal-$3^{+/+}$, Gal-$3^{+/-}$ and Gal-$3^{-/-}$ mice. On day 7 post intravenous injection of B16F10 cells in mice, no visible metastatic colonies were observed on mice lungs. On day 14, the numbers of lung metastatic colonies were almost equal in Gal-$3^{+/+}$ and Gal-$3^{-/-}$ mice and were found to be significantly lower in Gal-$3^{+/-}$ mice compared to Gal-$3^{+/+}$ and Gal-$3^{-/-}$ mice. Histopathological study of formalin fixed lung sections by hematoxylin-eosin staining confirmed these results. On day 21, number of lung metastatic colonies exceeded the manually countable limit and the lungs were flooded with melanoma colonies in Gal-$3^{+/+}$, Gal-$3^{+/-}$ and Gal-$3^{-/-}$ mice groups.

Immune responses in Gal-$3^{+/+}$, Gal-$3^{+/-}$ and Gal-$3^{-/-}$ mice in the lung metastasis model

Immune responses were monitored during progression of melanoma lung metastasis in Gal-$3^{+/+}$, Gal-$3^{+/-}$ and Gal-$3^{-/-}$ mice (Day 7, Day 14 and Day 21). On day 14 post intravenous B16F10 injection, Gal-$3^{-/-}$ mice exhibited significantly decreased levels of splenic NK cells as compared to Gal-$3^{+/+}$ and Gal-$3^{+/-}$ mice. On day 7, day 14 and day 21 of the experimental metastasis assay conditions, splenocytes of Gal-$3^{-/-}$ mice stimulated with PMA (50 ng/ well) + Ionomycin (50 ng/ well) or anti-CD3 (0.25 µg/ well) + anti-CD28 mAbs (0.25 µg/ well) showed significantly increased proliferative responses, than those of Gal-$3^{+/+}$ and Gal-$3^{+/-}$ mice as studied by [^{3}H] Thymidine incorporation assay. Levels of intracellular Ca^{++} flux in stimulated splenocytes were found to decrease with progression of lung metastasis in Gal-$3^{+/+}$, Gal-$3^{+/-}$ and Gal-$3^{-/-}$ mice. In the lung metastasis

model, upon *in vitro* stimulation of splenocytes (1 x 10^6 cells) using PMA (100 ng) + Ionomycin (500 ng) or anti-CD3 mAb (1 μg), Gal-$3^{+/-}$ and Gal-$3^{-/-}$ mice splenocytes showed decreased intracellular Ca^{++} flux compared to Gal-$3^{+/+}$ mice. On day 21, Gal-$3^{-/-}$ mice splenocytes (1.5 x 10^6 cells) exhibited significantly lower intracellular ROS generation compared to Gal-$3^{+/+}$ mice upon *in vitro* stimulation with PMA (100 ng) + Ionomycin (500 ng) or anti-CD3 mAb (1 μg). Further, the relative pattern of serum Th1, Th2 and Th17 cytokine levels in Gal-$3^{+/+}$, Gal-$3^{+/-}$ and Gal-$3^{-/-}$ mice changed gradually with the progression of lung metastasis. On Day 21, levels of pro-inflammatory cytokines IL-6 and IL-17A were found to be higher in Gal-$3^{-/-}$ mice sera than Gal-$3^{+/+}$ and Gal-$3^{+/-}$ mice groups.

Survival study in Gal-$3^{+/+}$, Gal-$3^{+/-}$ and Gal-$3^{-/-}$ mice bearing B16F10 lung metastases

Under B16F10 experimental metastasis assay conditions, Gal-$3^{+/+}$, Gal-$3^{+/-}$ and Gal-$3^{-/-}$ mice (10 mice per group) were monitored in Laboratory Animal Facility, ACTREC to study their overall survival. Survival rates were determined by standard Kaplan-Meier survival curve analysis. It was observed that, survival rates of Gal-$3^{+/+}$, Gal-$3^{+/-}$ and Gal-$3^{-/-}$ mice bearing lung metastases did not differ significantly.

<u>Objective 3</u>: To study the mechanisms involved in endogenous galectin-3 mediated regulation of anti-tumor immune responses in *LGALS3* transgenic mice

In the present study, striking differences were observed in the immune scenario of Gal-$3^{+/+}$, Gal-$3^{+/-}$ and Gal-$3^{-/-}$ mice under normal physiological conditions as well as during progression of B16F10 lung metastasis. It was therefore important to decipher the mechanisms involved in endogenous galectin-3 mediated regulation of anti-tumor immune responses in these mice.

NK cytotoxicity against YAC-1 and B16F10 tumor targets

NK cells are crucial players in host anti-tumor immune responses mediated by their cytolytic activities and IFN-γ production [27-29]. As mentioned earlier, we found reduced

splenic NK ($CD3^-NK1.1^+$) cell frequency in Gal-$3^{-/-}$ mice than in Gal-$3^{+/+}$ mice. It was interesting to analyze whether the cytotoxic function of splenic NK cells correlated with their phenotype in Gal-$3^{+/+}$, Gal-$3^{+/-}$ and Gal-$3^{-/-}$ mice. Immunomagnetically purified splenic NK cells from Gal-$3^{+/-}$ and Gal-$3^{-/-}$ mice exhibited significantly lower NK cytotoxicity against YAC-1 tumor cells than splenic NK cells from Gal-$3^{+/+}$ mice, as studied by [^{51}Cr] Release Assay. On the other hand, purified and recombinant murine IL-2 activated splenic NK cells from Gal-$3^{+/-}$ mice exhibited higher cytotoxicity against B16F10 melanoma cells than those from Gal-$3^{+/+}$ and Gal-$3^{-/-}$ mice. Thus, endogenous galectin-3 expression levels appeared to be important determinants of anti-tumor cytolytic function of splenic NK cells in these mice. NK cells provide first line of defense against transformed and tumorigenic cells in an organism. The impaired ability of NK cells to kill the tumor targets might be an important predisposing factor facilitating enhanced B16F10 lung metastasis observed in Gal-$3^{-/-}$ mice. This finding is further supported by increased NK cytotoxicity against B16F10 and significantly reduced pulmonary B16F10 melanoma metastases in Gal-$3^{+/-}$ mice as compared to Gal-$3^{+/+}$ and Gal-$3^{-/-}$ mice.

Serum cytokine milieu in mice under normal conditions and in lung metastasis model

The balance between pro-inflammatory and anti-inflammatory cytokine signaling is critical to maintain the immune homeostasis under normal physiological conditions. In the present study, the levels of pro-inflammatory cytokines TNF, IFN-γ and IL-17A had significantly strong positive correlations with each other exclusively in the sera of Gal-$3^{-/-}$ mice under normal physiological conditions. Interestingly, concentrations of pro-inflammatory cytokines IL-6, TNF and IL-17A correlated positively with anti-inflammatory cytokine IL-10 and these correlations were significant only in Gal-$3^{-/-}$ mice sera. All these correlations were not observed in the sera of non-tumor-bearing Gal-$3^{+/+}$ and Gal-$3^{+/-}$ mice. These findings indicated that, in the complete absence of endogenous host galectin-3, the serum cytokine

milieu may be disturbed, exhibiting dysregulation of the balance between pro-inflammatory and anti-inflammatory cytokines. Such imbalance in serum cytokine profile may further contribute to the observed immune dysregulation in Gal-$3^{-/-}$ mice. Comparison of the serum cytokine milieu under normal physiological conditions and in lung metastasis model clearly indicated that, the serum levels of most of the cytokines quantitated decreased gradually with progression of B16F10 lung metastasis on Day 7, Day 14 and Day 21 in Gal-$3^{+/+}$, Gal-$3^{+/-}$ and Gal-$3^{-/-}$ mice.

STAT1 mediated IFN-γ signaling in mice splenocytes

IFN-γ is a multifunctional cytokine produced mainly by NK cells and activated T cells. It is a key cytokine exerting anti-tumor immune responses against melanoma and various other cancers [17,30]. Under normal physiological conditions, serum levels of IFN-γ were found to be significantly lower in Gal-$3^{-/-}$ mice as compared to Gal-$3^{+/+}$ mice. IFN-γ exerts its effects by binding to IFN-γ receptor on the cell surface which is followed by STAT1 mediated signaling pathway. Immunophenotyping analysis revealed that, frequencies of IFN-γR1 expressing splenic T and NK cell were found to be significantly reduced in Gal-$3^{-/-}$ mice as compared to Gal-$3^{+/+}$ mice. STAT1 mediated IFN-γ signaling pathway intermediates in stimulated mice splenocytes were studied by western blotting. Total STAT1 and activated phospho-STAT1(Tyr701) protein levels were found to be higher in recombinant IFN-γ stimulated (1 and 10 ng, 30 minutes) splenocytes of Gal-$3^{+/-}$ mice compared to Gal-$3^{+/+}$ and Gal-$3^{-/-}$ mice. On the other hand, levels of SOCS1 and SOCS3 proteins, which are known to directly antagonize STAT1 activation by negative feedback mechanism, were remarkably higher in Gal-$3^{-/-}$ mice as compared to Gal-$3^{+/+}$ and Gal-$3^{+/-}$ mice splenocytes upon recombinant IFN-γ stimulation (1 and 10 ng, 12 hours). Together,

these findings suggest possible attenuation of STAT1 mediated IFN-γ signaling in the splenocytes of Gal-$3^{-/-}$ mice.

DISCUSSION AND CONCLUSION

In the present investigation, we compared the immune scenario with respect to different levels of endogenous host galectin-3 in Gal-$3^{+/+}$, Gal-$3^{+/-}$ and Gal-$3^{-/-}$ mice. Endogenous host galectin-3 appeared to exhibit its immunomodulatory effects in *LGALS3* gene dosage dependent manner and was reflected in the splenic NK cell frequency, NK mediated cytotoxicity, serum IL-2 and IFN-γ levels (Direct correlation with endogenous galectin-3 expression levels) as well as splenic T cell proliferative responses (Inverse correlation with endogenous galectin-3 expression levels) in Gal-$3^{+/+}$, Gal-$3^{+/-}$ and Gal-$3^{-/-}$ mice. On the other hand, endogenous galectin-3 appeared to exert paradoxical effects that are independent of *LGALS3* gene dosage in Gal-$3^{+/-}$ mice, including highest percentages of IFN-γR1 expressing splenic T and NK cells, elevated total STAT1 and activated phospho-STAT1(Tyr701) protein levels. The possible mechanisms underlying such a paradoxical immunoregulatory role of endogenous host galectin-3 in the Gal-$3^{+/-}$ mice warrants further investigation.

The findings of the present study collectively indicated dysregulation of immune responses in Gal-$3^{-/-}$ mice under normal physiological conditions, contributed by decreased NK cell frequency and NK cytotoxicity, disturbed serum Th1, Th2, Th17 cytokines milieu, reduced serum IFN-γ levels, lowest frequency of IFN-γR1 expressing splenic T and NK cells and attenuation of STAT1 mediated IFN-γ signaling in Gal-$3^{-/-}$ mice. We have comprehensively demonstrated that complete absence of endogenous galectin-3 may severely compromise host anti-tumor immunity and can adversely affect cancer progression.

Experimental metastasis assay using well characterized B1610 murine melanoma model for lung specific metastasis in Gal-$3^{+/+}$, Gal-$3^{+/-}$ and Gal-$3^{-/-}$ mice confirmed that apart from

promoting B16F10 melanoma cell interaction with endothelial cells in the lungs [9-12], galectin-3 has a major role in dictating the metastatic outcome by other mechanisms as well. Although, the functional redundancy by other galectins and the role of polyLacNAc on *N*-glycans in Gal-3$^{-/-}$ mice has been ruled out in our earlier study [12], the enhanced lung metastasis observed in Gal-3$^{-/-}$ mice is clearly due to the dysregulation of immune responses leading to compromised host immunity in the absence of endogenous galectin-3. The heightened anti-tumor immune responses in Gal-3$^{+/-}$ mice, including highest percentages of IFN-γR1 expressing splenic T and NK cells, increased NK mediated cytotoxicity against B16F10 cells, elevated total STAT1 and activated phospho-STAT1(Tyr701) protein levels might further explain the lowest incidence of B16F10 lung metastasis observed in these mice.

During metastatic spread of cancer cells to distant organs through the circulation, cancer cells encounter different types of immune cells. In an immunocompetent host, these immune cells can effectively eradicate majority of the circulating cancer cells by exerting anti-tumor effects. However, when the host immune system is not optimally performing, major frequency of the tumor cells can survive in the circulation ultimately reaching their secondary target organ site. In the present study, the chances of high number of circulating B16F10 melanoma cells reaching and getting mechanically trapped in the lungs of Gal-3$^{-/-}$ mice ultimately giving rise to metastatic melanoma colonies would be very high. It would be interesting to explore the mechanisms employed by B16F10 melanoma cells for lung homing in Gal-3$^{-/-}$ mice albeit the absence of endogenous galectin-3.

The present study opens new avenues in understanding the complex role of endogenous host galectin-3 in cancer metastasis process. The results collectively explain that endogenous galectin-3 exerts its effects through modulation of host immunity. Thus, thorough understanding of host immune scenario is indispensable while designing galectin-3 targeted therapeutic strategies against cancer.

REFERENCES

[1] Houzelstein D, Goncalves IR, Fadden AJ, Sidhu SS, Cooper DN, Drickamer K, et al. Phylogenetic analysis of the vertebrate galectin family. Molecular biology and evolution 2004;21:1177-1187.

[2] Liu FT, Patterson RJ, Wang JL. Intracellular functions of galectins. Biochimica et biophysica acta 2002;1572:263-273.

[3] Liu FT. Regulatory roles of galectins in the immune response. International archives of allergy and immunology 2005;136:385-400.

[4] Ochieng J, Furtak V, Lukyanov P. Extracellular functions of galectin-3. Glycoconjugate journal 2004;19:527-535.

[5] Fortuna-Costa A, Gomes AM, Kozlowski EO, Stelling MP, Pavao MS. Extracellular galectin-3 in tumor progression and metastasis. Frontiers in oncology 2014;4:138.

[6] Funasaka T, Raz A, Nangia-Makker P. Galectin-3 in angiogenesis and metastasis. Glycobiology 2014;24:886-891.

[7] Newlaczyl AU, Yu LG. Galectin-3--a jack-of-all-trades in cancer. Cancer letters 2011;313:123-128.

[8] Radosavljevic G, Volarevic V, Jovanovic I, Milovanovic M, Pejnovic N, Arsenijevic N, et al. The roles of Galectin-3 in autoimmunity and tumor progression. Immunologic research 2012;52:100-110.

[9] Dange MC, Srinivasan N, More SK, Bane SM, Upadhya A, Ingle AD, et al. Galectin-3 expressed on different lung compartments promotes organ specific metastasis by facilitating arrest, extravasation and organ colonization via high affinity ligands on melanoma cells. Clinical & experimental metastasis 2014;31:661-673.

[10] Krishnan V, Bane SM, Kawle PD, Naresh KN, Kalraiya RD. Altered melanoma cell surface glycosylation mediates organ specific adhesion and metastasis via lectin receptors on the lung vascular endothelium. Clinical & experimental metastasis 2005;22:11-24.

[11] Srinivasan N, Bane SM, Ahire SD, Ingle AD, Kalraiya RD. Poly N-acetyllactosamine substitutions on N- and not O-oligosaccharides or Thomsen-Friedenreich antigen facilitate lung specific metastasis of melanoma cells via galectin-3. Glycoconjugate journal 2009;26:445-456.

[12] More SK, Srinivasan N, Budnar S, Bane SM, Upadhya A, Thorat RA, et al. N-glycans and metastasis in galectin-3 transgenic mice. Biochemical and biophysical research communications 2015;460:302-307.

[13] Comodo AN, Lacerda Bachi AL, Soares MF, Franco M, Castro Teixeira VdP. Galectin-3 expression favors metastasis in murine melanoma. Advances in Bioscience and Biotechnology 2013;04:55-62.

[14] Radosavljevic G, Jovanovic I, Majstorovic I, Mitrovic M, Lisnic VJ, Arsenijevic N, et al. Deletion of galectin-3 in the host attenuates metastasis of murine melanoma by modulating tumor adhesion and NK cell activity. Clinical & experimental metastasis 2011;28:451-462.

[15] Eude-Le Parco I, Gendronneau G, Dang T, Delacour D, Thijssen VL, Edelmann W, et al. Genetic assessment of the importance of galectin-3 in cancer initiation, progression, and dissemination in mice. Glycobiology 2009;19:68-75.

[16] Jia W, Kidoya H, Yamakawa D, Naito H, Takakura N. Galectin-3 accelerates M2 macrophage infiltration and angiogenesis in tumors. The American journal of pathology 2013;182:1821-1831.

[17] Dunn GP, Koebel CM, Schreiber RD. Interferons, immunity and cancer immunoediting. Nature reviews Immunology 2006;6:836-848.

[18] Kim R, Emi M, Tanabe K. Cancer immunoediting from immune surveillance to immune escape. Immunology 2007;121:1-14.

[19] Chen HY, Liu FT, Yang RY. Roles of galectin-3 in immune responses. Archivum immunologiae et therapiae experimentalis 2005;53:497-504.

[20] Demetriou M, Granovsky M, Quaggin S, Dennis JW. Negative regulation of T-cell activation and autoimmunity by Mgat5 N-glycosylation. Nature 2001;409:733-739.

[21] Fukumori T, Takenaka Y, Yoshii T, Kim HR, Hogan V, Inohara H, et al. CD29 and CD7 mediate galectin-3-induced type II T-cell apoptosis. Cancer research 2003;63:8302-8311.

[22] Stillman BN, Hsu DK, Pang M, Brewer CF, Johnson P, Liu FT, et al. Galectin-3 and galectin-1 bind distinct cell surface glycoprotein receptors to induce T cell death. Journal of immunology 2006;176:778-789.

[23] Stowell SR, Qian Y, Karmakar S, Koyama NS, Dias-Baruffi M, Leffler H, et al. Differential roles of galectin-1 and galectin-3 in regulating leukocyte viability and cytokine secretion. Journal of immunology 2008;180:3091-3102.

[24] Yang RY, Hsu DK, Liu FT. Expression of galectin-3 modulates T-cell growth and apoptosis. Proceedings of the National Academy of Sciences of the United States of America 1996;93:6737-6742.

[25] Hsu DK, Yang RY, Saegusa J, Liu FT. Analysis of the intracellular role of galectins in cell growth and apoptosis. Methods in molecular biology 2015;1207:451-463.

[26] Liu FT, Yang RY, Saegusa J, Chen HY, Hsu DK. Galectins in regulation of apoptosis. Advances in experimental medicine and biology 2011;705:431-442.

[27] Waldhauer I, Steinle A. NK cells and cancer immunosurveillance. Oncogene 2008;27:5932-5943.

[28] Zamai L, Ponti C, Mirandola P, Gobbi G, Papa S, Galeotti L, et al. NK cells and cancer. Journal of immunology 2007;178:4011-4016.

[29] Pahl J, Cerwenka A. Tricking the balance: NK cells in anti-cancer immunity. Immunobiology 2015.

[30] Ikeda H, Old LJ, Schreiber RD. The roles of IFN gamma in protection against tumor development and cancer immunoediting. Cytokine & growth factor reviews 2002;13:95-109.

Publications in Refereed Journal:

a. Published: **Aparna D. Chaudhari**, Rajiv P. Gude, Rajiv D. Kalraiya, Shubhada V. Chiplunkar. Endogenous galectin-3 expression levels modulate immune responses in galectin-3 transgenic mice. **Molecular Immunology** 2015 Dec; 68(2 Pt. A):300-11.

b. Accepted: Nil

c. Communicated: Nil

d. Other Publications: Conference Proceedings

1. **Poster Presentation** titled 'Role of Galectin-3 in modulating tumor specific immunity and lung metastasis in mice' at the '32nd Annual Convention of Indian Association for Cancer Research & International Symposium on 'Infection and Cancer'' held at University of Delhi, North Campus between 13th-16th February, 2013.
   'RAJNIKANT BAXI AWARD' for Best Poster Presentation by Young Scientists

2. **Oral and Poster Presentation** titled 'Role of Galectin-3 in modulating tumor specific immunity and lung metastasis in mice' at the 'National Conference on Glycobiology of Cancer: Lectins as Tools and Targets' held at Karnataka University, Dharwad between 7th -9th November, 2013.

3. **Poster Presentation** titled 'Role of Galectin-3 in regulating tumor immunity in B16F10 lung metastasis model' at the 'IX DAE - BRNS Life Sciences Symposium (LSS - 2013) on 'Current Advances in Immunobiology and Cancer'' held at BARC, Mumbai between 28th -30th November, 2013.

4. **Poster Presentation** titled 'Absence of Galectin-3 contributes to immune dysfunction favoring lung metastasis of B16F10 melanoma in mice' at the International Conference 'Carcinogenesis 2015 - Molecular Pathways to Therapeutics: Paradigms and Challenges in Oncology' held at TMC-ACTREC, Mumbai between 11th-13th February, 2015.
   Abstract published: Aparna Chaudhari, Rajiv Gude, Rajiv Kalraiya, Shubhada V. Chiplunkar. Absence of galectin-3 contributes to immune dysfunction favoring lung metastasis of B16F10 melanoma in mice. **Journal of Carcinogenesis** 2015; 14, Suppl S1:21-38.

5. **Oral Presentation** titled 'Endogenous galectin-3 expression levels modulate immune responses and B16F10 lung metastasis in mice' at International Conference on 'Promotion of animal research, welfare and harmonization of Laboratory Animal Science - LASA 2015' held at TMC-ACTREC, Mumbai between 15th-16th October, 2015.

Signature of Student:

Date: 23/3/2016

Doctoral Committee

S. No.	Name	Designation	Signature	Date
1.	Dr. Sorab Dalal	Chairperson		23/3/16
2.	Prof. S. V. Chiplunkar	Guide & Convener		23/3/16
3.	Dr. Sanjay Gupta	Member		23/3/16
4.	Dr. N. N. Joshi	Member		23.3.16

Forwarded through:

23/3/16

Prof. S.V. Chiplunkar
Director, ACTREC
Chairperson,
Academic & Training Program, ACTREC

Dr. S. V. Chiplunkar
Director
Advanced Centre for Treatment, Research & Education in Cancer (ACTREC)
Tata Memorial Centre
Kharghar, Navi Mumbai 410210.

Prof. K. Sharma
Director, Academics
Tata Memorial Centre

Prof. K.S. Sharma
DIRECTOR - ACADEMICS, TMC
Mumbai - 400 012

List of Figures

List of Tables

Abbreviations

Gal-3	Galectin-3
LGALS3	Lectin, Galactoside-Binding, Soluble, 3
CRD	Carbohydrate Recognition Domain
kDa	Kilodalton
aa	Amino acids
TCR	T Cell Receptor
LPS	Lipopolysaccharide
IL-2	Interleukin-2
IFN-γ	Interferon-γ
TNF	Tumor Necrosis Factor
EAE	Experimental autoimmune encephalomyelitis
AGE	Advanced glycation end-product
Apo	Apolipoprotein
PolyLacNAc	Poly N-Acetyl Lactosamine
TTF-1	Thyroid Transcription Factor-1
Bcl-2	B-cell lymphoma-2
MUC2	Mucin 2
Rb	Retinoblastoma
ECM	Extracellular Matrix
mRNA	messenger Ribonucleic Acid
siRNA	silencer Ribonucleic Acid
DNA	Deoxyribonucleic acid
cDNA	Complementary Deoxyribonucleic acid
MMP	Matrix metalloproteinase
K-Ras	Kirsten Rat sarcoma

Raf	Rapidly Accelerated Fibrosarcoma
MEK	Mitogen-activated protein kinase kinase
ERK	Extracellular signal-regulated kinase
NFκB	Nuclear Factor kappa B
HIF-1α	Hypoxia-inducible factor- 1 α
FAK	Focal Adhesion Kinase
MAPK	Mitogen-activated protein kinase
CpG	5'—C—phosphate—G—3'
c-Myc	Myelocytomatosis cellular oncogene
MCL-1	Myeloid leukemia cell differentiation protein-1
VEGF	Vascular Endothelial Growth Factor
VEGFR	Vascular Endothelial Growth Factor Receptor
JNK	c-Jun NH2-terminal kinases
PI3-K	Phosphoinositide-3-kinase
EGF	Epidermal Growth Factor
ROS	Reactive Oxygen Species
COX-2	Cyclo-oxygenase-2
LAMP-1	Lysosome Associated Membrane Protein-1
NICD	Notch Intracellular Domain
SCID	Severe Combined Immunodeficiency
VCAM-1	Vascular cell adhesion molecule-1
NK	Natural Killer
Th	T helper
T_C	T cytotoxic
γδ	Gamma delta
T_{reg}	Regulatory T cells
CTL	Cytotoxic T Lymphocytes

mAb	monoclonal antibody
rmIL-2	recombinant murine IL-2
rmIFN-γ	recombinant murine IFN-γ
FBS	Fetal Bovine Serum
PBS	Phosphate Buffered Saline
DMSO	Dimethyl Sulphoxide
RPMI	Roswell Park Memorial Institute
PPO	2,5-Diphenyloxazole
POPOP	1,4-Di-2-(5-phenyloxazolyl)benzene
µl	microliter
ml	milliliter
µg	microgram
ng	nanogram
pg	picogram
µM	micromole
FITC	Fluorescein Isothiocyanate
PE	Phycoerythrin
PI	Propidium Iodide
FACS	Fluorescence Activated Cell Sorting
MACS	Magnetic Activated Cell Sorting
DCFH-DA	Dichloro-dihydro-fluorescein diacetate
CFSE	Carboxyfluorescein succinimidyl ester
SDS	Sodium dodecyl sulphate
APS	Ammonium persulphate
TEMED	Tetramethylethylenediamine
EDTA	Ethylenediaminetetraacetic acid
CBA	Cytometric Bead Array

CHAPTER 1

INTRODUCTION

Galectins are a family of β-galactoside-binding animal lectins that share a consensus sequence of about 130 amino acids in the carbohydrate recognition domain (CRD). Till date, fifteen mammalian galectins have been identified. Galectins show a high level of evolutionary conservation and members of this family are present in organisms from nematodes to mammals. Some galectins are widely expressed in different tissues, whereas others are more tissue specific. Members of galectin family differ in their carbohydrate-binding specificity and affinity. Emerging research on galectins indicates that they play important roles in diverse physiological and pathological processes, including cancer. Galectins have a broad variety of functions including mediation of cell-cell interactions, cell-matrix adhesion, migration, growth and transmembrane signaling [1,2].

Galectin-3 is one of the most widely studied members of the mammalian galectin family. It is a 31 kDa protein and a unique chimera-type galectin composed of an N-terminal domain, a repetitive collagen-like sequence rich in glycine, proline and tyrosine and a C-terminal carbohydrate recognition domain (CRD) [1]. Galectin-3 is found within the nucleus, in the cytoplasm, on the cell surface and in the extracellular compartment, depending on the cell type and the proliferative status [3-5]. Thus, it is a ubiquitously expressed molecule with diverse physiological functions based on its subcellular and extracellular localization. Galectin-3 plays important roles in various biological processes such as maintenance of cellular homeostasis, organogenesis, apoptosis, immune responses, angiogenesis, tumor invasion and metastasis [6-13].

Involvement of galectin-3 in various steps of cancer progression and metastasis has been extensively documented [14-18]. Majority of the studies have demonstrated the effects of galectin-3 produced either by the tumor cells themselves or the effects of endogenous host galectin-3 on the properties of tumor cells. Depending on the subcellular localization of galectin-3 produced by the tumor cells, various effects on the tumor cell

properties have been reported [6,9,11,14,16,19]. Using genetic manipulation techniques, effects of ectopic expression or complete knockdown of galectin-3 in cancer cell lines have been assessed through *in vitro* and *in vivo* approaches [20,21]. Further, endogenous host galectin-3 is known to exert its effects on the tumor cells via tumor cell surface carbohydrates associated with cancer progression, like TF-antigens on mucinous oligosaccharides [22-25] or poly N-acetyl lactosamine substituted *N*-oligosaccharides [26-30]. However, how different levels of expression of endogenous galectin-3 in the host influence tumor growth and metastasis remains poorly understood till date and warrants detailed investigation.

Galectin-3 has been found to be expressed in highest amounts on majority of the tissue compartments of lung and constitutively on lung vascular endothelium in mice [30,31]. Previous studies using B16F10 murine melanoma model have demonstrated that, interactions between galectin-3 present on the mice lung endothelium and its high affinity ligand poly-*N*-acetyl lactosamine (polyLacNAc) on β1,6 branched *N*-oligosaccharides present on B16F10 melanoma cells facilitate B16F10 colonization in the mice lungs exhibiting organ specific metastasis [26,30,32].

Earlier studies done in galectin-3 wild type (Gal-$3^{+/+}$) and null (Gal-$3^{-/-}$) mice have reported contradictory research findings related to comparison of primary tumor growth as well as metastatic frequencies in these two mice groups. A study done using C57BL/6 wild-type and galectin-3-null mice has shown that the growth of primary subcutaneous B16F10 melanoma tumor did not differ between these two genotypic groups of mice. However, the number of metastatic melanoma colonies in the lungs of wild-type mice was significantly increased in comparison to that observed in galectin-3-null mice [33]. Another group has reported that deletion of galectin-3 in the host attenuates lung metastasis of B16F1 malignant melanoma cells by modulating tumor cell adhesion to

lung tissue and NK cell mediated anti-tumor cytotoxicity. This study has focused on B16F1 cells, a variant of B16 melanoma possessing lower metastatic potential as compared to B16F10 cells [34]. Conversely, it has also been shown that in Gal-$3^{-/-}$ mice, both *Apc* intestinal tumors and *PyMT* mammary gland tumors appear at the same frequency as in Gal-$3^{+/+}$ animals. Further, it was reported that, absence of endogenous galectin-3 did not influence the frequency of dissemination of *PyMT* tumors to lungs in Gal-$3^{-/-}$ mice. Thus, no detectable effects of the absence of endogenous host galectin-3 on tumor formation as well as metastasis were evident in Gal-$3^{-/-}$ mice [35]. On the other hand, a study done using B16 mouse melanoma cells and LLC mouse lung cancer cells to develop allograft model in Gal-$3^{+/+}$ and Gal-$3^{-/-}$ mice as hosts, showed enhancement of primary solid tumor growth in Gal-$3^{-/-}$ mice compared with Gal-$3^{+/+}$ mice for both B16 and LLC tumors. However, the incidence of pulmonary metastases of B16 melanoma cells in Gal-$3^{+/+}$ and Gal-$3^{-/-}$ mice groups was not reported in this study [36]. Interestingly, it was recently documented that, the number and size of metastatic B16F10 melanoma colonies formed in the lungs of Gal-$3^{-/-}$ mice were very similar to those seen in Gal-$3^{+/+}$ mice. Gal-$3^{+/-}$ (galectin-3 hemizygous) mice that showed reduced expression of galectin-3 on the mice lungs also exhibited proportionate decrease in the number of metastatic melanoma colonies [32]. These studies highlight a paradoxical effect of endogenous galectin-3 expression on the tumor growth and metastasis in the host. It is therefore important to understand the possible underlying mechanisms of endogenous galectin-3 mediated regulation of tumorigenic and metastatic events in the host.

Role of immune system in the modulation of tumor progression and metastasis in the host has been widely reported [37,38]. Cancer immunoediting theory has explained that an optimally functioning immune system plays a crucial role in either elimination

or maintenance of metastatic cancer cells in dormancy over a prolonged time period in the host [38]. Galectin-3 is expressed in many cells subsets of immune system, including monocytes/macrophages, dendritic cells, eosinophils, neutrophils, mast cells, uterine NK cells, activated T and B cells. Accumulating evidence suggests the importance of galectin-3 in modulating host immune responses through the regulation of homeostasis and functions of various immune cell subsets [10,39-48]. The immunomodulatory functions of galectin-3 have been majorly studied either using recombinant galectin-3 or by genetic manipulation approaches to influence the expression of galectin-3 protein in the cell [9,12]. The immunoregulatory functions of galectin-3 have also been confirmed by other *in vitro* experimental strategies, such as the use of immune cells from Gal-$3^{-/-}$ mice or by knocking down the *LGALS3* gene expression in the immune cells by siRNA [8,49]. Although limited literature is available demonstrating the role of galectin-3 in immune regulation *in vivo* using Gal-$3^{+/+}$ and Gal-$3^{-/-}$ mice [8,34,36,39-42,49-52], the exact role of different endogenous galectin-3 expression levels in the modulation of host anti-tumor immune responses and the mechanisms involved therein remain unclear till date and necessitate in-depth investigation.

Based on these reported findings, we hypothesized that endogenous galectin-3 regulates immune responses in mice and thereby modulates lung metastasis of B16F10 murine melanoma cells in these mice. The present study therefore set out to delineate how different levels of expression of endogenous galectin-3 in the host regulate immune responses and what are the possible underlying mechanisms. *LGALS3* transgenic mice of C57BL/6 background strain, including Gal-$3^{+/+}$ (Wild-type), Gal-$3^{+/-}$ (Hemizygous) and Gal-$3^{-/-}$ (Knockout) genotypes were used and their immune scenario was thoroughly investigated under normal physiological conditions

as well as during progression of B16F10 experimental lung metastasis. This to our knowledge is the first experimental study done to investigate the gene dosage effect of endogenous galectin-3 on host immunity and the possible regulatory mechanisms using murine model system. The findings provide strong links to understand the crosstalk between galectin-3, immune system and cancer metastasis, which might facilitate the designing of more efficient galectin-3 targeted therapeutic strategies against cancer in the future.

Aims and objectives of the present thesis are as follows:

Aim

To investigate how endogenous galectin-3 contributes to anti-tumor immune responses and lung metastasis of B16F10 melanoma cells in mice.

Objectives

1. To study the immune scenario in Gal-3 wild type (Gal-$3^{+/+}$), Gal-3 hemizygous (Gal-$3^{+/-}$) and Gal-3 null (Gal-$3^{-/-}$) mice.
2. To monitor the immune responses in Gal-3 wild type (Gal-$3^{+/+}$), Gal-3 hemizygous (Gal-$3^{+/-}$) and Gal-3 null (Gal-$3^{-/-}$) mice during progression of B16F10 lung metastasis
3. To study the mechanisms involved in endogenous galectin-3 mediated regulation of anti-tumor immune responses in *LGALS3* transgenic mice.

CHAPTER 2

REVIEW OF LITERATURE

1. Galectins

Galectins constitute a family of soluble animal lectins defined by their evolutionary conserved carbohydrate recognition domain (CRD) and their affinity for β-galactosides containing glycoconjugates, such as *N*-acetyllactosamine, which can be bound to proteins by either N-linked or O-linked glycosylation. They are also termed S-type lectins due to their dependency on disulphide bonds for stability and carbohydrate binding [2,53,54].

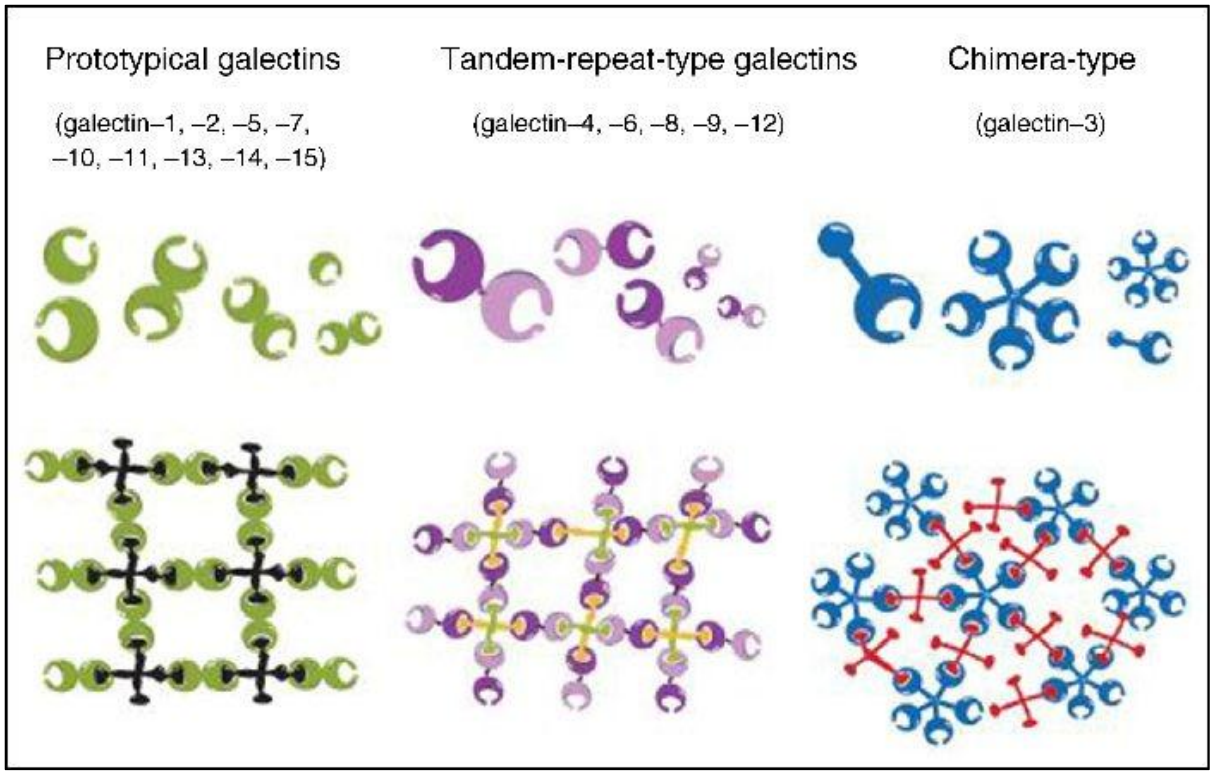

[Yang *et al.* Expert reviews in molecular medicine 2008;10:e17]

Figure 1: Galectin family members and formation of galectin-glycan lattices.

On the basis of the number and the organization of CRDs, galectins are divided into three types: (i) prototypical galectins, which contain a single CRD that may associate to form monomers or homodimers. Galectin-1, -2, -5, -7, -10, -11, -13, -14 and -15 belong to this type. (ii) tandem-repeat type galectins, composed of a single polypeptide chain

containing two CRDs connected by a small linker peptide (up to 70 amino acids) Galectin-4, -6, -8, -9, and -12 belong to this type. (iii) The chimera type galectin, characterized by the presence of a single C-terminal CRD and a large non-lectin amino-terminal domain, which is rich in proline, glycine, and tyrosine residues. Galectin-3 is the only member of this type (Figure 1).

Interestingly, galectins are found both extracellularly and intracellularly and regulate various cellular processes. Galectins are multifunctional proteins involved in cell-cell and cell-extracellular matrix interactions, organization of membrane domains, cell signaling, intracellular trafficking, apoptosis as well as regulation of cell cycle. Available literature indicates that galectins play important roles in diverse physiological and pathological processes, including immune and inflammatory responses, tumor development and progression, neural degeneration, atherosclerosis, diabetes, and wound repair. Some of these have been discovered or confirmed by using genetically engineered mice deficient in a particular galectin. Galectins therefore represent potential therapeutic targets, especially in the context of cancer, inflammatory diseases and several other diseases [2,10,13,16,53-55].

2. Galectin-3

Galectin-3 is one of the most studied members of the galectin family, originally identified as Mac-2, a 32-kDa cell surface antigen expressed on murine thioglycollate-elicited peritoneal macrophages [56]. Galectin-3 is encoded by a single gene, *LGALS3*, located on chromosome 14 [57]. It is the only known chimera-type galectin i.e. having both a lectin domain and a non-lectin domain [58]. It has a molecular weight of 29-35 kDa. Galectin-3 is a monomer in solution; however, it forms pentamers via the flexible N-terminal domains upon binding to its carbohydrate ligands (Figure 1).

3. Structure of galectin-3

Galectin-3 consists of two structural domains: (i) an N-terminal non-lectin domain containing a serine phosphorylation site, which is important in oligomerization of galectin-3 on ligand binding and in regulating its cellular signaling activity as well as a collagen-α-like sequence rich in glycine, tyrosine, and proline cleavable by matrix metalloproteinases (ii) a C-terminal domain with a globular structure containing a single CRD, which recognizes ligands containing β-galactosides [2,59] (Figure 2).

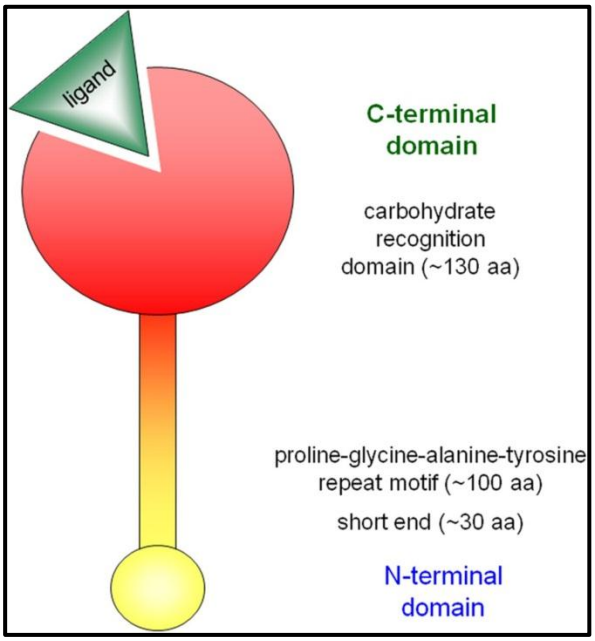

[Pugliese *et al.* Glycobiology 2015; 25 (2): 136-150]

Figure 2: Structure of Galectin-3.

4. Distribution and localization of galectin-3

Galectin-3 is widely spread among different types of cells and tissues of different animal species. Galectin-3 expression in tissues appears to be developmentally regulated, being more abundant during embryogenesis and development than in the adult life, when it is detected in various epithelial cells, cartilage and bone as well as in inflammatory cells, either constitutively or in an inducible fashion [9,60].

Galectin-3 is expressed in normal epithelial cells, fibroblasts, hematopoietic cells such as basophils, eosinophils, neutrophils, monocytes/macrophages, dendritic cells, mast cells as well as activated T and B cells [8,61,62]. Galectin-3 is also expressed in a variety of tumors and the intensity of the expression depends on tumor progression, invasiveness and metastatic potential [63-67].

Galectin-3 shows a ubiquitous localization within the cell and is found intracellularly in nucleus and cytoplasm [13]. However, its localization strongly depends on various factors such as cell type and proliferation status of the cell [3,68-70], cultivation conditions [71], neoplastic progression [19,72-77] and transformation [78]. Its intracellular distribution depends on the cell cycle, being mainly cytoplasmic in quiescent cells, and nuclear in replicating cells [9]. Phosphorylation at N-terminal serine 6 is a key event for galectin-3 shuttling from the nucleus to the cytoplasm, where only the phosphorylated form can be detected [79]. .

Galectin-3 lacks a signal sequence for transfer into the endoplasmic reticulum and Golgi compartments and entry into classical secretory pathways [80]. However, it secreted via non-classical pathway outside of cell, where it is found both on the cell surface as well as in the extracellular matrix [8,81].

5. Intracellular functions of galectin-3

Intracellular galectin-3 regulates various important cellular responses by functioning inside the nucleus or cytoplasm of the cells. Intracellular galectin-3 is known to be involved in pre-mRNA splicing, where galectin-3 functions as a component of spliceosomes [7]. It also regulates the expression of certain genes, including those for cyclin D1, thyroid-specific TTF-1 transcription factor, MUC2 mucin and c-Jun N-terminal

kinase etc. [8,9,53,82]. Intracellular galectin-3 regulates cell growth through its anti-apoptotic effect on various cell types by interacting with some components of the apoptosis signaling pathways. It protects cells from a variety of death signals, including Fas receptor cross-linking. In particular, the antiapoptotic activity of galectin-3 seems to be related to its sequence homology and association with *bcl-2* [83]. Galectin-3 has also been shown to protect cells against apoptosis induced by the loss of cell anchorage (anoikis) [11,47,84-86]. Earlier studies have demonstrated the dependence of intracellular galectin-3 expression on the cell cycle, by arresting the cells at G1 or G2/M phase, via downregulation of cyclin A and E, upregulation of p21 and p27 cyclin inhibitors and hypophosphorylation of Rb protein [86,87]. Galectin-3 controls intracellular trafficking of glycoproteins [88], which may be linked to its ability to translocate into the lumen of transport vesicles. Intracellular galectin-3 is associated with centrosomes in epithelial cells transiently during the process of epithelial polarization and may thus regulate epithelial polarization in enterocytes [89,90]. Galectin-3 contributes to maintenance of the barrier function of ocular surface epithelial cells [91].

6. Extracellular functions of galectin-3

The extracellular galectin-3 exhibits numerous regulatory effects in the host (Figure 3). It mediates cell adhesion and cell activation and acts as a chemo attractant for certain cell types. In that way, galectin-3 affects various biological processes such as maintenance of cellular homeostasis, immune responses, organogenesis, angiogenesis, tumor invasion and metastasis [12,14,28,92-98]. Extracellular galectin-3 regulates cell adhesion in a dual manner. Cell surface galectin-3 promotes homo- and heterotypic cell-to-cell interactions by serving as a cross-linking bridge between adjacent cells through attachment to a complementary serum glycoprotein(s) ([99,100]. On the contrary, galectin-3 downregulates

cell adhesion to the ECM component laminin via an association with the α1β1-integrin receptor in a lactose-inhibitable manner, thus producing an anti-adhesive effect [93,101]. Moreover, galectin-3 was found to interact with branched *N*-glycans on integrin α5β1, thus promoting turnover of focal adhesions and cell spreading and motility [101]. This dual function of galectin-3 on cell adhesion has made this lectin an interesting target for the study of tumor progression and invasiveness [102-104].

The secreted galectin-3 potentiates angiogenesis by facilitating migration, chemotaxis and morphogenesis of endothelial cells [15,36,94,105-108]. It is also known to induce T cell apoptosis [47,109].

Extracellular galectin-3 interacts with the β-galactoside residues of several extracellular matrix (ECM) and cell surface glycoproteins via the CRD; this is the classical lectin–glycoconjugate interaction. At the cell surface, galectin-3 forms multimeric structures up to pentamers, driven by increasing concentrations of multivalent glycoprotein ligands, resulting in higher order lattices or microdomains with irregular geometry [110,111]. The galectin-glycoprotein lattice is involved in the regulation of receptor clustering, endocytosis and signaling. Extracellular galectin-3 cross-links cell surface glyco-conjugates, form dimers and multimers, and delivers signals inside the cell. The ∼22 kDa fragment of MMP cleaved galectin-3 binds to the glycan receptors more efficiently than the intact protein, the functions of smaller fragments are as yet unknown [112].

However, it should be mentioned that majority of these studies were performed using exogenously introduced galectin-3 in high concentrations, thus biological functions of extracellular galectin-3 in physiological conditions remain to be elucidated till date.

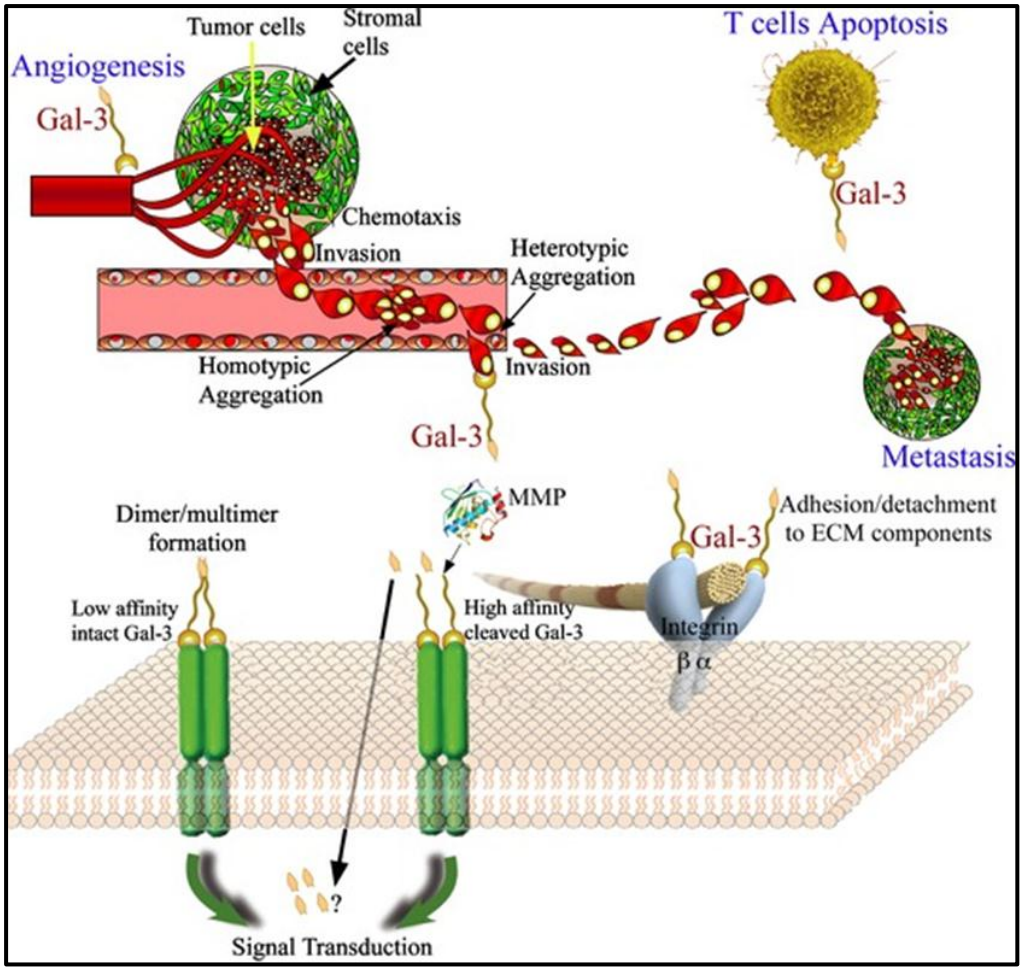

[Raz *et al*., Cancer Microenviron. 2008 ; 1(1):43-51]

Figure 3: Extracellular functions of galectin-3

7. Role of galectin-3 in tumor progression and metastasis

The involvement of Galectin-3 in tumor growth, progression and metastasis has been comprehensively documented [14,15,17,18,35,64-67,92,113-124]. By virtue of its pro-proliferative and anti-apoptotic action, galectin-3 is considered as an immediate early gene possibly implicated in tumor growth. There is evidence that Galectin-3 expression is necessary for the initiation of the transformed phenotype of tumors, possibly related to its ability to interact with oncogenic K-Ras [125,126]. The promoter region as well as the first exon of galectin-3 encoding *LGALS-3* gene, exhibit a high content

of CpG islands, indicating that epigenetic mechanisms also control galectin-3 expression, as observed during malignant transformation and tumor progression [127,128].

Galectin-3 expression in human cancers

Galectin-3 expression is altered in a variety of human cancers in comparison to normal tissues [65,129]. For instance, the expression of galectin-3 is found to be upregulated in gastric, liver, thyroid, colorectal, melanoma, head and neck and tongue cancers; while it is downregulated in prostate, head and neck, breast, cervical, bladder, colon, cholangiocarcinoma and pancreatic cancers and uterine sarcoma when compared to normal tissues [6,19,130-143]. Numerous studies have also reported elevated or reduced serum levels of galectin-3 in cancer patients as compared to healthy individuals, that may serve as a potential prognostic marker of various cancers [144-162].

Galectin-3 in tumor cell growth and apoptosis

Endogenous galectin-3 is known to promote tumor cell growth [75,163-166]. One mechanism may involve interaction with transcription factors, such as interaction between nuclear galectin-3 and TTF-1 transcription factor in transformed thyroid cells [78]. Another mechanism through which endogenous galectin-3 has been found to promote tumor cell growth may be facilitation of the signaling of K-Ras to Raf and PI3 kinase [167]. It has also been reported that, endogenous galectin-3 regulates tumor progression by influencing cell cycling; it binds to β-catenin and stimulates the expression of cyclin D and c-Myc [168]. Another study demonstrated that, vascular endothelial growth factor C enhances cervical cancer cell invasiveness via upregulation of galectin-3 protein [169]. A recent study has revealed that, cell surface interaction of annexin A2 and galectin-3 modulates epidermal growth factor receptor signaling in Her-2 negative breast cancer cell [170].

The most extensively studied function of Galectin-3 is its inhibition of apoptosis in a range of tumor cell types exposed to diverse apoptotic stimuli [11,53,84,171-180]. The mechanisms by which Galectin-3 modulates apoptosis in tumor cells have been extensively studied [11,16,85,143,176,178,179,181-186]. It has been demonstrated that, apoptosis induced by the tumor suppressor protein p53 involves repression of anti-apoptotic galectin-3 through homeodomain-interacting protein kinase 2-activated p53 [187]. Galectin-3-targeting small molecule inhibitors enhance apoptosis induced by chemo- and radio-therapy in papillary thyroid cancer *in vitro* [175]. GCS-100, a novel galectin-3 antagonist, has been shown to modulate MCL-1, NOXA and cell cycle to induce myeloma cell death *in vitro* [188].

Galectin-3 in tumor cell invasion and migration

Exogenous as well as endogenous galectin-3 has been shown to affect the motility of tumor cells and influence their invasiveness *in vitro* [85,98,189-191]. However, both positive and negative effects have been reported [75,192-194]. It has been reported that, extracellular galectin-3 promotes tumor cell migration through interaction with mediators, such as integrins and caveolin, leading to FAK stabilization [121,195-197] (Figure 4B).

Galectin-3 in tumor angiogenesis

Galectin-3 can affect tumor metastasis by exerting its effect in the tumor microenvironment [16,120,121]. It has been reported that, galectin-3 has angiogenic activity [15,106,198], which may be related to its ability to induce migration of endothelial cells [105,107,199]. The full-length galectin-3 can form oligomers and bind to endothelial cell surface, preventing VEGFR and integrin internalization [94,199]. In addition, galectin-3 induces VEGF release by platelets upon activation through a PKC-dependent pathway [198,200]. Furthermore,

galectin-3 is known to promote monocyte/macrophage chemotaxis toward tumor microenvironment potentializing macrophage-induced angiogenesis [36,108] (Figure 4C).

Galectin-3 in cancer cell signaling

In tumor cells, galectin-3 has been reported to regulate signaling pathways like, Ras/Raf/MEK/ERK and Notch, modulating the cell survival, proliferation and migration [121] (Figure 4A).

MAPK signaling

The involvement of galectin-3 in tuning stress signaling pathways (MAPK family) within the tumor microenvironment, which play a key role in the development and progression of cancer, is well documented. MAPK family includes K-Ras-Raf-MEK-ERK cascade, p38 and c-Jun NH2-terminal kinases (JNK). Galectin-3 was first associated with Ras signaling in cancers, as galectin-3 was found to interact selectively through its CRD with activated K-Ras (K-Ras-GTP) and stabilize it in the activated state [201]. Activated K-Ras has been shown to enhance the translocation of galectin-3 to the plasma membrane and thereby galectin-3 increases K-Ras signaling, promoting phosphoinositide 3-kinase (PI3-K) activation and controlling both the intensity and duration of the K-Ras signal. Through this mechanism, galectin-3 and Ras regulate important processes in tumor cells, such as proliferation and survival, playing key roles in different cancer cells e.g., breast cancer cells [202]. Additional data revealed that galectin-3 is an integral component of nanoclusters containing K-Ras, that are essential for high fidelity signal transduction, with the ability to increase K-Ras activation to drive tumorigenesis *via* constitutive activation of Raf/MEK/ERK signaling cascade [125]. It has also been demonstrated that, galectin-3 down regulation leads to decreased activation of AKT and

ERK; thus, decreasing cell invasion and reducing tumor growth in an orthotopic mouse model of pancreatic cancer [203].

There are few reports about galectin-3 and its relation with p38 or JNK kinases. Earlier study has demonstrated that the copper treatment increased the levels of intracellular reactive oxygen species (ROS), which was accompanied by p38 activation in galectin-3-expressing melanoma cells [204]. In addition, it has been reported that extracellular galectin-3 induces MMP-9 expression via p38 MAPK pathway in melanoma cells [28]. These results show a different function of galectin-3 in p38 regulation, associated with the malignant phenotype, invasion, and metastasis of cancer cells. Further, it is known that intracellular galectin-3 activates elements of the JNK pathway. Evidence exists that the activation of both ERK and JNK1/2 depend on the phosphorylation status of the Ser6 residue of galectin-3. Phosphorylation of galectin-3 by kinases, such as casein kinase, seems necessary to the activation of antiapoptotic circuits dependent on ERK and JNK [205]. Although it is known that galectin-3 regulates the activity of MAPK pathway in several cancer models, further studies are still necessary to elucidate the mechanistic details of the pro-survival activity of galectin-3.

NF-κB and HIF-1

NF-κB is a family of transcription factors that plays important roles in the immune system and regulates the expression of cytokines, cyclooxygenase 2 (COX-2), growth factors and inhibitors of apoptosis. Dysregulation of NF-κB is known to be associated with inflammatory and autoimmune diseases as well as cancer [206]. Previous studies have revealed a link between galectin-3, NF-κB, hypoxia, nutrient deprivation and common stressing conditions within the tumor microenvironment. NF-κB inhibition by specific proteasomal inhibitors was found to decrease the expression of galectin-3 in

glioblastoma cells [207]. Similarly, it was also shown that the interference in NF-κB activation can inhibit galectin-3 expression leading to apoptotic processes [180].

HIF-1α is a master regulator of gene transcription under hypoxia, upregulating several genes, including galectin-3, in order to maintain cellular homeostasis and promote cell survival in skeletal tissues [208]. It has been previously demonstrated that, under hypoxic conditions, galectin-3 transcription requires protein synthesis and depends on both HIF-1α and NF-κB activities. Hypoxic/nutrient-deprived microenvironments are enriched in galectin-3, which protects cells from death [209]. More recently, another study has shown that galectin-3 deficiency reduces proliferation of hepatoma cells and increases their rate of apoptosis both *in vitro* and *in vivo*. Conversely, it was demonstrated that galectin-3 expression induced by NF-κB transactivation led to a more invasive phenotype of tumor cells, which developed larger tumors as compared to those found in Gal-$3^{-/-}$ mice [210].

Notch Signaling

Notch signaling plays a key role in differentiation, survival and/or proliferation. Alterations in the regulation of these processes contribute to malignant transformation. Abnormal activation of Notch pathway is often found in various types of cancers [211-216] . A study has described galectin-3-dependent activation of Notch1 signaling in a system that models tumor cell/osteoblast and osteoclast interactions, critical events in the maintenance of bone metastasis found in different cancers, such as breast and prostate cancers. In this study, extracellular galectin-3 was shown to interact with Notch1, in a CRD-dependent manner, activating Notch through its proteolytic cleavage, which leads to the formation of Notch intracellular domain (NICD) and its subsequent translocation to the nucleus leading to Notch target genes upregulation. The results indicated that, the

intact galectin-3 is more efficient in the induction of Notch cleavage than its truncated form [217]. These findings highlight the potential of targeting various Notch-dependent processes in the tumor therapies, including maintenance of a non-differentiated state of cells/tumor cells, activation of survival pathways leading to resistance to different therapeutic strategies and angiogenesis [218,219].

Collectively, the available literature studies shed light on the homeostatic roles of galectin-3 in tumors, as (i) it favors tumor cell adaptation for survival in stressed conditions; (ii) upon secretion, galectin-3 induces tumor cell detachment and migration; (iii) it attracts monocyte/macrophage and endothelial cells to the tumor mass, inducing the process of angiogenesis both directly and indirectly (Figure 4). The activities of galectin-3 related to invasion, adhesion, migration as well as chemotaxis of monocytes and endothelial cells are potentially targetable and specific interventions may be designed to counteract the pro-tumoral role of extracellular galectin-3.

Studies with animal models have provided evidence for the role of galectin-3 in tumor metastasis *in vivo* [16,18,114,220-222]. For example, liver metastases of human adenocarcinoma xenotransplants in SCID mice are inhibitable by anti-galectin-3 antibody. Breast carcinoma cells overexpressing transgenic galectin-3 have higher metastatic potential. In an orthotopic nude mouse model of human breast cancer, tumor metastasis is inhibitable by C-terminal domain fragment of galectin-3 (galectin-3C) [165]. In a human melanoma tumor model in immunodeficient mice, administration of galectin-3 results in suppressing the tumor killing effect of tumor-reactive T cells [122]. Tumor-associated galectin-3 may also contribute to tumor immune escape by rendering tumor-infiltrating $CD8^+$ cytolytic lymphocytes anergic [223]. Galectin-3 has been found to contribute to chemotherapeutic resistance of thyroid cancer cells *in vitro* [174], the progression of disease in prostate cancer [224] and development of carcinogen-induced lung tumorigenesis [225] in mouse models.

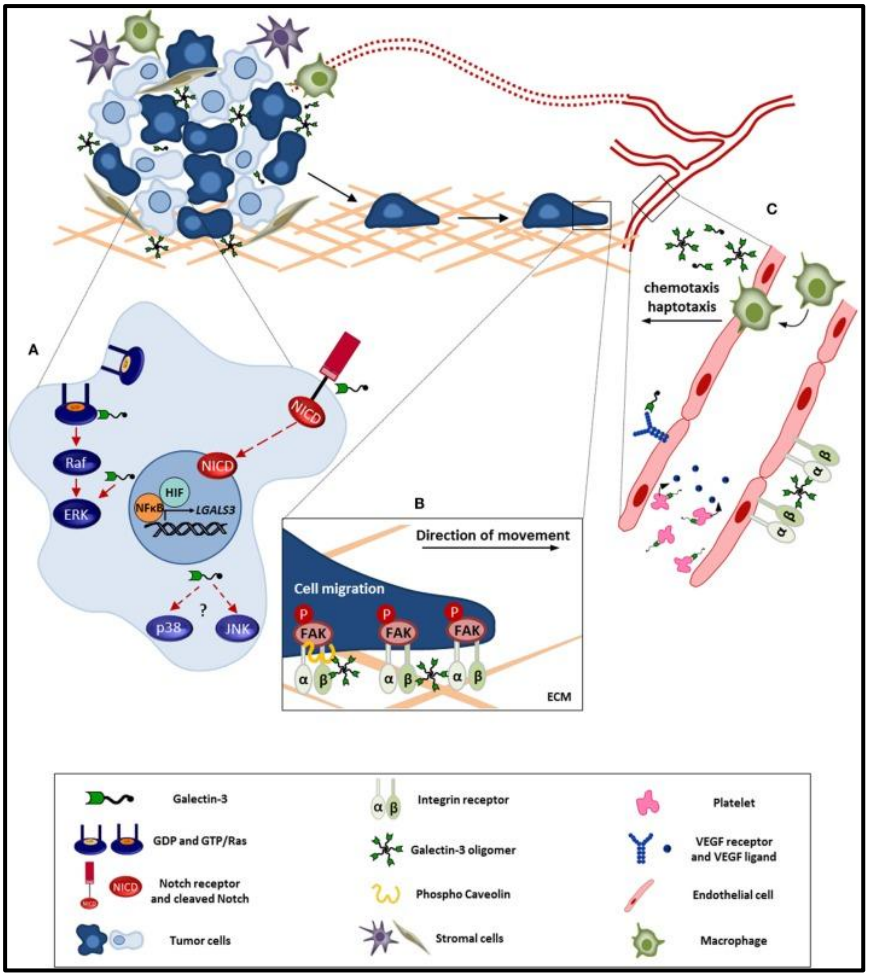

[Cardoso *et al*., Front Oncol. 2016; 6:127]

Figure 4: Involvement of galectin-3 in tumor progression and metastasis

Galectin-3 interactions with certain glycans and extracellular matrix (ECM) proteins have been described to promote and/ or antagonize tumor cell apoptosis, to induce endothelial cell proliferation and angiogenesis, to promote tumor cell adhesion and invasion, thus both potentially facilitating as well as hindering metastasis [113]. Moreover, although galectin-3 is expressed in several types of malignancies and its expression has been correlated with transformation and metastasis-related events, its downregulation has also been associated with malignancy and tumor progression [65-67,226]. These apparently conflicting data demonstrate that the role of galectin-3 in metastasis remains to be fully understood.

8. Role of endogenous galectin-3 in lung specific metastasis of B16F10 melanoma

B16F10 murine melanoma model

Cell culture experiments as well as *in vitro* biochemical studies have contributed many recent advances in our understanding of various physiological and pathological processes. However, the complexity of biological processes often requires *in vivo* analysis. The study of human biology *in vivo* is severely limited by ethical and technical constraints. Thus, there is a growing need for animal models to improve our understanding of human diseases without putting individuals at risk [227-229].

This notion also holds true for cancers, including melanoma which is the focus of the present study. Indeed, several mouse melanoma models have been developed [228,230-237]. These models have been used: (i) to determine the function of particular proteins in melanoma progression; (ii) to approximate certain biological aspects of human melanomas; and (iii) to critically evaluate novel drugs or therapies.

The most frequently used syngeneic murine melanoma model is B16 derived from a spontaneously arising melanoma in C57BL/6J background strain. This model was originally developed by Fidler *et al.* [238,239] by alternate *in vitro* and *in vivo* passages of melanoma cells derived from these spontaneous subcutaneous melanoma tumors. The first in vitro passage of the cells yielded B16F1 cell line having a low metastatic potential, whereas the tenth in vitro passage gave rise to B16F10 cell line, which is a highly metastatic variant of B16 melanoma cells (Figure 5).

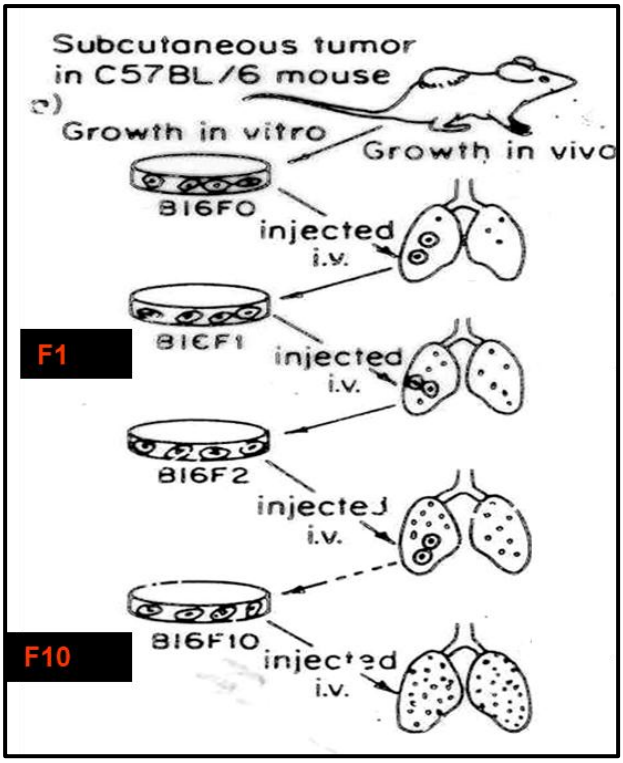

[Fidler and Nicolson, J Natl Cancer Inst. 1976;57(5):1199-202]

Figure 5: Development of B16 murine melanoma model

Following are the properties of B16F10 cell line, which make it a suitable model to study lung specific melanoma metastasis:

- It has high metastatic potential
- B16F10 cells express β1,6 branched *N*-glycans substituted terminally with polyNAcetylLactosamine (PolyLacNAc), which is a high affinity ligand for galectin-3 present on lung vascular endothelium
- B16F10 cells have inherent property for lung specific metastasis
- Melanin pigment (black) in B16F10 cells helps in the quantitation of metastatic colonies developed on the mice lungs.

Galectin-3 has been found to be expressed in highest amounts on majority of the tissue compartments of lung and constitutively on lung vascular endothelium in mice [30,31]. Previous studies using B16F10 murine melanoma model have shown that, interactions between galectin-3 on the mice lung endothelium and its high affinity ligand poly-*N*-acetyl lactosamine (polyLacNAc) on β1,6 branched N-oligosaccharides present on B16F10 melanoma cells facilitates B16F10 colonization in the lungs of the mice [26,30,32].

Earlier studies done in transgenic *LGALS3* mice that are wild type (Gal-$3^{+/+}$) or null (Gal-$3^{-/-}$) for galectin-3 expression have reported conflicting findings related to primary melanoma tumor growth as well as melanoma metastatic frequency. A study done using C57BL/6 Gal-$3^{+/+}$ or Gal-$3^{-/-}$ mice has shown that primary subcutaneous B16F10 melanoma tumor growth did not differ between these two groups. However, the number of lung metastatic colonies in wild-type mice was significantly increased in comparison to that observed in galectin-3-null mice [33]. Another group has reported that deletion of galectin-3 in the host attenuates lung metastasis of B16F1 malignant melanoma by modulating tumor adhesion and NK cell activity. This study has focused on B16F1 cells, a variant of B16 melanoma possessing lower metastatic potential than B16F10 cells [34]**.** On the other hand, a study has used B16 mouse melanoma cells for the allograft model using Gal-$3^{+/+}$ and Gal-$3^{-/-}$ mice as hosts. Their findings showed enhancement of primary solid tumor growth in Gal-$3^{-/-}$ mice compared with Gal-$3^{+/+}$ mice in B16 tumors. However, the frequency of pulmonary metastases of B16 melanoma in Gal-$3^{+/+}$ and Gal-$3^{-/-}$ mice groups was not reported in this study [36]. Interestingly, it was recently documented that the number and size of metastatic B16F10 melanoma colonies formed in lungs of Gal-$3^{-/-}$ mice was very similar to that seen in Gal-$3^{+/+}$ mice. Gal-$3^{+/-}$ mice that showed reduced expression of galectin-3 on the lungs showed proportionate decrease in the number of metastatic melanoma colonies [32]. To resolve the ambiguity in the reported

findings, it is important to unveil the possible underlying mechanisms in endogenous galectin-3 mediated regulation of tumorigenic and metastatic events in the host.

9. Role of galectin-3 in immune responses

Role of galectin-3 in the modulation of immune responses has been extensively documented [10,39,40,43,49,52,240-252]. Galectin-3 plays a pivotal role in both innate and adaptive immune responses, where it participates in the activation or differentiation of immune cells. Galectin-3 is expressed in a variety of cell types in the immune system, constitutively or in response to stimuli (Figure 6) [62].

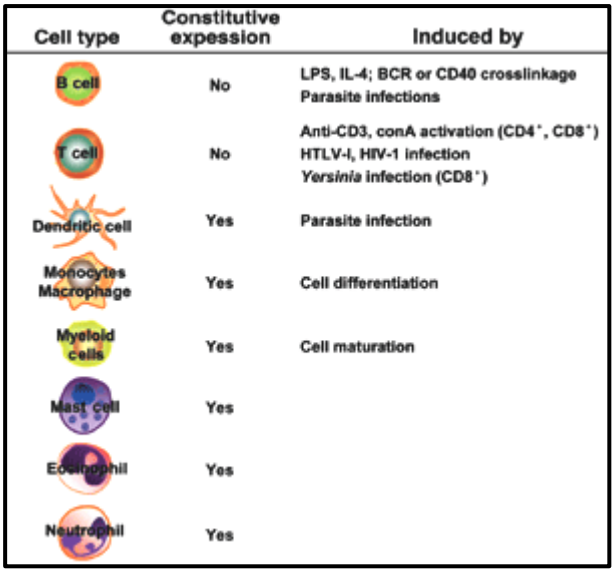

[Liu and Hsu, Drug News Perspect 2007, 20(7): 455]

Figure 6: Expression of galectin-3 in leukocytes

Galectin-3 has been shown to regulate the functions of various immune cell subsets (Figure 7) as mentioned below:

T and B cells

Recombinant galectin-3 is known to induce IL-2 production [253] and calcium influx [254] in Jurkat T cells. Extracellular galectin-3 induces apoptosis in human T leukemic

cell lines, human peripheral blood mononuclear cells, mouse activated T cells [109,255-257], normal human T cells [258] and a human tumor infiltrating T cell line [122]. In some T cell lines, such as MOLT-4 cells, galectin-3 induces phosphatidylserine exposure, an early event in apoptosis, but not cell death [258]. It has been reported that, galectin-3 induces apoptosis in both Th1 and Th2 cells [259]. It is pro-apoptotic in $CD4^-CD8^-$ human thymocytes [255] and attenuates the interaction of thymocytes with thymic nurse cells [260]. On the other hand, endogenous Galectin-3 has anti-apoptotic activity in the human T cell line Jurkat [47].

Galectin-3 binds to Mgat5-modified T cell receptor (TCR) and suppresses T cell activation induced by TCR engagement, which is associated with a decrease in lateral mobility of TCR [110]. It attenuates association of CD8 and TCR on $CD8^+$ tumor-infiltrating lymphocytes, thus causing anergy [223]. Intracellular galectin-3 negatively regulates TCR-mediated $CD4^+$ T cell activation at the immunological synapse, by intracellular action [261]. Endogenous galectin-3 regulates differentiation of B cells into plasma cells and memory B cells [48] and is anti-apoptotic in B cell lines [262].

Monocytes/Macrophages

Endogenous galectin-3 is anti-apoptotic in macrophages treated with LPS and IFN-γ [263]. It plays a critical role in the phagocytic function of macrophages in ingesting opsonized sheep red blood cells and apoptotic thymocytes. It plays a critical role in alternative macrophage activation [264].

Earlier studies have demonstrated that, recombinant galectin-3 triggers human peripheral blood monocytes to produce superoxide anion [265] and potentiates LPS-induced IL-1 production [266]. It functions as a chemoattractant for monocytes and macrophages [44]. Galectin-3 is an opsonin and enhances the macrophage clearance of apoptotic neutrophils

[267]. It activates microglia (tissue macrophages of the central nervous system) to phagocytose degenerated myelin mediated by complement receptor-3 and scavenger receptor [248]. Galectin-3 binds to a major xenoantigen, α-Gal [Galα(1,3)Galβ(1,4)GlcNAc], expressed on porcine endothelial cells [268] and mediates adhesion of human monocytes to porcine endothelial cells. It was shown to suppress LPS-induced production of inflammatory cytokines by macrophages, including IL-6, IL-12, and TNF-α [269].

Dendritic cells

Endogenous Galectin-3 suppresses the production of IL-12 by dendritic cells [270] and can thereby suppress Th1 responses [271]. It promotes Th2 polarization in the setting of antigen presentation to T cells by dendritic cells [271]. Another study suggested that, galectin-3 suppresses the antigen-presenting function of dendritic cells [42] and promotes dendritic cell trafficking by functioning intracellularly [272]. It also promotes adhesion of mouse dendritic cells [273].

Neutrophils

Galectin-3 induces oxidative burst [274-276] and L-selectin shedding as well as IL-8 production [277] in neutrophils. It promotes neutrophil adhesion to the extracellular protein laminin [278] and endothelial cells [45]. Extracellular galectin-3 induces phosphatidylserine exposure in the absence of cell death [258] and induces apoptosis [279] in neutrophils. On the other hand, endogenous galectin-3 protects neutrophils from apoptosis [277].

Mast cells

Galectin-3 induces mediator release from both IgE-sensitized and nonsensitized mast cells [280,281], but apoptosis following prolonged treatment (18-44 h) [282]. Endogenous Galectin-3 is a positive regulator of mast cell mediator release and cytokine production [283].

Eosinophils

Recombinant galectin-3 suppresses IL-5 production by human eosinophils [284]. It mediates rolling and adhesion of eosinophils on immobilized VCAM-1 under conditions of flow [285].

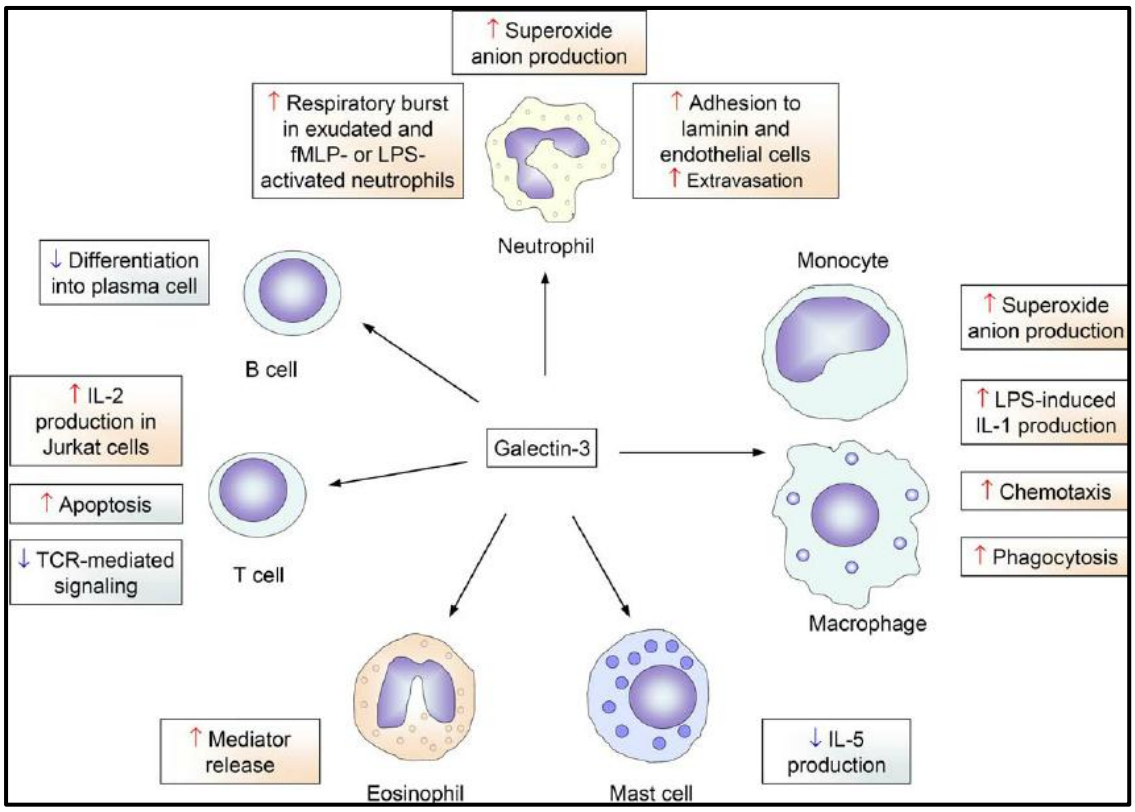

[Dumic *et al*., Biochim Biophys Acta. 2006;1760(4):616-35]

Figure 7: The effects of galectin-3 on immune cells

Immunomodulatory functions of galectin-3 demonstrated in vivo

A number of biological functions of galectin-3 have been identified *in vivo* by using Gal-$3^{+/+}$ (wild type) and Gal-$3^{-/-}$ (null) mice.

<u>Galectin-3 in inflammmation</u>

Galectin-3 has a proinflammatory role in acute inflammation induced by intraperitoneal injection of thioglycollate broth, in terms of the neutrophil response [263] and

macrophage response [51]. It promotes allergic airway inflammation, airway hyperresponsiveness, and a Th2 response in a mouse model of asthma in which mice are sensitized with ovalbumin systemically and challenged with the same antigen through the airways [286]. Galectin-3 is known to promote allergic skin inflammation and a systemic Th2 response in a model of atopic dermatitis, in which mice are repeatedly sensitized with ovalbumin epicutaneously [271]. Galectin-3 enhances allergic contact hypersensitivity, in which mice are sensitized with the hapten oxazalone, and then challenged with the same hapten at another skin site [272]. However, rats and mice treated by intranasal delivery of cDNA encoding Galectin-3 showed reduced eosinophil infiltration following airway antigen challenge [287,288]. Galectin-3 has also been suggested to be a pro-inflammatory mediator, since it induces the production of reactive oxygen species (ROS) in human neutrophils and promotes chemotaxis in monocytes [43,44,275]. Further, the interaction of galectin-3 with T cells induces anti-apoptotic activity, a phenomenon often correlated with a prolonged inflammatory response [84].

Galectin-3 in autoimmunity

Previous study has reported that, galectin-3 contributes to the disease severity in a mouse model of autoimmune encephalomyelitis (EAE) induced by immunization with a myelin oligodendrocyte glycoprotein peptide [289]. Galectin-3 suppresses the development of glomerulopathy in mice rendered diabetic with streptozotocin, associated with lower accumulation of advanced glycation end products (AGE) in the kidneys [290]. It may serve as an AGE receptor and protects from AGE-induced tissue injury [291] and age-dependent changes [292]. Galectin-3 contributes to development of diabetes induced by multiple low doses of streptozotocin [293]; this may be related to its upregulation of

TNF-α and nitric oxide production by macrophages. Galectin-3 is known to be involved in ischemia and neovascularization in retina in a mouse model of oxygen-induced proliferative retinopathy after perfusion of preformed AGEs [294]. It is expressed in foam cells and macrophages in atherosclerotic lesions [295] and contributes to the development of atherosclerosis in apolipoprotein (Apo)E-deficient mice [296].

Galectin-3 in infectious diseases

The roles of galectin-3 in a large number of mouse models of infectious disease have been studied. It was shown that, galectin-3 suppresses LPS-induced shock accompanied by lower inflammatory cytokine and nitric oxide production, possibly a result of its ability to bind to this endotoxin. However, it enhances sensitivity to *Salmonella* infection [269]. Galectin-3 contributes to recruitment of neutrophils to lungs of mice infected with *Streptococcus pneumoniae* and has a protective role in development of pneumonia after the infection, possibly by augmenting the function of neutrophils [297]. It is involved in the inflammatory responses in intestines, liver, and brain (but not in lungs) and a lower systemic Th1-polarized response in mice infected by *Toxoplasma gondii* [270]; galectin-3 suppresses parasite burden in the brain. Galectin-3 promotes development of T and B responses in the spleen, as well formation of liver granulomas, but suppresses the Th1-polarized response in mice infected with *Schistosoma mansoni* [42]. It induces sensitivity in lethal effects of *Rhodococcus equi*, a facultative intracellular bacterium of macrophages [52], where it suppresses inflammatory responses, including production of the Th1 cytokines IL-12 and IFN-γ, as well as IL-1β. Galectin-3 promotes resistance of mice to infection by *Paracoccidioides brasiliensis* and favors a Th1-polarized immune response [298]. Interestingly, recombinant Galectin-3 is able to induce cell death in the yeast Candida albicans *in vitro* [299].

CHAPTER 3

MATERIALS AND METHODS

1. Mice

6-8 Weeks old female *LGALS3* transgenic mice (C57BL/6 background strain) of 3 genotype groups: Gal-$3^{+/+}$ (Wild type), Gal-$3^{+/-}$ (Hemizygous) and Gal-$3^{-/-}$ (Knockout) were used for the study. Galectin-3 knockout mice generated by targeted disruption of the galectin-3 gene [51] were procured from Prof. F.T. Liu, University of California, Davis, California, USA. Initially, two pairs of male and female transgenic *LGALS3* mice i.e. hemizygous (Gal-$3^{+/-}$) and null (Gal-$3^{-/-}$) were purchased. The wild type (Gal-$3^{+/+}$) littermates were obtained by breeding the hemizygous pair. All the animals were propagated and maintained in pathogen-free environments in the Laboratory Animal Facility, ACTREC - Tata Memorial Centre. Standard laboratory diet and filtered water were available *ad libitum*. All animal experiments were done as per the guidelines of Institutional Animal Ethics Committee, ACTREC-Tata Memorial Centre.

2. Cell lines

YAC-1 Murine T cell Lymphoma cell line, a suspension cell line and B16F10 murine melanoma cell line, an adherent cell line were obtained from National Centre for Cell Sciences (NCCS, Pune, India). YAC-1 cells were cultured in RPMI 1640 medium supplemented with 10% Fetal Bovine Serum, 2mM L-Glutamine and antibiotics cocktail (Penicillin, Streptomycin, gentamycin, mycostatin). B16F10 cells were cultured in Dulbecco's Modified Eagle Medium supplemented with 10% Fetal Bovine Serum, 2mM L-Glutamine and antibiotics cocktail (Penicillin, Streptomycin, gentamycin, mycostatin). The cell lines were maintained at 37ºC in humidified CO_2 incubator containing 5% CO_2 and 95% air for up to 4-5 passages.

The YAC-1 suspension cell line was maintained in sterile 25 cm^2 culture flasks and split when confluent. The cell aggregates were dissociated to form a single cell suspension

by mechanical disaggregation using glass pipette. The cells were washed with plain RPMI medium before being used for the experiments. For maintaining the YAC-1 cell line culture, cells were seeded at the density of $0.5x10^6$ cells/ 25 cm^2 flask with 5 ml of complete RPMI medium.

The B16F10 adherent cell line was maintained in sterile 25 cm^2 culture flasks and passaged upon attaining confluence. The cells were stripped from the flask using PBS-trypsin (Sigma, USA; 0.3% trypsin in 0.01 M PBS pH 7.5, containing 0.02% EDTA, sterilized using Millipore filter). The cells were washed with plain DMEM medium to remove the traces of trypsin before use. For passaging, $0.5x10^6$ cells were seeded in a 25 cm^2 flask with 5 ml of complete DMEM medium.

For cryopreservation of the cultured cells, cells were pelleted by centrifugation at 1000 rpm for 10 minutes. The culture medium was removed, the pellet was dissociated by gentle tapping and chilled freezing mixture (10% Dimethyl Sulphoxide [DMSO] + 90% FBS) was added drop-wise with constant shaking. $2\text{-}3x10^6$ cells/ ml of freezing mixture were transferred to a sterile cryotube (Nunc, Denmark) and were frozen in liquid nitrogen.

For reviving cells, frozen vials were thawed quickly in a water bath at 37ºC and the cells were transferred to a sterile centrifuge tube. Prewarmed plain medium was added drop-wise with constant mixing to dilute the DMSO. Cells were washed thrice using plain medium and were checked for the viability using vital dye trypan blue (0.4% trypan blue [Fluke AG, Buchse SG, Switzerland] in normal saline, was sterilized by filtration and 0.01% thiomersal [BDH Laboratory Reagents, UK] added).

3. Culture Media

To prepare plain medium, RPMI 1640 (Invitrogen Life Technologies, USA) or DMEM (Invitrogen Life Technologies, USA) media powders were dissolved in deionized water and were supplemented with sodium bicarbonate (Sarabhai Chemicals, India) and HEPES buffer (Sigma, St. Louis, USA) if required as per the manufacturer's instructions. The plain medium was sterilized by membrane filtration using 0.45 µm filters (Millipore, USA), checked for sterility and stored at -20ºC until use.

To prepare the complete medium, RPMI / DMEM plain medium was supplemented with 10% Fetal Bovine Serum (Gibco, Invitrogen Life Technologies, USA), 2mM L-Glutamine (HiMedia, India) and antibiotics cocktail including Penicillin (100 IU/ml; Alembic Chemical, India), streptomycin (100 mg/ml; Alembic Chemical, India), gentamycin (40 mg/ml; Schering Corp., India), mycostatin (5 mg/ml; Sigma, USA).

4. Recombinant Proteins

Protein	**Source**
Recombinant murine Interleukin-2 (rIL-2)	PeproTech, NJ, USA
Recombinant murine Interferon-γ (rIFN-γ)	PeproTech, NJ, USA

5. Antibodies

Conjugated / Unconjugated Antibodies	**Source**
Alexa Fluor 647 rat anti-mouse CD3	BD Pharmingen, USA
PE rat anti-mouse CD3	BD Pharmingen, USA

PE rat anti-mouse CD4	BD Pharmingen, USA
PE-CF594 rat anti-mouse CD4	BD Pharmingen, USA
FITC rat anti-mouse CD8	BD Pharmingen, USA
Pacific Blue rat anti-mouse CD8	BD Pharmingen, USA
FITC rat anti-mouse CD45R/B220	BD Pharmingen, USA
PE-Cy7 rat anti-mouse CD45R/B220	BD Pharmingen, USA
PE mouse anti-mouse NK1.1	BD Pharmingen, USA
PerCP-Cy5.5 mouse anti-mouse NK1.1	BD Pharmingen, USA
FITC hamster anti-mouse γδ TCR	BD Pharmingen, USA
FITC rat anti-mouse CD209	BD Pharmingen, USA
FITC rat anti-mouse CD14	BD Pharmingen, USA
FITC rat anti-mouse CD25	BD Pharmingen, USA
Alexa Fluor 647 rat anti-mouse Foxp3	BD Pharmingen, USA
PE hamster anti-mouse CD119	eBioscience, USA
FITC Annexin V	BD Pharmingen, USA
Purified rat anti-mouse CD3 Molecular Complex	BD Pharmingen, USA
Purified hamster anti-mouse CD28	BD Pharmingen, USA
STAT1 rabbit polyclonal antibody	Cell Signaling Technology, USA
Phospho-Stat1 (Tyr701) (58D6) rabbit mAb	Cell Signaling Technology, USA
SOCS1 (A156) Rabbit Polyclonal antibody	Cell Signaling Technology, USA
SOCS3 Rabbit Polyclonal antibody	Cell Signaling Technology, USA
Anti-β-actin mouse mAb	Sigma-Aldrich, USA

Secondary Antibodies	Source
Goat anti-rabbit IgG HRPO	Sigma-Aldrich, USA
Goat anti-mouse IgG HRPO	Sigma-Aldrich, USA

6. Isolation of splenocytes and thymocytes from mice

Mice were sacrificed under deep anesthesia and spleens were collected. Spleens were gently minced using sterile piston and wire mesh. Single cell suspension of splenocytes was prepared in sterile plain RPMI 1640 medium. The cells were pelleted by centrifugation and treated with 1X RBC lysis buffer (eBioscience) to lyse erythrocytes. The lysed erythrocytes were removed by washing twice with plain RPMI 1640 at 1000 rpm for 10 minutes each. The splenocytes were suspended in sterile complete RPMI 1640 medium. Thymuses were minced gently using sterile piston and wire mesh. Single cell suspension of thymocytes was prepared in sterile normal saline. The thymocytes were washed twice using normal saline at 1000 rpm for 10 minutes each. The thymocytes were suspended in complete RPMI 1640 medium.

Splenocytes and thymocytes counts were calculated using hemocytometer by trypan blue dye exclusion method. The cells were aliquoted as per the experimental requirements and used further for all the cell based assays.

7. Preparation of Single cell suspension from mice lungs

The lungs with or without metastatic melanoma colonies were dissected from mice and minced finely. The minced pieces of lung tissue were incubated in sterile plain RPMI 1640 medium supplemented with a double strength of antibiotics (double strength

RMPI medium) and enzyme mixture (0.05% collagenase, 0.02% DNase and 5U/ml hyaluronidase along with 1 mg/ml trypsin [Sigma-Aldrich, USA]) at 37ºC for 2 hours in a shaker incubator (neoLab, Heidelberg, Germany). The lung tissue pieces were then passed through a 200-gauge wire mesh with gentle mincing using a piston. The cells were washed twice at 1000 rpm for 10 minutes each using plain RPMI medium to remove the traces of enzyme mixture. The cells were suspended in complete RPMI medium. Leukocyte count was calculated using hemocytometer using trypan blue dye exclusion method. The viability of the cells was ~95%.

8. Immunomagnetic purification of NK cells from mice splenocytes

NK cells were purified from mice splenocytes using mouse NK Cell Isolation Kit (Miltenyi Biotech, Germany).

8.1 Magnetic Labeling

Freshly isolated mice splenocytes were washed, pelleted and suspended in MACS buffer (Degassed PBS pH 7.2, 0.5% BSA, 2 mM EDTA) at the concentration of 40 µl buffer per 10 x 10^6 cells. 10 µl of NK Cell biotin-antibody cocktail was added per 10 x 10^6 total cells, mixed well and incubated for 5 minutes at 4 °C. Cells were washed by adding 2 ml of buffer per 10 x 10^6 cells and centrifuged at 1000 rpm for 10 minutes. Supernatant was removed completely. 80 µl of buffer and 20 µl of anti-biotin microbeads were added per 10 x 10^6 cells, mixed well and incubated for an additional 10 minutes at 4°C.

8.2 Magnetic Separation of negatively selected cells

MACS LS column (for up to 10^8 magnetically labeled cells) was placed in the magnetic field of MACS Separator. The column was prepared by rinsing 3 times each

with 3 ml of MACS buffer. 1 ml of cell suspension was applied onto the column. Flow-through containing unlabeled cells representing the enriched NK cells was collected. The column was washed 3 times each with 3 ml of MACS buffer. Unlabeled cells that pass through were collected, representing the enriched NK cells and were combined with the flow-through from the cell suspension. Negatively selected NK cells ($CD3^{-}NK1.1^{+}$) were checked for purity using anti-mouse CD3 Alexa Fluor 647 and anti-mouse NK1.1 PE antibodies (BD Pharmingen, USA) by flow cytometry.

9. Immunomagnetic purification of T cells from mice splenocytes

T cells were purified from mice splenocytes using mouse pan T Cell Isolation Kit (Miltenyi Biotech, Germany).

9.1 Magnetic Labelling

Freshly isolated mice splenocytes were washed, pelleted and suspended in MACS buffer (Degassed PBS pH 7.2, 0.5% BSA, 2 mM EDTA) at the concentration of 40 µl buffer per 10 x 10^6 cells. 10 µl of biotin-antibody cocktail was added per 10 x 10^6 total cells, mixed well and incubated for 5 minutes at 4 °C. 30 µl of buffer and 20 µl of anti-biotin microbeads were added per 10 x 10^6 cells, mixed well and incubated for an additional 10 minutes at 4°C.

9.2 Magnetic Separation of negatively selected cells

MACS LS column (for up to 10^8 magnetically labeled cells) was placed in the magnetic field of MACS Separator. The column was prepared by rinsing 3 times each with 3 ml of MACS buffer. 1 ml of cell suspension was applied onto the column. Flow-through containing unlabeled cells representing the enriched T cells was

collected. The column was washed 3 times each with 3 ml of MACS buffer. Unlabeled cells that pass through were collected, representing the enriched T cells and were combined with the flow-through from the cell suspension. Negatively selected T cells ($CD3^+$) were checked for purity using anti-mouse CD3 PE antibodies (BD Pharmingen, USA) by flow cytometry.

10. Flow cytometric analysis of immune cell subsets

Freshly isolated mice splenocytes and thymocytes were rinsed with 1X PBS and cold-fixed in 1% paraformaldehyde in PBS for 15 minutes at 4ºC. The fixed cells were washed with 1X PBS and suspended in cold FACS buffer (1X PBS containing 1% FBS and 0.02% sodium azide) at the concentration of 1 x 10^6 cells/ 50 µl buffer in each tube.

10.1 Surface markers analysis

For surface markers analysis of mice splenocytes by single color or multicolor immunophenotyping, the non-permeabilized splenocytes were stained with fluorochrome-conjugated anti-mouse antibodies: CD3 Alexa Fluor 647, CD4 PE-CF594, CD8 Pacific blue, B220 FITC, NK1.1 PerCP-Cy5.5, γδ TCR FITC, CD14 FITC, CD209 FITC (BD Biosciences, CA, USA) and CD119 PE (eBioscience, CA, USA) for 45 minutes at 4ºC.

For surface markers analysis of mice thymocytes by dual color immunophenotyping, the non-permeabilized thymocytes were stained with fluorochrome-conjugated anti-mouse antibodies: CD4 PE and CD8 FITC (BD Biosciences, CA, USA) for 45 minutes at 4ºC.

After the incubation period, splenocytes and thymocytes were washed by centrifugation using FACS buffer, resuspended in 300 µl FACS buffer and were acquired on FACSAria flow cytometer (BD Biosciences, CA, USA). Cells were selectively gated for lymphocytes or macrophages populations based on their forward scatter (FSC) and side scatter (SSC) characteristics during acquisition and analysis. Results were analyzed by FlowJo software (Tree Star, OR, USA).

10.2 Intracellular markers analysis

For intracellular staining, paraformaldehyde fixed splenocytes were washed with PBS and permeabilized for 15 minutes at room temperature in saponin buffer (FACS buffer with 0.1% saponin). Permeabilized cells were washed with saponin buffer and suspended in FACS buffer at the concentration of 1 x 10^6 cells/ 50 µl buffer in each tube. These cells were stained with fluorochrome-conjugated anti-mouse antibodies: CD4 PE, CD25 FITC and Foxp3 Alexa Fluor 647 for 30 minutes at room temperature. Appropriate isotype controls were used in all experiments. After the incubation period, the cells were washed by centrifugation using FACS buffer, cell pellet was suspended in 300 µl FACS buffer and cells were acquired on FACSAria flow cytometer (BD Biosciences, CA, USA). Cells were selectively gated for lymphocyte population based on their forward scatter (FSC) and side scatter (SSC) characteristics during flow cytometric acquisition and analysis. Results were analyzed by FlowJo software (Tree Star, OR, USA).

11. Annexin V PI staining

Freshly isolated splenocytes were washed in 1X PBS and surface stained using anti-mouse CD3 AF647, CD4 PE-CF594, CD8 Pacific blue and B220 PE-Cy7 antibodies.

After surface staining, the splenocytes were suspended in 100 µl annexin binding buffer (10 mM HEPES pH 7.4, 150 mM NaCl, 0.25 mM $CaCl_2$). Cells were incubated with PI and FITC-conjugated Annexin V Ab (BD Biosciences) in dark for 15 min at room temperature. After incubation, 400 µl binding buffer was added and cells were acquired immediately on FACSAria flow cytometer (BD Biosciences, CA, USA). Acquired data were analyzed using FlowJo software (Tree Star, OR, USA).

12. Splenocytes proliferation by [^{3}H] thymidine incorporation assay

Proliferation of splenocytes was determined by the [^{3}H] thymidine incorporation assay. Freshly isolated splenocytes were cultured at a density of 1.5 x 10^5 cells/100 µl complete RPMI medium/ well in 96 well microtiter plates. The cells were stimulated with either PMA (50 ng, Sigma-Aldrich, MO, USA) + ionomycin (50 ng, Sigma-Aldrich, MO, USA) or plate bound anti-CD3 mAb (0.25 µg; BD Biosciences, USA) + soluble anti-CD28 mAb (0.25 µg; BD Biosciences, USA) for 72 hours. Unstimulated splenocytes in complete medium were used as controls. Cells were incubated at 37 °C in humidified CO_2 incubator containing 5% CO_2 and 95% air. [^{3}H] thymidine (0.5 µCi/ 10 µl/ well; Board of Radiation and Isotope Technology, Mumbai, India) was added during the last 18 hours of the assay. After the incubation period, the cells were harvested onto glass-fiber filter paper (Titertek, Norway) using a cell harvester (Titertek, Norway). The filter paper was dried at 50ºC in a dry heat oven and each disc corresponding to a single well was placed in 3 ml of scintillation fluid (0.5 g PPO, 7 g POPOP in 1 liter Toluene) in a glass scintillation vial. The radioactivity incorporated into DNA was measured as β emission using a liquid scintillation counter (Packard TRI-CARB 2100 TR counters, IL, USA). Data were expressed as counts per minute (CPM).

13. CFSE Proliferation assay

To study the proliferation of total splenocytes and purified splenic T cell population 0from mice, CFSE proliferation assay was performed. T cells were immunomagnetically purified from freshly isolated mice splenocyte suspension by negative selection using Mouse Pan T cell isolation kit (Miltenyi Biotec, Bergisch Gladbach, Germany) as per the manufacturer's instructions. Splenocytes as well as purified splenic T cells were separately labeled with 5 μM CFSE (Invitrogen, Life Technologies, USA) dye as described earlier [300]. Briefly, 15 x 10^6 T cells were thoroughly suspended in 1 ml of 1X PBS containing 5% (v/v) FBS in a fresh tube and were incubated with 5 μM CFSE for 5 min at room temperature in dark. Cells were washed thrice with PBS containing 5% (v/v) FCS by centrifugation at 1000 rpm for 5 min each to remove excess dye. CFSE labeled mice splenocytes or purified splenic T cells (1.5 x 10^5 cells/ 100 μl complete RPMI/ well) were stimulated with either PMA (50 ng) + Ionomycin (50 ng) or plate bound anti-CD3 mAb (0.25 μg) + soluble anti-CD28 mAb (0.25 μg) in 96-well microtiter plates for 3 days or 6 days. A fraction of CFSE labeled splenocytes or purified T cells were treated with mitomycin C (50 μg/ml) for 30 minutes at 37ºC in 5% CO_2 incubator to serve as non-proliferating control for each group. On day 3 and day 6, cells were harvested and CFSE fluorescence intensities of $CD3^+$ splenocytes as well as of purified splenic T cells were measured by flow cytometer (FACSAria, BD Biosciences, CA, USA). Results were analyzed using FlowJo software (Tree Star, OR, USA).

14. Intracellular calcium flux measurement

Splenocytes as well as immunomagnetically purified splenic T cells (1 x 10^6 cells/ ml PBS) were separately loaded with 5 μM Fluo-3-AM (Sigma-Aldrich, MO, USA) for 30 minutes

at 37ºC in CO_2 incubator. Cells were washed with 1X PBS to remove excess dye, suspended in 1 ml calcium estimation buffer (137 mM NaCl, 5 mM KCl, 1 mM Na_2HPO_4, 5 mM Glucose, 0.5 mM $MgCl_2$, 10 mM HEPES, 1 mM $CaCl_2$, 1g/L BSA) and acquired on FACSAria flow cytometer (BD Biosciences, CA, USA) for 30 seconds to determine the baseline Fluo-3 fluorescence intensity in unstimulated cells. PMA (100 ng) + Ionomycin (500 ng) or soluble anti-CD3 (1 μg) were added as stimulants in mice splenocytes, whereas PMA (100 ng) + Ionomycin (500 ng) or soluble anti-CD3 (10 μg) + anti-CD28 mAbs (10 μg) were added as stimulants in purified splenic T cells *in vitro*. Immediately after the addition of the stimulants *in vitro*, changes in the Fluo-3 fluorescence intensities of splenocytes as well as that of purified T cells were measured for up to 10 minutes in a continuous manner. Data were analyzed by FlowJo software (Tree Star, OR, USA).

15. Intracellular ROS Generation Assay

Reactive oxygen species (ROS) generation in stimulated murine splenocytes was measured using oxidation sensitive dye 2, 7 dichloro-fluorescein diacetate (DCFH-DA) (Sigma-Aldrich, USA). Splenocytes (1 x 10^6 cells/250 μl PBS) were stained with 4 μM DCFH-DA dye and incubated for 30 minutes at 37ºC. Cells were washed and resuspended in 1 ml PBS. Cells were acquired on the FACSAria flow cytometer (BD Biosciences, CA, USA) to determination baseline DCF fluorescence. PMA (100 ng) + Ionomycin (500 ng) or soluble anti-CD3 mAb (1 μg) were added as stimulants and increase in DCF fluorescence intensity was measured from 0 to 90 minutes at regular time intervals i.e. at 0, 3, 5, 10, 15, 20, 25, 30, 45 and 90 minutes on FACSAria flow cytometer (BD Biosciences, CA, USA). Analysis was done using FlowJo software (Tree Star, OR, USA).

16. ^{51}Chromium Release Cytotoxicity Assay

[^{51}Cr] release assay was used to measure the cytotoxicity of splenic NK cells (effectors) against murine T lymphoma cell line (YAC-1) and murine melanoma cell line (B16F10) used as target cells. YAC-1 or B16F10 cells were labeled with 50 μCi [^{51}Cr] for 90 minutes at 37°C in CO_2 incubator. Labeled YAC-1 and B16F10 target cells were washed using plain RPMI 1640 or plain DMEM medium, respectively. Freshly isolated unstimulated NK cells were incubated with [^{51}Cr] labeled YAC-1 (3000 cells/well) at different Effector to Target (E:T) ratios including 80:1, 40:1, 20:1 and 10:1 at 37°C in 5% CO_2 for 4 hours. On the other hand, purified NK cells were stimulated using recombinant murine IL-2 for 3 days (Day 1: 100 U/ 10 μl, Day 2: 50 U/ 10 μl, Day 3: 50 U/ 10 μl). IL-2 stimulated NK cells (effectors) were incubated with [^{51}Cr] labeled B16F10 targets (3000 cells/well) at the Effector to Target (E:T) ratios of 100:1, 50:1, 25:1 and 12.5:1 at 37°C in 5% CO_2 for 4 hours. After incubation, the plates were centrifuged, 100 μl supernatants were collected from each well and radioactive chromium release was measured as counts per minute (CPM) using 1470 Wallac automated gamma counter (Perkin-Elmer, IL, USA). Spontaneous release was determined by incubating the target cells with complete RPMI 1640 medium alone, and maximum release was determined by incubating target cells with 10% Triton X-100. The percent specific lysis (% cytotoxicity) was calculated as: [(experimental release - spontaneous release) / (maximum release - spontaneous release)] x 100.

17. Cytometric Bead Array

Blood was collected from mice before sacrifice by retro-orbital puncture and serum was separated by centrifugation. Sera samples were stored at -80ºC until used.

Also, cell free supernatants were collected from splenocytes cultured in the presence of PMA (50 ng/ well) + Ionomycin (50 ng/ well) or plate-bound anti-CD3 mAb (0.25 μg/well) + soluble anti-CD28 (0.25 μg/well) in 96-well microtiter plates for 24 hours in 5% CO_2 incubator at 37ºC. Concentrations (pg/ml) of different Th1 (IL-2, IFN-γ, TNF), Th2 (IL-4, IL-6, IL-10) and Th17 (IL-17A) cytokines in mice sera and supernatants were quantitated by Th1/Th2/Th17 Cytometric Bead Array kit (BD Biosciences, USA) as per manufacturer's instructions. Briefly, test samples (50 μl) and PE detection antibody (50 μl) were incubated along with mixed capture bead reagent (50 μl) for 2 hours in dark at room temperature. Excess unbound antibodies were washed with 1 ml wash buffer, supernatant was carefully removed and samples were resuspended in 300 μl wash buffer. Samples were acquired on FACSAria flow cytometer (BD Biosciences, CA, USA) and data were analyzed using FCAP Array software (BD Biosciences, CA, USA). Arbitrary ranges (High, medium, low) were assigned for the mean values of serum concentrations (pg/ml) for all the cytokines in each mice group and Heat maps were generated using Plotly software.

18. Western Blotting

STAT1 mediated IFN-γ signaling pathway intermediates in stimulated mice splenocytes were studied by western blotting. Freshly isolated splenocytes of mice (2.5 x 10^6 cells/ml complete RPMI 1640/ well) were stimulated *in vitro* using recombinant murine IFN-γ (PeproTech, NJ, USA) at two different concentrations (1 and 10 ng/ well) in 24-well microtiter plates for 30 minutes or 12 hours. Unstimulated cells cultured in medium alone were used as controls.

18.1 Cell lysate preparation

The cells were harvested at the desired time points, washed with 1X PBS and whole-cell lysates (10 x 10^6 cells/ group) were prepared in 150 µl SDS sample buffer (62.5 mM Tris-HCl, 2% w/v SDS, 10% glycerol, 50 mM DTT, and 0.01% bromophenol blue, pH 6.8). Lysates were sonicated to reduce sample viscosity, denatured by boiling and then cooled on ice.

18.2 Sodium Dodecyl Sulphate Polyacrylamide Gel Electrophoresis (SDS-PAGE)

Samples were loaded and resolved on 10% SDS-PAGE gels at 120 V in the presence of the electrophoresis running buffer (3.0275 g Tris, 14.413 g Glycine and 1 g SDS in 1 liter final volume of Milli-Q water).

The following solutions were mixed to cast 10% resolving polyacrylamide gel and 5% stacking gel:

Components	**10% Resolving gel**	**5% Stacking gel**
30% Acrylamide	5 ml	1 ml
1% Bisacrylamide	1.95 ml	1 ml
1.5 M Tris (pH 8.8)	3.75 ml	-
1 M Tris (pH 6.8)	-	2.5 ml
10% SDS	150 µl	100 µl
10% Ammonium persulphate (Freshly prepared)	50 µl	100 µl
TEMED	40 µl	10 µl
Milli-Q water	4.1 ml	5.35 ml

18.3 Immunoblotting

After electrophoresis under reducing conditions, the proteins separated on the gel were electrophoretically transferred onto Hybond-ECL nitrocellulose membrane (Amersham Pharmacia Biotech, NJ, USA) in the presence of electrophoresis transfer buffer (3.0275 g Tris, 14.413 g Glycine, 200 ml methanol and Milli-Q water to final volume of 1 liter) at 80 V for 2 hours under cooling conditions using the vertical electrophoresis transfer apparatus (Bio-Rad, USA). Post transfer, the membranes containing the standard molecular weight marker along with the protein lysates were stained with Ponceau S stain (10 ml Milli-Q Water, 0.3 ml glacial acetic acid, 0.033 g Ponceau S, final volume adjusted to 30 ml with Milli-Q water) to visualize the transferred protein bands. The membranes containing the lysate were completely destained in 1X TBS-T wash buffer (1X TBS [20 mM Tris, 137 mM NaCl, pH7.6] + 0.1% Tween) and were blocked with blocking buffer (5% skimmed milk in 1X TBS-T) for 1 hour at room temperature. The membranes were then blotted with the appropriate concentrations (1:1000 dilution) of primary Abs to total STAT1, phospho-STAT1(Tyr701), SOCS1, SOCS3 (Cell Signaling Technology, USA) using dilution buffer (5% BSA in 1X TBS-T buffer) followed by overnight incubation at 4ºC with gentle shaking. β-actin antibody (Sigma-Aldrich) was used as loading control at the appropriate concentration (1:1000 dilution) using dilution buffer (3% skimmed milk in 1X TBS-T) with overnight incubation at 4ºC with gentle shaking. After washing, the membranes were incubated with appropriate secondary antibodies conjugated to horseradish peroxidase (HRPO) including GAR-HRPO (Sigma-Aldrich, USA) for total STAT1, phospho-STAT1(Tyr701), SOCS1, SOCS3 and GAM-HRPO (Sigma-Aldrich, USA) for β-actin at a dilution of 1:1000 using dilution buffer (3% skimmed milk in 1X TBS-T) at room temperature for 2 hours. The blots were washed with 1X TBS-T

buffer to remove excess of the secondary antibodies and protein bands were detected by enhanced chemiluminescence using ECL plus Western blot detection system (GE Healthcare, UK). Densitometric analysis of western blots was done using ImageJ software (NIH, USA).

19. Experimental Metastasis Assay

To establish experimental metastasis, B16F10 murine melanoma cells were intravenously injected at the concentration of 1 x 10^5 cells/ 100 µl plain DMEM/ mouse in the lateral tail vein of mice. On day 7, day 14 and day 21 post intravenous B16F10 injection, mice were sacrificed and lungs were collected by dissection. The melanoma colonies on each mouse lung were counted using a dissecting microscope. The lungs were fixed using 10% neutral buffered formalin (10 ml 37% formaldehyde, 0.4 g NaH_2PO_4, 0.65 g Na_2HPO_4, adjusted to a final volume of 100 ml with milli-Q water, pH 6.8). Paraffin embedded 5 µm thin sections of formalin fixed lungs were stained by hematoxylin and eosin (H&E) for histopathological analysis of melanoma colonies in the mice lungs. The H&E stained lung sections were observed under upright microscope and images were captured at 5X magnification.

20. Survival Study

Gal-$3^{+/+}$, Gal-$3^{+/-}$ and Gal-$3^{-/-}$ mice (10 mice per group) were monitored in Laboratory Animal Facility, ACTREC to study their overall survival under normal physiological conditions (control mice) as well as under experimental metastasis assay conditions. Survival rates were determined by standard Kaplan-Meier survival curves. Log-rank test was employed to determine whether the differences between the survival curves of Gal-$3^{+/+}$, Gal-$3^{+/-}$ and Gal-$3^{-/-}$ mice groups are statistical significant.

21. Statistical Analysis

Statistical analyses were performed using GraphPad Prism Software version 5.0 (La Jolla, USA). Student's *t* test was used to determine the statistical significance. Results were represented as Mean±SE. A value of $P<0.05$ was considered statistically significant.

CHAPTER 4

Immune scenario in Gal-3 wild type (Gal-$3^{+/+}$), Gal-3 hemizygous (Gal-$3^{+/-}$) and Gal-3 null (Gal-$3^{-/-}$) mice

Galectin-3 is a unique chimera-type member of the β-galactoside-binding mammalian galectin family. It is a ubiquitously expressed molecule with diverse physiological functions based on its subcellular and extracellular localization. Galectin-3 is involved in various biological processes such as maintenance of cellular homeostasis, organogenesis, immune responses, angiogenesis, tumor invasion and metastasis [6-13]. Involvement of galectin-3 in various steps of cancer progression and metastasis has been extensively documented [14-18]. However, how the levels of expression of endogenous galectin-3 in the host influence tumor growth and metastasis remains poorly understood till date.

Role of immune system in the modulation of tumor progression and metastasis has been widely reported [37,38]. According to the cancer immunoediting theory, an optimally functioning immune system plays a pivotal role in either elimination or maintenance of metastatic tumor cells in dormancy over a prolonged time period [38]. Galectin-3 is expressed in many cells subsets of immune system, including monocytes/macrophages, dendritic cells, eosinophils, neutrophils, mast cells, uterine NK cells, activated T and B cells. Accumulating evidence suggests the importance of galectin-3 in functionally regulating the host immune responses [10,39-43]. However, the role of endogenous galectin-3 in the modulation of host immunity and the mechanisms involved therein remain poorly understood till date and need to be further investigated. Experiments carried out in this chapter are aimed at thoroughly investigating the immune scenario in the three genotypic groups of *LGALS3* transgenic mice with different endogenous galectin-3 expression levels viz. Gal-$3^{+/+}$ (wild-type), Gal-$3^{+/-}$ (hemizygous) and Gal-$3^{-/-}$ (null) mice under normal physiological conditions.

Immune cell subsets in Gal-$3^{+/+}$, Gal-$3^{+/-}$ and Gal-$3^{-/-}$ mice splenocytes

To assess whether reduction or total absence of galectin-3 levels in host affects the frequency of major immune cell subtypes, immunophenotyping of splenocytes isolated from Gal-$3^{+/+}$, Gal-$3^{+/-}$ and Gal-$3^{-/-}$ mice was performed. Freshly isolated mice splenocytes were stained with fluorochrome labeled antibodies specific to immune cell surface markers including NK1.1, γδ TCR, CD209, CD14, CD3, CD4, CD8 and B220. Lymphocytes or macrophages populations in the splenocytes were gated based on their forward scatter (FSC) and side scatter (SSC) characteristics during flow cytometric analysis, followed by subsequent analysis based on the expression of particular cell surface markers characteristic for different immune cell subsets studied as mentioned below.

Innate immune cell subsets in mice splenocytes

It was observed that, in the innate immune compartment, percentages of splenic NK ($CD3^{-}NK1.1^{+}$) cells were found to be significantly lower in Gal-$3^{-/-}$ mice compared to Gal-$3^{+/+}$ mice. The percentages of splenic NK cells correlated with the *LGALS3* gene dosage in Gal-$3^{+/+}$, Gal-$3^{+/-}$ and Gal-$3^{-/-}$ mice (Figure 8A). No significant differences were observed in the percentages of NKT cells ($CD3^{+}NK1.1^{+}$), γδ T cells ($CD3^{+}\gamma\delta^{+}$), dendritic cells ($CD209^{+}$) and macrophages ($CD14^{+}$) in the splenocytes of Gal-$3^{+/+}$, Gal-$3^{+/-}$ and Gal-$3^{-/-}$ mice (Figure 8B-E).

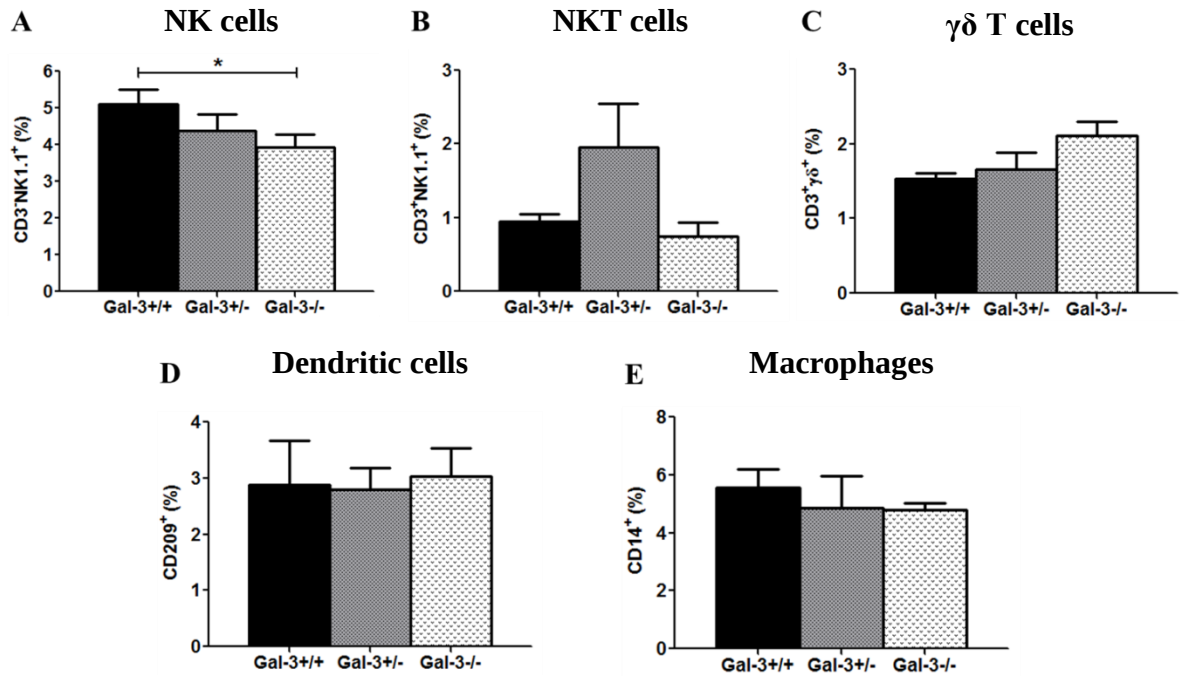

Figure 8: Innate immune cell subsets in the splenocytes of Gal-3$^{+/+}$, Gal-3$^{+/-}$ and Gal-3$^{-/-}$ mice. Single cell suspensions of splenocytes were prepared from Gal-3$^{+/+}$, Gal-3$^{+/-}$ and Gal-3$^{-/-}$ mice. The cells were fixed, subjected to surface antibody staining and analyzed by multicolor flow cytometry. The graphs indicate frequencies of **(A)** NK cells ($CD3^-NK1.1^+$) **(B)** NKT cells ($CD3^+NK1.1^+$) **(C)** γδ T cells ($CD3^+\gamma\delta^+$) **(D)** Dendritic cells ($CD209^+$) and **(E)** macrophages ($CD14^+$) in Gal-3$^{+/+}$, Gal-3$^{+/-}$ and Gal-3$^{-/-}$ mice splenocytes. The graphs represent consolidated data of 5 independent experiments. **P* <0.05.

Adaptive immune cell subsets in mice splenocytes

To study the key players of adaptive immune responses, the percentages of total T cells ($CD3^+$), helper T cells (T_H, $CD3^+CD4^+$), cytotoxic T cells (T_C, $CD3^+CD8^+$) and B cells ($B220^+$) were analyzed in the splenocytes of Gal-3$^{+/+}$, Gal-3$^{+/-}$ and Gal-3$^{-/-}$ mice. No significant differences were observed in the percentages of total $CD3^+$ T cells, helper T cells (T_H, $CD3^+CD4^+$) and cytotoxic T cells (T_C, $CD3^+CD8^+$) in the three groups of mice (Figure 9A-B). Higher levels of splenic B cells ($B220^+$) were found in Gal-3$^{+/-}$ mice than in Gal-3$^{-/-}$ mice (Figure 9C).

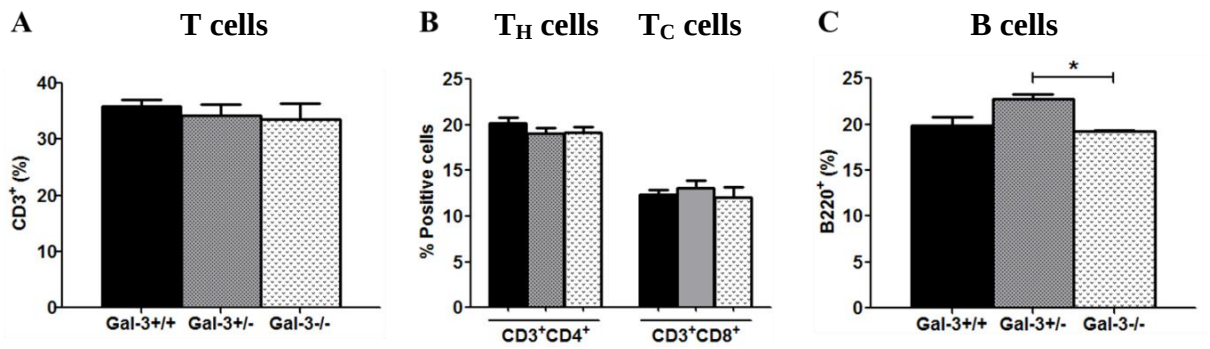

Figure 9: Adaptive immune cell subsets in splenocytes of Gal-3$^{+/+}$, Gal-3$^{+/-}$ and Gal-3$^{-/-}$ mice. Single cell suspensions of spleen cells were prepared from Gal-3$^{+/+}$, Gal-3$^{+/-}$ and Gal-3$^{-/-}$ mice. The cells were fixed, subjected to surface antibody staining and analyzed by multicolor flow cytometry. The graphs indicate frequencies of **(A)** T cells (CD3^{+}), **(B)** helper T cells (T_H, CD3^{+}CD4^{+}) and cytotoxic T cells (T_C, CD3^{+}CD8^{+}) and **(C)** B cells (B220^{+}) in Gal-3$^{+/+}$, Gal-3$^{+/-}$ and Gal-3$^{-/-}$ mice splenocytes. The graphs represent consolidated data of 5 independent experiments. *P <0.05.

Regulatory T cells in mice splenocytes

Regulatory T cells (Treg) play an indispensable role in immune homeostasis, by maintaining immunological unresponsiveness to self-antigens and in suppressing excessive immune responses deleterious to the host [301,302]. In the present investigation, multicolor immunophenotyping was done to compare the splenic CD4^{+}CD25^{+}Foxp3^{+} regulatory T cell (T_{reg}) populations in Gal-3$^{+/+}$, Gal-3$^{+/-}$ and Gal-3$^{-/-}$ mice. Lymphocytes were gated based on their forward scatter (FSC) and side scatter (SSC) characteristics followed by subsequent gating for T_{reg} as represented (Figure 10, upper panel). No significant differences were observed in the percentages of CD4^{+}CD25^{+}Foxp3^{+} T_{reg} in the splenocytes of Gal-3$^{+/+}$, Gal-3$^{+/-}$ and Gal-3$^{-/-}$ mice (Figure 10, lower panel).

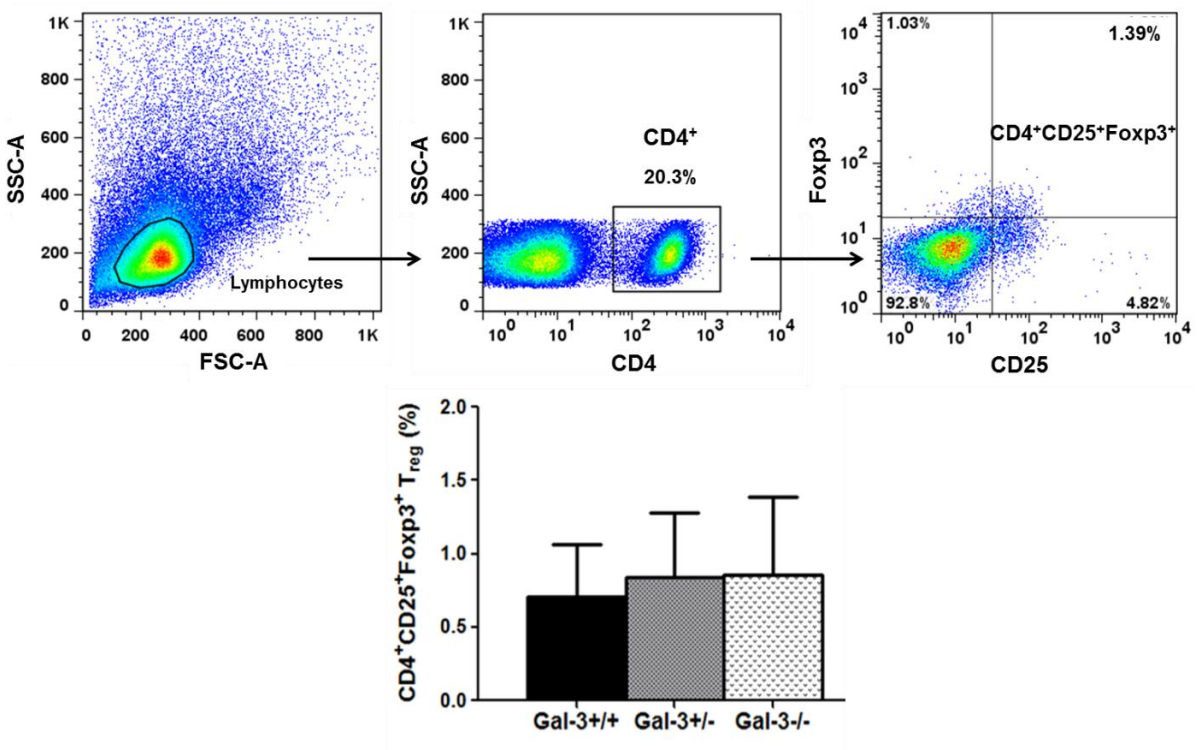

Figure 10: Regulatory T cells in Gal-3$^{+/+}$, Gal-3$^{+/-}$ and Gal-3$^{-/-}$ mice splenocytes. Gating strategy (upper panel) and percentages (lower panel) of $CD4^+CD25^+Foxp3^+$ regulatory T cells in Gal-3$^{+/+}$, Gal-3$^{+/-}$ and Gal-3$^{-/-}$ mice splenocytes. The graph represents consolidated data of 5 independent experiments. *$P < 0.05$.

T cell subsets in Gal-3$^{+/+}$, Gal-3$^{+/-}$ and Gal-3$^{-/-}$ mice thymocytes

The thymus is a primary lymphoid organ in which bone marrow-derived T cell precursors undergo differentiation, ultimately leading to migration of positively selected thymocytes to the T cell-dependent areas of peripheral lymphoid organs. This process involves sequential expression of various proteins and rearrangements of T cell receptor (TCR) genes [303].

Intrathymic T cell differentiation

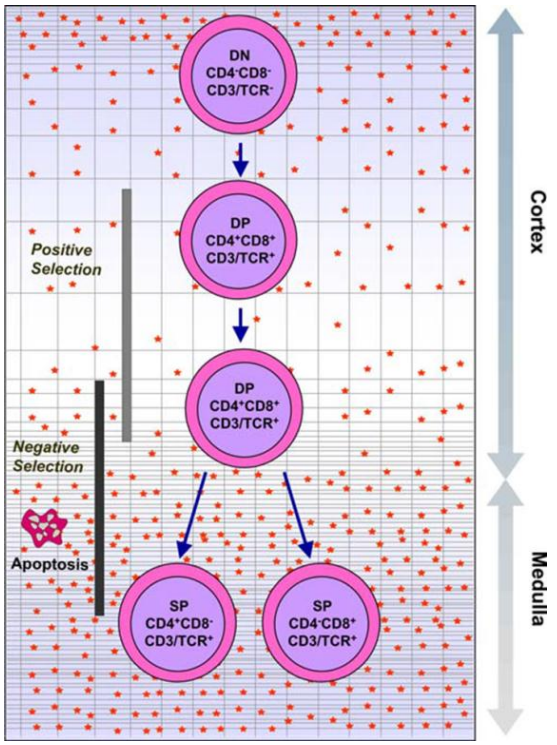

[Savino W., PLoS Pathogen, 2006; 2(6):e62]

Figure 11: Intrathymic T cell differentiation. Thymocytes are classified into a number of distinct maturational stages based on the expression of cell surface markers. The earliest thymocyte stage is the double negative stage (DN, negative for both CD4 and CD8). The next major stage is the double positive stage (DP, positive for both CD4 and CD8). The final stage in maturation is the single positive stage (SP, positive for either CD4 or CD8).

It was further assessed whether differences in endogenous galectin-3 levels affect intrathymic T cell differentiation and maturation in Gal-$3^{+/+}$, Gal-$3^{+/-}$ and Gal-$3^{-/-}$ mice. Based on T cell lineage markers, the percentages of thymocytes at different stages of maturation viz. $CD4^{+}CD8^{-}$ (CD4 Single positive), $CD4^{-}CD8^{+}$ (CD8 Single positive), $CD4^{+}CD8^{+}$ (Double positive) and $CD4^{-}CD8^{-}$ (Double negative) were analyzed by dual color immunophenotyping using flow cytometry.

It was observed that, there were no significant differences in the percentages of $CD4^{+}CD8^{-}$ (CD4 Single positive), $CD4^{-}CD8^{+}$ (CD8 Single positive), $CD4^{+}CD8^{+}$ (Double positive) and $CD4^{-}CD8^{-}$ (Double negative) cell subsets in the thymocytes of Gal-$3^{+/+}$, Gal-$3^{+/-}$ and Gal-$3^{-/-}$ mice (Figure 12). The results indicated that changes in the expression levels of endogenous galectin-3 do not influence the intrathymic T cell differentiation in Gal-$3^{+/+}$, Gal-$3^{+/-}$ and Gal-$3^{-/-}$ mice.

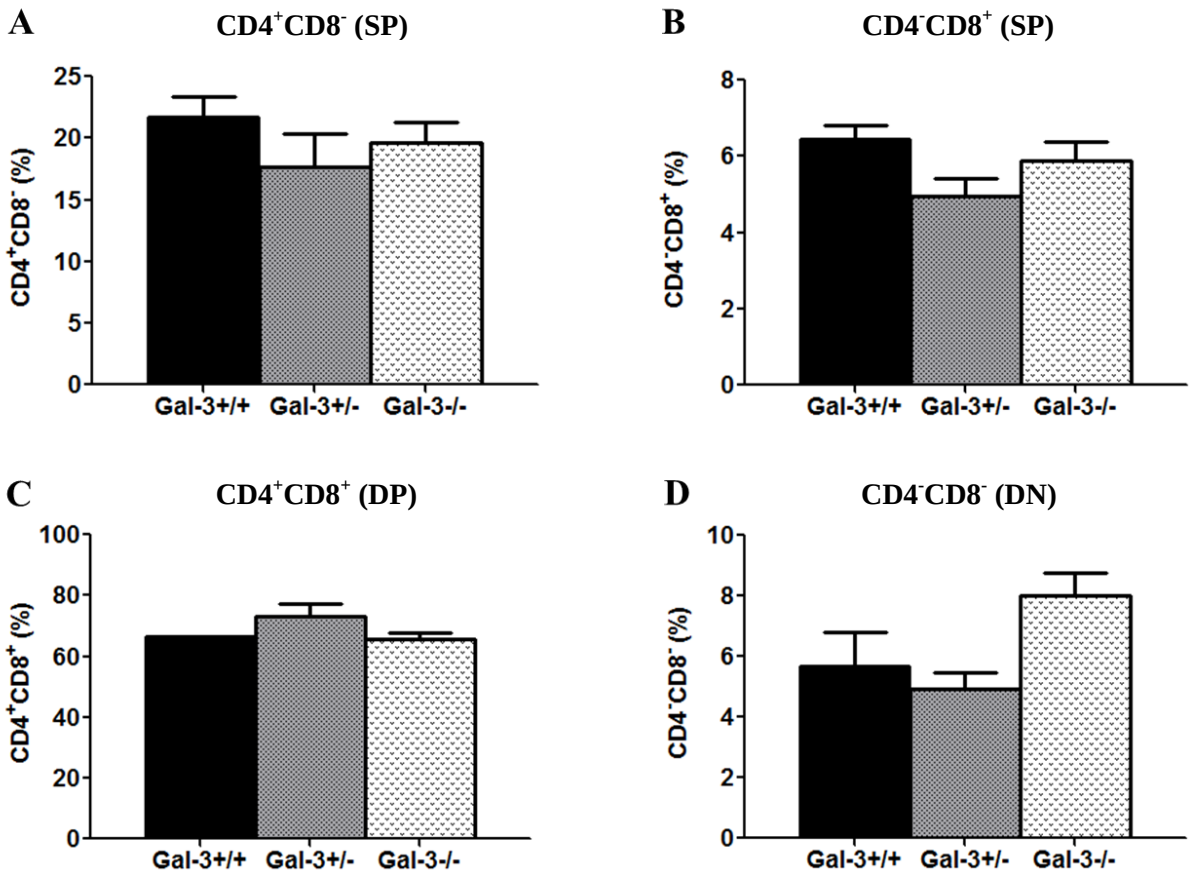

Figure 12: Thymic T cell subsets in Gal-3$^{+/+}$, Gal-3$^{+/-}$ and Gal-3$^{-/-}$ mice. Single cell suspensions of thymocytes were prepared from Gal-3$^{+/+}$, Gal-3$^{+/-}$ and Gal-3$^{-/-}$ mice. The cells were fixed, subjected to surface antibody staining and analyzed by dual color immunophenotyping using flow cytometry. The graphs indicate frequencies of **(A)** CD4^{+}CD8^{-} (CD4 Single positive, SP), **(B)** CD4^{-}CD8^{+} (CD8 Single positive, SP), **(C)** CD4^{+}CD8^{+} (Double positive, DP) and **(D)** CD4^{-}CD8^{-} (Double negative, DN) thymocytes in Gal-3$^{+/+}$, Gal-3$^{+/-}$ and Gal-3$^{-/-}$ mice. The graphs represent consolidated data of 5 independent experiments.

Proliferative responses in splenocytes from Gal-3$^{+/+}$, Gal-3$^{+/-}$ and Gal-3$^{-/-}$ mice upon *in vitro* stimulation

In order to study whether functional immune responses differ with galectin-3 expression levels in the host, the ability of splenocytes isolated from Gal-3$^{+/+}$, Gal-3$^{+/-}$ and Gal-3$^{-/-}$ mice to respond to stimulants *in vitro* was studied.

Splenocytes proliferation by [^{3}H] thymidine incorporation assay

The proliferative responses of splenocytes upon *in vitro* stimulation were compared between Gal-3$^{+/+}$, Gal-3$^{+/-}$ and Gal-3$^{-/-}$ mice groups using [^{3}H] thymidine incorporation assay. It was observed that, on stimulation with PMA (50 ng/ well) + Ionomycin (50 ng/ well), Gal-3$^{-/-}$ mice splenocytes showed remarkably higher proliferation as compared to that of Gal-3$^{+/+}$ and Gal-3$^{+/-}$ mice. On stimulation using plate-bound anti-CD3 mAb (0.25 µg/ well) + soluble anti-CD28 mAb (0.25 µg/ well), proliferation of Gal-3$^{+/-}$ and Gal-3$^{-/-}$ splenocytes was found to be significantly increased than that of Gal-3$^{+/+}$ splenocytes. Upon TCR-mediated stimulation using anti-CD3/CD28 mAbs, proliferative responses in Gal-3$^{+/+}$, Gal-3$^{+/-}$ and Gal-3$^{-/-}$ mice splenocytes exhibited negative correlation with endogenous galectin-3 expression levels in these mice groups (Figure 13).

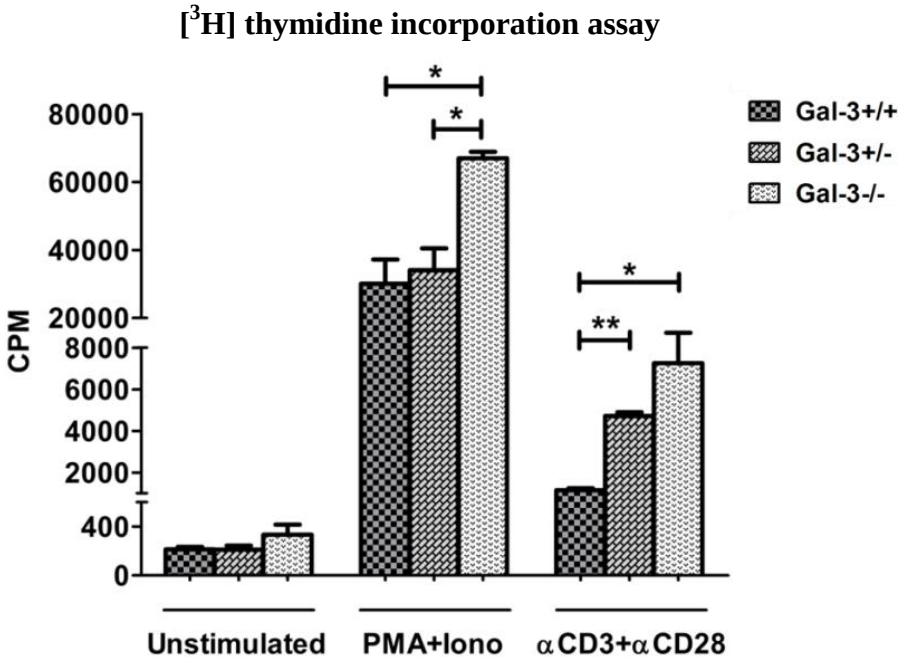

Figure 13: Proliferative responses in splenocytes of Gal-3$^{+/+}$, Gal-3$^{+/-}$ and Gal-3$^{-/-}$ mice as measured by [^{3}H] thymidine incorporation assay. Freshly isolated splenocytes (1.5 x 10^5 cells/ 100 µl medium/ well) of Gal-3$^{+/+}$, Gal-3$^{+/-}$ and Gal-3$^{-/-}$ mice were stimulated *in vitro* with either PMA (50 ng/ 10µl/ well) + Ionomycin (50 ng/ 10µl/ well) or plate bound anti-CD3 mAb (0.25 µg/ 30µl/ well) + soluble anti-CD28

mAb (0.25 µg/ 10µl/ well) in 96-well microtiter plate for 72 hours. Unstimulated splenocytes were used as control. The graph represents consolidated data of 5 independent assays as radioactive counts per minute (CPM). Each set in the assay was performed in triplicate wells. *P<0.05, **P<0.01.

Splenocytes proliferation by CFSE assay

Simultaneously, splenocytes freshly isolated from Gal-$3^{+/+}$, Gal-$3^{+/-}$ and Gal-$3^{-/-}$ mice were labeled with CFSE. Proliferative responses in CFSE labeled splenocytes upon *in vitro* stimulation using PMA (50 ng/ well) + Ionomycin (50 ng/ well) or plate-bound anti-CD3 mAb (0.25 µg/ well) + soluble anti-CD28 mAb (0.25 µg/ well) were monitored using CFSE assay *in vitro* at two different time points i.e. Day 3 and Day 6 post stimulation. At the desired time points, the cells were harvested, washed, stained with anti-mouse CD3 PE antibody and analyzed by flow cytometry to quantitate the percentages of divided $CD3^+$ T cells in the total splenocytes population in Gal-$3^{+/+}$, Gal-$3^{+/-}$ and Gal-$3^{-/-}$ mice groups.

On day 3 and day 6 post stimulation, splenic $CD3^+$ T cells of Gal-$3^{+/-}$ and Gal-$3^{-/-}$ mice exhibited higher proliferative responses to stimulants than that observed in splenic $CD3^+$ T cells of Gal-$3^{+/+}$ mice (Figure 14A and 14B). On day 3, distinct peaks representing different generations of dividing splenic T cells were observed (Figure 14A). This distinction was less evident on Day 6 (Figure 14B).

CFSE Proliferation assay: Splenocytes

A

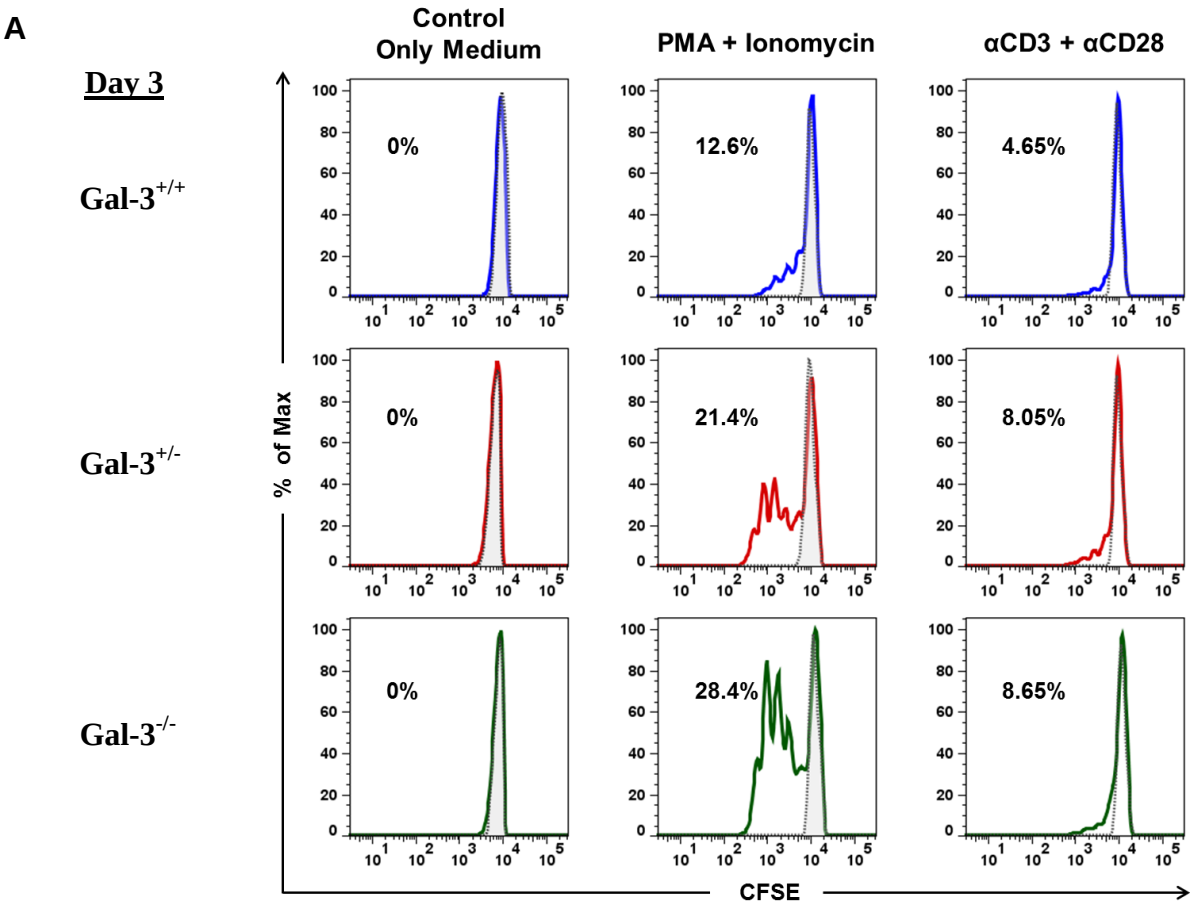

B

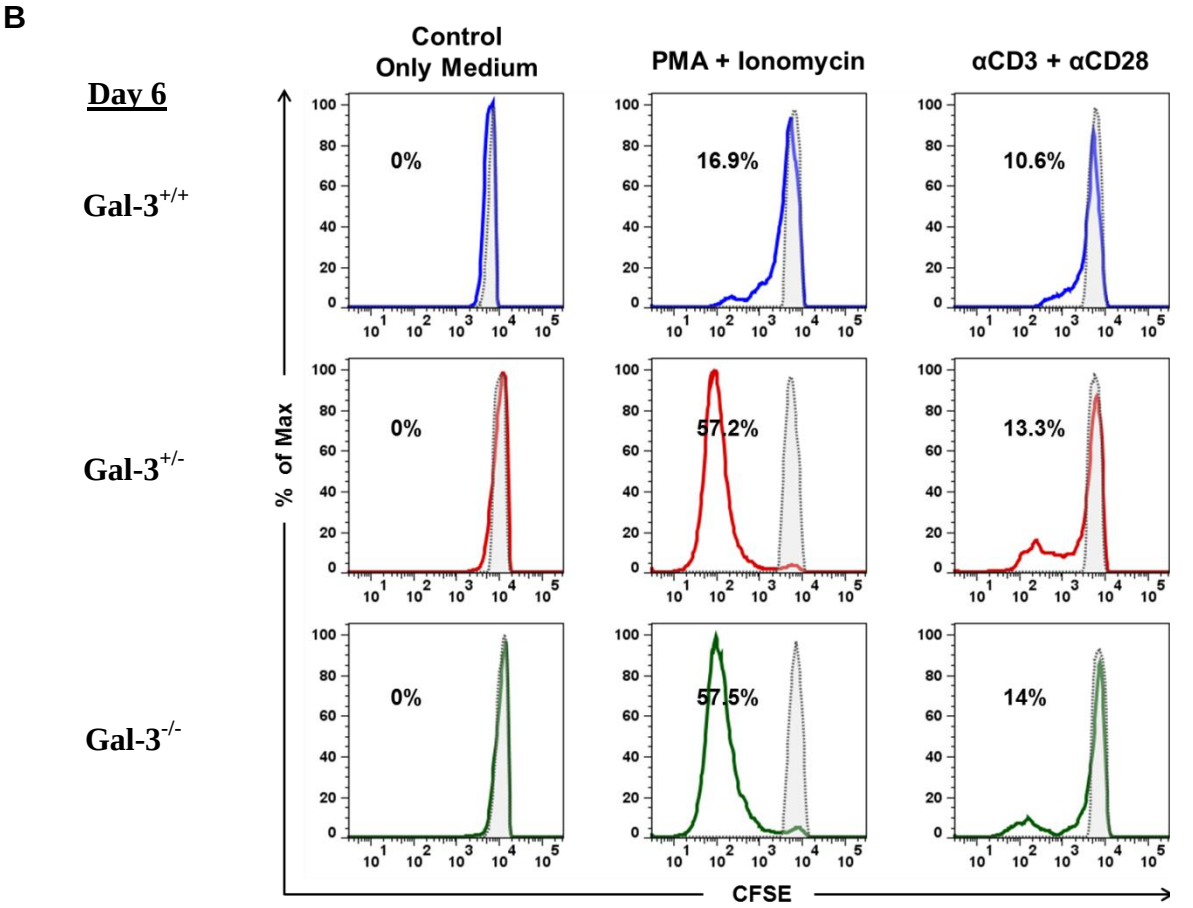

Figure 14: Proliferative responses of Gal-$3^{+/+}$, Gal-$3^{+/-}$ and Gal-$3^{-/-}$ mice splenocytes as assessed by CFSE staining assay. Freshly isolated splenocytes of Gal-$3^{+/+}$, Gal-$3^{+/-}$ and Gal-$3^{-/-}$ mice were subjected to CFSE staining. CFSE labeled splenocytes (1.5 x 10^5 cells/ 100 µl medium/ well) were stimulated *in vitro* with either PMA (50 ng/ 10µl/ well) + Ionomycin (50 ng/ 10µl/ well) or plate bound anti-CD3 mAb (0.25 µg/ 30µl/ well) + soluble anti-CD28 mAb (0.25 µg/ 10µl/ well) in 96-well microtiter plates for (**A)** 3 days and (**B)** 6 days. Unstimulated splenocytes served as control. A fraction of CFSE labeled splenocytes was treated with mitomycin C (50 µg/ml) to block the cell proliferation and cultured under the conditions mentioned above to serve as non-proliferating control for each group (Gray filled histogram in each graph). Each histogram represents CFSE fluorescence intensity of splenic $CD3^+$ T cell population. The numbers in histogram plots represent percentages of divided $CD3^+$ T cell population. The histogram graphs show representative data of 3 independent assays. Each set in the assay was performed in triplicate wells.

Purified splenic T cell proliferation by CFSE assay

Further, *in vitro* proliferative responses of purified splenic T cells from Gal-$3^{+/+}$, Gal-$3^{+/-}$ and Gal-$3^{-/-}$ mice were assessed. T cells were isolated from splenocyte suspensions of Gal-$3^{+/+}$, Gal-$3^{+/-}$ and Gal-$3^{-/-}$ mice by immunomagnetic purification (Negative selection) using Mouse Pan T cell isolation kit (MACS, Mitenyi Biotec, Bergisch Gladbach, Germany). Yield of purified T cells obtained from murine splenocytes after immunomagnetic separation was calculated and was found to be ~30% for each isolation with no significant differences between Gal-$3^{+/+}$, Gal-$3^{+/-}$ and Gal-$3^{-/-}$ mice groups (Table 1, Figure 15A). The viability of purified T cells as assessed by trypan blue dye exclusion method was found to be >95% in Gal-$3^{+/+}$, Gal-$3^{+/-}$ and Gal-$3^{-/-}$ mice. Purity of the T cells was checked using anti-mouse CD3 PE antibody and was found to be ~90-95% ($CD3^+$ cells) for each isolation in Gal-$3^{+/+}$, Gal-$3^{+/-}$ and Gal-$3^{-/-}$ mice groups (Figure 15B).

Table 1: Yield of purified T cells from Gal-3$^{+/+}$, Gal-3$^{+/-}$ and Gal-3$^{-/-}$ mice splenocytes

Experiment No.	Splenocytes subjected to MACS (x 10^6)			T Cells count after MACS (x 10^6)			Yield (%)		
	Gal-3$^{+/+}$	Gal-3$^{+/-}$	Gal-3$^{-/-}$	Gal-3$^{+/+}$	Gal-3$^{+/-}$	Gal-3$^{-/-}$	Gal-3$^{+/+}$	Gal-3$^{+/-}$	Gal-3$^{-/-}$
1	36	36	36	10.1	11.2	10.2	28.06	31.11	28.33
2	48	48	48	15	14.1	15.3	31.25	29.38	31.88
3	48	48	48	15.2	13.9	14.5	31.67	28.96	30.21
Mean Yield (%)							30.33 ± 1.14	29.82 ± 0.66	30.14 ± 1.03

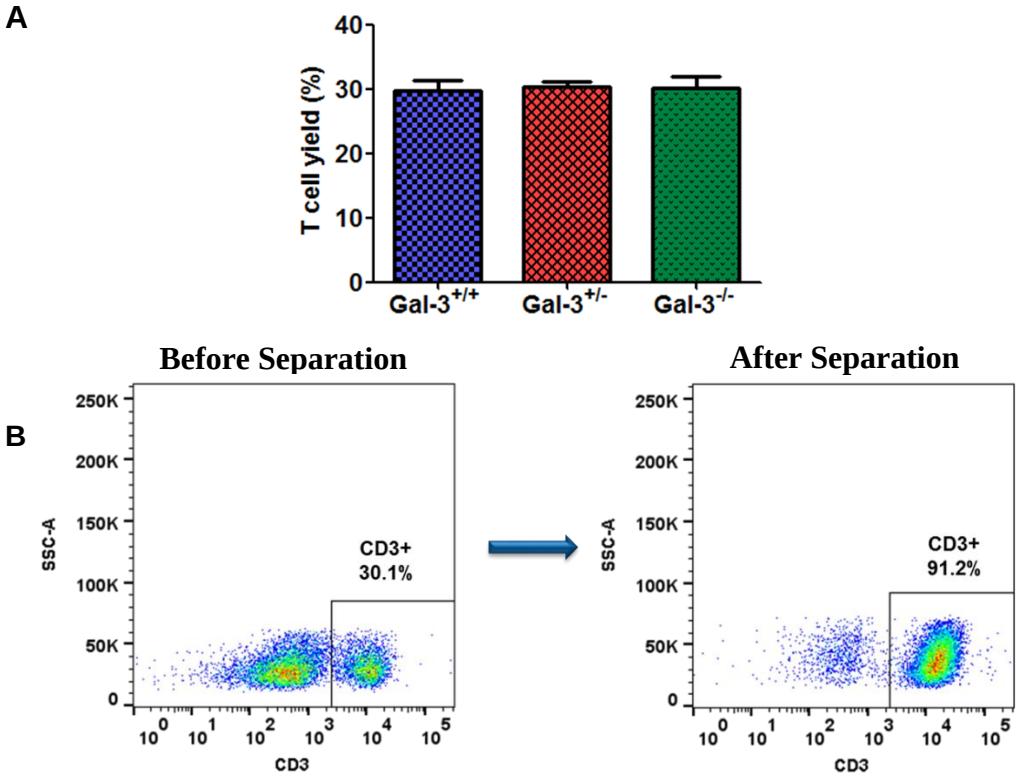

Figure 15: Yield and purity of T cells isolated from the splenocytes of Gal-3$^{+/+}$, Gal-3$^{+/-}$ and Gal-3$^{-/-}$ mice. T cells were purified from the freshly isolated splenocyte suspensions of Gal-3$^{+/+}$, Gal-3$^{+/-}$ and Gal-3$^{-/-}$ mice by immunomagnetic purification (Negative selection) using Mouse T cell isolation kit (Mitenyi Biotec, Bergisch Gladbach, Germany) as per the manufacturer's protocol. (**A)** Splenic T cell yields from Gal-3$^{+/+}$, Gal-3$^{+/-}$ and Gal-3$^{-/-}$ mice. Yield of T cells obtained after immunomagnetic purification was calculated as a percentage (%) of splenocytes number subjected to isolation in Gal-3$^{+/+}$, Gal-3$^{+/-}$ and Gal-3$^{-/-}$ mice group. The graph represents consolidated data of 3 independent experiments. **(B)** Purity of splenic T cells (CD3$^+$) assessed using anti-mouse CD3 PE antibody before and after immunomagnetic isolation. The dot plots are representative data of 3 independent experiments.

The immunomagnetically purified splenic T cells from Gal-$3^{+/+}$, Gal-$3^{+/-}$ and Gal-$3^{-/-}$ mice were subjected to CFSE labeling and cultured in 96 well microtiter plates (1.5 x 10^5 cells/100 µl complete RPMI/ well) in the presence of stimulants including PMA (50 ng/ well) + Ionomycin (50 ng/ well) or plate bound anti-CD3 mAb (0.25 µg/ well) + soluble anti-CD28 mAb (0.25 µg/ well) or in the medium only for 3 days and 6 days. It was confirmed that, upon *in vitro* stimulation with PMA + Ionomycin and anti-CD3/CD28 mAbs, purified T cells from Gal-$3^{+/-}$ and Gal-$3^{-/-}$ mice exhibited higher proliferative responses than those from Gal-$3^{+/+}$ mice as observed on day 3 (Figure 16A) and day 6 (Figure 16B). Using purified T cell population, distinct peaks of dividing T cells were observed on day 3 (Figure 16A). The distinction was less evident on day 6 (Figure 16B).

CFSE Proliferation assay: Purified splenic T cells

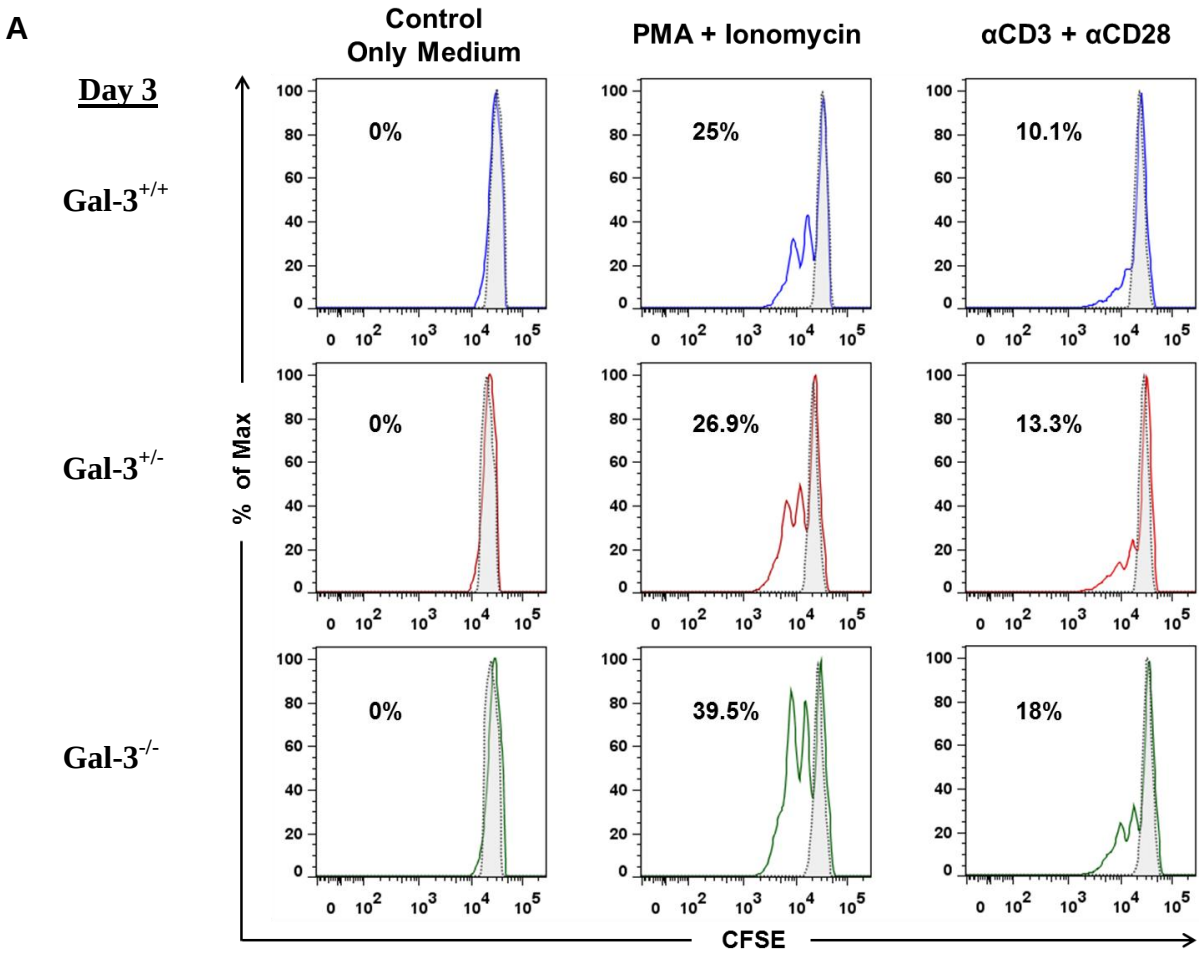

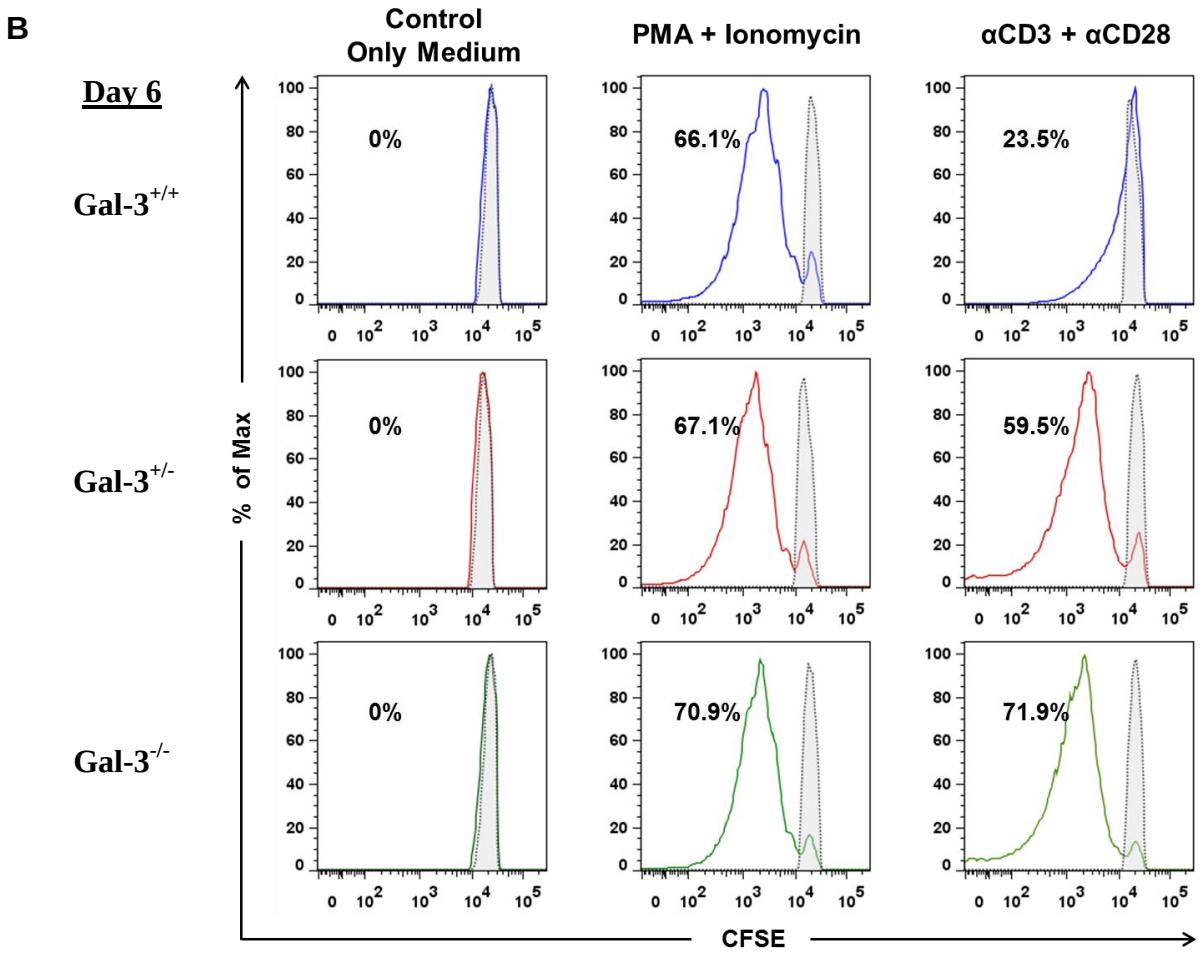

Figure 16: Proliferative responses in purified splenic T cells form Gal-3$^{+/+}$, Gal-3$^{+/-}$ and Gal-3$^{-/-}$ mice as assessed by CFSE staining assay. Immunomagnetically purified T cells from Gal-3$^{+/+}$, Gal-3$^{+/-}$ and Gal-3$^{-/-}$ mice were subjected to CFSE staining. CFSE labeled T cells (1.5 x 10^5 cells/ 100 µl medium/ well) were stimulated *in vitro* with either PMA (50 ng/ 10µl/ well) + Ionomycin (50 ng/ 10µl/ well) or plate bound anti-CD3 mAb (0.25 µg/ 30µl/ well) + soluble anti-CD28 mAb (0.25 µg/ 10µl/ well) in 96-well microtiter plates for **(A)** 3 days and **(B)** 6 days. Unstimulated T cells served as control. A fraction of CFSE labeled splenocytes was treated with mitomycin C (50 µg/ml) to block the cell proliferation and cultured under the conditions mentioned above to serve as non-proliferating control for assay in each group (Gray filled histogram in each graph). Each histogram represents CFSE fluorescence intensity of purified T lymphocyte population. The numbers in each histogram plot represent percentages of divided T cell population in Gal-3$^{+/+}$, Gal-3$^{+/-}$ and Gal-3$^{-/-}$ mice groups. The histogram graphs show representative data of 3 independent assays. Each set in the assay was performed in triplicate wells.

Intracellular calcium flux in splenocytes from Gal-3$^{+/+}$, Gal-3$^{+/-}$ and Gal-3$^{-/-}$ mice upon *in vitro* stimulation

Calcium ions (Ca^{++}) act as important secondary messengers in T cell activation and signaling cascade leading to various T cell responses. Fluo-3 is a calcium indicator dye widely used to probe the levels of cytosolic Ca^{++} ions produced on stimulation of cells. In the present study, the flux of intracellular Ca^{++} ions produced in Fluo-3-AM labeled splenocytes from Gal-3$^{+/+}$, Gal-3$^{+/-}$ and Gal-3$^{-/-}$ mice was analyzed upon *in vitro* stimulation using PMA (100 ng) + Ionomycin (500 ng) or anti-CD3 mAb (1 µg) as per the protocol described in the Materials and Methods chapter. It was observed that, freshly isolated splenocytes from Gal-3$^{+/-}$ and Gal-3$^{-/-}$ mice produced higher levels of intracellular Ca^{++} flux compared to those from Gal-3$^{+/+}$ mice, in response to *in vitro* stimulation using PMA (100 ng) + Ionomycin (500 ng) or anti-CD3 mAb (1 µg) (Figure 17).

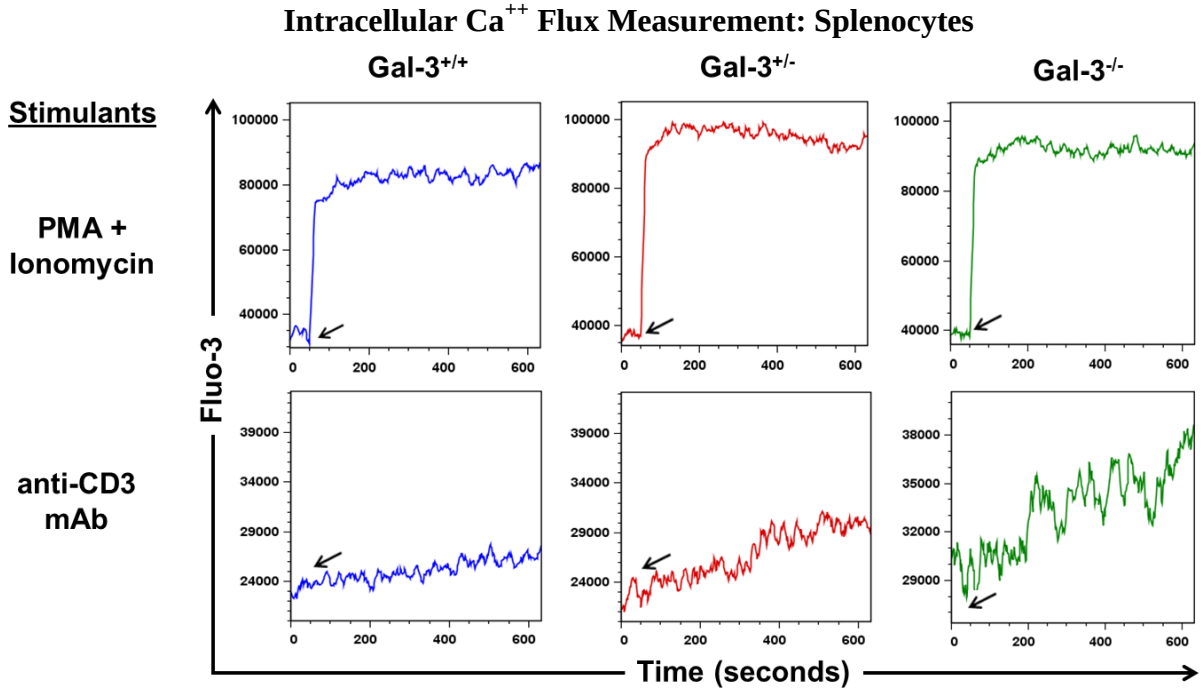

Figure 17: Intracellular calcium flux in Gal-3$^{+/+}$, Gal-3$^{+/-}$ and Gal-3$^{-/-}$ mice splenocytes upon *in vitro* stimulation. Freshly isolated splenocytes of Gal-3$^{+/+}$, Gal-3$^{+/-}$ and Gal-3$^{-/-}$ mice were stained with calcium indicator dye Fluo-3-AM. The baseline fluorescence intensity of splenocytes was measured by flow cytometry. The splenocytes were stimulated with either

PMA (100 ng) + Ionomycin (500 ng) (upper panel) or soluble anti-CD3 mAb (1 μg) (lower panel) and the changes in the Fluo-3 fluorescence intensity were quantitated over a period of up to 10 minutes continuously by flow cytometry. The histograms show representative data of 3 independent experiments. Arrows indicate the time points of addition of stimulants.

Intracellular calcium flux in purified splenic T cells from Gal-3$^{+/+}$, Gal-3$^{+/-}$ and Gal-3$^{-/-}$ mice upon *in vitro* stimulation

Further, immunomagnetically purified and Fluo-3-AM labeled splenic T cells from Gal-3$^{+/+}$, Gal-3$^{+/-}$ and Gal-3$^{-/-}$ mice were subjected to intracellular Ca^{++} flux measurement. Titration was performed using different concentrations of soluble anti-CD3 mAb to select the optimum concentration needed for stimulation of purified T cells to produce a substantial intracellular Ca^{++} flux response. It was observed that, by providing a co-stimulatory signal using soluble anti-CD28 mAb along with soluble anti-CD3 mAb resulted in more rapid and robust pattern of intracellular Ca^{++} flux in Gal-3$^{+/+}$ mice T cells as compared to stimulation with soluble anti-CD3 mAb alone (Figure 18; Figure 19, lower panel).

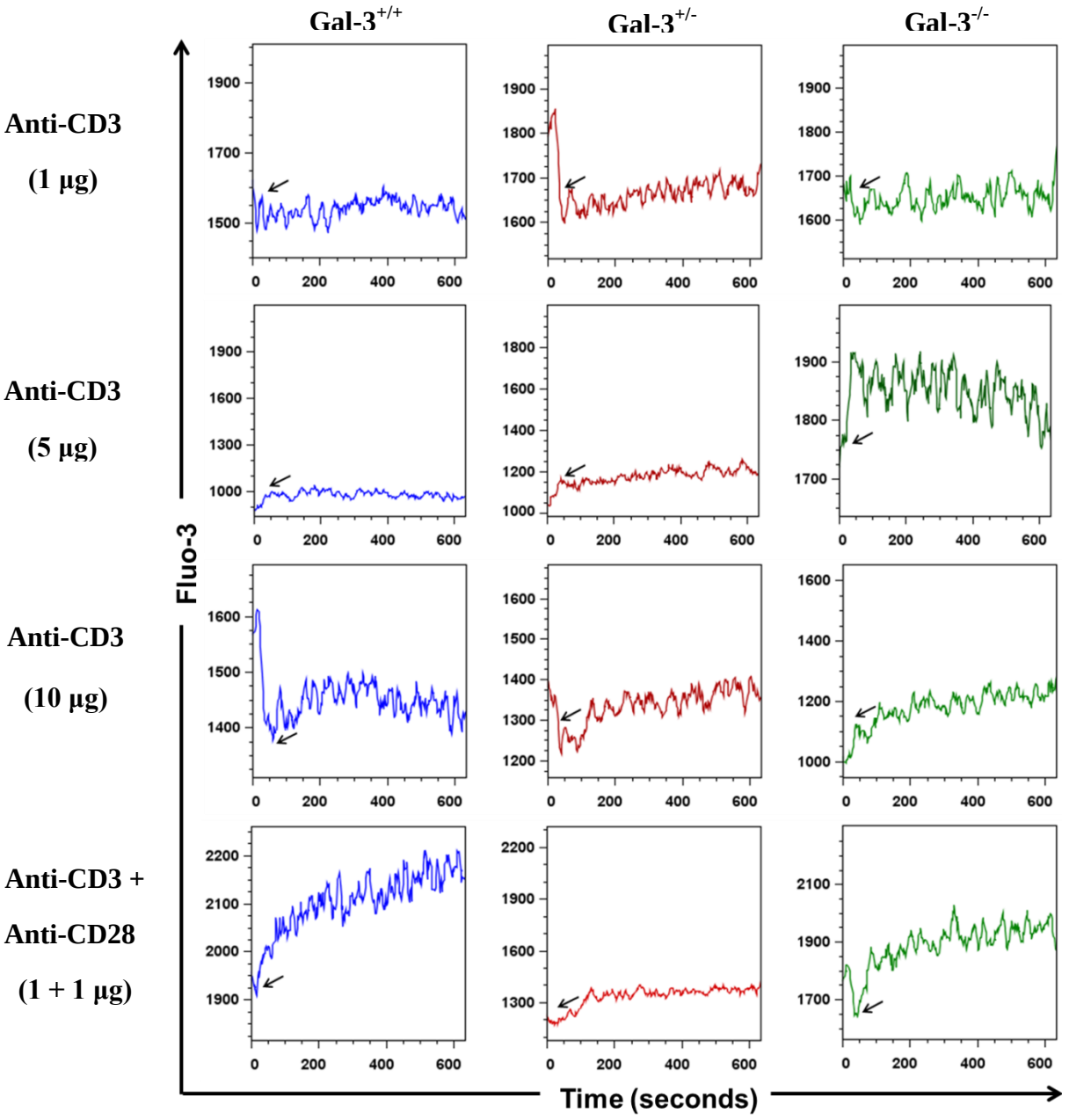

Figure 18: Intracellular calcium flux in purified splenic T cells from Gal-3$^{+/+}$, Gal-3$^{+/-}$ and Gal-3$^{-/-}$ mice upon *in vitro* stimulation with different concentrations of anti-CD3/CD28 mAbs. Immunomagnetically purified splenic T cells of Gal-3$^{+/+}$, Gal-3$^{+/-}$ and Gal-3$^{-/-}$ mice were stained with calcium indicator dye Fluo-3-AM. The baseline fluorescence intensity of T cells was measured by flow cytometry for 30 seconds. Titration was performed by stimulating purified T cells with different concentrations of soluble anti-CD3 or using combination of anti-CD3 + anti-CD28 mAbs as indicated. The changes in the Fluo-3 fluorescence intensity were then quantitated over a period of up to 10 minutes by flow cytometry.

The measurement of intracellular Ca^{++} flux in the purified murine T cells upon *in vitro* stimulation with PMA (100 ng) + Ionomycin (500 ng) and soluble anti-CD3 mAb (10 μg) + soluble anti-CD28 mAb (10 μg) was performed as per the protocol mentioned in the Materials and Methods section. Purified splenic T cells from Gal-$3^{-/-}$ mice were found to produce lower levels of intracellular Ca^{++} flux compared to those from Gal-$3^{+/+}$ and Gal-$3^{+/-}$ mice, in response to *in vitro* stimulation with PMA + Ionomycin (Figure 19, upper panel) and soluble anti-CD3/CD28 mAbs (Figure 19, lower panel). These results differed from those of the intracellular Ca^{++} flux measurement done using total splenocytes population, where increased intracellular Ca^{++} levels were observed in splenocytes of Gal-$3^{+/-}$ and Gal-$3^{-/-}$ mice than in Gal-$3^{+/+}$ mice (Figure 17). Further, the overall intracellular Ca^{++} levels produced before and after stimulation with PMA + Ionomycin and soluble anti-CD3/CD28 mAbs are lower in purified murine T cells (Figure 19) as compared to total splenocytes population (Figure 17). These differences in intracellular Ca^{++} levels may be possibly due to the contribution of Ca^{++} flux generated by the other immune cell subsets (macrophages, neutrophils) along with the T cells in the total splenocytes population, when compared to purified T cells alone. Further, reduced intracellular Ca^{++} flux observed in stimulated T cells of Gal-$3^{-/-}$ mice highlights the crucial role of endogenous galectin-3 expression in the regulation of T cell calcium signaling in the host.

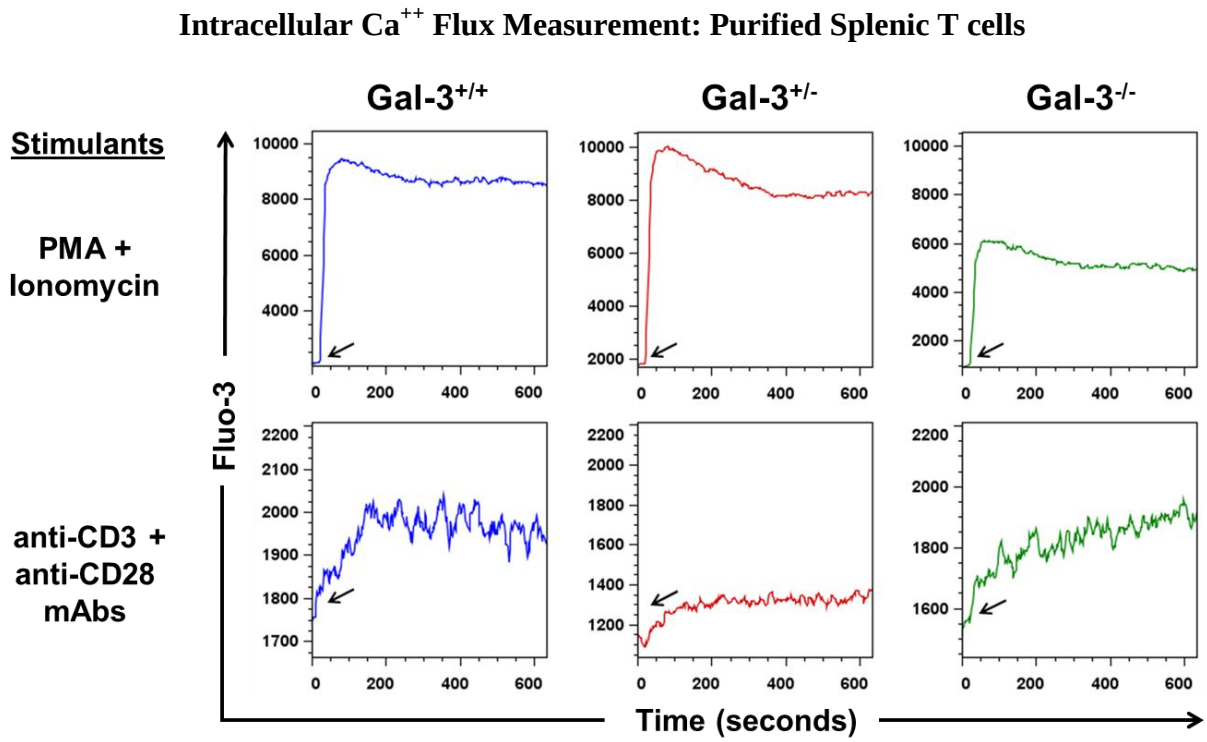

Figure 19: Intracellular calcium flux in purified T cells upon *in vitro* stimulation. Immunomagnetically purified splenic T cells of Gal-$3^{+/+}$, Gal-$3^{+/-}$ and Gal-$3^{-/-}$ mice were stained with calcium indicator dye Fluo-3-AM. The baseline fluorescence intensity of T cells was measured by flow cytometry for 30 seconds. The T cells were stimulated with either PMA (100 ng) + Ionomycin (500 ng) (upper panel) or soluble anti-CD3 mAb (10 µg) + anti-CD28 mAb (10 µg) (lower panel) and the changes in the Fluo-3 fluorescence intensity were then quantitated over a period of up to 10 minutes by flow cytometry. The histograms show representative data of 3 independent experiments. Arrows indicate the time points of addition of stimulants.

Intracellular ROS generation in splenocytes from Gal-$3^{+/+}$, Gal-$3^{+/-}$ and Gal-$3^{-/-}$ mice upon *in vitro* stimulation

Reactive oxygen species (ROS) play an important role in the regulation of cellular signaling, thereby modulating immune responses in the host. To understand whether ROS production is affected by endogenous galectin-3 expression levels in the host, intracellular ROS generation in freshly isolated splenocytes of Gal-$3^{+/+}$, Gal-$3^{+/-}$ and Gal-$3^{-/-}$ mice upon *in vitro* stimulation with PMA + Ionomycin and anti-CD3 mAb was studied by flow cytometry as

described in the Materials and Methods chapter. It was observed that, splenocytes of Gal-$3^{+/-}$ and Gal-$3^{-/-}$ mice stimulated *in vitro* with PMA (100 ng) + Ionomycin (500 ng) or with soluble anti-CD3 mAb (1 μg) exhibited significantly lower intracellular ROS generation compared to those of Gal-$3^{+/+}$ mice (Figure 20).

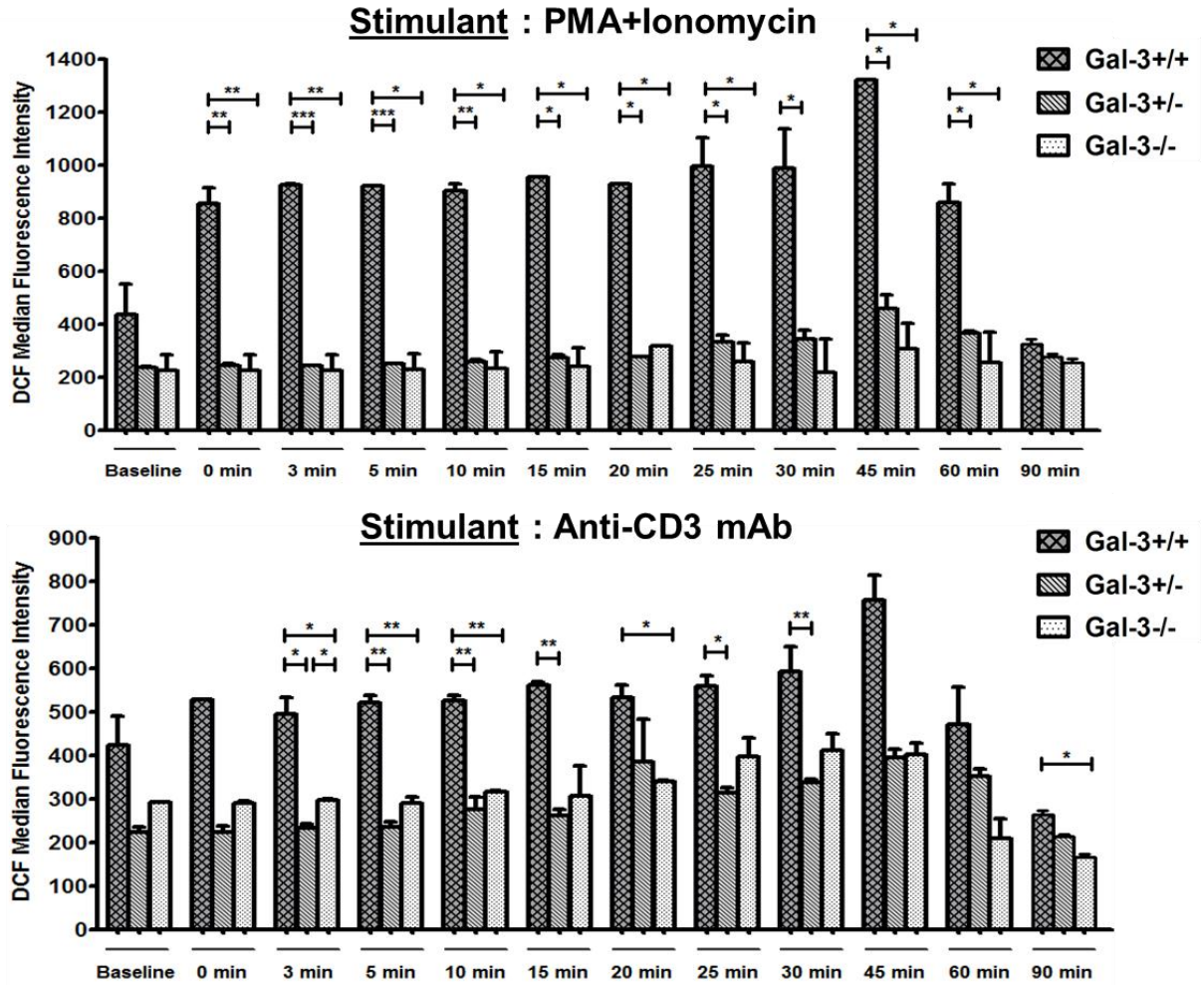

Figure 20: Intracellular ROS generation in Gal-$3^{+/+}$, Gal-$3^{+/-}$ and Gal-$3^{-/-}$ mice splenocytes upon *in vitro* stimulation. Freshly isolated splenocytes of Gal-$3^{+/+}$, Gal-$3^{+/-}$ and Gal-$3^{-/-}$ mice were stained with DCFH-DA. The baseline DCF fluorescence intensity of labeled splenocytes was measured by flow cytometry. The splenocytes were then stimulated with either PMA (100 ng) + Ionomycin (500 ng; upper panel) or soluble anti-CD3 mAb (1 μg; lower panel) and the changes in the Fluo-3-AM fluorescence intensity were quantitated at the indicated time intervals by flow cytometry. The graphs represent consolidated data of 3 independent experiments. **P*<0.05, ***P*<0.01, ****P*<0.001.

Frequency of spontaneous apoptosis in freshly isolated splenocytes of Gal-3$^{+/+}$, Gal-3$^{+/-}$ and Gal-3$^{-/-}$ mice

Extracellular galectin-3 is known to induce apoptosis in human T leukemia cell lines, human peripheral blood mononuclear cells, and activated mouse T cells [109,255,258]; whereas intracellular galectin-3 has been found to be anti-apoptotic in various cell types including human leukemia T cells [47,55,304]. In the present investigation, it was assessed whether differences in endogenous galectin-3 expression levels affected the frequencies of spontaneously apoptotic cells in Gal-3$^{+/+}$, Gal-3$^{+/-}$ and Gal-3$^{-/-}$ mice splenocytes. Freshly isolated splenocytes of Gal-3$^{+/+}$, Gal-3$^{+/-}$ and Gal-3$^{-/-}$ mice were analyzed for the presence of early apoptotic and late apoptotic/ necrotic cell populations by Annexin V-PI staining as described in the Materials and Methods chapter. The apoptotic cell percentages in total lymphocyte population as well as in T cells (CD3^{+}), helper T cells (CD3^{+} CD4^{+}), cytotoxic T cells (CD3^{+}CD8^{+}) and B (B220^{+}) cell subsets were quantitated.

In the total splenic lymphocytes population, no significant differences were observed in the frequencies of early apoptotic cell (Annexin V^{+}PI^{-}) cells as well as of late apoptotic/ necrotic cells (Annexin V^{+}PI^{+}) in Gal-3$^{+/+}$, Gal-3$^{+/-}$ and Gal-3$^{-/-}$ mice groups (Figure 21).

Frequency of spontaneously apoptotic lymphocyte population in mice splenocytes

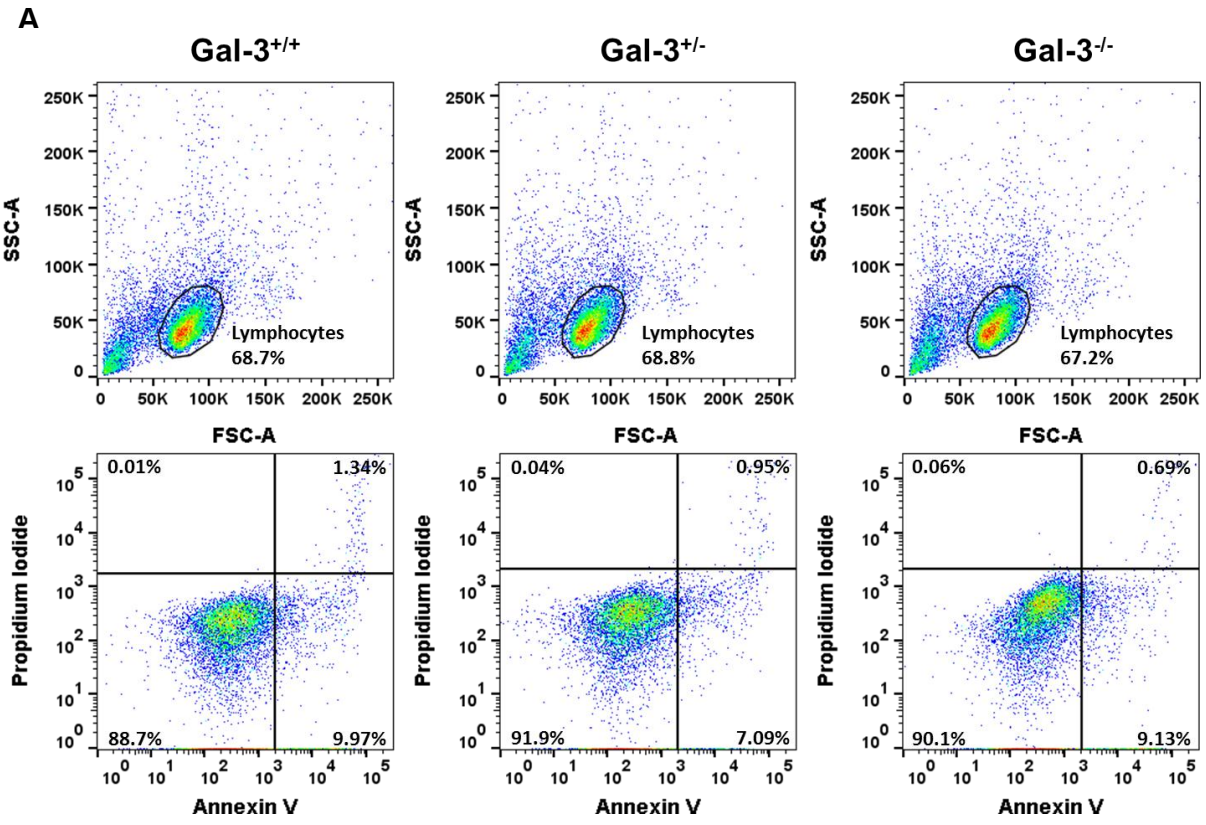

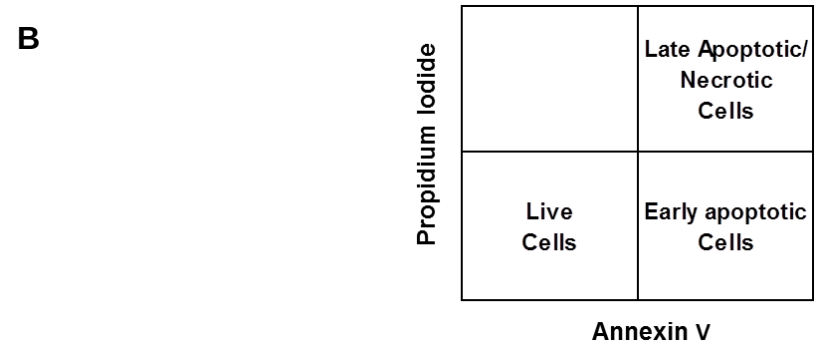

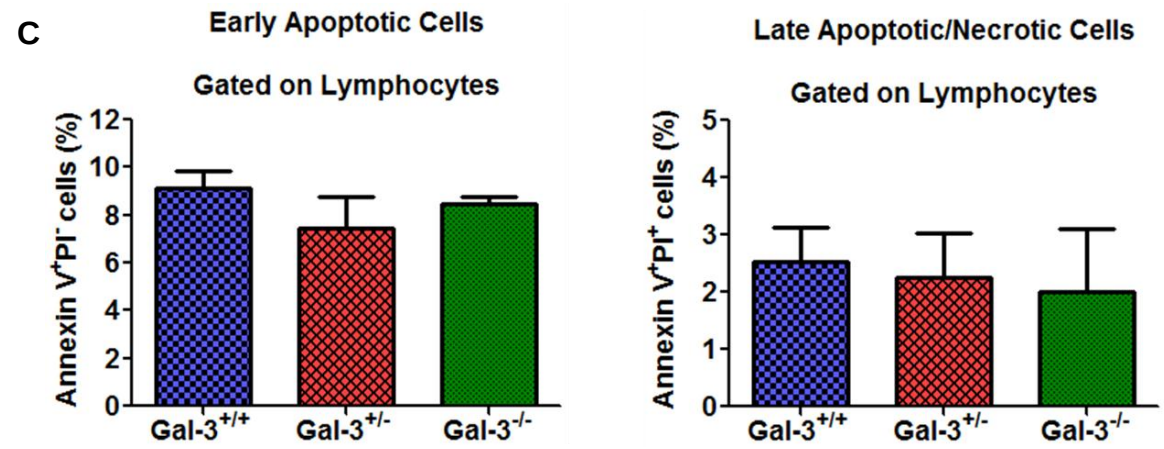

Figure 21: Frequency of spontaneously apoptotic lymphocyte population in Gal-3$^{+/+}$, Gal-3$^{+/-}$ and Gal-3$^{-/-}$ mice splenocytes. Freshly isolated splenocytes from Gal-3$^{+/+}$, Gal-3$^{+/-}$ and Gal-3$^{-/-}$ mice were stained with anti-Annexin V FITC antibody and propidium iodide and were analyzed by flow cytometry. **(A)** Representative dot plots of Annexin V and Propidium Iodide stained splenocytes in Gal-3$^{+/+}$, Gal-3$^{+/-}$ and Gal-3$^{-/-}$ mice groups. **(B)** The quadrant diagram indicates different types of cell subsets within a population based on their Annexin-V and PI staining properties. **(C)** Frequencies of early apoptotic cells (Annexin V^{+}PI^{-}) and late apoptotic/necrotic cells (Annexin V^{+}PI^{+}) were quantitated amongst total lymphocyte population. The graphs represent consolidated data of 3 independent experiments. *P<0.05.

It was observed that, in splenic CD3^{+} (total T cells) and CD3^{+}CD4^{+} (helper T cell) subsets, frequencies of early apoptotic (Annexin V^{+}PI^{-}) cell populations were found to be significantly higher in Gal-3$^{-/-}$ mice than those in Gal-3$^{+/-}$ mice (Figure 22B, left panel). No significant differences were found in the levels of early apoptotic cells (Annexin V^{+}PI^{-}) in splenic CD3^{+}CD8^{+} (cytotoxic T cell) and B220^{+} (B cell) subsets amongst Gal-3$^{+/+}$, Gal-3$^{+/-}$ and Gal-3$^{-/-}$ mice groups (Figure 22B, left panel). Further, it was noted that, percentages of late apoptotic/ necrotic cells (Annexin V^{+}PI^{+}) in splenic CD3^{+} (total T cells), CD3^{+}CD4^{+} (helper T cell) and CD3^{+}CD8^{+} (cytotoxic T cell) remained almost comparable in Gal-3$^{+/+}$, Gal-3$^{+/-}$ and Gal-3$^{-/-}$ mice groups (Figure 22B, right panel). On the other hand, splenic B220^{+} (B cells) in Gal-3$^{-/-}$ mice exhibited significantly lower percentages of late apoptotic/ necrotic cells (Annexin V^{+}PI^{+}) as compared to those in Gal-3$^{+/+}$ and Gal-3$^{+/-}$ mice splenocytes (Figure 22B, right panel).

A

CD3$^+$ (T cells)

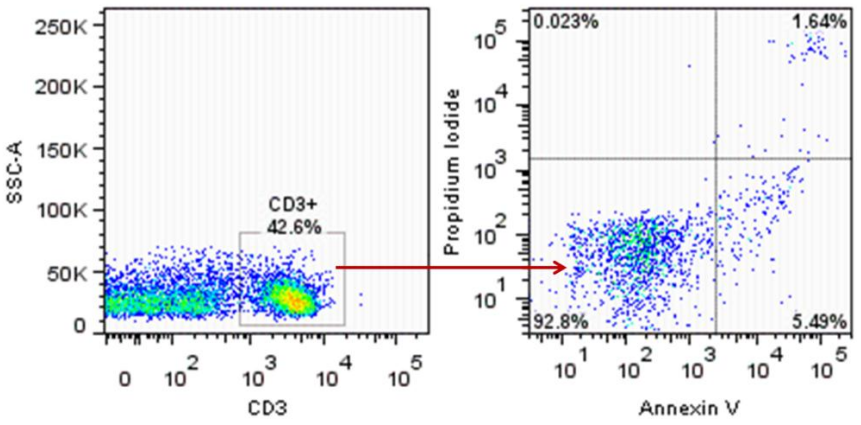

CD3$^+$CD4$^+$

(T_H cells)

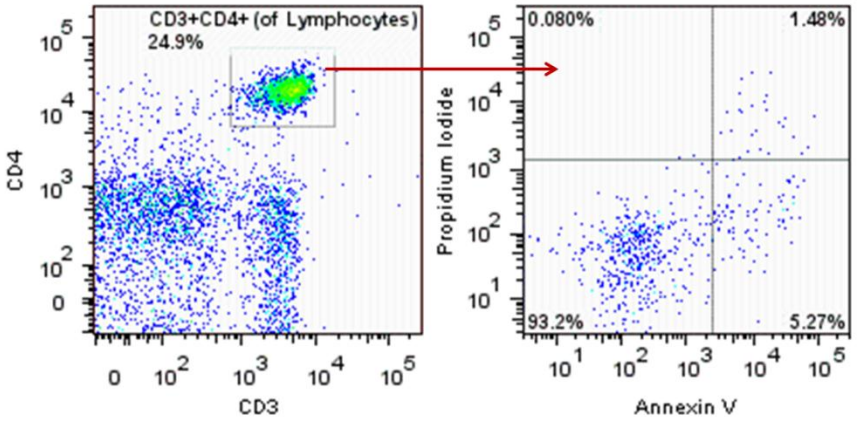

CD3$^+$CD8$^+$

(T_C cells)

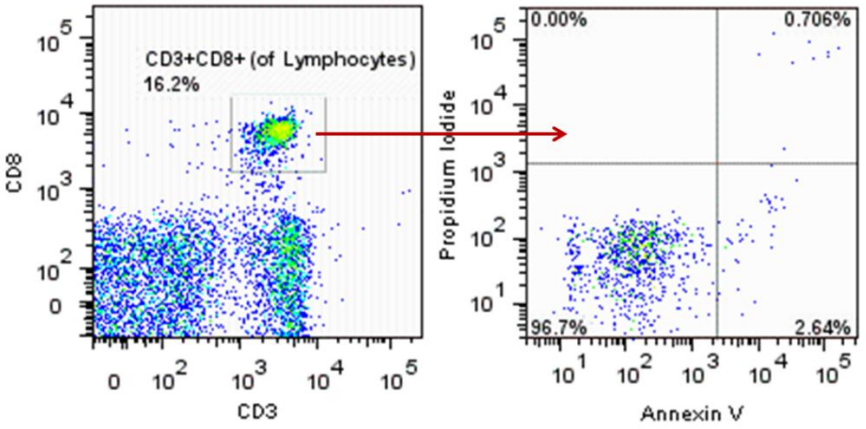

B220$^+$

(B cells)

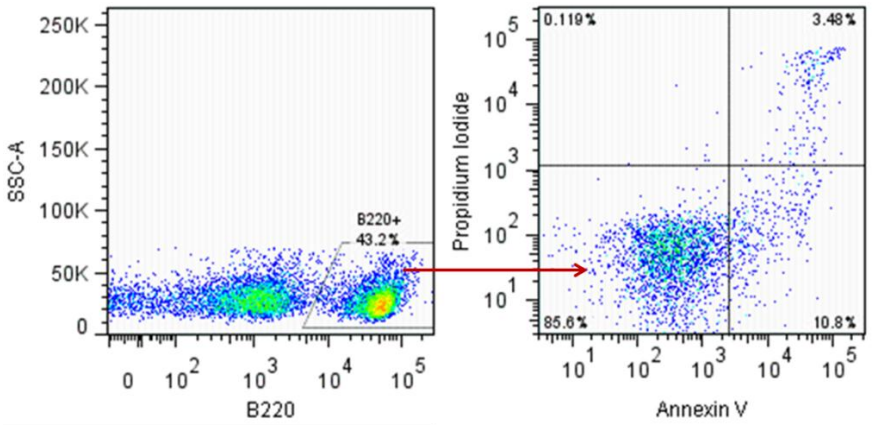

B

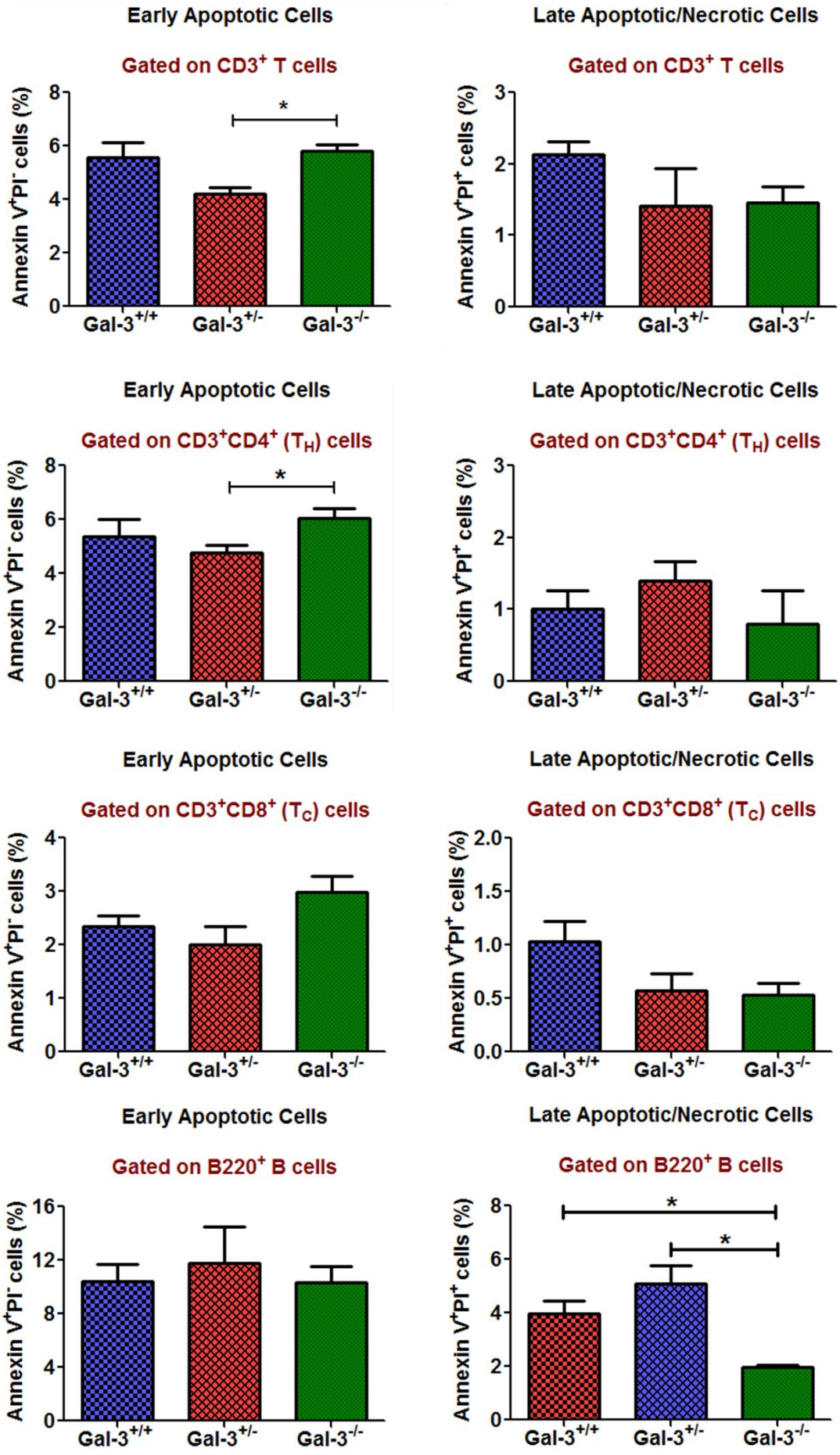
Early Apoptotic Cells
Gated on CD3+ T cells
Annexin V+PI- cells (%)
Gal-3+/+
Gal-3+/-
Gal-3-/-
Late Apoptotic/Necrotic Cells
Gated on CD3+ T cells
Annexin V+PI+ cells (%)
Early Apoptotic Cells
Gated on CD3+CD4+ (TH) cells
Late Apoptotic/Necrotic Cells
Gated on CD3+CD4+ (TH) cells
Early Apoptotic Cells
Gated on CD3+CD8+ (TC) cells
Late Apoptotic/Necrotic Cells
Gated on CD3+CD8+ (TC) cells
Early Apoptotic Cells
Gated on B220+ B cells
Late Apoptotic/Necrotic Cells
Gated on B220+ B cells

Figure 22: Frequencies of early apoptotic and late apoptotic T and B cells in Gal-3$^{+/+}$, Gal-3$^{+/-}$ and Gal-3$^{-/-}$ mice splenocytes. Freshly isolated splenocytes of Gal-3$^{+/+}$, Gal-3$^{+/-}$ and Gal-3$^{-/-}$ mice were washed in PBS and surface stained using antibodies for mouse CD3, CD4, CD8 and B220 surface markers. After surface staining, splenocytes were stained with Annexin V FITC antibody and Propidium Iodide. Splenic T and B cell subsets were analysed for the presence of early apoptotic (Annexin V$^+$PI$^-$) and late apoptotic/ necrotic (Annexin V$^+$PI$^+$) cell populations following Annexin V-PI staining. (**A)** Representative dot plots of Annexin V- PI stained CD3$^+$ (total T cells), CD3$^+$CD4$^+$ (helper T cells), CD3$^+$CD8$^+$ (cytotoxic T cells) and B220$^+$ (B cells). (**B)** The graphs represent percentages of early apoptotic cells (Annexin V$^+$PI$^-$, left panel) and late apoptotic/ necrotic cells (Annexin V$^+$PI$^+$, right panel) in respective splenocyte subsets as consolidated data of 3 independent experiments. **P*<0.05.

Serum cytokine profile in Gal-3$^{+/+}$, Gal-3$^{+/-}$ and Gal-3$^{-/-}$ mice

Cytokines are the important modulators of balance between humoral and cell mediated immune responses in normal physiological processes as well as during pathological conditions; including infection, inflammation and cancer. It was important to explore the serum cytokine profile in Gal-3$^{+/+}$, Gal-3$^{+/-}$ and Gal-3$^{-/-}$ mice with different endogenous galectin-3 expression levels.

The levels of Th1 (IL-2, IFN-γ, TNF), Th2 (IL-4, IL-6, IL-10) and Th17 (IL-17A) cytokines were measured in the sera of Gal-3$^{+/+}$, Gal-3$^{+/-}$ and Gal-3$^{-/-}$ mice by cytometric bead array using flow cytometry. It was observed that, Gal-3$^{+/-}$ and Gal-3$^{-/-}$ mice showed reduced serum cytokine levels as compared to Gal-3$^{+/+}$ mice. The Th1, Th2 and Th17 cytokine levels were found to be affected the most in the total absence of endogenous galectin-3 in Gal-3$^{-/-}$ mice as the sera of Gal-3$^{-/-}$ mice showed marked reduction in all cytokine levels (Figure 23).

Serum Th1/Th2/Th17 cytokine profile in Gal-3$^{+/+}$, Gal-3$^{+/-}$ and Gal-3$^{-/-}$ mice

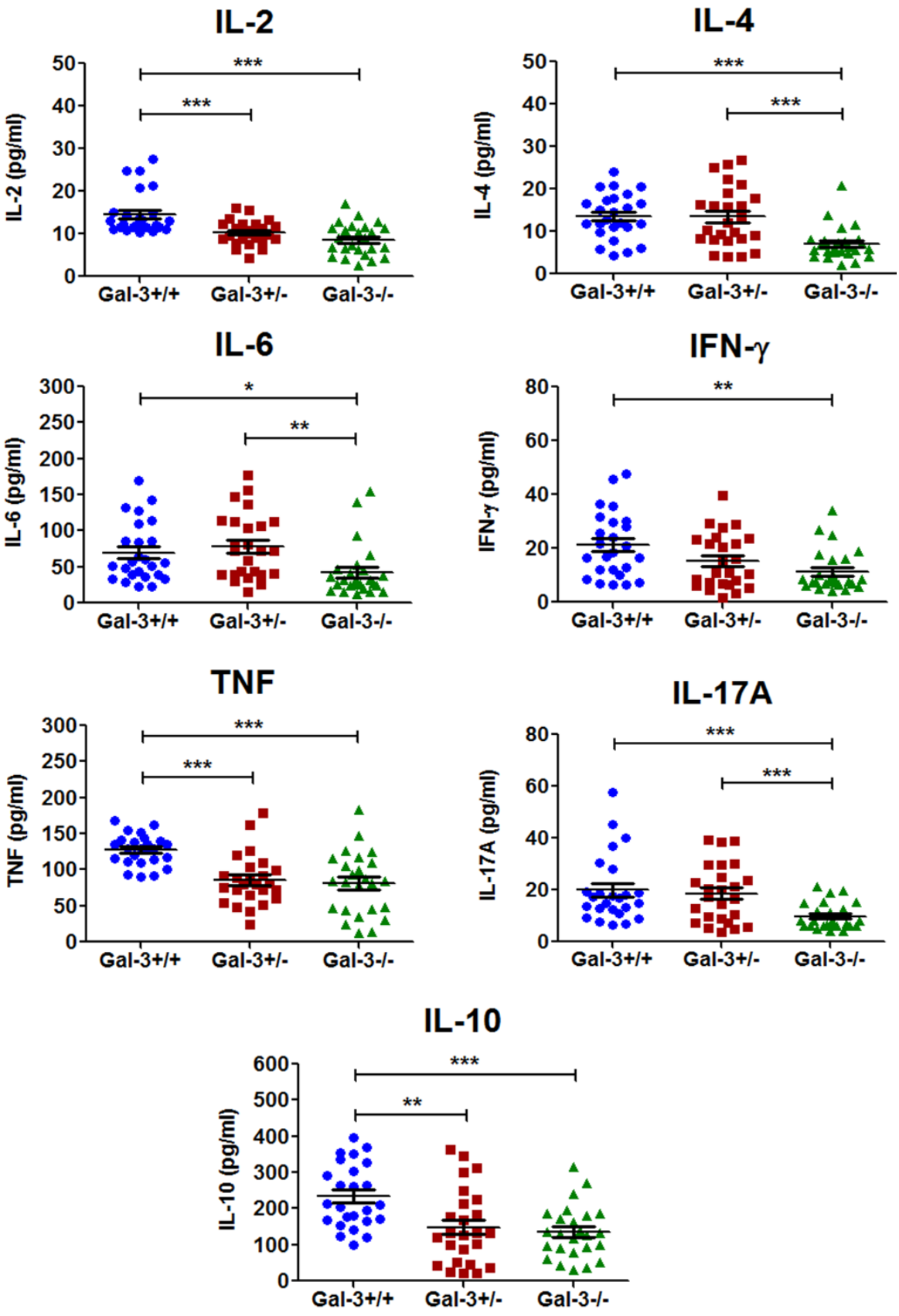

Figure 23: Serum Th1/Th2/Th17 cytokine profile in Gal-3$^{+/+}$, Gal-3$^{+/-}$ and Gal-3$^{-/-}$ mice. Blood was collected from Gal-3$^{+/+}$, Gal-3$^{+/-}$ and Gal-3$^{-/-}$ mice before sacrifice by retro-orbital puncture and serum was separated by centrifugation. Serum cytokine profile was assessed by Th1/Th2/Th17 Cytometric Bead Array using flow cytometry. The graphs indicate concentrations of Th1 (IL-2, IFN-γ, TNF), Th2 (IL-4, IL-6, IL-10) and Th17 (IL-17A) cytokines in Gal-3$^{+/+}$, Gal-3$^{+/-}$ and Gal-3$^{-/-}$ mice sera. Each dot in the dot plot represents serum cytokine concentration (pg/ml) of one mouse from the corresponding group (n=25 mice per group). *P<0.05, **P<0.01, ***P<0.001.

It was interesting to note that, serum levels of IL-2 and IFN-γ showed a trend that correlated with endogenous galectin-3 expression levels in Gal-3$^{+/+}$, Gal-3$^{+/-}$ and Gal-3$^{-/-}$ mice (Figure 23). However, correlation analysis revealed that, there was no significant correlation between serum IL-2 and IFN-γ levels in all the three groups of mice (Figure 24).

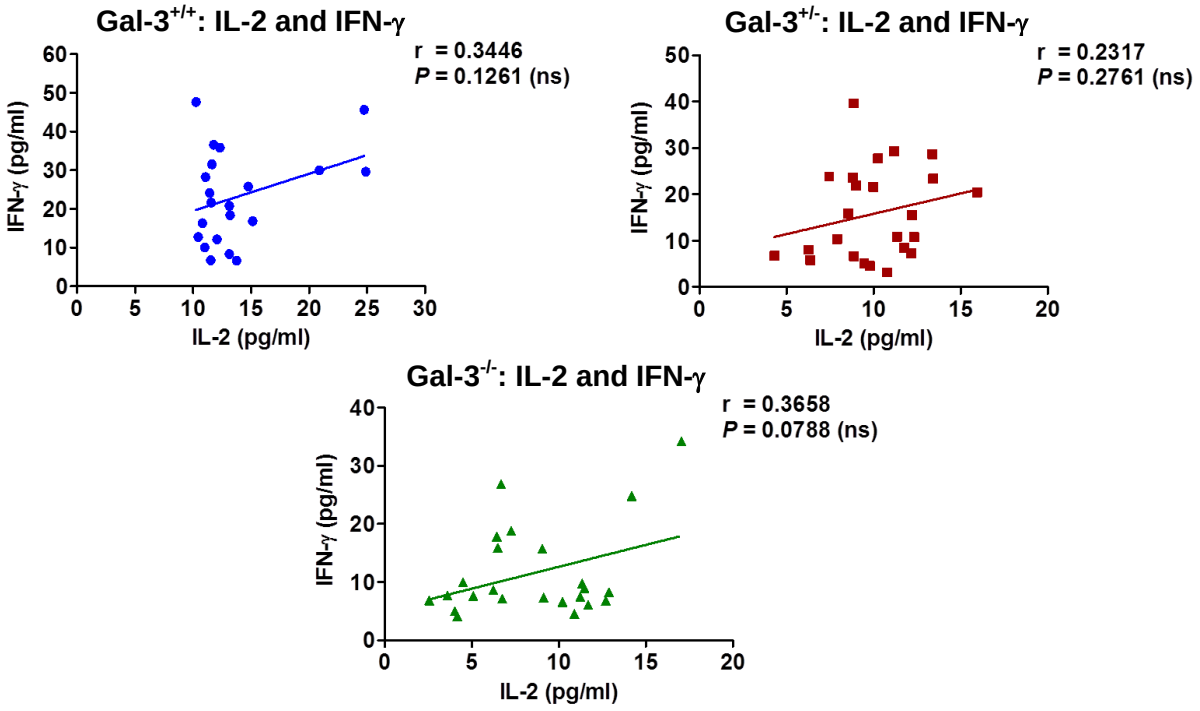

Figure 24: Correlation analysis of serum IL-2 and IFN-γ levels in Gal-3$^{+/+}$, Gal-3$^{+/-}$ and Gal-3$^{-/-}$ mice sera. The graphs show correlations between concentrations (pg/ml) of IL-2 and IFN-γ in Gal-3$^{+/+}$, Gal-3$^{+/-}$ and Gal-3$^{-/-}$ mice sera. Pearson's correlation coefficients (r) and *P* values indicating significance of correlation between the groups are mentioned next to each correlation graph.

The levels of pro-inflammatory cytokines TNF, IFN-γ and IL-17A had significantly strong positive correlations with each other exclusively in Gal-3$^{-/-}$ mice sera (Figure 25). Interestingly, concentrations of pro-inflammatory cytokines IL-6, TNF and IL-17A correlated positively with anti-inflammatory cytokine IL-10 and these correlations were found to be significant only in Gal-3$^{-/-}$ mice sera (Figure 25). These findings indicate that, in the complete absence of endogenous host galectin-3, the serum cytokine milieu may be disturbed, exhibiting dysregulation of the balance between pro-inflammatory and anti-inflammatory cytokines in Gal-3$^{-/-}$ mice.

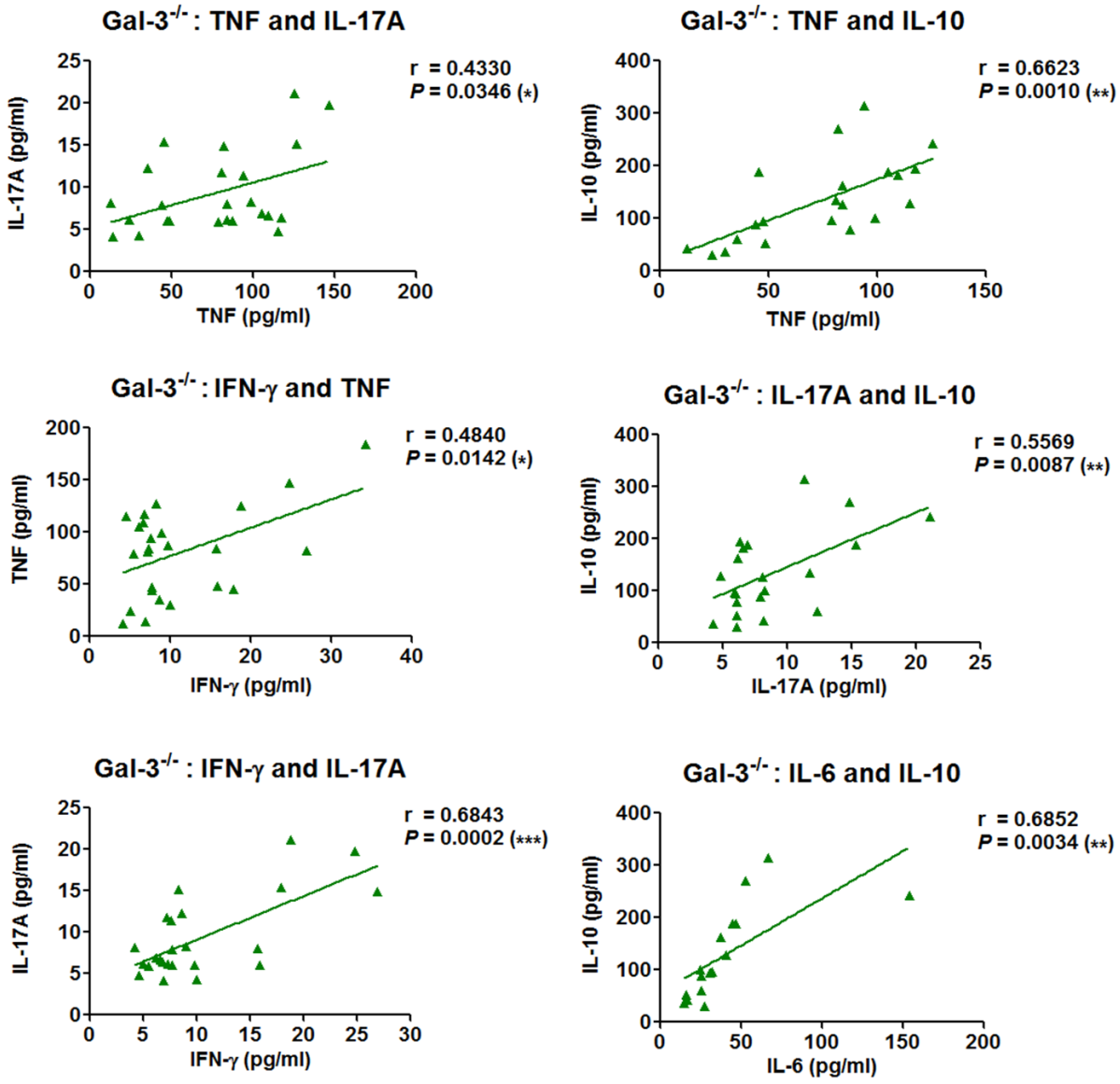

Figure 25: Correlation analysis of serum pro-inflammatory and anti-inflammatory cytokines in Gal-3$^{-/-}$ mice sera. The graphs show correlations between concentrations (pg/ml) of pro-inflammatory cytokines including IFN-γ, TNF and IL-17A with each other in Gal-3$^{-/-}$ mice sera (left panel). Correlations of IL-6, TNF and IL-17A concentrations (pg/ml) each independently with IL-10 concentrations (pg/ml) were also analyzed in Gal-3$^{-/-}$ mice sera (right panel). Pearson's correlation coefficients (r) and *P* values indicating significance of correlation between the respective cytokines are mentioned next to each correlation graph. **P*<0.05, ***P*<0.01.

Cytokine profiles in the cell-free supernatants of *in vitro* stimulated splenocytes from Gal-3$^{+/+}$, Gal-3$^{+/-}$ and Gal-3$^{-/-}$ mice

It was further analyzed whether differences in endogenous galectin-3 levels affect the ability of Gal-3$^{+/+}$, Gal-3$^{+/-}$ and Gal-3$^{-/-}$ mice splenocytes to produce cytokines upon *in vitro* stimulation. Freshly isolated splenocytes from Gal-3$^{+/+}$, Gal-3$^{+/-}$ and Gal-3$^{-/-}$ mice were cultured in the presence of either PMA + Ionomycin or anti-CD3/CD28 mAbs for 24 hours. After 24 hours, cell free supernatants were carefully collected and subjected to Th1 (IL-2, IFN-γ, TNF), Th2 (IL-4, IL-6, IL-10) and Th17 (IL-17A) cytokine profiling by cytometric bead array using flow cytometry. Upon *in vitro* stimulation with PMA (50 ng/ well) + Ionomycin (50 ng/ well) or with plate-bound anti-CD3 mAb (0.25 μg/ well) + soluble anti-CD28 mAb (0.25 μg/ well), levels of IL-2 in splenocytes culture supernatants of Gal-3$^{+/-}$ and Gal-3$^{-/-}$ mice were found to be significantly lower than that of Gal-3$^{+/+}$ mice. There were no significant differences observed in the concentrations of other cytokines analyzed in the culture supernatants of Gal-3$^{+/+}$, Gal-3$^{+/-}$ and Gal-3$^{-/-}$ mice splenocytes upon *in vitro* stimulation using PMA + Ionomycin or anti-CD3/CD28 mAbs (Figure 26). These results indicated possible role of endogenous galectin-3 expression levels in the regulation of IL-2 production by *in vitro* stimulated splenocytes of mice.

Th1/Th2/Th17 cytokine profiles in cell-free supernatants of stimulated mice splenocytes

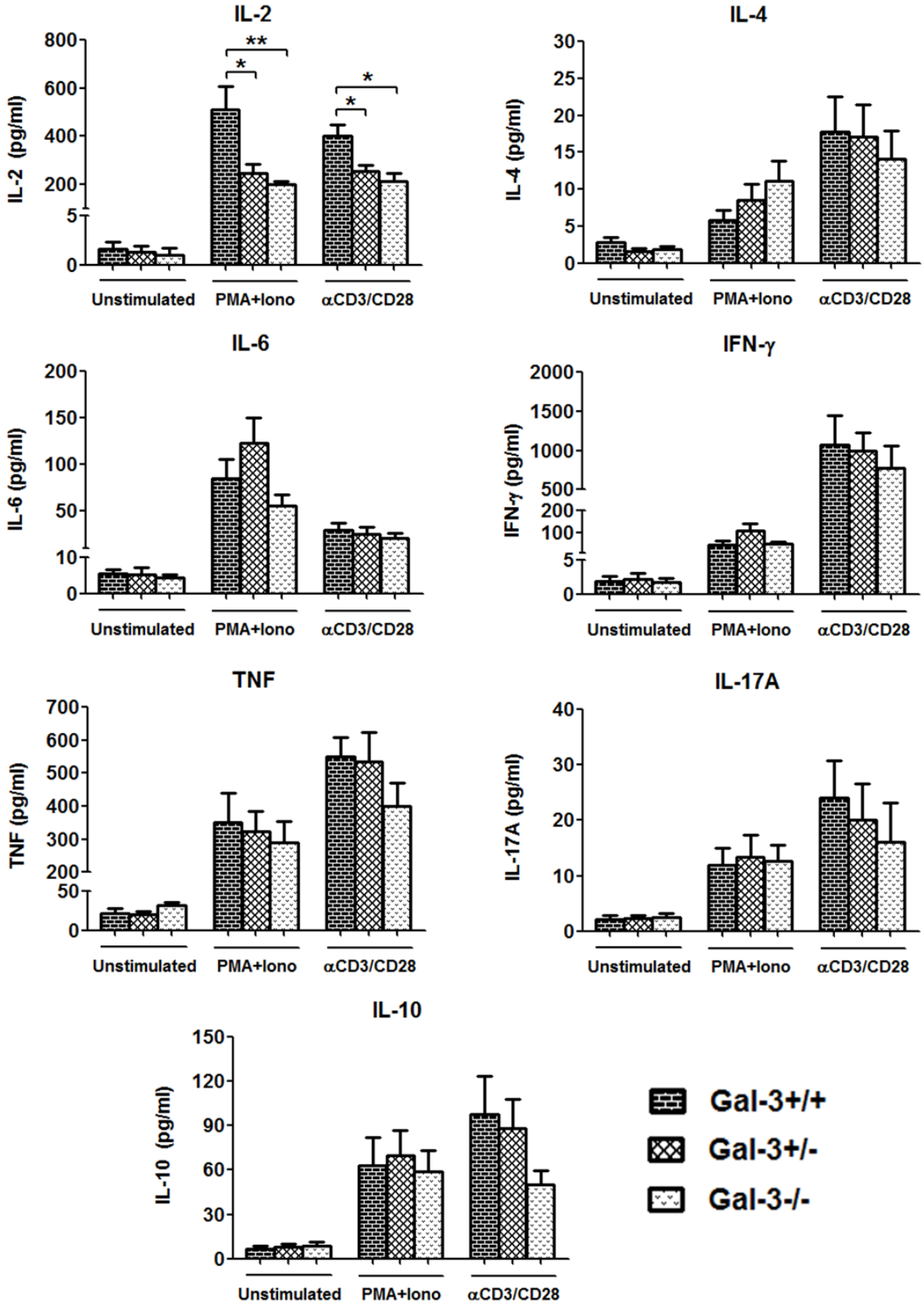

Figure 26: Th1/Th2/Th17 cytokine profile in cell free supernatants of *in vitro* stimulated splenocytes from Gal-3$^{+/+}$, Gal-3$^{+/-}$ and Gal-3$^{-/-}$ mice. Freshly isolated splenocytes (1.5 x 10^5 cells/ 100 µl medium/ well) of Gal-3$^{+/+}$, Gal-3$^{+/-}$ and Gal-3$^{-/-}$ mice were stimulated *in vitro* with either PMA (50 ng/ 10 µl/ well) + Ionomycin (50 ng/ 10 µl/ well) or plate bound anti-CD3 mAb (0.25 µg/ 30 µl/ well) + soluble anti-CD28 mAb (0.25 µg/ 10 µl/ well) in 96-well microtiter plates for 24 hours. Unstimulated splenocytes were used as control. After 24 hours, cell free supernatants were collected from each well and their cytokine profile was assessed by Th1/Th2/Th17 Cytometric Bead Array using flow cytometry. The graphs indicate concentrations (pg/ml) of respective Th1 (IL-2, IFN-γ, TNF), Th2 (IL-4, IL-6, IL-10) and Th17 (IL-17A) cytokines in splenocytes culture supernatants of Gal-3$^{+/+}$, Gal-3$^{+/-}$ and Gal-3$^{-/-}$ mice. Each graph represents consolidated data of 5 independent assays. Each set in the assay was performed in triplicate wells. *P<0.05, **P<0.01.

Survival study in Gal-3$^{+/+}$, Gal-3$^{+/-}$ and Gal-3$^{-/-}$ mice

Galectin-3 is an important regulator of diverse physiological functions in host [6-13]. In the present study, it was assessed whether endogenous galectin-3 levels influence overall survival in Gal-3$^{+/+}$, Gal-3$^{+/-}$ and Gal-3$^{-/-}$ mice under normal physiological conditions. Gal-3$^{+/+}$, Gal-3$^{+/-}$ and Gal-3$^{-/-}$ mice (10 mice per group) were kept under observation in the Laboratory Animal Facility, ACTREC to study their overall survival. Log-rank test was employed to determine whether the differences between the survival rates are statistically significant. By Kaplan-Meier survival curve analysis, it was observed that, the overall survival rate of Gal-3$^{+/-}$ mice group was significantly lower (P = 0.0232) than that of Gal-3$^{+/+}$ mice group (Figure 27). Further, the median survival rates of Gal-3$^{+/+}$, Gal-3$^{+/-}$ and Gal-3$^{-/-}$ mice exhibited striking differences i.e. 854 days, 674 days and 575 days, respectively.

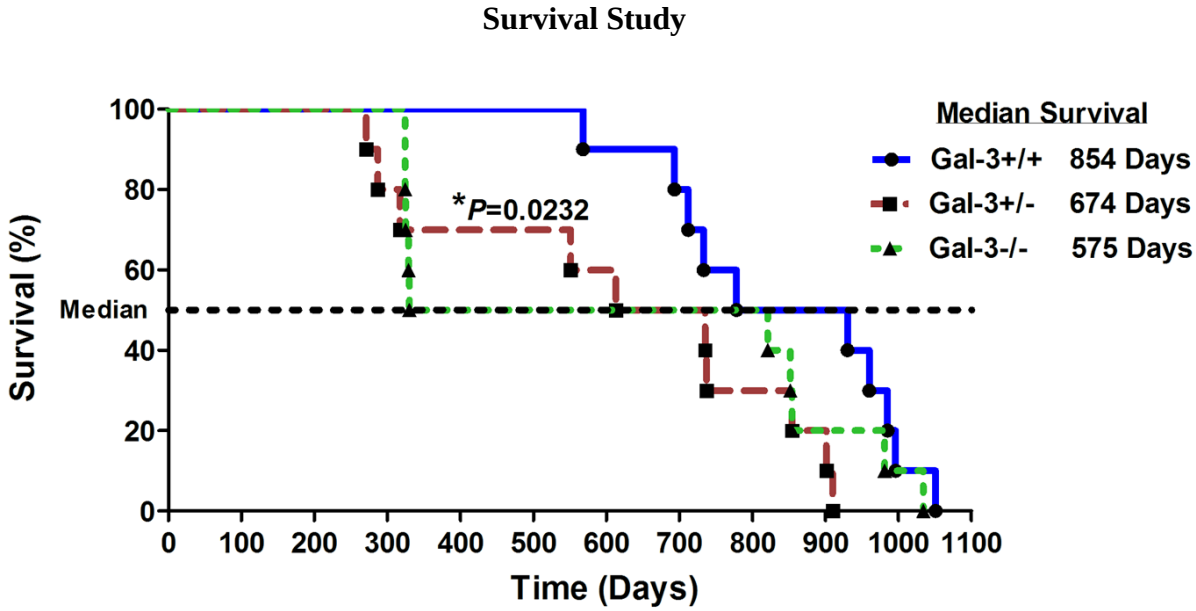

Figure 27: Survival curve of Gal-3$^{+/+}$, Gal-3$^{+/-}$ and Gal-3$^{-/-}$ mice groups. Gal-3$^{+/+}$, Gal-3$^{+/-}$ and Gal-3$^{-/-}$ mice (10 mice per group) were monitored till death to study their overall survival under normal physiological conditions. Survival rates were determined by standard Kaplan-Meier survival curve analysis. Each symbol in the graph represents age of one mouse calculated at the time of death (number of days). Black dotted horizontal line on the graph represents median survival rate of Gal-3$^{+/+}$, Gal-3$^{+/-}$ and Gal-3$^{-/-}$ mice groups (50% survival).

CHAPTER 5

Immune responses in Gal-3 wild type (Gal-$3^{+/+}$), Gal-3 hemizygous (Gal-$3^{+/-}$) and Gal-3 null (Gal-$3^{-/-}$) mice during progression of B16F10 lung metastasis

B16F10 murine melanoma pulmonary metastasis model is a well-established model system widely used to study organ specific metastasis of cancer cells. B16F10 murine melanoma is a highly aggressive and metastatic cell line [230,238,239]. Previous studies done using B16F10 murine melanoma model have shown that, interactions between galectin-3 on the mice lung endothelium and its high affinity ligand poly-*N*-acetyl lactosamine (polyLacNAc) on β1,6 branched N-oligosaccharides present on B16F10 melanoma cells facilitates B16F10 colonization in the lungs of the mice [26,30,32]. In the present study, striking differences were observed in the immune scenario of Gal-$3^{+/+,}$ Gal-$3^{+/-}$ and Gal-$3^{-/-}$ mice under normal physiological conditions i.e. in non-tumor-bearing conditions (Chapter 4). The results indicated possible dysregulation of immune responses in the complete absence of endogenous galectin-3 in Gal-$3^{-/-}$ mice. It was therefore interesting to analyze the immune status of Gal-$3^{+/+}$, Gal-$3^{+/-}$ and Gal-$3^{-/-}$ mice under the experimental metastasis assay conditions. The experiments performed were aimed at establishing lung metastasis of B16F10 murine melanoma cells in Gal-$3^{+/+,}$ Gal-$3^{+/-}$ and Gal-$3^{-/-}$ mice by experimental metastasis assay, assessing the frequency of pulmonary metastases developed at different time points (Day 7, Day 14 and Day 21) during progression of lung metastasis and simultaneously monitoring the immune responses (Day 7, Day 14 and Day 21) in Gal-$3^{+/+}$, Gal-$3^{+/-}$ and Gal-$3^{-/-}$ mice.

Experimental pulmonary metastasis assay using B16F10 murine melanoma cells

To establish experimental lung metastasis, single cell suspensions of B16F10 murine melanoma cells (1 x 10^5 cells/ 100 µl plain DMEM) were administered intravenously in the lateral tail vein of each mouse. At the desired time point post intravenous B16F10 injection, mice were sacrificed and lungs were collected by dissection to

assess the frequency of black colored (due to melanin pigment) metastatic melanoma colonies formed in the mice lungs.

Experimental Metastasis Assay: Day 7

On day 7 post intravenous injection of B16F10 cells in mice, visible metastatic melanoma colonies were not observed on the lungs of mice from any of the groups studied i.e. Gal-3$^{+/+}$, Gal-3$^{+/-}$ and Gal-3$^{-/-}$ mice (Figure 28A, lower panel) and the lungs appeared to be similar to those observed in Gal-3$^{+/+}$, Gal-3$^{+/-}$ and Gal-3$^{-/-}$ mice under normal physiological conditions (control mice) (Figure 28A, upper panel). Histopathological study of formalin fixed lung sections by hematoxylin-eosin staining confirmed the absence of melanoma colonies in Gal-3$^{+/+}$, Gal-3$^{+/-}$ and Gal-3$^{-/-}$ mice on day 7 under experimental metastasis assay conditions (Figure 1B, lower panel). Also, the histology of the lungs from Gal-3$^{+/+}$, Gal-3$^{+/-}$ and Gal-3$^{-/-}$ mice did not show any remarkable changes on day 7 post intravenous B16F10 injection (Figure 28B, lower panel) when compared with lung histology of control Gal-3$^{+/+}$, Gal-3$^{+/-}$ and Gal-3$^{-/-}$ mice i.e. under normal physiological conditions (Figure 28B, upper panel).

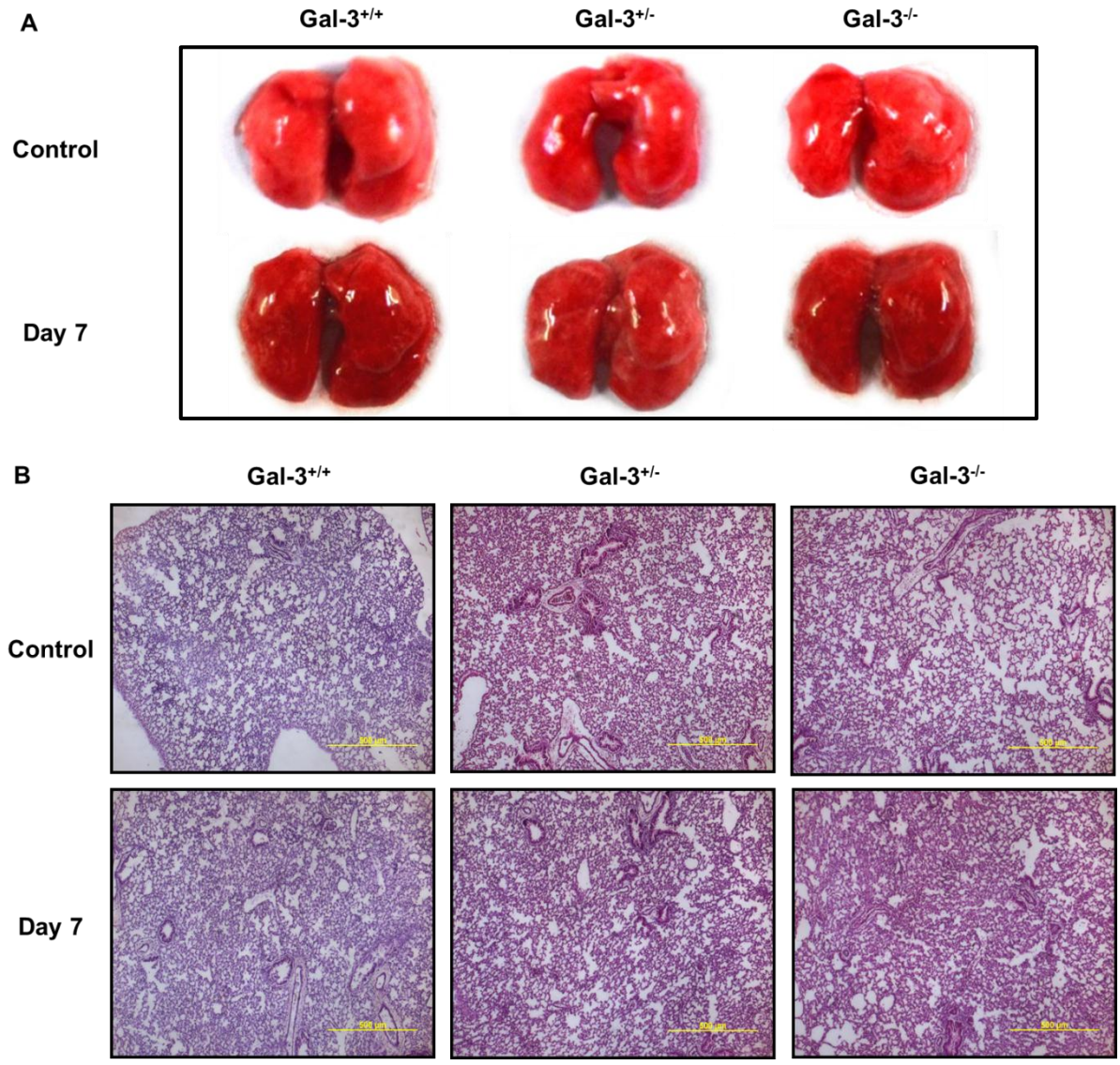

Figure 28: Absence of metastatic melanoma colonies in the lungs of Gal-3$^{+/+}$, Gal-3$^{+/-}$ and Gal-3$^{-/-}$ mice on day 7 post intravenous B16F10 injection. Experimental metastasis assay was done by lateral tail vein injection of B16F10 murine melanoma cells (1 x 10^5 cells / 100 µl plain DMEM) in each mouse of the Gal-3$^{+/+}$, Gal-3$^{+/-}$ and Gal-3$^{-/-}$ group. On day 7 post intravenous B16F10 injection, mice were sacrificed and lungs were collected by dissection. **(A)** The representative images of freshly dissected lungs from Gal-3$^{+/+}$, Gal-3$^{+/-}$ and Gal-3$^{-/-}$ mice group show absence of metastatic melanoma colonies on Day 7 (lower panel) similar to that as in control mice (upper panel). The assay was done 3 times independently using 6 mice per group in each assay. **(B)** Histopathology of Gal-3$^{+/+}$, Gal-3$^{+/-}$ and Gal-3$^{-/-}$ mice lungs under normal physiological conditions (Control mice; Upper panel) and on Day 7 post intravenous B16F10 injection using hematoxylin &

eosin staining. Paraffin embedded 5 µm thin sections of formalin fixed lungs were stained by hematoxylin (nuclear stain, violet) and eosin (cytoplasmic stain, Red). The stained sections were observed under upright microscope and the images were taken at 5X magnification. Scale Bar = 500 µm.

Experimental Metastasis Assay: Day 14

On day 14, black colored melanoma colonies were observed on the lungs of Gal-$3^{+/+}$, Gal-$3^{+/-}$ and Gal-$3^{-/-}$ mice. Metastatic melanoma colonies on the surfaces of the lungs were counted using dissecting microscope. Interestingly, the numbers of lung melanoma colonies were almost equal in Gal-$3^{+/+}$ and Gal-$3^{-/-}$ mice and were found to be significantly lower in Gal-$3^{+/-}$ mice compared to Gal-$3^{+/+}$ and Gal-$3^{-/-}$ mice (Figure 29A-B). Histopathological study of formalin fixed lung sections by hematoxylin-eosin staining confirmed these results (Figure 29C).

Experimental Metastasis Assay: Day 14

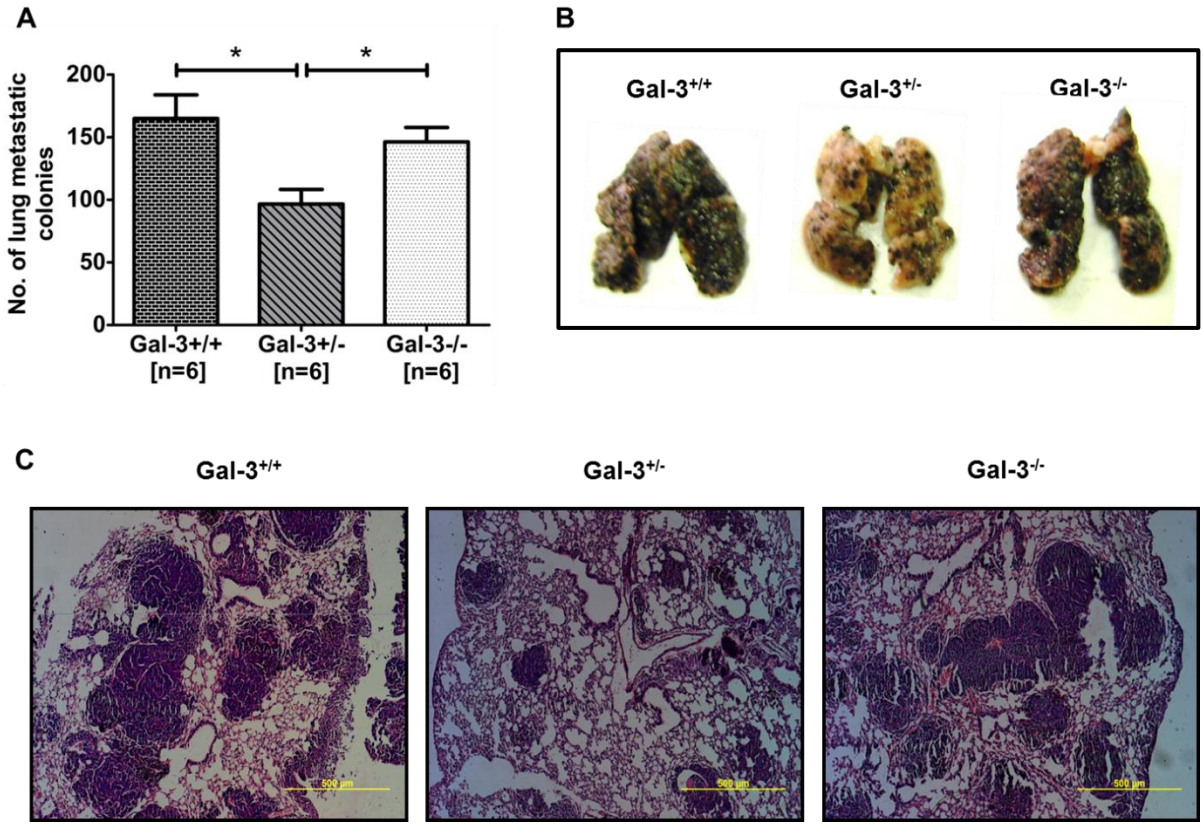

Figure 29: Pulmonary metastasis of B16F10 murine melanoma cells in Gal-3$^{+/+}$, Gal-3$^{+/-}$ and Gal-3$^{-/-}$ mice on day 14. Experimental metastasis assay was performed by lateral tail vein injection of B16F10 murine melanoma cells (1 x 10^5 cells / 100 µl plain DMEM) in each mouse of the Gal-3$^{+/+}$, Gal-3$^{+/-}$ and Gal-3$^{-/-}$ group. On day 14 post intravenous B16F10 injection, mice were sacrificed and lungs were collected by dissection. The assay was done 3 times independently using 6 mice per group in each assay. **(A)** Frequencies of metastatic melanoma colonies on the mice lungs on Day 14. The numbers of melanoma colonies on each mouse lung were counted using a dissecting microscope. The graph shows mean data of one representative experiment done using 6 mice per group. *p<0.05. **(B)** Representative images of lungs bearing black colored metastatic B16F10 melanoma colonies on Day 14 in each mice group. The lungs were fixed in 10% neutral buffered formalin after dissection. Each black colored dot on the lungs represents a melanoma colony. **(C)** Histopathology of mice lungs showing metastatic melanoma colonies on Day 14 using hematoxylin & eosin staining. Paraffin embedded 5 µm thin sections of formalin fixed lungs were stained by hematoxylin (nuclear stain, violet) and eosin (cytoplasmic stain, Red). The stained sections were observed under upright microscope and the images were taken at 5X magnification. Scale Bar = 500 µm.

Experimental Metastasis Assay: Day 21

On Day 21 of the experimental metastasis assay, numbers of metastatic melanoma colonies formed in Gal-3$^{+/+}$, Gal-3$^{+/-}$ and Gal-3$^{-/-}$ mice lungs exceeded the manually countable limit and the lungs were flooded with black colored melanoma colonies in all the three groups of mice studied (Figure 30A). Histopathological study of formalin fixed lung sections by hematoxylin-eosin staining confirmed these findings. On day 21, large sized metastatic melanoma colonies formed in the mice lungs seemed to merge with each other, as observed in the hematoxylin-eosin stained lung sections of Gal-3$^{+/+}$, Gal-3$^{+/-}$ and Gal-3$^{-/-}$ mice using upright microscope (Figure 30B).

Experimental Metastasis Assay: Day 21

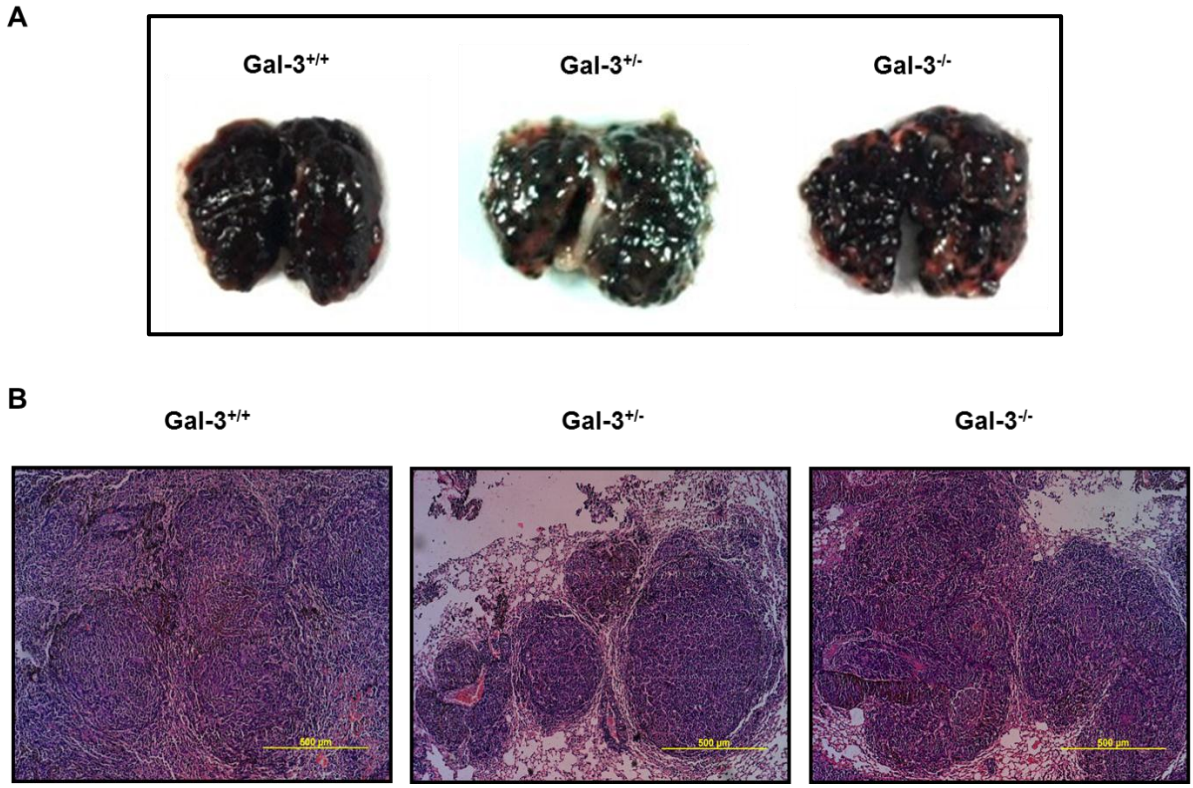

Figure 30: B16F10 lung metastasis in Gal-3$^{+/+}$, Gal-3$^{+/-}$ and Gal-3$^{-/-}$ mice on day 21 of experimental metastasis assay. On day 21 post intravenous B16F10 injection, mice were sacrificed and lungs were collected by dissection. The assay was done 3 times independently using 6 mice per group in each assay. **(A)** Representative images of dissected mice lungs flooded with metastatic B16F10 melanoma colonies in each mice group on day 21. The lungs were fixed in 10% neutral buffered formalin after dissection. Each black dot on the lungs represents a melanoma colony. **(B)** Histopathology of lungs showing melanoma colonies using hematoxylin & eosin staining. Paraffin embedded 5 µm thin sections of formalin fixed lungs were stained by hematoxylin (nuclear stain, violet) and eosin (cytoplasmic stain, Red). The stained sections were observed under upright microscope and the images were taken at 5X magnification. Scale Bar = 500 µm.

Immune cell subsets in splenocytes of Gal-3$^{+/+}$, Gal-3$^{+/-}$ and Gal-3$^{-/-}$ mice bearing pulmonary melanoma metastases

To check whether reduction or total absence of endogenous galectin-3 levels in the host influences the frequency of major immune cell subtypes in the splenocytes of mice under experimental metastasis assay conditions, immunophenotyping of splenocytes isolated from Gal-3$^{+/+}$, Gal-3$^{+/-}$ and Gal-3$^{-/-}$ mice on day 7, day 14 and day 21 post intravenous B16F10 injection was performed. Lymphocyte or macrophage populations were gated based on their forward scatter (FSC) and side scatter (SSC) characteristics in the flow cytometric analysis.

Innate immune cell subsets in mice splenocytes

To study the cell subsets of innate immune compartment in Gal-3$^{+/+}$, Gal-3$^{+/-}$ and Gal-3$^{-/-}$ mice during progression of lung melanoma metastasis, immunophenotyping of splenocytes was done. On day 7 as well as on day 21 of the experimental metastasis assay, no significant differences were observed in the percentages of splenic NK (CD3^{-}NK1.1^{+}) cells, NKT cells (CD3^{+}NK1.1^{+}), γδ T cells (CD3^{+}γδ^{+}), dendritic cells (CD209^{+}) and macrophages (CD14^{+}) in the splenocytes of Gal-3$^{+/+}$, Gal-3$^{+/-}$ and Gal-3$^{-/-}$ mice (Figure 31A and 31C). Interestingly, on day 14, percentages of splenic NK (CD3^{-}NK1.1^{+}) cells were found to be significantly lower in Gal-3$^{-/-}$ mice compared to Gal-3$^{+/+}$ and Gal-3$^{+/-}$ mice. The percentages of splenic NK cells correlated positively with the *LGALS3* gene dosage in Gal-3$^{+/+}$, Gal-3$^{+/-}$ and Gal-3$^{-/-}$ mice on day 14. No significant differences were observed in the percentages of NKT cells (CD3^{+}NK1.1^{+}), γδ T cells (CD3^{+}γδ^{+}), dendritic cells (CD209^{+}) and macrophages (CD14^{+}) in splenocytes of Gal-3$^{+/+}$, Gal-3$^{+/-}$ and Gal-3$^{-/-}$ mice on day 14 of experimental metastasis assay (Figure 31B).

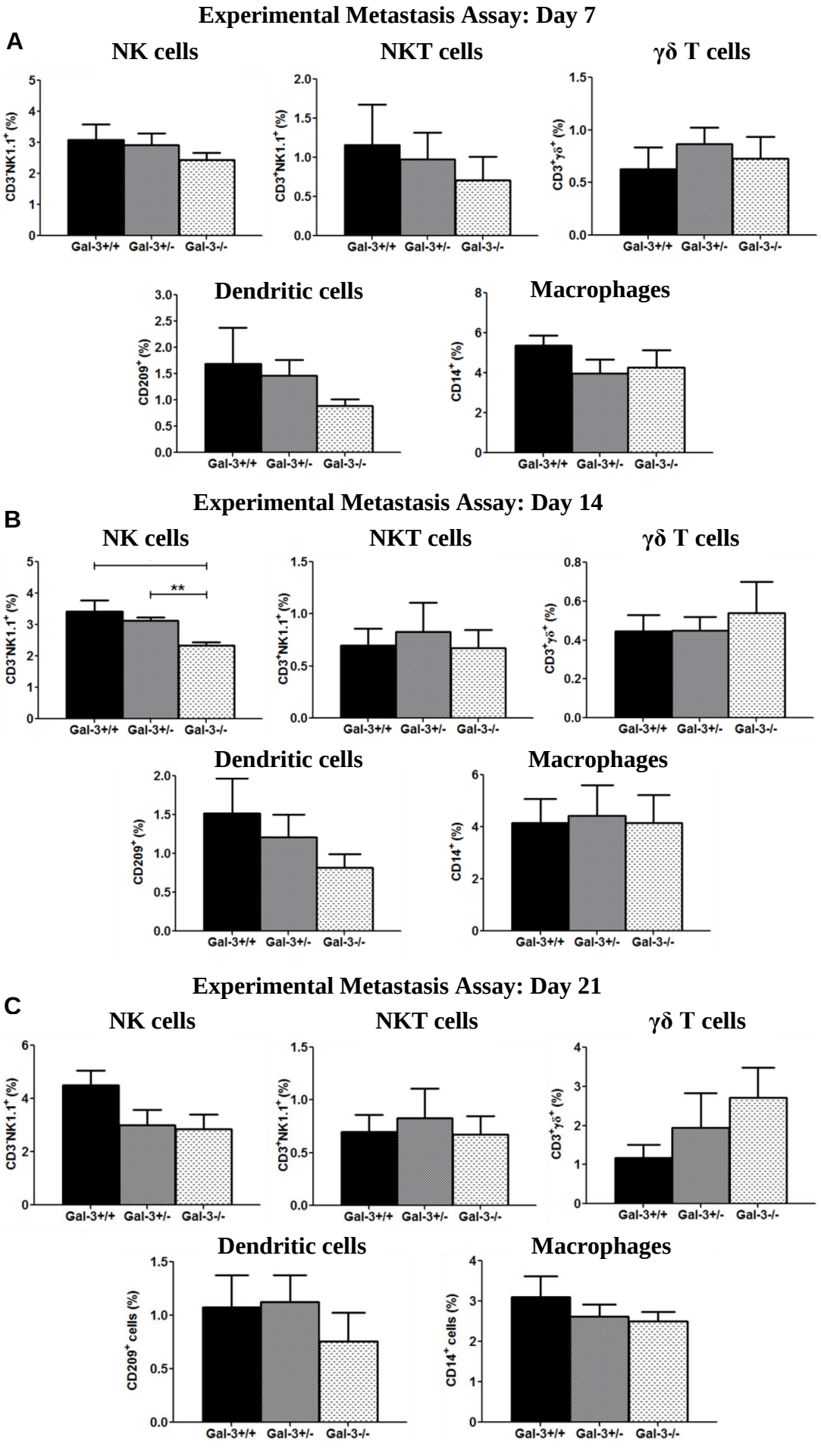
Experimental Metastasis Assay: Day 7
A
NK cells
NKT cells
γδ T cells
CD3⁻NK1.1⁺ (%)
CD3⁺NK1.1⁺ (%)
CD3⁺γδ⁺ (%)
Gal-3+/+ Gal-3+/- Gal-3-/-
Dendritic cells
Macrophages
CD209⁺ (%)
CD14⁺ (%)
Experimental Metastasis Assay: Day 14
B
NK cells
NKT cells
γδ T cells
**
Dendritic cells
Macrophages
Experimental Metastasis Assay: Day 21
C
NK cells
NKT cells
γδ T cells
Dendritic cells
Macrophages
CD209⁺ cells (%)
CD14⁺ cells (%)

Figure 31: Innate immune cell subsets in splenocytes of Gal-3$^{+/+}$, Gal-3$^{+/-}$ and Gal-3$^{-/-}$ mice bearing lung melanoma metastases. Single cell suspensions of spleen cells were prepared from Gal-3$^{+/+}$, Gal-3$^{+/-}$ and Gal-3$^{-/-}$ mice sacrificed on day 7, day 14 and day 21 post intravenous B16F10 melanoma cell injection. The cells were fixed, subjected to surface antibody staining and analyzed by multicolor flow cytometry. Frequencies of NK cells ($CD3^{-}NK1.1^{+}$), NKT cells ($CD3^{+}NK1.1^{+}$), γδ T cells ($CD3^{+}\gamma\delta^{+}$)**,** dendritic cells ($CD209^{+}$) and macrophages ($CD14^{+}$) in mice splenocytes on (**A**) day 7, (**B**) day 14 and (**C**) day 21 of experimental metastasis assay conditions. The graphs represent consolidated data of 3 independent experiments for each time point. *P <0.05, **P <0.01.

Adaptive immune cell subsets in mice splenocytes

To study the key players of adaptive immune responses, the levels of total $CD3^{+}$ T cells, helper T cells (T_H, $CD3^{+}CD4^{+}$), cytotoxic T cells ($T_{C,}$ $CD3^{+}CD8^{+}$) and B cells ($B220^{+}$) in Gal-3$^{+/+}$, Gal-3$^{+/-}$ and Gal-3$^{-/-}$ mice splenocytes were checked by immunophenotyping analysis. No significant differences were observed in the percentages of any of these cell subsets in the splenocytes of Gal-3$^{+/+}$, Gal-3$^{+/-}$ and Gal-3$^{-/-}$ mice on day 7 (Figure 32A), day 14 (Figure 32B) as well as on day 21 (Figure 32C) post intravenous B16F10 injection.

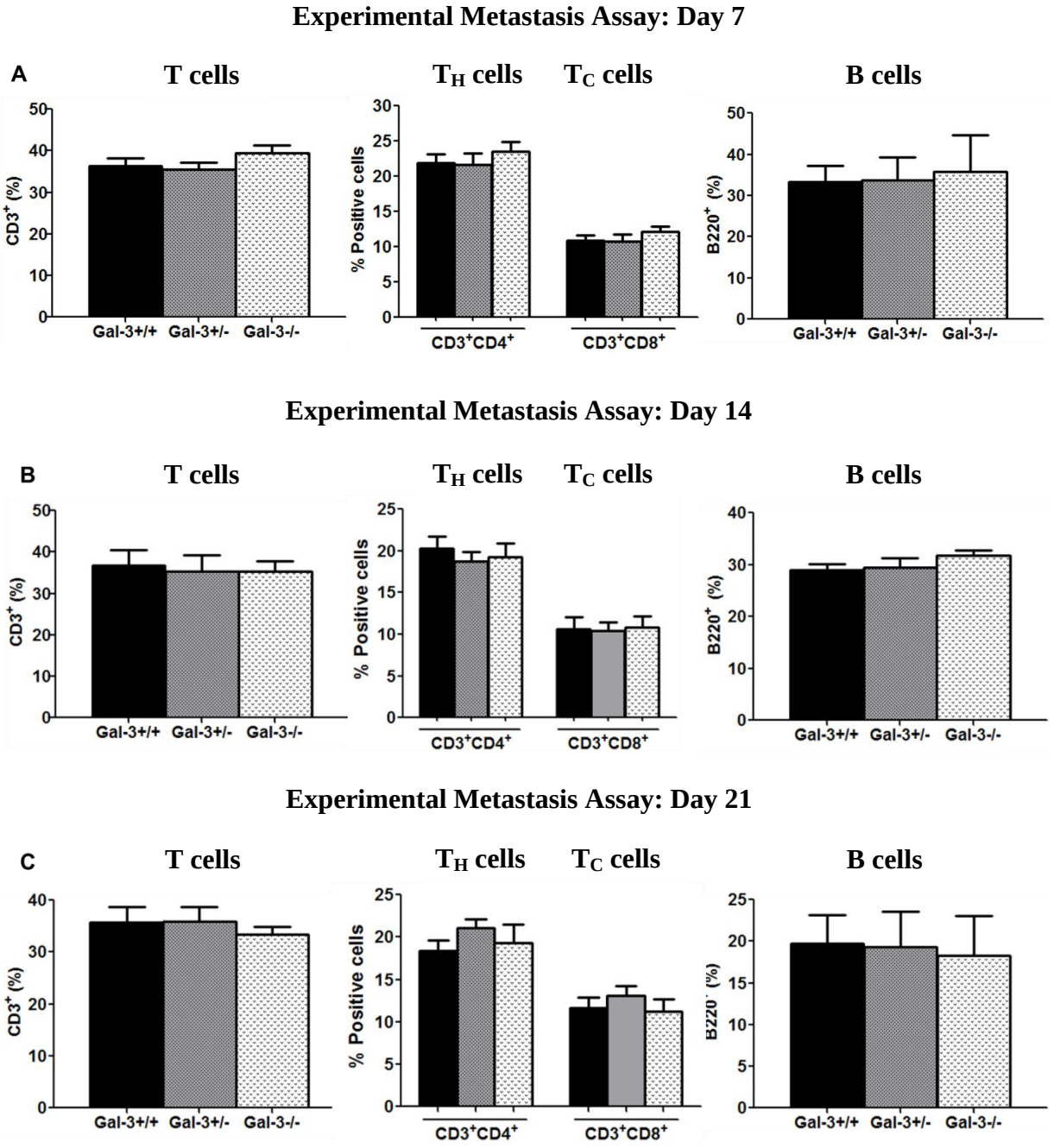

Figure 32: Adaptive immune cell subsets in splenocytes of Gal-3$^{+/+}$, Gal-3$^{+/-}$ and Gal-3$^{-/-}$ mice bearing lung melanoma metastases. Single cell suspensions of spleen cells were prepared from Gal-3$^{+/+}$, Gal-3$^{+/-}$ and Gal-3$^{-/-}$ mice sacrificed on day 7, day 14 and day 21 post intravenous B16F10 melanoma cell injection. The cells were fixed, subjected to surface antibody staining and analyzed by multicolor flow cytometry. Frequencies of T cells (CD3$^+$), helper T cells (T_H, CD3$^+$CD4$^+$), cytotoxic T cells (T_C, CD3$^+$CD8$^+$) and B cells (B220$^+$) in mice splenocytes on (**A**) day 7, (**B**) day 14 and (**C**) day 21 in experimental metastasis assay conditions. The graphs represent consolidated data of 3 independent experiments for each time point.

Regulatrory T cells in mice splenocytes

Regulatory T cells (T_{reg}) play an active and significant role in the progression of cancer and have an important role in suppressing tumor-specific immunity [305]. In the present study, immunophenotyping of T_{reg} was performed to compare the splenic $CD4^+CD25^+Foxp3^+$ T_{reg} populations in Gal-$3^{+/+}$, Gal-$3^{+/-}$ and Gal-$3^{-/-}$ mice during progression of lung melanoma metastasis. Lymphocytes were gated based on their forward scatter (FSC) and side scatter (SSC) characteristics followed by subsequent gating as represented (Figure 33A). It was observed that, percentages of $CD4^+CD25^+Foxp3^+$ T_{reg} in the splenocytes of Gal-$3^{+/+}$, Gal-$3^{+/-}$ and Gal-$3^{-/-}$ mice sacrificed on day 7 (Figure 33B), day 14 (Figure 33C) as well as on day 21 (Figure 33D) post intravenous B16F10 injection did not differ significantly.

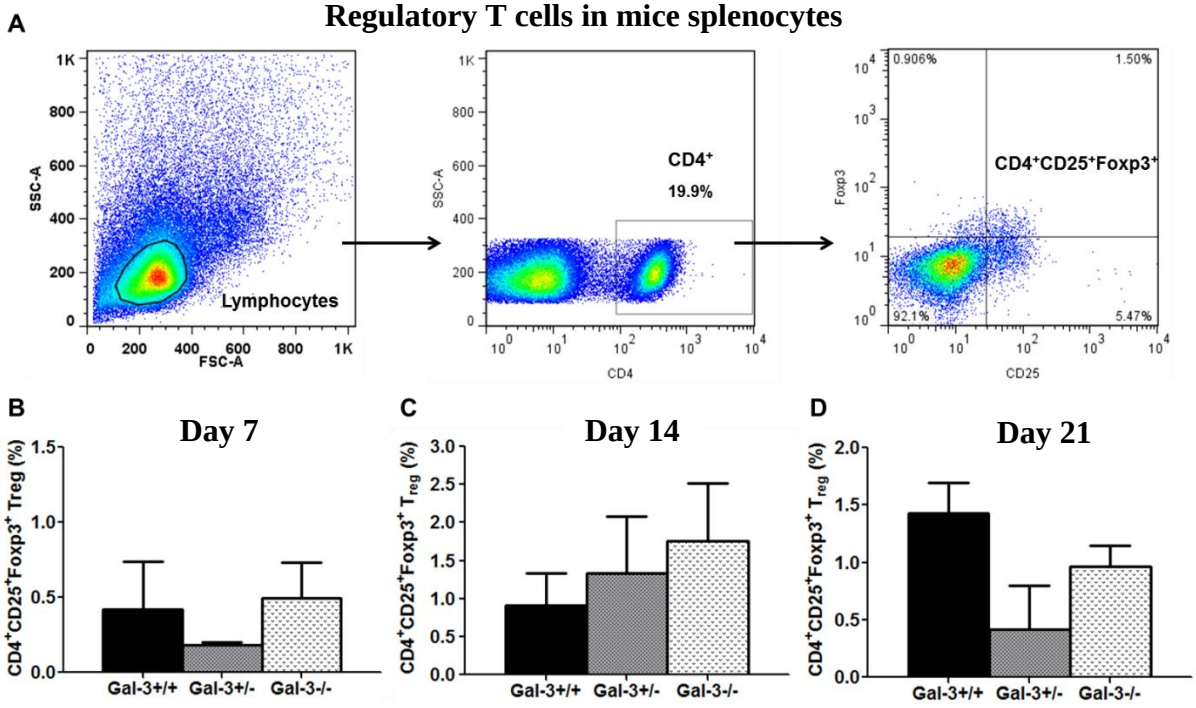

Figure 33: Regulatory T cells in Gal-$3^{+/+}$, Gal-$3^{+/-}$ and Gal-$3^{-/-}$ mice splenocytes during progression of lung metastasis. (A) Gating strategy of $CD4^+CD25^+Foxp3^+$ regulatory T cells (T_{reg}) in mice splenocytes. Percentages of $CD4^+CD25^+Foxp3^+$ T_{reg} in the splenocytes of Gal-$3^{+/+}$, Gal-$3^{+/-}$ and Gal-$3^{-/-}$ mice sacrificed on **(B)** day 7 **(C)** day 14 and **(D)** day 21 of the experimental metastasis assay. The graphs represent consolidated data of 3 independent experiments for each time point.

T cell subsets in mice thymocytes

Immunophenotyping of thymocytes from Gal-$3^{+/+}$, Gal-$3^{+/-}$ and Gal-$3^{-/-}$ mice indicated that intrathymic T cell differentiation was not affected by different endogenous galectin-3 expression levels in these mice under normal physiological conditions (Chapter 4). It was further analyzed whether differences in endogenous galectin-3 levels influence T cell differentiation and maturation in Gal-$3^{+/+}$, Gal-$3^{+/-}$ and Gal-$3^{-/-}$ mice thymocytes during progression of B16F10 lung metastasis. Based on T cell lineage markers, the percentages of thymocytes at different stages of maturation i.e. $CD4^+CD8^-$ (CD4 Single positive), $CD4^-CD8^+$ (CD8 Single positive), $CD4^+CD8^+$ (Double positive) and $CD4^-CD8^-$ (Double negative) were analyzed by dual color immunophenotyping using flow cytometry under experimental metastasis assay conditions in Gal-$3^{+/+}$, Gal-$3^{+/-}$ and Gal-$3^{-/-}$ mice.

It was noted that, on day 7, day 14 and day 21 post intravenous B16F10 injection, percentages of $CD4^+CD8^-$ (CD4 Single positive), $CD4^-CD8^+$ (CD8 Single positive), $CD4^+CD8^+$ (Double positive) as well as $CD4^-CD8^-$ (Double negative) thymocyte subsets in Gal-$3^{+/+}$, Gal-$3^{+/-}$ and Gal-$3^{-/-}$ mice did not differ significantly (Figure 34A-C). The results indicated that intra thymic T cell differentiation remains unaffected by differences in the expression levels of endogenous galectin-3 in Gal-$3^{+/+}$, Gal-$3^{+/-}$ and Gal-$3^{-/-}$ mice during progression of experimental lung metastasis.

A **Experimental Metastasis Assay: Day 7**

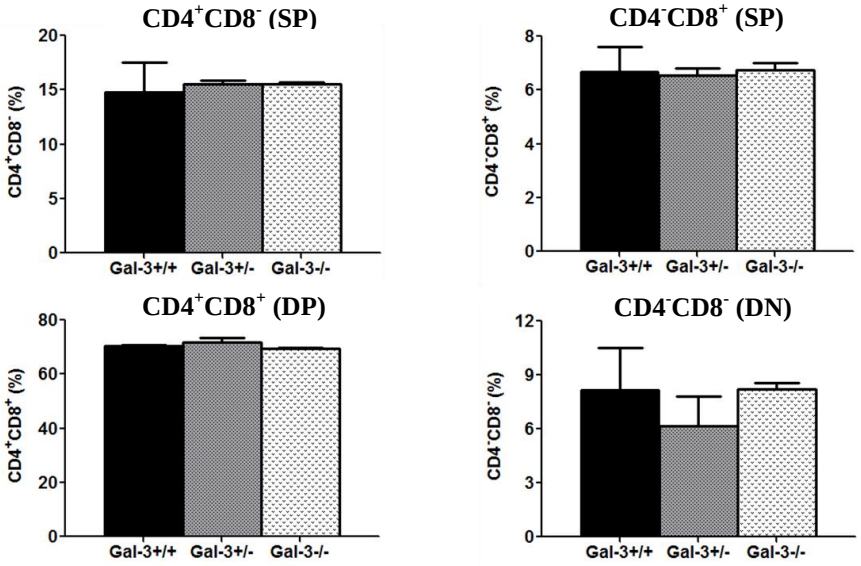

B **Experimental Metastasis Assay: Day 14**

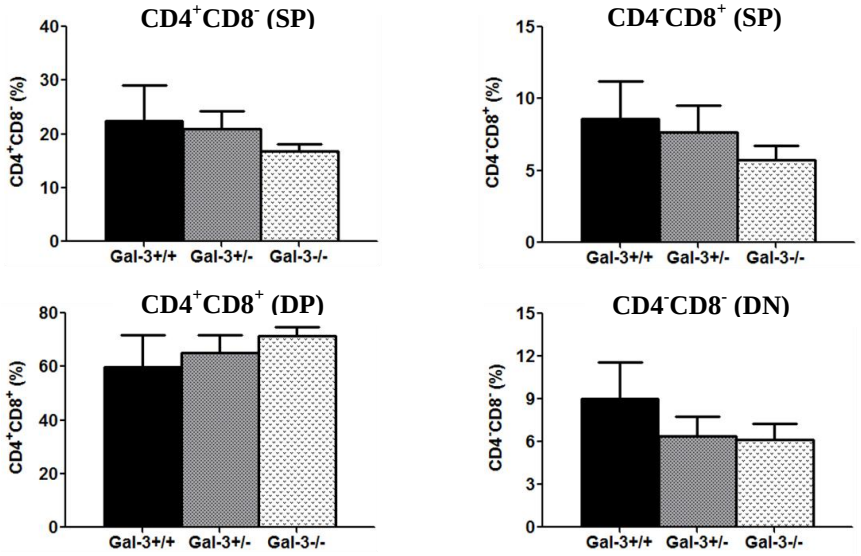

C **Experimental Metastasis Assay: Day 21**

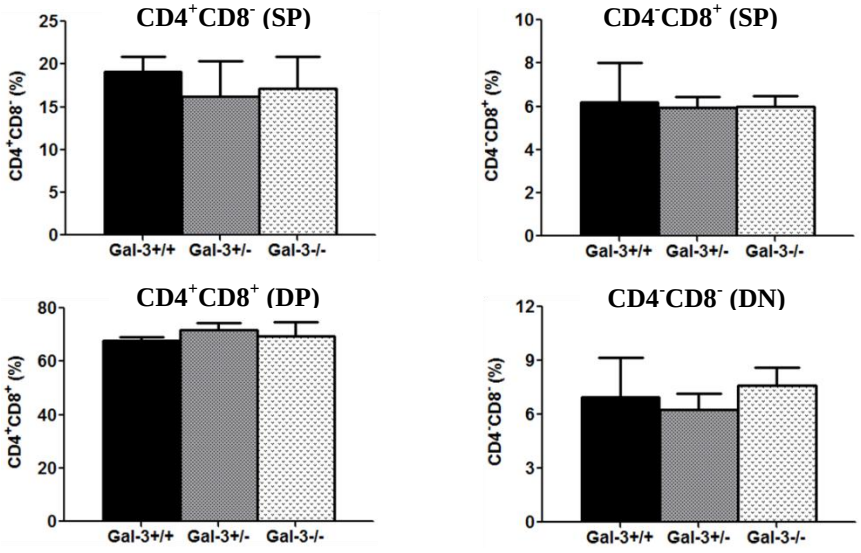

Figure 34: Thymic T cell subsets in Gal-3$^{+/+}$, Gal-3$^{+/-}$ and Gal-3$^{-/-}$ mice during progression of B16F10 lung metastasis. Single cell suspensions of thymocytes were prepared from Gal-3$^{+/+}$, Gal-3$^{+/-}$ and Gal-3$^{-/-}$ mice sacrificed on day 7, day 14 and day 21 post intravenous B16F10 injection. The cells were fixed, subjected to surface antibody staining and analyzed by dual color immunophenotyping using flow cytometry. The graphs indicate frequencies of $CD4^+CD8^-$ (CD4 Single positive, SP), $CD4^-CD8^+$ (CD8 Single positive, SP), $CD4^+CD8^+$ (Double positive, DP) and $CD4^-CD8^-$ (Double negative, DN) thymocytes in Gal-3$^{+/+}$, Gal-3$^{+/-}$ and Gal-3$^{-/-}$ mice on **(A)** day 7, **(B)** day 14 and **(C)** day 21. The graphs represent consolidated data of 3 independent experiments for each time point.

Lung infiltrating leukocytes in Gal-3$^{+/+}$, Gal-3$^{+/-}$ and Gal-3$^{-/-}$ mice bearing pulmonary melanoma metastases

As mentioned earlier, a distinct pattern of B16F10 melanoma metastasis was observed in the lungs of Gal-3$^{+/+}$, Gal-3$^{+/-}$ and Gal-3$^{-/-}$ mice on day 14 post intravenous B16F10 injection. At this time point, numbers of lung melanoma colonies were almost equal in Gal-3$^{+/+}$ and Gal-3$^{-/-}$ mice and were found to be significantly lower in Gal-3$^{+/-}$ mice compared to Gal-3$^{+/+}$ and Gal-3$^{-/-}$ mice (Figure 29). It was therefore interesting to analyze whether the percentages of lung infiltrating leukocytes, which could possibly recognize and target metastatic cancer cells in the mice lungs, differed in Gal-3$^{+/+}$, Gal-3$^{+/-}$ and Gal-3$^{-/-}$ mice during experimental metastasis assay conditions. Single cell suspensions of freshly dissected mice lungs were prepared by enzymatic degradation as described in the Materials and Methods chapter. Immunophenotyping was performed to analyze the frequencies of different immune cell subsets infiltrating the mice lungs on day 7, day 14 and day 21 post intravenous B16F10 injection in Gal-3$^{+/+}$, Gal-3$^{+/-}$ and Gal-3$^{-/-}$ mice (Figure 35A-C).

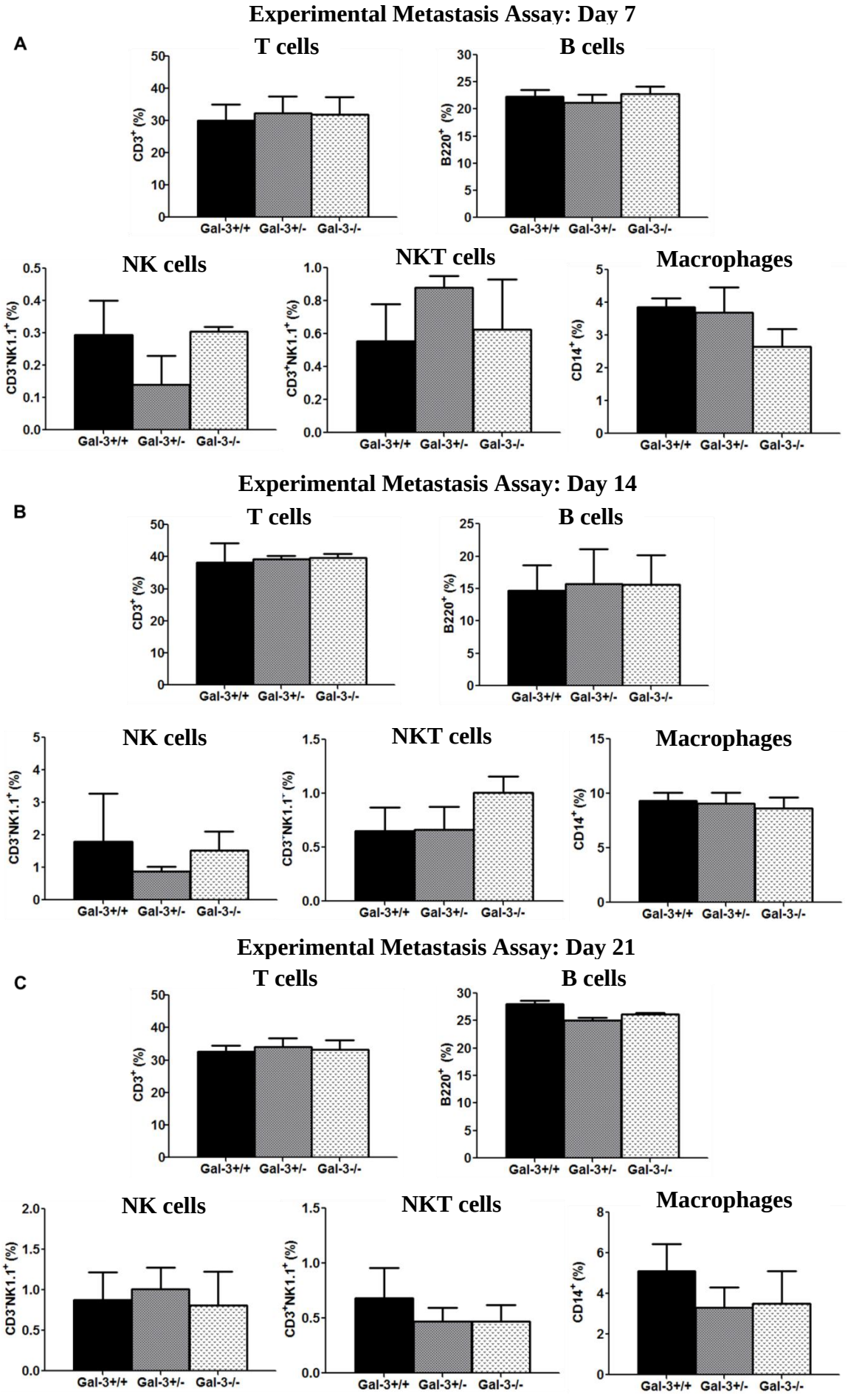
Experimental Metastasis Assay: Day 7
A
T cells
B cells
NK cells
NKT cells
Macrophages
Experimental Metastasis Assay: Day 14
B
T cells
B cells
NK cells
NKT cells
Macrophages
Experimental Metastasis Assay: Day 21
C
T cells
B cells
NK cells
NKT cells
Macrophages
Gal-3+/+ Gal-3+/- Gal-3-/-

Figure 35: Lung infiltrating leukocytes in Gal-3$^{+/+}$, Gal-3$^{+/-}$ and Gal-3$^{-/-}$ mice bearing pulmonary melanoma metastases. Single cell suspensions were prepared by enzymatic digestion from the lungs of Gal-3$^{+/+}$, Gal-3$^{+/-}$ and Gal-3$^{-/-}$ mice sacrificed on day 7, day 14 and day 21 post intravenous B16F10 melanoma injection. The cells were fixed, subjected to surface antibody staining and analyzed by multicolor flow cytometry. Frequencies of T cells ($CD3^+$), B cells ($B220^+$), NK cells ($CD3^-NK1.1^+$), NKT cells ($CD3^+NK1.1^+$) and macrophages ($CD14^+$) in mice on **(A)** day 7, **(B)** day 14 and **(C)** day 21 of experimental metastasis assay conditions. The graphs represent consolidated data of 3 independent experiments for each time point.

Lymphocytes or macrophages populations were gated based on their forward scatter (FSC) and side scatter (SSC) characteristics followed by subsequent gating for cell surface markers expressions on each of the immune cell types studied. It was observed that, percentages of lung infiltrating T cells ($CD3^+$), B cells ($B220^+$), NK cells ($CD3^-NK1.1^+$), NKT cells ($CD3^+NK1.1^+$) and macrophages ($CD14^+$) did not differ significantly in Gal-3$^{+/+}$, Gal-3$^{+/-}$ and Gal-3$^{-/-}$ mice bearing lung metastases on day 7 (Figure 35A), day 14 (Figure 35B) as well as on day 21 (Figure 35C) post intravenous B16F10 injection.

Proliferative responses of *in vitro* stimulated splenocytes from Gal-3$^{+/+}$, Gal-3$^{+/-}$ and Gal-3$^{-/-}$ mice bearing lung melanoma metastases

Functional immune responses were monitored during progression of B16F10 lung metastasis in Gal-3$^{+/+}$, Gal-3$^{+/-}$ and Gal-3$^{-/-}$ mice i.e. on Day 7, Day 14 and Day 21. The ability of splenocytes isolated from Gal-3$^{+/+}$, Gal-3$^{+/-}$ and Gal-3$^{-/-}$ mice to respond to stimulants *in vitro* was assessed. The proliferative responses of stimulated splenocytes were compared between the three groups of mice using [^{3}H] thymidine incorporation assay as described in the Material and Methods chapter. On Day 7, Day 14 as well as Day 21 of the experimental metastasis assay conditions, splenocytes (1.5 x 10^5 cells/ well) of Gal-3$^{-/-}$

mice stimulated *in vitro* with PMA (50 ng/ well) + Ionomycin (50 ng/ well) as well as plate-bound anti-CD3 mAb (0.25 μg/ well) + soluble anti-CD28 mAb (0.25 μg/ well) showed remarkably higher proliferative responses, than Gal-$3^{+/+}$ and Gal-$3^{+/-}$ mice splenocytes (Figure 36A-C). Upon *in vitro* stimulation using anti-CD3/CD28 (0.25 μg each/ well), proliferation of Gal-$3^{+/-}$ and Gal-$3^{-/-}$ splenocytes was found to be significantly increased than that of Gal-$3^{+/+}$ splenocytes on day 7 (Figure 36A). On day 14 post intravenous B16F10 injection in mice, proliferative responses of Gal-$3^{+/+}$, Gal-$3^{+/-}$ and Gal-$3^{-/-}$ mice splenocytes stimulated *in vitro* using PMA (50 ng/ well) + Ionomycin (50 ng/ well) exhibited *LGALS3* gene dosage effect, with inverse correlation to endogenous galectin-3 expression levels in the three mice groups (Figure 36B). Interestingly, on day 21 of the experimental metastasis assay when the lungs of mice from all the three groups were flooded with metastatic melanoma colonies, a marked decrease in the proliferative ability of splenocytes from Gal-$3^{+/+}$, Gal-$3^{+/-}$ and Gal-$3^{-/-}$ mice, in response to *in vitro* stimulation with PMA + Ionomycin as well as anti-CD3/CD28 mAbs, was noted as indicated by remarkably lower radioactive counts of ^{3}H-TdR incorporated (CPM) (Figure 36C).

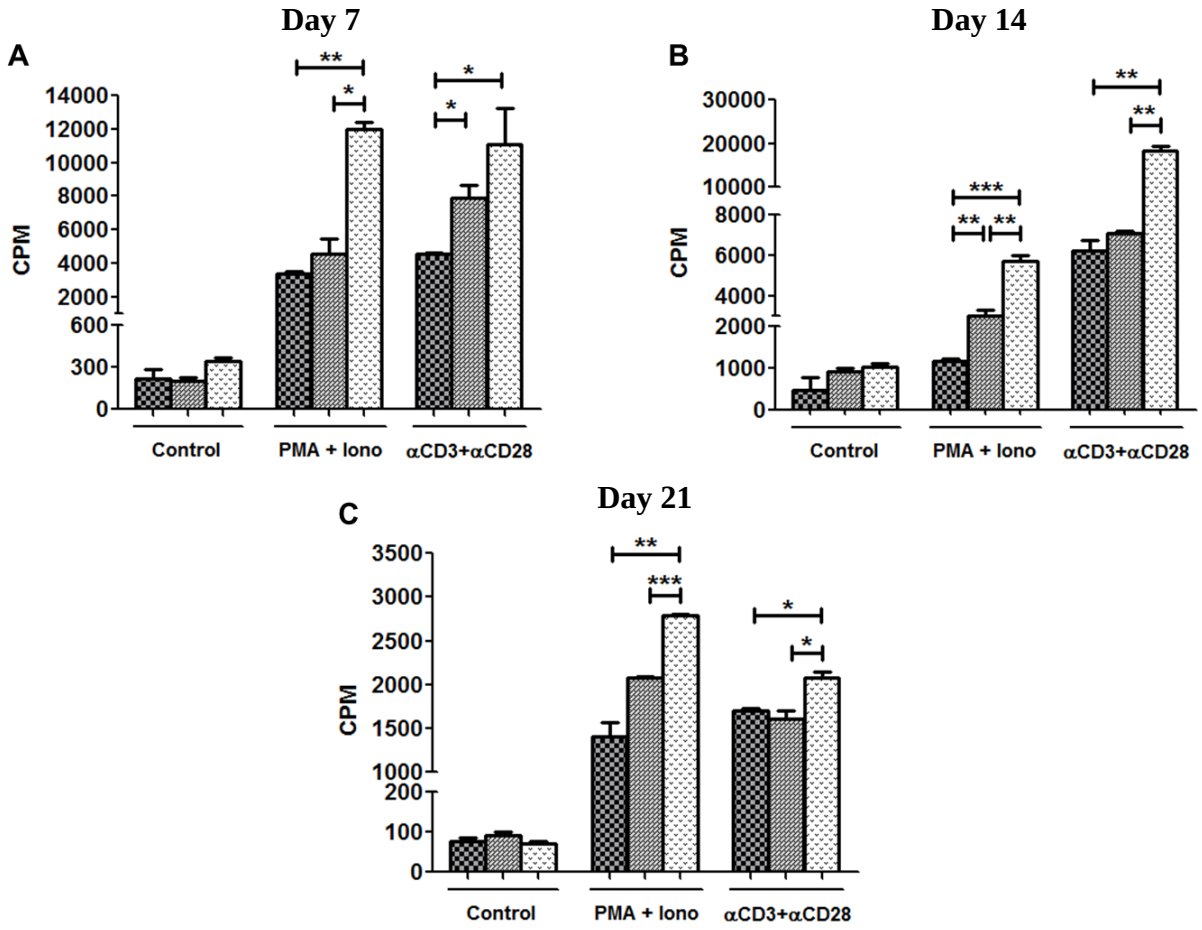

Figure 36: Proliferative responses in Gal-3$^{+/+}$, Gal-3$^{+/-}$ and Gal-3$^{-/-}$ mice splenocytes as measured by [^{3}H] thymidine incorporation assay during progression of experimental lung metastasis. Gal-3$^{+/+}$, Gal-3$^{+/-}$ and Gal-3$^{-/-}$ mice were sacrificed on **(A)** day 7, **(B)** day 14 and **(C)** day 21 post intravenous B16F10 melanoma cell injection. Freshly isolated splenocytes (1.5 x 10^5 cells/ 100 µl medium/ well) of mice were stimulated with either PMA (50 ng/ 10 µl/ well) + Ionomycin (50 ng/ 10 µl/ well) or plate bound anti-CD3 mAb (0.25 µg/ 30 µl/ well) + soluble anti-CD28 mAb (0.25 µg/ 10 µl/ well) in 96-well microtiter plate for 72 hours. Unstimulated splenocytes were used as control. The graphs represent consolidated data of 3 independent assays for each time point as radioactive counts per minute (CPM). Each set in the assay was performed in triplicate wells. **P*<0.05, ***P*<0.01, ****P*<0.001.

Intracellular calcium flux upon *in vitro* stimulation of lymphocytes from Gal-3$^{+/+}$, Gal-3$^{+/-}$ and Gal-3$^{-/-}$ mice during experimental metastasis assay conditions

Calcium ions (Ca^{++}) act as important secondary messengers in T cell signaling leading to various T cell responses. In the present study, the flux of intracellular Ca^{++} ions on stimulation of Fluo-3-AM labeled splenocytes *in vitro* was analyzed as per the protocol described in the Materials and Methods chapter. In the lung metastasis model, upon *in vitro* stimulation of freshly isolated mice splenocytes (1×10^6 cells) using PMA (100 ng) + Ionomycin (500 ng) (Figure 37A) or anti-CD3 mAb (1 μg) (Figure 37B), Gal-3$^{+/-}$ and Gal-3$^{-/-}$ mice splenocytes showed reduced intracellular Ca^{++} flux compared to Gal-3$^{+/+}$ mice.

On day 7, when no metastatic melanoma colonies were observed in the mice lungs from any of the three groups, *in vitro* stimulated splenocytes of Gal-3$^{-/-}$ mice exhibited lower intracellular Ca^{++} flux compared to those of Gal-3$^{+/+}$ and Gal-3$^{+/-}$ mice (Figure 37A-B). On day 14 and day 21 post intravenous B16F10 injection, when pulmonary metastatic melanoma colonies were developed in mice, splenic intracellular Ca^{++} levels at the baseline as well as upon *in vitro* stimulation were remarkably lower in Gal-3$^{+/-}$ and Gal-3$^{-/-}$ mice than those in Gal-3$^{+/+}$ mice splenocytes (Figure 37A-B). On day 21, a marked reduction in the levels of intracellular Ca^{++} ions in Gal-3$^{+/+}$, Gal-3$^{+/-}$ and Gal-3$^{-/-}$ mice splenocytes was noted upon *in vitro* stimulation with PMA + Ionomycin (Figure 37A) as well as with anti-CD3 mAb (Figure 37B). Further, on day 21, overall levels of intracellular Ca^{++} flux at baseline as well as after *in vitro* stimulation of splenocytes were significantly lower in all the three mice groups as indicated by Fluo-3 fluorescence intensity.

A

Stimulant : PMA + Ionomycin

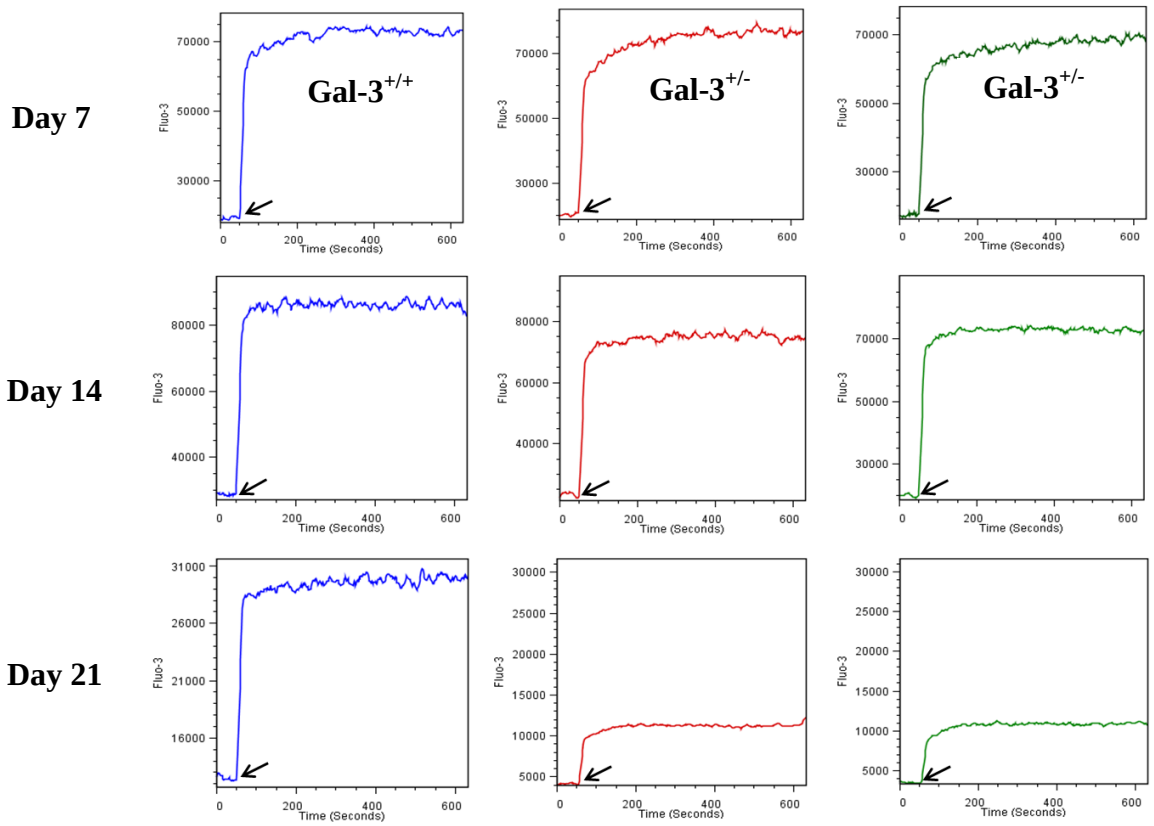

B

Stimulant : anti-CD3 mAb

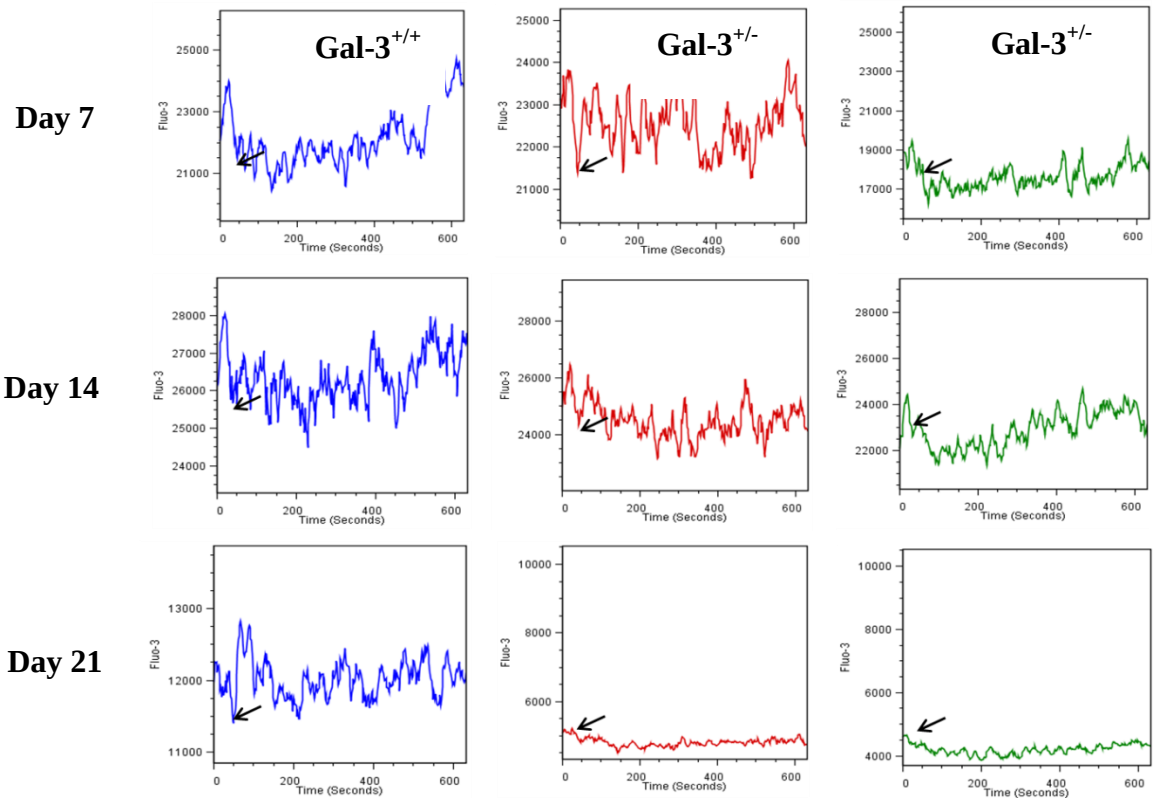

Figure 37: Intracellular calcium flux upon *in vitro* stimulation of splenocytes from Gal-3$^{+/+}$, Gal-3$^{+/-}$ and Gal-3$^{-/-}$ mice during progression of lung metastasis. Freshly isolated splenocytes of Gal-3$^{+/+}$, Gal-3$^{+/-}$ and Gal-3$^{-/-}$ mice sacrificed on day 7, day 14 and day 21 of the experimental metastasis assay conditions were stained with calcium indicator dye Fluo-3-AM. The baseline fluorescence intensity of splenocytes was measured by flow cytometry. The splenocytes were stimulated with either **(A)** PMA (100 ng) + Ionomycin (500 ng) or **(B)** soluble anti-CD3 mAb (1 μg) and the changes in the Fluo-3 fluorescence intensity were quantitated over a period of up to 10 minutes continuously by flow cytometry. The histograms show representative data of 3 independent experiments for each time point. Arrows indicate the time points of addition of stimulants.

Intracellular ROS generation upon *in vitro* stimulation of splenocytes from Gal-3$^{+/+}$, Gal-3$^{+/-}$ and Gal-3$^{-/-}$ mice in the lung metastasis model

Reactive oxygen species (ROS) are known to be involved in the modulation of immune responses and tumor microenvironment in the host. In the present study, it was analyzed whether intracellular ROS production is affected by endogenous galectin-3 expression levels in the splenocytes of Gal-3$^{+/+}$, Gal-3$^{+/-}$ and Gal-3$^{-/-}$ mice during progression of lung metastasis. Mice from Gal-3$^{+/+}$, Gal-3$^{+/-}$ and Gal-3$^{-/-}$ groups were sacrificed on day 7, day 14 and day 21 post intravenous B16F10 cell injection. Intracellular ROS generation in freshly isolated DCFH-DA labeled splenocytes (1.5 x 10^6 cells) of Gal-3$^{+/+}$, Gal-3$^{+/-}$ and Gal-3$^{-/-}$ mice upon *in vitro* stimulation with PMA (100 ng) + Ionomycin (500 ng) and anti-CD3 mAb (1 μg) was quantitated by flow cytometry as described in the Materials and Methods chapter.

On day 7 and day 14 of the experimental metastasis assay conditions, no significant differences were noted in the levels of intracellular ROS generated in the splenocytes of Gal-3$^{+/+}$, Gal-3$^{+/-}$ and Gal-3$^{-/-}$ mice upon *in vitro* stimulation (Figure 38A-B). On day 21, when mice lungs were flooded with metastatic melanoma colonies, Gal-3$^{-/-}$ mice splenocytes exhibited significantly lower intracellular ROS generation compared to Gal-3$^{+/+}$ mice upon *in vitro* stimulation with PMA + Ionomycin or anti-CD3 mAb (Figure 38C).

A

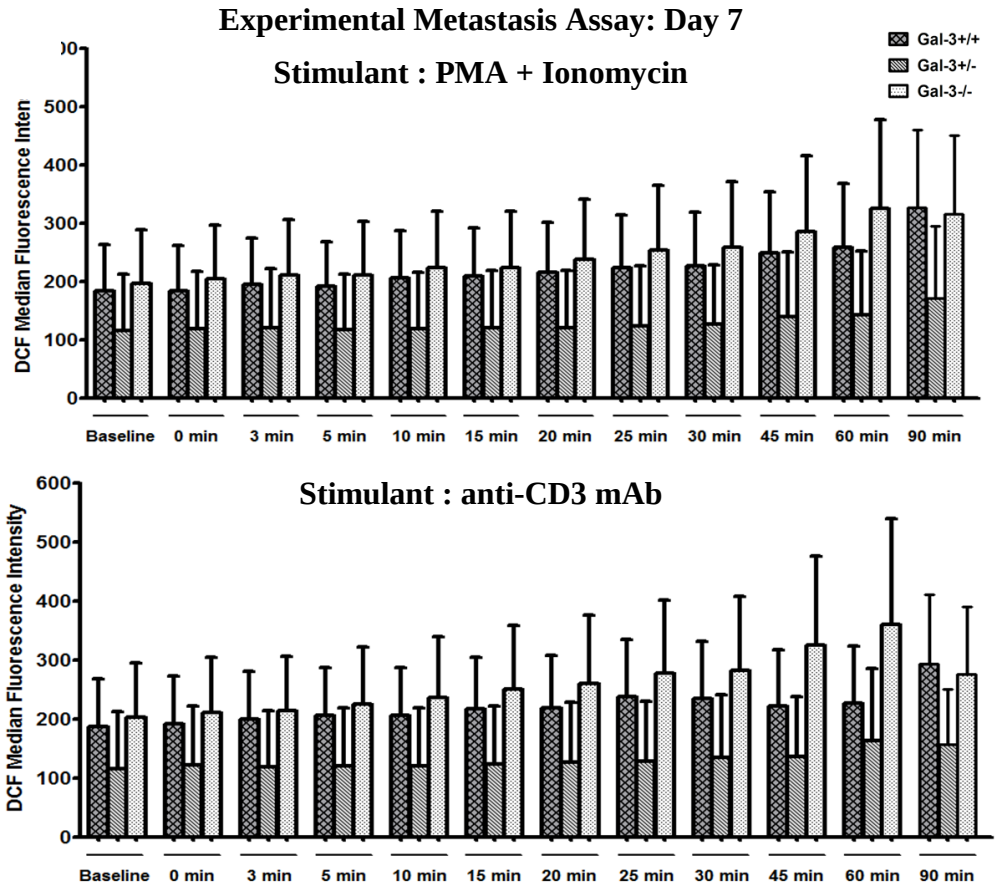
Experimental Metastasis Assay: Day 7
Stimulant : PMA + Ionomycin
Gal-3+/+
Gal-3+/-
Gal-3-/-
DCF Median Fluorescence Inten
0
100
200
300
400
500
Baseline
0 min
3 min
5 min
10 min
15 min
20 min
25 min
30 min
45 min
60 min
90 min
Stimulant : anti-CD3 mAb
DCF Median Fluorescence Intensity
0
100
200
300
400
500
600
Baseline
0 min
3 min
5 min
10 min
15 min
20 min
25 min
30 min
45 min
60 min
90 min

B

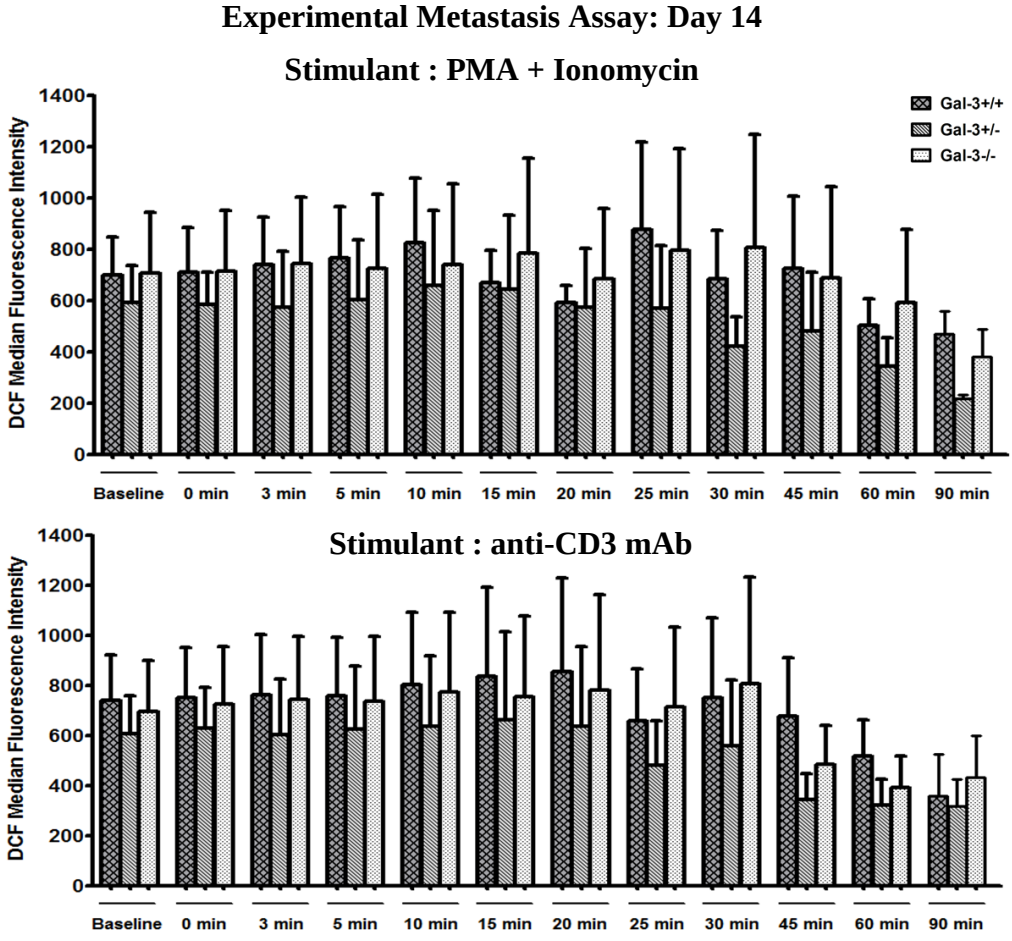
Experimental Metastasis Assay: Day 14
Stimulant : PMA + Ionomycin
Gal-3+/+
Gal-3+/-
Gal-3-/-
DCF Median Fluorescence Intensity
0
200
400
600
800
1000
1200
1400
Baseline
0 min
3 min
5 min
10 min
15 min
20 min
25 min
30 min
45 min
60 min
90 min
Stimulant : anti-CD3 mAb
DCF Median Fluorescence Intensity
0
200
400
600
800
1000
1200
1400
Baseline
0 min
3 min
5 min
10 min
15 min
20 min
25 min
30 min
45 min
60 min
90 min

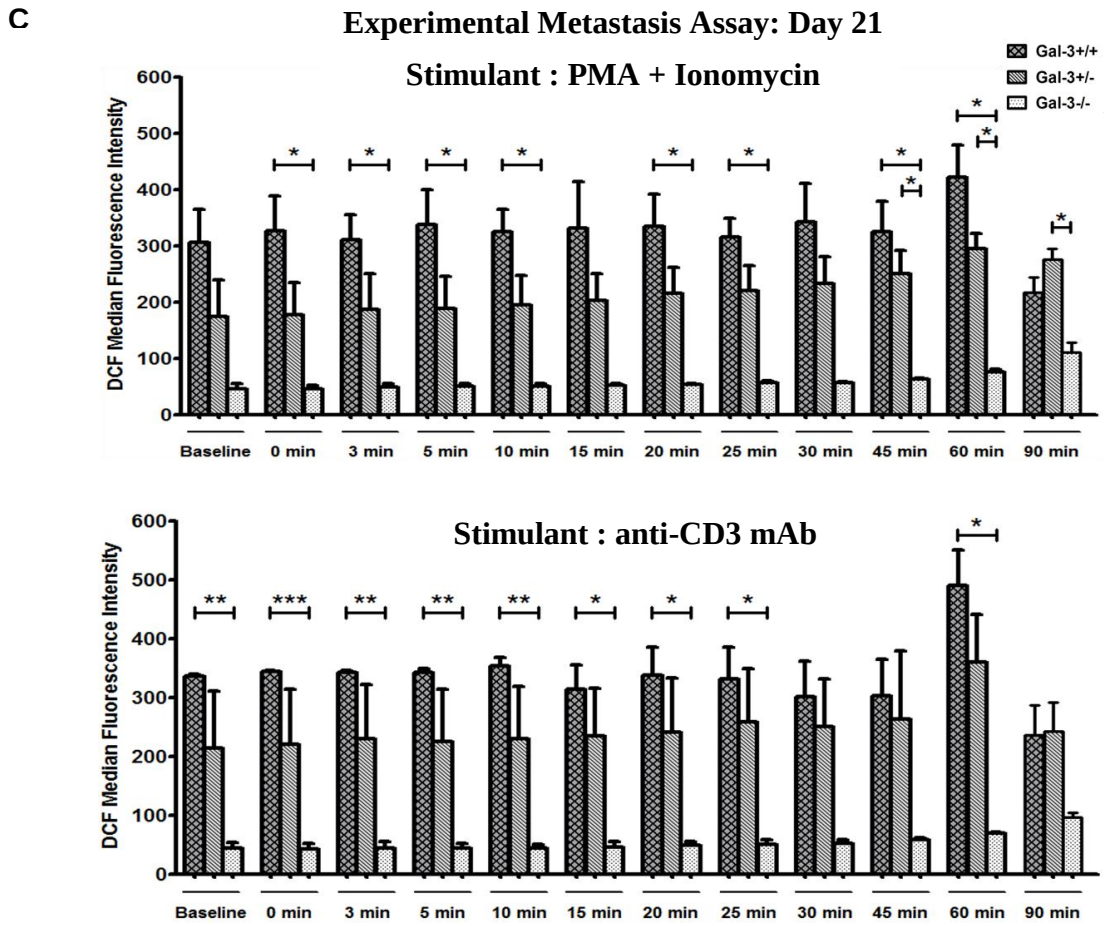

Figure 38: Intracellular ROS generation upon *in vitro* stimulation of splenocytes from Gal-3$^{+/+}$, Gal-3$^{+/-}$ and Gal-3$^{-/-}$ mice in lung metastasis model. Freshly isolated splenocytes of Gal-3$^{+/+}$, Gal-3$^{+/-}$ and Gal-3$^{-/-}$ mice sacrificed on **(A)** day 7, **(B)** day 14 and **(C)** day 21 of the experimental metastasis assay conditions were stained with DCFH-DA. The baseline DCF fluorescence intensity of labelled splenocytes was measured by flow cytometry. The splenocytes were then stimulated with either PMA (100 ng) + Ionomycin (500 ng; upper panel) or soluble anti-CD3 mAb (1 μg; lower panel) and the changes in the Fluo-3-AM fluorescence intensity were quantitated at the indicated time intervals by flow cytometry. The graphs represent consolidated data of 3 independent experiments for each time point. *P<0.05, **P<0.01, ***P<0.001.

Serum cytokine profile in Gal-3$^{+/+}$, Gal-3$^{+/-}$ and Gal-3$^{-/-}$ mice during progression of B16F10 lung metastasis

Cytokines are crucial modulators of host immune responses in normal physiological processes as well as during pathological conditions; including infection, inflammation and cancer.

Systemic dysregulation in various cytokines can contribute to enhancement or suppression of immunological responses to cancer in the host. As mentioned in the previous chapter, serum cytokine milieu in Gal-$3^{+/+}$, Gal-$3^{+/-}$ and Gal-$3^{-/-}$ mice was studied under normal physiological conditions. It was observed that, Gal-$3^{-/-}$ mice exhibited marked reduction in serum cytokine production with dysregulated pro-inflammatory and anti-inflammatory cytokine balance (Chapter 4). It was therefore important to understand the changes in the cytokine milieu in the sera of Gal-$3^{+/+}$, Gal-$3^{+/-}$ and Gal-$3^{-/-}$ mice during progression of melanoma lung metastasis.

The levels of Th1 (IL-2, IFN-γ, TNF), Th2 (IL-4, IL-6, IL-10) and Th17 (IL-17A) cytokines were quantitated in the sera of lung metastasis-bearing Gal-$3^{+/+}$, Gal-$3^{+/-}$ and Gal-$3^{-/-}$ mice by cytometric bead array using flow cytometry. The relative pattern of serum Th1, Th2 and Th17 cytokine levels in Gal-$3^{+/+}$, Gal-$3^{+/-}$ and Gal-$3^{-/-}$ mice changed gradually with the progression of lung metastasis from day 7, day 14 to day 21 post intravenous B16F10 injection. On day 7, when no melanoma colonies were developed in mice lungs, Gal-$3^{-/-}$ mice exhibited marked reduction in serum Th1 (IL-2, IFN-γ, TNF) and Th2 (IL-4, IL-6, IL-10) cytokine levels (Figure 39A) as seen in non-tumor-bearing Gal-$3^{-/-}$ mice without B16F10 injection (Chapter 4). On day 14, although the frequencies of pulmonary melanoma metastases differed in the Gal-$3^{+/+}$, Gal-$3^{+/-}$ and Gal-$3^{-/-}$ mice, no significant differences were observed in the levels of Th1, Th2 and Th17 cytokines amongst these mice groups (Figure 39B). On day 21, when Gal-$3^{+/+}$, Gal-$3^{+/-}$ and Gal-$3^{-/-}$ mice exhibited uncountably high numbers of pulmonary metastatic melanoma colonies, levels of pro-inflammatory cytokines IL-6 and IL-17A were found to be highest in Gal-$3^{-/-}$ mice sera amongst the three mice groups. Interestingly, on day 21, serum levels of IFN-γ as well as IL-10 were significantly lower in Gal-$3^{+/-}$ mice as compared to Gal-$3^{+/+}$ and Gal-$3^{-/-}$ mice (Figure 39C).

A

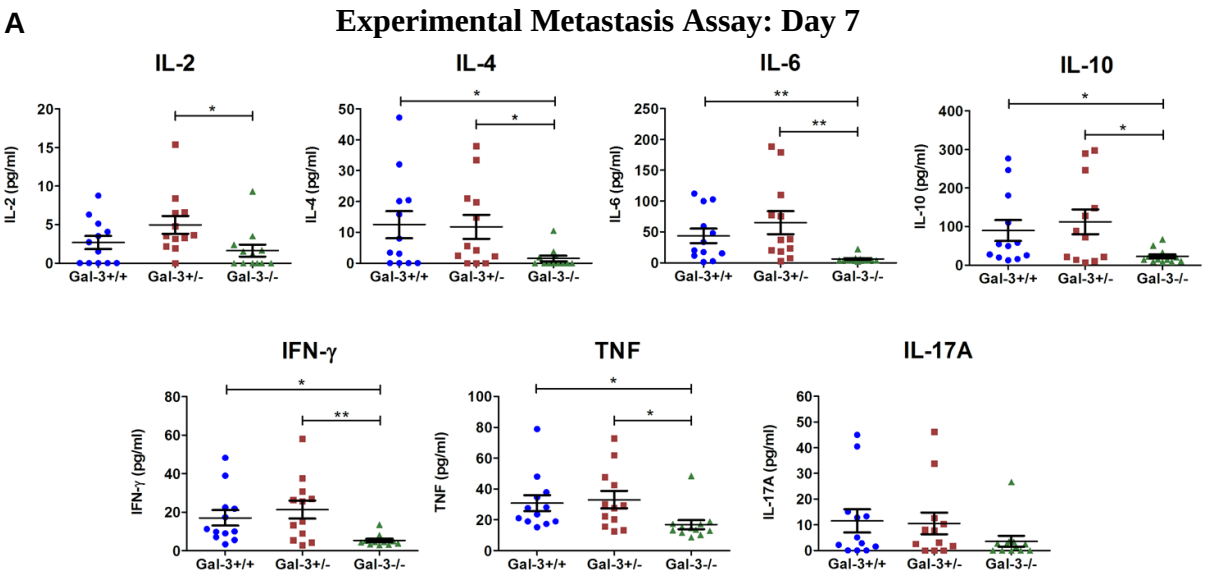
Experimental Metastasis Assay: Day 7
IL-2
IL-4
IL-6
IL-10
IFN-γ
TNF
IL-17A
IL-2 (pg/ml)
IL-4 (pg/ml)
IL-6 (pg/ml)
IL-10 (pg/ml)
IFN-γ (pg/ml)
TNF (pg/ml)
IL-17A (pg/ml)
Gal-3+/+
Gal-3+/-
Gal-3-/-

B

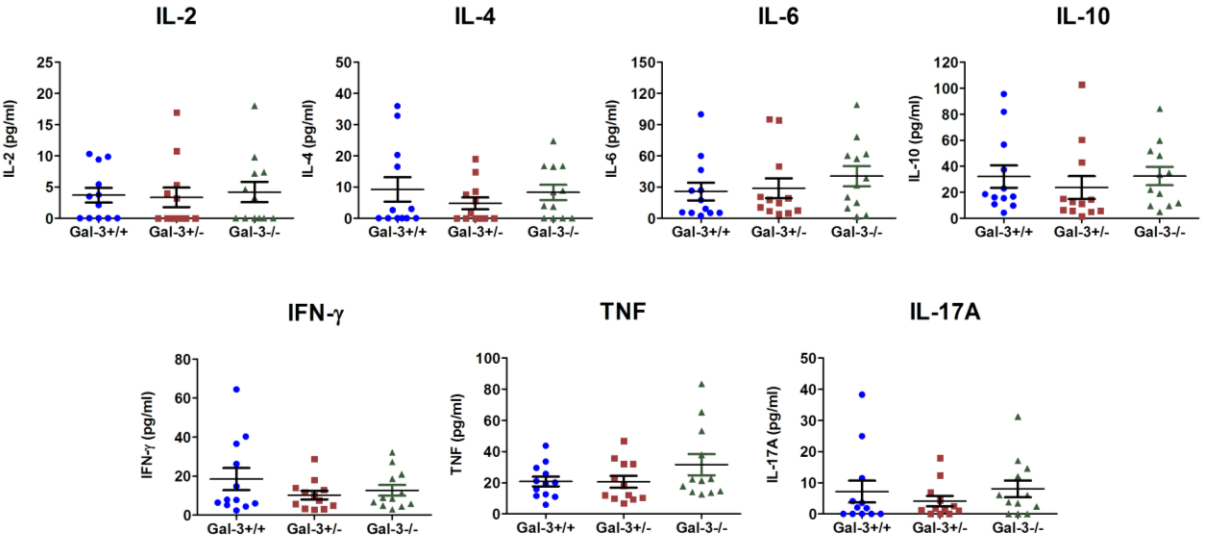
Experimental Metastasis Assay: Day 14
IL-2
IL-4
IL-6
IL-10
IFN-γ
TNF
IL-17A
IL-2 (pg/ml)
IL-4 (pg/ml)
IL-6 (pg/ml)
IL-10 (pg/ml)
IFN-γ (pg/ml)
TNF (pg/ml)
IL-17A (pg/ml)
Gal-3+/+
Gal-3+/-
Gal-3-/-

C

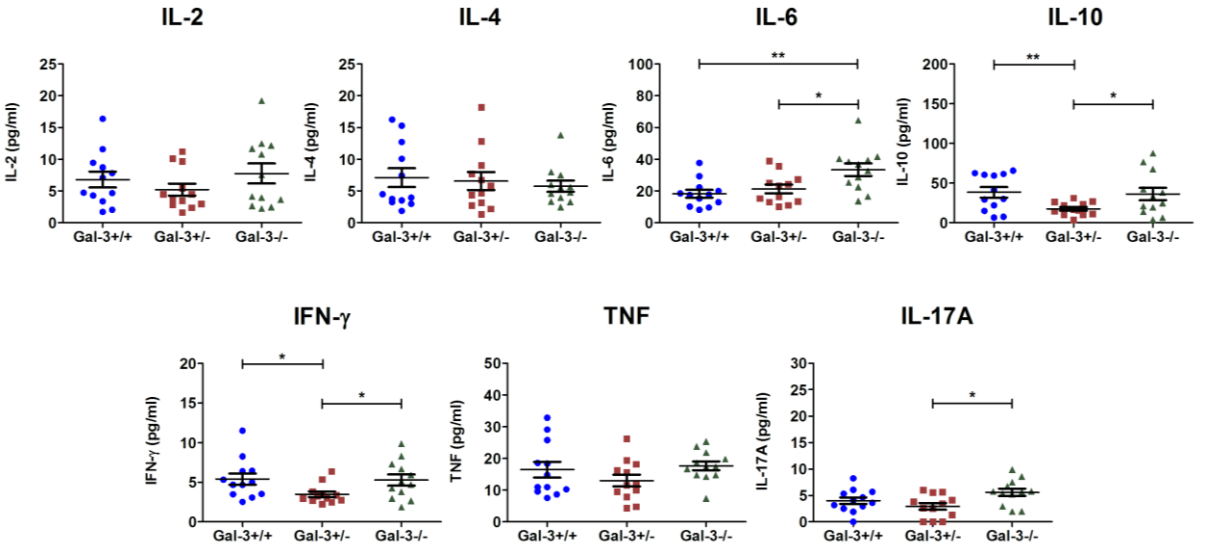
Experimental Metastasis Assay: Day 21
IL-2
IL-4
IL-6
IL-10
IFN-γ
TNF
IL-17A
IL-2 (pg/ml)
IL-4 (pg/ml)
IL-6 (pg/ml)
IL-10 (pg/ml)
IFN-γ (pg/ml)
TNF (pg/ml)
IL-17A (pg/ml)
Gal-3+/+
Gal-3+/-
Gal-3-/-

Figure 39: Serum Th1/Th2/Th17 cytokine profile in Gal-3$^{+/+}$, Gal-3$^{+/-}$ and Gal-3$^{-/-}$ mice during progression of lung metastasis. Blood was collected from Gal-3$^{+/+}$, Gal-3$^{+/-}$ and Gal-3$^{-/-}$ mice before sacrifice by retro-orbital puncture and serum was separated by centrifugation. Serum cytokine profile was assessed on **(A)** day 7, **(B)** day 14 and **(C)** day 21 post intravenous B16F10 injection by Th1/Th2/Th17 Cytometric Bead Array using flow cytometry. The graphs indicate concentrations of respective Th1 (IL-2, IFN-γ, TNF), Th2 (IL-4, IL-6, IL-10) and Th17 (IL-17A) cytokines in mice sera. Each dot in the dot plots represents serum cytokine concentration (pg/ml) of one mouse from the corresponding group (n=12 mice per group). *P<0.05, **P<0.01.

Survival study in Gal-3$^{+/+}$, Gal-3$^{+/-}$ and Gal-3$^{-/-}$ mice bearing B16F10 lung metastases

It was interesting to study whether differences in endogenous galectin-3 expression levels affect the survival of Gal-3$^{+/+}$, Gal-3$^{+/-}$ and Gal-3$^{-/-}$ mice bearing lung metastasis. Under experimental metastasis assay conditions, Gal-3$^{+/+}$, Gal-3$^{+/-}$ and Gal-3$^{-/-}$ mice (10 mice per group) bearing B16F10 lung metastases were monitored in Laboratory Animal Facility, ACTREC to study their overall survival. When mice died, their lungs were dissected out and fixed in 10% neutral buffered formalin. Survival rates were determined by standard Kaplan-Meier survival curve analysis. It was observed that, survival rates of Gal-3$^{+/+}$, Gal-3$^{+/-}$ and Gal-3$^{-/-}$ mice bearing lung metastases did not differ significantly (Figure 40A). The results indicated that the differences in endogenous galectin-3 levels did not influence the survival rates in Gal-3$^{+/+}$, Gal-3$^{+/-}$ and Gal-3$^{-/-}$ mice under experimental metastasis assay conditions. However, mice died due to respiratory arrest caused by heavy burden of metastatic melanoma colonies developed in their lungs in all the three mice groups (Figure 40B).

Experimental Metastasis Assay

Survival Study

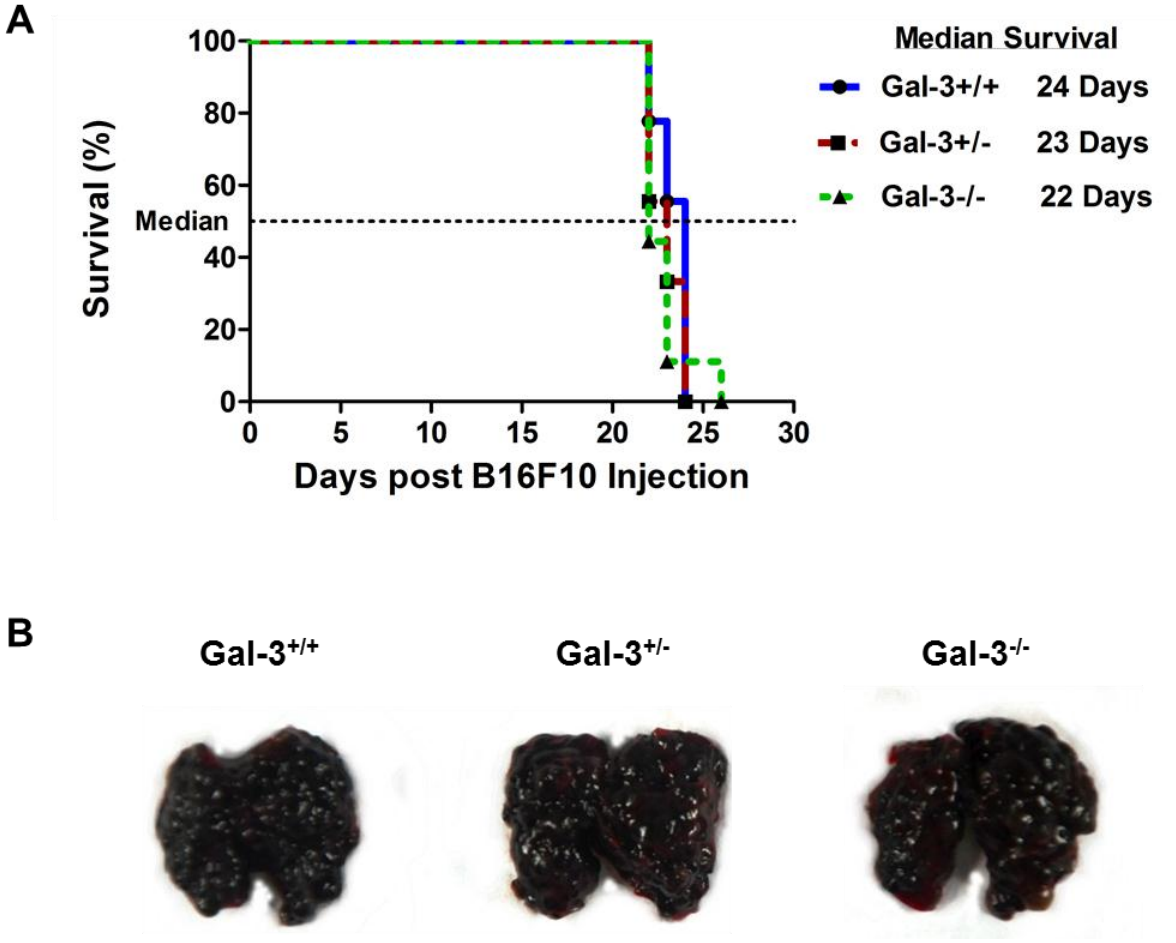

Figure 40: Survival study in Gal-3$^{+/-}$, Gal-3$^{-/-}$ and Gal-3$^{-/-}$ mice under experimental metastasis assay conditions. Groups of Gal-3$^{+/+}$, Gal-3$^{+/-}$ and Gal-3$^{-/-}$ mice [n=10 mice/ group] were monitored for their overall survival. **(A)** Survival curve of Gal-3$^{+/+}$, Gal-3$^{+/-}$ and Gal-3$^{-/-}$ mice bearing B16F10 lung metastasis. Ages of the animals (in days) were calculated at the time of death. Survival rates are represented using the standard Kaplan-Meier survival curve. Differences in the survival rates between the three groups were calculated using Log-rank test. Median survival is marked as a thin dotted line. The graph shows data of a representative experiment out of 2 independent experiments. (**B**) Representative images of dissected mice lungs flooded with metastatic B16F10 melanoma colonies (black colored) in dead mice of each mice group. The lungs were fixed in 10% neutral buffered formalin after dissection.

CHAPTER 6

Mechanisms involved in endogenous galectin-3 mediated regulation of anti-tumor immune responses in *LGALS3* transgenic mice

Galectin-3 is involved in cancer progression and metastasis [14-18]. It is also known to be an important regulator of immune responses [10,39-43]. However, the role of endogenous galectin-3 in the modulation of tumor-specific immunity in the host and the mechanisms involved therein remain poorly understood till date. In the present study, striking differences were observed in the immune scenario of Gal-$3^{+/+,}$ Gal-$3^{+/-}$ and Gal-$3^{-/-}$ mice under normal physiological conditions as well as during progression of B16F10 lung metastasis (Chapter 4 and Chapter 5). The results so far indicated dysregulation of immune responses in the absence of endogenous galectin-3 as seen in Gal-$3^{-/-}$ mice. Experiments included in this chapter are aimed at deciphering the mechanisms involved in endogenous galectin-3 mediated regulation of anti-tumor immune responses in *LGALS3* transgenic mice i.e. Gal-$3^{+/+,}$ Gal-$3^{+/-}$ and Gal-$3^{-/-}$ mice.

Comparison of splenic NK cell cytotoxicity in Gal-$3^{+/+}$, Gal-$3^{+/-}$ and Gal-$3^{-/-}$ mice

NK cells are the key players of innate immune responses, providing first line of defense against transformed and tumorigenic cells [306-308]. Reduced frequency of splenic NK cells was found in Gal-$3^{-/-}$ mice than in Gal-$3^{+/+}$ mice under normal physiological conditions (Chapter 4). It was therefore interesting to analyze whether the cytotoxic function of splenic NK cells correlated with their phenotype in Gal-$3^{+/+}$, Gal-$3^{+/-}$ and Gal-$3^{-/-}$ mice.

NK cells were isolated from splenocyte suspensions of Gal-$3^{+/+}$, Gal-$3^{+/-}$ and Gal-$3^{-/-}$ mice by immunomagnetic purification (Negative selection) using Mouse NK cell isolation kit (Mitenyi Biotec, Bergisch Gladbach, Germany). Yield of purified NK cells isolated from murine splenocytes ranged between 1-3% for each isolation and was not significantly different in Gal-$3^{+/+}$, Gal-$3^{+/-}$ and Gal-$3^{-/-}$ mice groups (Table 2, Figure 41A). Purity of the NK cells was checked using anti-mouse CD3 Alexa Fluor 647 and anti-mouse NK1.1 PE antibodies and was found to be ~90% ($CD3^{-}NK1.1^{+}$) for each isolation (Figure 41B).

Table 2: Yield of purified NK cells from Gal-3$^{+/+}$, Gal-3$^{+/-}$ and Gal-3$^{-/-}$ mice splenocytes

Experiment No.	Splenocytes subjected to MACS (x 10^6)			NK Cell count after MACS (x 10^6)			Yield (%)		
	Gal-3$^{+/+}$	Gal-3$^{+/-}$	Gal-3$^{-/-}$	Gal-3$^{+/+}$	Gal-3$^{+/-}$	Gal-3$^{-/-}$	Gal-3$^{+/+}$	Gal-3$^{+/-}$	Gal-3$^{-/-}$
1	158	143.5	89.5	2.12	2.33	0.73	1.34	1.62	0.82
2	118.8	90	71.6	2.1	1.23	0.95	1.77	1.37	1.33
3	150	150	150	3.04	3.52	1.9	2.03	2.35	1.27
4	150	150	150	3.3	3.12	3.06	2.20	2.08	2.04
5	150	150	150	3.24	2.65	2.34	2.16	1.77	1.56
Mean Yield (%)							1.90 ± 0.15	1.84 ± 0.17	1.40 ± 0.19

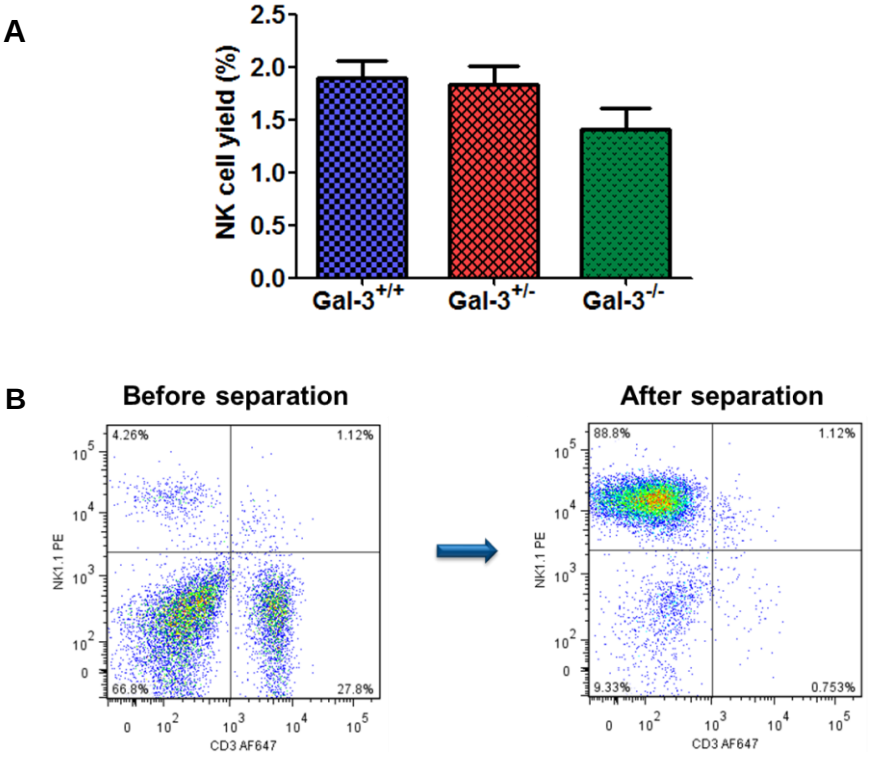

Figure 41: Yield and purity of NK cells isolated from the splenocytes of Gal-3$^{+/+}$, Gal-3$^{+/-}$ and Gal-3$^{-/-}$ mice. NK cells were purified from the freshly isolated splenocyte suspensions of Gal-3$^{+/+}$, Gal-3$^{+/-}$ and Gal-3$^{-/-}$ mice by immunomagnetic purification (Negative selection) using Mouse NK cell isolation kit (Mitenyi Biotec, Bergisch Gladbach, Germany) as per the manufacturer's protocol. (**A)** Splenic NK cell yield in Gal-3$^{+/+}$, Gal-3$^{+/-}$ and Gal-3$^{-/-}$ mice. Yield of NK cells obtained after purification was calculated as a percentage (%) of splenocytes number subjected to isolation in each mice group. The graph represents consolidated data of 5 independent experiments. (**B)** Purity of splenic NK cells (CD3$^-$NK1.1$^+$) assessed using anti-mouse CD3 Alexa Fluor 647 and anti-mouse NK1.1 PE

antibodies before and after immunomagnetic isolation. The dot plots are representative data of 5 independent experiments.

YAC-1 mouse T lymphoma cells have been used as classical tumor targets of NK cells in murine system in numerous studies because of their NK sensitive nature. In the present study, ability of purified NK cells from Gal-$3^{+/+}$, Gal-$3^{+/-}$ and Gal-$3^{-/-}$ mice to kill YAC-1 tumor targets was assessed by standard ^{51}Chromium Release Cytotoxicity Assay as described in the Materials and Methods chapter. Purified splenic NK cells were used as effectors against YAC-1 cells at the Effector: Target (E:T) ratios of 80:1, 40:1, 20:1 and 10:1 It was observed that freshly isolated purified NK cells from Gal-$3^{+/-}$ and Gal-$3^{-/-}$ mice exhibited significantly decreased cytotoxicity against YAC-1 tumor cells, as compared to that of Gal-$3^{+/+}$ mice at all the E:T ratios tested (Figure 42). Thus, endogenous galectin-3 expression levels in Gal-$3^{+/+}$, Gal-$3^{+/-}$ and Gal-$3^{-/-}$ mice appear to be important determinants of anti-tumor cytolytic function of NK cells from these mice.

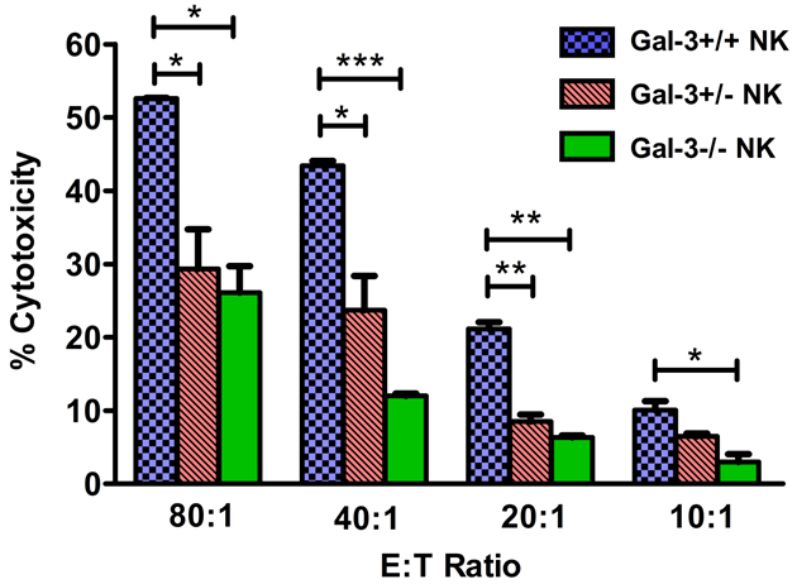

Figure 42: Ability of splenic NK cells isolated from Gal-$3^{+/+}$, Gal-$3^{+/-}$ and Gal-$3^{-/-}$ mice to kill YAC-1 tumor targets. NK cells were immunomagnetically purified from freshly isolated splenocytes of Gal-$3^{+/+}$, Gal-$3^{+/-}$ and Gal-$3^{-/-}$ mice by negative selection. NK cells were co-cultured with [^{51}Cr] labeled YAC-1 tumor targets at the indicated Effector: Target ratios in

a standard 4-hour [^{51}Cr] release assay. The graph represents percentage (%) cytotoxicity calculated as described in the Materials and Methods chapter. Data shows mean±SE of % cytotoxicity of triplicate wells of a representative experiment. The cytotoxicity assay was performed 3 times using purified splenic NK cells from mice. *P<0.05, **P<0.01, ***P<0.001.

In the present study, the lung-specific metastasis of B16F10 melanoma cells in Gal-3$^{+/+}$, Gal-3$^{+/-}$ and Gal-3$^{-/-}$ mice exhibiting different endogenous galectin-3 expression levels was studied as described in Chapter 4. Interestingly, the ability of B16F10 melanoma cells to form metastatic colonies in the lungs of Gal-3$^{+/+}$ and Gal-3$^{-/-}$ mice remained comparable, whereas it was found to be reduced in Gal-3$^{+/-}$ mice (Chapter 5). It was therefore interesting to study the cytotoxic potential of NK cells isolated from Gal-3$^{+/+}$, Gal-3$^{+/-}$ and Gal-3$^{-/-}$ mice against B16F10 melanoma cells. B16F10 cells are not the natural targets of murine NK cells. The purified NK cells from Gal-3$^{+/+}$, Gal-3$^{+/-}$ and Gal-3$^{-/-}$ mice were therefore stimulated *in vitro* for 3 days using recombinant murine IL-2. Recombinant IL-2 stimulated NK cells were used as effectors against [^{51}Cr] labeled B16F10 melanoma cells as targets at the effector: target (E:T) ratios of 100:1, 50:1, 25:1 and 12.5:1 in the standard 4 hour [^{51}Cr] release assay. Interestingly, purified and *in vitro* stimulated NK cells from Gal-3$^{+/-}$ mice exhibited relatively higher cytotoxic potential against B16F10 murine melanoma cells as compared to those from Gal-3$^{+/+}$ and Gal-3$^{-/-}$ mice (Figure 43).

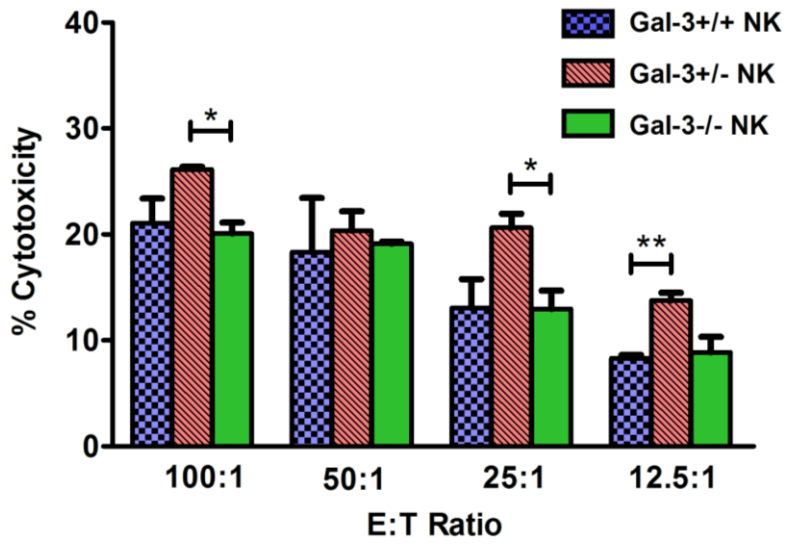

Figure 43: Cytotoxic potential of splenic NK cells from Gal-3$^{+/+}$, Gal-3$^{+/-}$ and Gal-3$^{-/-}$ mice against B16F10 murine melanoma cells. NK cells were immunomagnetically purified from freshly isolated splenocytes of Gal-3$^{+/+}$, Gal-3$^{+/-}$ and Gal-3$^{-/-}$ mice by negative selection. Purified NK cells were stimulated *in vitro* for 3 days using recombinant murine IL-2 (Day 1: 100 U/ 100 µl, Day 2: 50 U/ 100 µl, Day 3: 50 U/ 100 µl). *In vitro* stimulated NK cells were co-cultured with [^{51}Cr] labeled YAC-1 tumor targets at the indicated Effector: Target ratios in a standard 4-hour [^{51}Cr] release assay. The graph represents percentage (%) cytotoxicity calculated as described in the Materials and Methods chapter. Data shows mean±SE of % cytotoxicity of triplicate wells of a representative experiment. The cytotoxicity assay was performed 2 times each using purified splenic NK cells from Gal-3$^{+/+}$, Gal-3$^{+/-}$ and Gal-3$^{-/-}$ mice. *P<0.05, **P<0.01.

Serum cytokine milieu in Gal-3$^{+/+}$, Gal-3$^{+/-}$ and Gal-3$^{-/-}$ mice

In the present study, the serum levels of Th1 (IL-2, IFN-γ, TNF), Th2 (IL-4, IL-6, IL-10) and Th17 (IL-17A) cytokines was found to be decreased in the non-tumor-bearing Gal-3$^{+/-}$ and Gal-3$^{-/-}$ mice, concomitant with the reduced expression or complete absence of endogenous galectin-3 in these mice, respectively (Chapter 4). Correlation analysis indicated that, the cytokine milieu was disturbed in Gal-3$^{-/-}$ mice, with dysregulation of balance between pro-inflammatory and anti-inflammmatory cytokines (Chapter 4). In tumor bearing mice,

relative pattern of serum Th1, Th2 and Th17 cytokine levels in Gal-$3^{+/+}$, Gal-$3^{+/-}$ and Gal-$3^{-/-}$ mice was found to be varying during progression of lung metastasis i.e. on Day 7, Day 14 and Day 21 post intravenous injection of B16F10 melanoma cells in mice (Chapter 5).

To assess the overall changes in the serum cytokine profile of Gal-$3^{+/+}$, Gal-$3^{+/-}$ and Gal-$3^{-/-}$ mice during progression of lung metastasis, serum concentrations (pg/ml) of Th1 (IL-2, IFN-γ, TNF), Th2 (IL-4, IL-6, IL-10) and Th17 (IL-17A) cytokines under normal physiological conditions (control) as well as under experimental metastasis assay conditions on day 7, day 14 and day 21 were collectively represented in the form of a heat map (Figure 44). Heat map data clearly indicated that, the serum Th1/Th2/Th17 cytokine levels reduced gradually in most cases in Gal-$3^{+/+}$, Gal-$3^{+/-}$ and Gal-$3^{-/-}$ mice during progression of experimental lung metastasis (day 7, day 14, day 21) as compared to control mice. Further, serum concentrations of most of the cytokines assessed, particularly IL-2, TNF, IL-10 exhibited striking reductions in Gal-$3^{+/+}$, Gal-$3^{+/-}$ as well as Gal-$3^{-/-}$ mice groups under experimental metastasis assay conditions (day 7, day 14, day 21) when compared with normal physiological conditions (control mice). Also, on day 21 post intravenous B16F10 injections when lungs of mice from Gal-$3^{+/+}$, Gal-$3^{+/-}$ and Gal-$3^{-/-}$ groups were flooded with metastatic melanoma colonies, serum levels of IFN-γ reduced remarkably as compared to normal physiological conditions as well as those during early stages of metastatic progression i.e. day 7 and day 14. Serum levels of IL-6, which is known to be a key metastasis promoting cytokine, were found to be significantly reduced during initial stages of experimental metastasis assay (day 7) compared to normal physiological conditions (control) in Gal-$3^{-/-}$ mice, but increased remarkably with the progression of lung metastasis (day 14 and day 21) in this mice group.

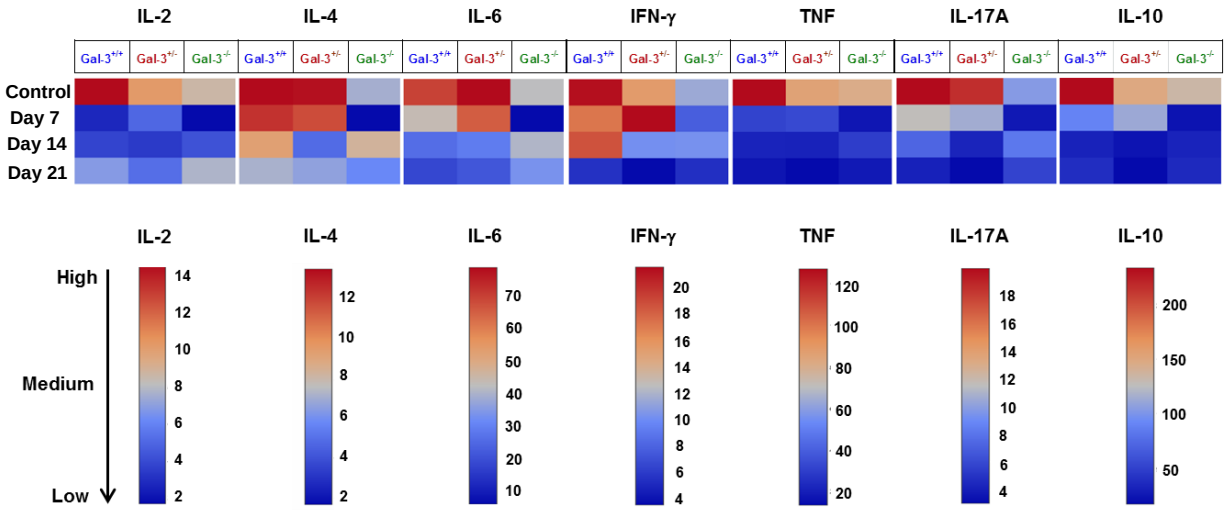

Figure 44: Heat map of serum Th1/Th2/Th17 cytokine levels in Gal-3$^{+/+}$, Gal-3$^{+/-}$ and Gal-3$^{-/-}$ mice. Upper panel represents serum levels of indicated cytokines in Gal-3$^{+/+}$, Gal-3$^{+/-}$ and Gal-3$^{-/-}$ mice under normal physiological conditions (Control) and during experimental pulmonary metastasis assay conditions (Day 7, Day 14, Day 21). Lower panel includes scale bars for respective cytokines with a range from high to low concentrations (pg/ml) corresponding to the assigned color gradient.

Role of endogenous galectin-3 in IFN-γ mediated regulation of tumor progression

IFN-γ is a multifunctional cytokine produced mainly by NK cells and activated T cells that plays a critical role in host immune responses against pathogens and cancer [37]. IFN-γ has also been found to have direct anti-proliferative and pro-apoptotic effects on tumor cells in animal models. IFN-γ is known to prevent B16 experimental metastasis by directly inhibiting cell growth [309]. In the present study, serum levels of IFN-γ were found to be significantly lower in Gal-3$^{-/-}$ mice as compared to Gal-3$^{+/+}$ under normal physiological conditions i.e. in non-tumor-bearing mice (Chapter 4). On day 7 post B16F10 intravenous injection i.e. when no metastatic melanoma colonies were observed on mice lungs, Gal-3$^{-/-}$ mice exhibited significantly lower serum IFN-γ levels than Gal-3$^{+/+}$ and Gal-3$^{+/-}$ mice. On Day 14 when differences in the frequency of B16F10 lung metastasis in the three

mice groups were observed, Gal-$3^{+/+}$ and Gal-$3^{+/-}$ mice exhibited reduction in serum IFN-γ levels, however the differences were statistically insignificant. On Day 21 when the lungs in all the three mice groups were flooded with melanoma colonies, Gal-$3^{+/-}$ mice exhibited significantly reduced serum IFN-γ levels, compared to Gal-$3^{+/+}$ and Gal-$3^{-/-}$ mice (Chapter 5). Relative pattern of serum IFN-γ levels changed gradually amongst the three mice groups i.e. Gal-$3^{+/+}$, Gal-$3^{+/-}$ and Gal-$3^{-/-}$ on day 7, day 14 and day 21 of experimental metastasis assay conditions, as evident from the heat map for serum IFN-γ concentrations (Figure 45).

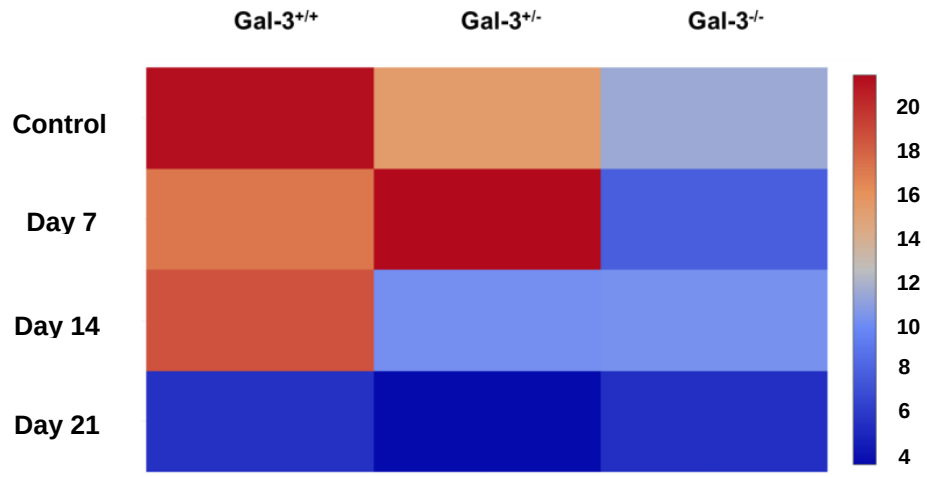

Figure 45: Heat map of serum IFN-γ levels in Gal-$3^{+/+}$, Gal-$3^{+/-}$ and Gal-$3^{-/-}$ mice. Heat map represents serum levels of IFN-γ in Gal-$3^{+/+}$, Gal-$3^{+/-}$ and Gal-$3^{-/-}$ mice under normal physiological conditions (control mice) and at different stages of experimental B16F10 melanoma lung metastasis (Day 7, Day 14, Day21). Scale bar at right indicates a range from high to low concentrations (pg/ml) of IFN-γ corresponding to the assigned color gradient.

STAT1 mediated IFN-γ signaling in Gal-$3^{+/+}$, Gal-$3^{+/-}$ and Gal-$3^{-/-}$ mice

IFN-γ exerts its effects on cells by binding to IFN-γ Receptor (IFN-γR) on the cell surface followed by signal transduction through STAT1 mediated pathway. In the present study, immunophenotyping was performed to quantitate the frequency of T cell subsets, B cells,

NK cells and macrophages expressing the ligand binding chain of IFN-γ Receptor i.e. IFN-γR1 (CD119) in Gal-$3^{+/+}$, Gal-$3^{+/-}$ and Gal-$3^{-/-}$ mice splenocytes. Percentages of IFN-γR1 receptor expressing splenic T cell subsets ($CD3^+CD119^+$ T cells, $CD4^+CD119^+$ T_H cells and $CD8^+CD119^+$ T_C cells) and NK cells ($NK1.1^+CD119^+$) were found to be higher in Gal-$3^{+/-}$ mice and lower in Gal-$3^{-/-}$ mice as compared to Gal-$3^{+/+}$ mice. No significant differences were observed in the percentages of B cells ($B220^+CD119^+$) and macrophages ($CD14^+CD119^+$) expressing IFN-γR1 (Figure 46).

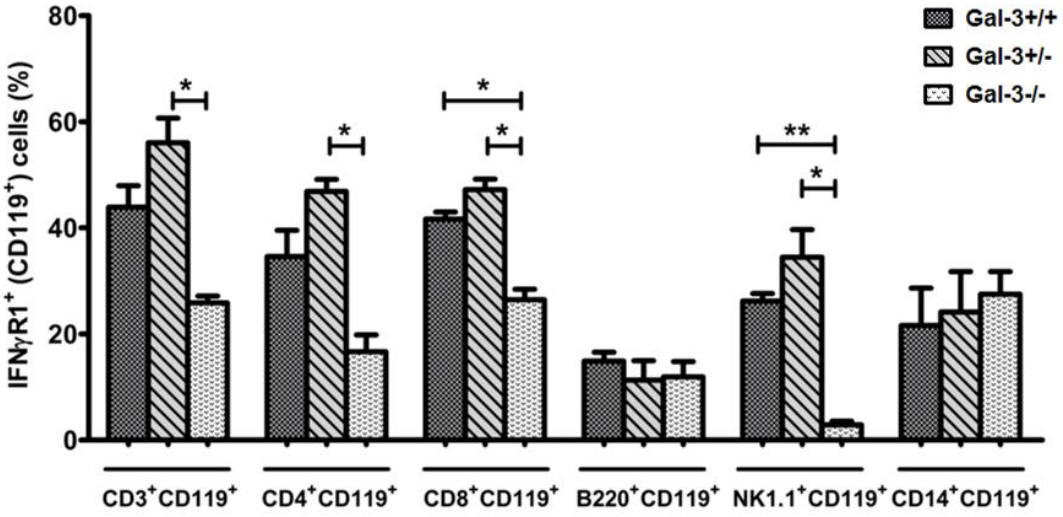

Figure 46: IFN-γR1 (CD119) expressing splenocyte subsets in Gal-$3^{+/+}$, Gal-$3^{+/-}$ and Gal-$3^{-/-}$ mice. Freshly isolated splenocytes of Gal-$3^{+/+}$, Gal-$3^{+/-}$ and Gal-$3^{-/-}$ mice were fixed and stained using fluorochrome conjugated antibodies against CD3, CD4, CD8, B220, NK1.1, CD14 and CD119 by multicolor immunophenotyping. The percentages of $CD119^+$ cells amongst each splenocyte subset were analyzed by flow cytometry. The graph shows consolidated data of 3 independent experiments. *P<0.05, **P<0.01.

The Signal Transducer and Activator of Transcription 1 (STAT1) transcription factor is activated in response to IFN-γ binding to the IFN-γ receptor. Phosphorylation of STAT1 at Tyr701 induces STAT1 dimerization, nuclear translocation and binding to promoter IFN-γ-activation site (GAS) elements to initiate/ suppress transcription of IFN-γ-regulated

genes. Positive feedback regulation of IFN-γ signaling is caused by increased expression of STAT1 [310]. To understand whether the differences in the splenic IFN-γR1 expression affect the subsequent STAT1 mediated signal transduction, levels of total STAT1 and activated phospho-STAT1(Tyr701) proteins were examined in the IFN-γ stimulated splenocytes of Gal-$3^{+/+}$, Gal-$3^{+/-}$ and Gal-$3^{-/-}$ mice by western blotting. On stimulation of splenocytes with recombinant murine IFN-γ (1 and 10 ng/ml) for 30 minutes, total STAT1 and activated phospho-STAT1(Tyr701) protein levels were found to be higher in Gal-$3^{+/-}$ mice splenocytes compared to Gal-$3^{+/+}$ and Gal-$3^{-/-}$ mice splenocytes (Figure 47A).

Suppressors of cytokine signaling (SOCS)1 and SOCS3 proteins are inhibitors of JAK-mediated phosphorylation of STAT1, thus creating a negative feedback loop that attenuates IFN-γ induced signal transduction [310,311]. In the present study, when splenocytes were stimulated using recombinant murine IFN-γ (1 and 10 ng/ml) for 12 hours, levels SOCS1 and SOCS3 proteins were remarkably higher in Gal-$3^{-/-}$ mice as compared to Gal-$3^{+/+}$ and Gal-$3^{+/-}$ mice splenocytes (Figure 47B). Together, these findings suggested possible attenuation of STAT1 mediated IFN-γ signaling in the complete absence of endogenous galectin-3 in Gal-$3^{-/-}$ mice splenocytes.

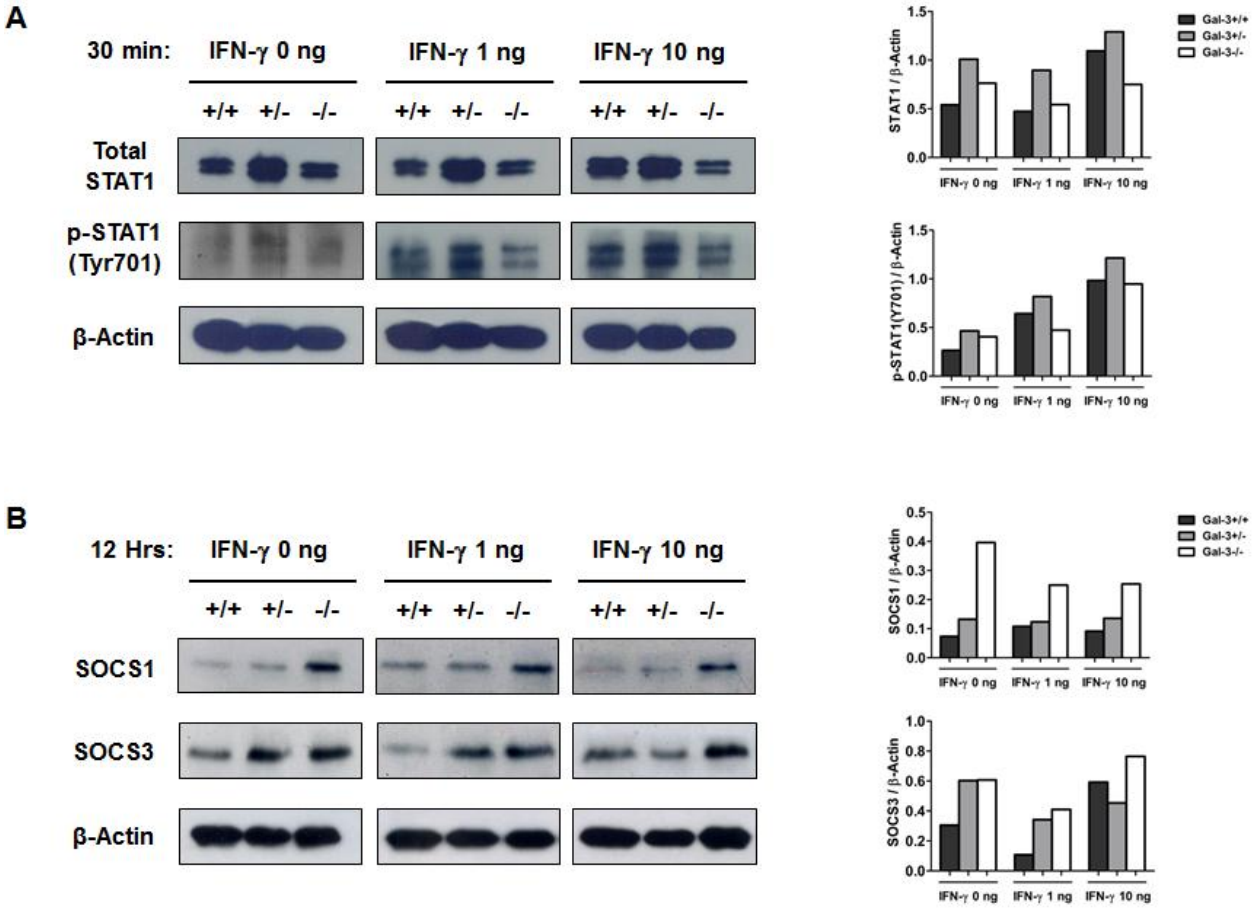

Figure 47: STAT1 mediated IFN-γ signaling in Gal-3$^{+/+}$, Gal-3$^{+/-}$ and Gal-3$^{-/-}$ mice splenocytes. (A) IFN-γ induced STAT1 signaling in mice splenocytes. Freshly isolated splenocytes of Gal-3$^{+/+}$, Gal-3$^{+/-}$ and Gal-3$^{-/-}$ mice (2.5 x 10^{6} cells/ ml complete medium/ well) were stimulated *in vitro* using recombinant murine IFN-γ (1 and 10 ng/ml) in 24-well microtiter plates for 30 minutes. Unstimulated cells cultured in medium alone were used as controls (IFN-γ 0 ng/ml). The cells were then harvested, lysed and equal amounts of lysates were analyzed by western blotting to detect protein levels of total STAT1 (STAT1α: 91 kDa and STAT1β: 84 kDa) and phospho-STAT1(Tyr701). β-actin (42 kDa) served as loading control. The blots are representative of 3 independent experiments (Left panel). Densitometry results are indicated as ratios of optical densities for STAT1 or phospho-STAT1(Tyr701) protein bands relative to loading control i.e. β-Actin band for the representative blots (Right panel). **(B)** Suppressors of IFN-γ signaling pathway in mice splenocytes. Freshly isolated splenocytes of Gal-3$^{+/+}$, Gal-3$^{+/-}$ and Gal-3$^{-/-}$ mice (2.5 x 10^{6} cells/ ml complete medium/ well) were stimulated using recombinant murine IFN-γ (1 and 10 ng/ml) in 24-well plates for 12 hours. Unstimulated cells cultured in medium alone were used as

controls (IFN-γ 0 ng/ml). The cells were then harvested, lysed and equal amounts of lysates were analyzed by western blotting to detect protein levels of SOCS1 (23 kDa) and SOCS3 (26 kDa). β-actin (42 kDa) served as loading control. The blots are representative of 3 independent experiments (Left panel). Densitometry results are indicated as ratios of optical densities for SOCS1 or SOCS3 protein bands relative to loading control i.e. β-Actin band for the representative blots (Right panel).

CHAPTER 7

DISCUSSION

Galectin-3 is known to be an important regulator of cancer progression and metastasis by promoting cell-cell and cell-ECM adhesion, invasion, migration, angiogenesis, cell proliferation, malignant transformation and inhibition of tumor cell apoptosis [18,92,93,98,107]. Interactions between galectin-3 and its glycosylated ligands have been shown to be involved in the early steps of the metastatic process. In earlier reported studies, galectin-3 has been found to be expressed in highest amounts on majority of the tissue compartments of lung and constitutively on lung vascular endothelium in mice [30,31]. Earlier studies done to understand organ specific metastasis using B16F10 murine melanoma model have demonstrated that, interactions between galectin-3 on the mice lung endothelium and its high affinity ligand poly-*N*-acetyl lactosamine (polyLacNAc) on β1,6 branched *N*-oligosaccharides present on B16F10 melanoma cells facilitates B16F10 colonization in the lungs of the mice [26,30,32].

The studies done so far to assess the role of endogenous galectin-3 in galectin-3 wild type (Gal-$3^{+/+}$) and null (Gal-$3^{-/-}$) mice have reported conflicting findings with respect to primary tumor growth as well as metastatic frequency compared between these two mice groups [32-36]. These studies highlight a paradoxical effect of endogenous galectin-3 expression on the tumor growth and metastasis in the host. The precise role of endogenous galectin-3 in the regulation of cancer progression and metastasis is poorly understood and warrants further investigation.

Involvement of immune system in the modulation of tumor progression and metastasis in the host has been extensively studied [37,38]. Accumulating evidence suggests the importance of galectin-3 in modulating host immune responses through the regulation of homeostasis and functions of various immune cell subsets [10,39-48]. Although limited literature is available demonstrating the role of galectin-3 in immune regulation *in vivo* using Gal-$3^{+/+}$ and Gal-$3^{-/-}$ mice [8,34,36,39-42,49-52],

the effects of endogenous galectin-3 expression levels on the modulation of host anti-tumor immune responses and the mechanisms involved therein remain elusive till date and necessitate in-depth investigation.

Based on these reported findings, we hypothesized that endogenous galectin-3 regulates immune responses in mice and thereby modulates lung metastasis of B16F10 murine melanoma cells in these mice. The present study attempts to investigate the role of endogenous galectin-3 expression levels in orchestrating anti-tumor immune responses in mice and relate them to the lectin's role in melanoma metastasis studied using B16F10 murine melanoma model. Comparative analysis of the host immune scenario with respect to different expression levels of endogenous galectin-3 was performed using Gal-$3^{+/+}$, Gal-$3^{+/-}$ and Gal-$3^{-/-}$ mice under normal physiological conditions (control mice) and during progression of B16F10 experimental lung metastasis. To our knowledge, this is the first experimental study done to investigate the gene dosage effects of endogenous galectin-3 on host immune responses and the possible regulatory mechanisms involved using murine model system.

In the present study, differences in the endogenous galectin-3 expression levels did not influence the frequencies of most of the splenic immune cell subsets as well as the intrathymic T cell differentiation in Gal-$3^{+/+}$, Gal-$3^{+/-}$ and Gal-$3^{-/-}$ mice under normal physiological conditions (control mice) as well as during progression of melanoma lung metastasis (day 7, day 14, day 21). However, percentages of splenic NK cells exhibited marked reduction in Gal-$3^{-/-}$ mice compared to Gal-$3^{+/+}$ and Gal-$3^{+/-}$ mice under normal physiological conditions (control mice) as well as on day 14 during experimental lung metastasis of B16F10 melanoma cells. Also, the percentages of splenic $B220^{+}$ (B cells) were found to be remarkable lower in Gal-$3^{-/-}$ mice compared to Gal-$3^{+/-}$ mice group under normal physiological conditions (control mice).

Further, the frequencies of T cells, B cells and NK cells and macrophages amongst the lung infiltrating leukocytes were not found to be significantly different between Gal-$3^{+/+}$, Gal-$3^{+/-}$ and Gal-$3^{-/-}$ mice groups during progression of melanoma lung metastasis (day 7, day 14, day 21). Together, the immunophenotyping results indicated that endogenous galectin-3 expression levels might modulate the functional responses rather than frequencies of most of the immune cell types studied in Gal-$3^{+/+}$, Gal-$3^{+/-}$ and Gal-$3^{-/-}$ mice, with exception of splenic NK and B cells whose percentages exhibited striking differences in these mice groups.

Higher splenic T cell proliferative responses were exhibited by Gal-$3^{+/-}$ and Gal-$3^{-/-}$ mice as compared to Gal-$3^{+/+}$ mice upon *in vitro* stimulation with PMA + Ionomycin and anti-CD3/CD28 mAbs. These responses showed *LGALS3* gene dosage effects, albeit with an inverse correlation to galectin-3 expression levels. The relative trend in the *in vitro* proliferative responses exhibited by the splenocytes of Gal-$3^{+/+}$, Gal-$3^{+/-}$ and Gal-$3^{-/-}$ mice during progression of B16F10 lung metastasis was found to be similar to that observed under non-tumor-bearing conditions in these mice groups. However, marked reduction in the *in vitro* proliferative responses of stimulated splenocytes from Gal-$3^{+/+}$, Gal-$3^{+/-}$ and Gal-$3^{-/-}$ mice groups was noted during progression of melanoma lung metastasis (day 7, day 14, day 21) compared to normal physiological conditions indicated by reduced radioactive counts of ^{3}H-TdR (CPM) incorporated in DNA suggesting immune suppression in Gal-$3^{+/+}$, Gal-$3^{+/-}$ and Gal-$3^{-/-}$ mice during the course of metastasis (Results chapters 1 and 2). It has been previously reported that galectin-3 is absent in resting $CD4^{+}$ and $CD8^{+}$ T cells, but is inducible by various stimuli such as viral trans-activating factors, TCR ligation, calcium ionophores etc. [46]. Further, extracellular galectin-3 is known to form multivalent lattices with glycoproteins of TCR and restrains lateral mobility of

TCR complex necessary for clustering, thereby Inhibiting TCR mediated signal transduction and activation of T cells [110]. The enhancement of splenic T cell proliferative responses observed in Gal-$3^{+/-}$ and Gal-$3^{-/-}$ mice compared to that in Gal-$3^{+/+}$ mice might be possibly due to abrogation of inhibitory effects of galectin-3 on TCR signaling in Gal-$3^{+/-}$ and Gal-$3^{-/-}$ mice groups.

Calcium is an important intracellular secondary messenger involved in the regulation of many signaling pathways in a multitude of different biological processes including cell growth, proliferation and apoptosis [312-314]. Stimulation of T cells with soluble antibodies to the CD3/T-cell receptor complex causes rapid increases in the intracellular concentration of calcium, which plays a crucial role during the activation and homeostasis of T cells [315-318]. In the present study, upon *in vitro* stimulation of splenocytes using PMA + Ionomycin or anti-CD3 mAb, Gal-$3^{+/-}$ and Gal-$3^{-/-}$ mice showed increased intracellular calcium flux compared to Gal-$3^{+/+}$ mice. On the other hand, reduced intracellular Ca^{++} flux was observed in PMA + Ionomycin or soluble anti-CD3/CD28 mAbs stimulated purified splenic T cells of Gal-$3^{-/-}$ mice as compared to those of Gal-$3^{+/+}$ and Gal-$3^{+/-}$ mice. Further, the overall intracellular Ca^{++} levels produced before as well as after stimulation with PMA + Ionomycin or soluble anti-CD3/CD28 mAbs were lower in purified splenic T cells as compared to those in total splenocytes population in Gal-$3^{+/+,}$ Gal-$3^{+/-}$ and Gal-$3^{-/-}$ mice. These differences in intracellular Ca^{++} levels observed between splenocytes and purified T cells might be possibly due to the contribution of intracellular Ca^{++} flux generated by the other immune cell subsets (macrophages, neutrophils, dendritic cells etc.) along with the T cells in the total splenocytes population, when compared to purified T cells alone. An earlier study has reported that galectin-3 stimulates uptake of extracellular Ca^{++} in human Jurkat T cells [254]. This study has also pointed out that galectin-3 released by accessory cells such as macrophages may

bind *in vivo* to T-cell activation antigens and also participate in Ca^{++} signaling [254]. In the present study, the increased T cell proliferation but the reduced intracellular Ca^{++} flux observed in stimulated T cells of Gal-$3^{-/-}$ mice compared to those of Gal-$3^{+/+}$ and Gal-$3^{+/-}$ mice, indicates possible impairment of functional T cell responses in the complete absence of endogenous galectin-3 expression in Gal-$3^{-/-}$ mice. Collectively, these results highlight the importance of endogenous galectin-3 expression in the regulation of T cell calcium signaling in the host. On day 21 during experimental pulmonary metastasis assay conditions when the lungs of Gal-$3^{+/+}$, Gal-$3^{+/-}$ and Gal-$3^{-/-}$ mice were flooded with metastatic melanoma colonies, marked reduction in the intracellular Ca^{++} flux indicated by reduced Fluo-3 fluorescence intensity was noted in the *in vitro* stimulated splenocytes from Gal-$3^{+/+}$, Gal-$3^{+/-}$ and Gal-$3^{-/-}$ mice. This pointed towards a decline in the ability of splenocytes to respond to stimulants at the advanced stage of lung melanoma metastasis.

Reactive Oxygen Species (ROS) are essential for various biological functions, including cell survival, cell growth, proliferation, differentiation and immune responses [319]. In immune cells, intracellular ROS generated upon exogenous stimulation play a critical role in directing the appropriate immune responses [320,321]. In the present study, we observed that, under normal physiological conditions as well as on day 21 of the experimental metastasis assay conditions, splenocytes derived from Gal-$3^{+/-}$ and Gal-$3^{-/-}$ mice produced much less intracellular ROS *in vitro* compared with Gal-$3^{+/+}$ mice splenocytes, in response to the potent ROS inducer PMA+ Ionomycin as well as upon TCR mediated stimulation using anti-CD3 mAb. The data indicate the importance of endogenous galectin-3 expression levels in the appropriate intracellular ROS production by the activated immune cells in the host, the absence of which might lead to suboptimal or weaker immune responses as seen in Gal-$3^{-/-}$ mice.

Extracellular galectin-3 is known to induce apoptosis in human T leukemia cell lines, human peripheral blood mononuclear cells, and activated mouse T cells [109,255,258]; whereas intracellular galectin-3 has been found to be anti-apoptotic in various cell types including human leukemia T cells [47,55,304]. Analysis of spontaneously apoptotic immune cell populations in the freshly isolated splenocytes of Gal-$3^{+/+}$, Gal-$3^{+/-}$ and Gal-$3^{-/-}$ mice by Annexin V-PI staining revealed some interesting findings. It was observed that, frequencies of early apoptotic (Annexin V^+PI^-) as well as late apoptotic/ necrotic (Annexin V^+PI^+) cells in total splenic lymphocytes population were not significantly different amongst Gal-$3^{+/+}$, Gal-$3^{+/-}$ and Gal-$3^{-/-}$ mice groups. However, the differences became apparent when early apoptotic cell populations (Annexin V^+PI^-) were compared in Gal-$3^{+/-}$ and Gal-$3^{-/-}$ mice groups within total T cells ($CD3^+$) and helper T cell ($CD3^+CD4^+$) subsets. Gal-$3^{-/-}$ mice splenocytes exhibited significantly higher percentages of early apoptotic (Annexin V^+PI^-) cells as compared to Gal-$3^{+/-}$ mice splenocytes. On the other hand, frequencies of late apoptotic/ necrotic (Annexin V^+PI^+) splenic B cells ($B220^+$) were found to be significantly lower in Gal-$3^{-/-}$ mice than in Gal-$3^{+/+}$ and Gal-$3^{+/-}$ mice. Collectively, these results indicated that, the differences in the functional immune responses observed in splenic T cells from Gal-$3^{+/+}$ and Gal-$3^{-/-}$ mice might not result from the prevalence of apoptotic cell populations in either of these two mice groups, as no significant differences were noted in the frequencies of spontaneously apoptotic cells in the splenic T cell subsets of Gal-$3^{+/+}$ and Gal-$3^{-/-}$ mice.

NK cells are crucial players in host anti-tumor immune responses mediated by their cytolytic activities and IFN-γ production [306-308]. In the present study, immunophenotyping results indicated differences in the percentages of splenic NK cells ($CD3^-NK1.1^+$) in Gal-$3^{+/+}$, Gal-$3^{+/-}$ and Gal-$3^{-/-}$ mice that correlated with endogenous galectin-3 expression levels in these mice groups. Gal-$3^{-/-}$ mice exhibited significantly

lower percentages of splenic NK cells ($CD3^{-}NK1.1^{+}$) under normal physiological conditions. Further, marked decrease in splenic NK cell-mediated cytotoxicity against YAC-1 murine T lymphoma cells was observed in Gal-$3^{+/-}$ and Gal-$3^{-/-}$ mice compared to Gal-$3^{+/+}$ mice. On day 14 post intravenous B16F10 injection, Gal-$3^{-/-}$ mice exhibited significantly decreased levels of splenic NK cells as compared to Gal-$3^{+/+}$ and Gal-$3^{+/-}$ mice. It has been previously demonstrated that, treatment of B16F10 murine melanoma cells with swainsonine, an *N*-glycosylation inhibitor, inhibits their lung metastasis in syngeneic C57BL/6 mice by prevention of *N*-glycosylation in these cells [26]. Earlier study has reported that, systemic administration of swainsonine to C57BL/6 mice also results in inhibition of metastasis of untreated B16F10 cells. In contrast, the inhibitory activity of swainsonine was completely abrogated when assays were performed in mice depleted of their NK cell activity either experimentally (C57BL/6 mice treated with anti-asialo-GM1 antibody or cyclophosphamide) or as a result of genetic mutation (homozygous $C57BL/6^{bg/bg}$ beige mice) [322]. NK cells are known to provide first line of defense against transformed and tumorigenic cells in an organism. These findings suggested that, the impaired ability of NK cells to kill the tumor targets in Gal-$3^{-/-}$ mice might be an important predisposing factor facilitating enhanced melanoma lung metastasis observed in Gal-$3^{-/-}$ mice despite the complete absence of endogenous galectin-3 on day 14 under experimental assay conditions. This finding is further supported in Gal-$3^{+/-}$ mice, as increased cytotoxicity of freshly isolated NK cells against YAC-1 tumor targets as well as that of IL-2 stimulated NK cells against B16F10 tumor targets was observed *in vitro* along with reduced pulmonary B16F10 melanoma metastases *in vivo* in Gal-$3^{+/-}$ mice as compared to Gal-$3^{-/-}$ mice.

The studies done previously to elucidate the role of galectin-3 in functional immune responses using Gal-$3^{-/-}$ mice have also revealed the protein's ability to regulate Th1/Th2 polarization under various pathological conditions [52,270,271,286]. It has been reported

that, *Toxoplasma gondii* infected Gal-3$^{-/-}$ mice mounted a higher Th1-polarized response compared to infected Gal-3$^{+/+}$ mice. Further, it was demonstrated that presence of endogenous galectin-3 suppressed the production of IL-12 by dendritic cells in Gal-3$^{+/+}$ mice, which is the major cytokine that drives the Th1 response [270]. Several *in vitro* and *in vivo* studies have suggested that, galectin-3 may modulate inflammatory responses through its functions on cell activation, cell migration or inhibition of apoptosis thus prolonging the survival of inflammatory cells [323]. The emerging data from studies of Gal-3$^{+/+}$ and Gal-3$^{-/-}$ mice support the role of galectin-3 in the promotion of inflammatory responses [39,50,51,286]. In the present study, the levels of Th1 (IL-2, IFN-γ, TNF), Th2 (IL-4, IL-6, IL-10) and Th17 (IL-17A) cytokines were found to be decreased in Gal-3$^{+/-}$ and Gal-3$^{-/-}$ mice sera compared to Gal-3$^{+/+}$ mice sera under normal physiological conditions, highlighting the importance of endogenous galectin-3 in the regulation of serum cytokine milieu in the host. Serum IL-2 and IFN-γ levels showed positive correlation with endogenous galectin-3 protein levels in Gal-3$^{+/+}$, Gal-3$^{+/-}$ and Gal-3$^{-/-}$ mice. Correlation analysis of serum cytokine levels indicated that, the cytokine milieu was disturbed in Gal-3$^{-/-}$ mice, with dysregulation of pro-inflammatory and anti-inflammmatory cytokine balance in these mice. The balance between pro-inflammatory and anti-inflammatory signaling is critical to maintain the immune homeostasis under normal physiological conditions. In Gal-3$^{-/-}$ mice, the immune homeostasis appeared to be disturbed, which may contribute to the observed immune dysregulation in these mice.

Cytokines are key regulators of immune responses in cancer. They can modulate tumor growth and metastasis by either elevating or suppressing anti-tumor immune responses. In the present study, the relative pattern of serum Th1, Th2 and Th17 cytokine profiles in Gal-3$^{+/+}$, Gal-3$^{+/-}$ and Gal-3$^{-/-}$ mice altered gradually with the progression of lung metastasis from day 7, day 14 to day 21 post intravenous

B16F10 injection. Further, serum concentrations of most of the cytokines assessed, particularly IL-2, TNF, IL-10 exhibited striking reductions in Gal-$3^{+/+}$, Gal-$3^{+/-}$ as well as Gal-$3^{-/-}$ mice groups under experimental metastasis assay conditions (day 7, day 14, day 21) when compared with normal physiological conditions (control mice). Also, on day 21 post intravenous B16F10 injections when lungs of mice from Gal-$3^{+/+}$, Gal-$3^{+/-}$ and Gal-$3^{-/-}$ groups were flooded with metastatic melanoma colonies, serum levels of IFN-γ reduced remarkably as compared to normal physiological conditions as well as those during early stages of metastatic progression i.e. day 7 and day 14. Serum levels of IL-6, which is known to be a key metastasis promoting cytokine, were found to be significantly reduced during initial stages of experimental metastasis assay (day 7) compared to normal physiological conditions (control) in Gal-$3^{-/-}$ mice, but increased remarkably with the progression of lung metastasis (day 14 and day 21) in this mice group. These alterations seen in systemic cytokine production in Gal-$3^{+/+}$, Gal-$3^{+/-}$ and Gal-$3^{-/-}$ mice groups pointed towards a complex dynamics of immune regulation by endogenous galectin-3 expression levels during progression of melanoma lung metastasis in these mice.

Majority of the literature data which reported upregulation, downregulation or no significant differences in the Th1 and Th17 type cytokine levels (IFN-γ, TNF, IL-17 etc.) in Gal-$3^{-/-}$ mice as compared to Gal-$3^{+/+}$ mice have emerged from studies of patho-physiological conditions developed in animal models using Gal-$3^{+/+}$ and Gal-$3^{-/-}$ mice genotypic groups [34,52,289,293,298,324-328]. Also, many of these reports have focused on studying cytokine expression in lymphoid organs or a specific organ/tissue with diseased condition in Gal-$3^{+/+}$ and Gal-$3^{-/-}$ mice or the cytokines secreted under *in vitro* culture conditions by a particular subset of immune cells isolated from these mice. There is scarcity of studies reporting serum cytokine levels in Gal-$3^{+/+}$ and

Gal-3$^{-/-}$ mice under normal physiological conditions. To our knowledge, this is the first study which reports serum Th1/Th2/Th17 cytokine profile in Gal-3$^{+/+}$, Gal-3$^{+/-}$ and Gal-3$^{-/-}$ mice under normal physiological conditions as well as during progression of experimental B16F10 lung metastasis. The findings help to understand how endogenous galectin-3 at different expression levels modulates serum cytokine production in Gal-3$^{+/+}$, Gal-3$^{+/+}$ and Gal-3$^{-/-}$ mice.

IFN-γ is a multifunctional cytokine produced mainly by NK cells and activated T cells. IFN-γ is a key cytokine exerting anti-tumor immunity against melanoma and various other cancers [37,329]. It has been found to have direct anti-proliferative and pro-apoptotic effects on tumor cells in animal models [309,330-334]. IFN-γ prevents B16 experimental metastasis by directly inhibiting cell growth [309]. Another study reported that, HTLV-1-Tax$^{+/+}$IFNγ$^{-/-}$ mice develop increased numbers of soft tissue tumors with enhanced tumor-associated angiogenesis and up-regulation of vascular endothelial growth factor expression [331].

In the present study, serum IFN-γ levels as well as splenic IFN-γR1 (CD119) expressing T and NK cell frequencies were found to be significantly reduced in Gal-3$^{-/-}$ mice as compared to Gal-3$^{+/+}$ mice. Interestingly, percentages of IFN-γR1 (CD119) expressing T and NK cells were highest in Gal-3$^{+/-}$ mice splenocytes amongst the three groups of mice. IFN-γ exerts its effects by binding to IFN-γ receptor on the cell surface which is followed by STAT1 mediated signaling pathway. On stimulation of splenocytes using recombinant IFN-γ, activated phospho-STAT1 (Tyr701) protein levels were found to be higher in Gal-3$^{+/-}$ mice than in Gal-3$^{+/+}$ and Gal-3$^{-/-}$ mice, which correlated with the highest frequency of IFN-γR1 expressing splenic T and NK cells in Gal-3$^{+/-}$ mice. On the other hand, IFN-γ stimulated Gal-3$^{-/-}$

mice splenocytes exhibited highest intracellular expression of SOCS1 and SOCS3 proteins, which are known to directly antagonize STAT1 activation by negative feedback mechanism [335,336]. Thus, complete absence of endogenous host galectin-3 appeared to contribute in the attenuation of STAT1 mediated IFN-γ signaling in Gal-3$^{-/-}$ mice splenocytes.

SOCS1 and SOCS3 proteins can both inhibit JAK phosphorylation of STAT, thus creating a negative feedback loop that attenuates cytokine signal transduction, although the mechanisms by which they act appear to differ. Whereas SOCS1 functions by binding directly to JAK proteins, SOCS3 inhibits signaling by binding to phosphorylated tyrosine sites on the cytoplasmic domain of the receptor [337,338]. In addition, SOCS1 is known to exhibit a much stronger inhibitory activity toward the activation of STAT1 than did SOCS3 [336]. The literature data indicate that induction of SOCS1 and SOCS3 proteins in host cells upon IFN-γ stimulation is a result of a complex interplay between several different factors; including cell type, concentration of exogenous IFN-γ used for stimulation, levels of other cytokines present in the cellular environment, expression of cytokine receptors, relative abundance and activation level of IFN-γ/STAT1 and IL-6, IL-10/STAT3 signaling in cells and galectin-3 expression levels in host. In the present study, due to striking reduction in IFN-γR1 expression observed in Gal-3$^{-/-}$ mice, stimulation of murine splenocytes with increasing doses of exogenous IFN-γ might not lead to a gradual and sustained increase in SOCS1 production in IFN-γ dose dependent manner in Gal-3$^{-/-}$ mice, as expected. Further, galectin-3 being an important regulator of SOCS1 and SOCS3 expression in host [339,340], this regulatory mechanism appears to be impaired in Gal-3$^{+/-}$ and Gal-3$^{-/-}$ mice, leading to abrupt decrease in splenic SOCS1

and SOCS3 levels upon stimulation with increasing doses of recombinant murine IFN-γ *in vitro.*

Survival study of Gal-$3^{+/+}$, Gal-$3^{+/-}$ and Gal-$3^{-/-}$ mice under normal physiological conditions revealed that their median survival rates were strikingly different and correlated positively with endogenous galectin-3 expression levels in these mice groups. Gal-$3^{+/-}$ (674 days) and Gal-$3^{-/-}$ (575 days) mice had remarkably lower median survival rates, compared to Gal-$3^{+/+}$ (854 days) mice, highlighting the vital role of endogenous galectin-3 in the maintenance of homeostasis and physiological functioning during the lifespan of mice. On the other hand, overall survival as well as median survival rates of Gal-$3^{+/+}$, Gal-$3^{+/-}$ and Gal-$3^{-/-}$ mice bearing metastatic melanoma colonies in their lungs did not differ significantly, indicating that the differences in endogenous galectin-3 levels did not influence the survival rates in Gal-$3^{+/+}$, Gal-$3^{+/-}$ and Gal-$3^{-/-}$ mice groups under experimental metastasis assay conditions. However, under these conditions, mice from all the three groups died due to respiratory arrest caused by heavy burden of metastatic melanoma colonies developed in their lungs and could not survive for a prolonged period of time after intravenous B16F10 melanoma cells injection.

In the present investigation, detailed analysis of immune scenario in Gal-$3^{+/+}$, Gal-$3^{+/-}$ and Gal-$3^{-/-}$ mice having different endogenous galectin-3 expression levels revealed that their immune system has striking differences. Two broad categories of immune responses were observed: (a) Immune responses that correlated with levels of endogenous galectin-3 expression and clearly showed *LGALS3* gene dosage effects in Gal-$3^{+/+}$, Gal-$3^{+/-}$ and Gal-$3^{-/-}$ mice. These included splenic NK cell frequency, NK mediated cytotoxicity against YAC-1 tumor targets, serum IL-2 and IFN-γ levels (Direct correlation

with endogenous galectin-3 expression levels) as well as T cell proliferative responses (Inverse correlation with endogenous galectin-3 expression levels) in Gal-$3^{+/+}$, Gal-$3^{+/-}$ and Gal-$3^{-/-}$ mice and were predominantly noted under normal physiological conditions (control mice). (b) Immune responses in which no *LGALS3* gene dosage effects were observed with respect to endogenous galectin-3 expression levels in Gal-$3^{+/+}$, Gal-$3^{+/-}$ and Gal-$3^{-/-}$ mice. For example, Gal-$3^{+/-}$ mice demonstrated highest percentages of IFN-γR1 expressing splenic T cells and NK cells, elevated total STAT1 and activated phospho-STAT1(Tyr701) protein levels as well as highest NK mediated cytotoxicity against B16F10 tumor targets amongst Gal-$3^{+/+}$, Gal-$3^{+/-}$ and Gal-$3^{-/-}$ mice groups under normal physiological conditions. Further, on day 21 under experimental metastasis assay conditions, serum IFN-γ and IL-10 concentrations were found to be significantly lower in Gal-$3^{+/-}$ mice as compared to both Gal-$3^{+/+}$ and Gal-$3^{-/-}$ mice groups. The possible mechanisms underlying such a paradoxical immunoregulatory role of endogenous host galectin-3 observed in the Gal-$3^{+/-}$ mice warrant further in-depth investigation.

We assessed whether incidence of organ specific metastasis of tumor cells was affected by different endogenous galectin-3 expression levels in Gal-$3^{+/+}$, Gal-$3^{+/-}$ and Gal-$3^{-/-}$ mice. B16F10 murine melanoma model was used to establish lung specific metastasis of B16F10 melanoma cells in Gal-$3^{+/+}$, Gal-$3^{+/-}$ and Gal-$3^{-/-}$ mice by experimental metastasis assay. On day 14 post lateral tail vein injection of B16F10 cells, it was observed that frequency of B16F10 pulmonary metastasis was not significantly different between Gal-$3^{+/+}$ and Gal-$3^{-/-}$ mice groups. However, in Gal-$3^{+/-}$ mice, the number of metastatic melanoma colonies present on the lungs were found to be significantly lower than that in Gal-$3^{+/+}$ and Gal-$3^{-/-}$ mice. These results were in accordance with an earlier published study done by our group using Gal-$3^{+/+}$, Gal-$3^{+/-}$ and Gal-$3^{-/-}$ mice to study lung metastasis of B16F10 cells by

experimental metastasis assay [32]. This previously reported study had used two different doses of B16F10 cells to induce lung metastasis in mice (1.8×10^5 cells/ mouse and 0.75×10^5 cells/ mouse) and also, the duration of the assay was different (21 days). In the present thesis, experimental metastasis assay was performed using 1×10^5 cells/ mouse and the progression of lung metastasis was monitored at 3 different time points i.e. day 7, day 14 and day21 post intravenous injection of B16F10 cells in Gal-$3^{+/+}$, Gal-$3^{+/-}$ and Gal-$3^{-/-}$ mice groups. The reason for using this protocol was to assess early time points where the differences in the number of metastatic melanoma colonies in the lungs could be clearly noted between Gal-$3^{+/+}$, Gal-$3^{+/-}$ and Gal-$3^{-/-}$ mice groups. At the later time points i.e. after 19 days, the lungs were flooded with the melanoma colonies and the differences in the pulmonary metastatic frequency were difficult to quantitate.

In the present study, we have also done the histopathological analysis (Hematoxylin - Eosin staining) of lungs bearing metastatic B16F10 melanoma colonies from Gal-$3^{+/+}$, Gal-$3^{+/-}$ and Gal-$3^{-/-}$ mice groups. The lung histopathology provided additional confirmatory evidence with respect to number and size of melanoma colonies in the interiors of the mice lungs from Gal-$3^{+/+}$, Gal-$3^{+/-}$ and Gal-$3^{-/-}$ genotypic groups.

Further, survival study done in Gal-$3^{+/+}$, Gal-$3^{+/-}$ and Gal-$3^{-/-}$ mice groups under experimental pulmonary metastasis assay conditions pointed out that their survival did not differ significantly across the three genotypic groups. Thus, different expression levels of endogenous galectin-3 did not seem to dictate the survival rates in mice bearing lung-specific melanoma metastases. Instead, all the mice in Gal-$3^{+/+}$, Gal-$3^{+/-}$ and Gal-$3^{-/-}$ groups under experimental metastasis assay condition died due to extremely heavy load of metastatic melanoma colonies that flooded the lungs, causing respiratory arrest ultimately leading to death in all the three mice groups studied.

Experimental metastasis assay using well characterized B16 murine melanoma model for lung specific metastasis in Gal-$3^{+/+}$, Gal-$3^{+/-}$ and Gal-$3^{-/-}$ mice confirmed that apart from promoting interaction with cells in the lungs, galectin-3 has a major role in dictating the metastatic outcome by other mechanisms as well. The functional redundancy by other galectins including galectin-1, -8 and -9 as well as the role of polyLacNAc on *N*-glycans in Gal-$3^{-/-}$ mice has already been ruled out as reported in a previously published study [32]. The enhanced melanoma lung metastasis observed in Gal-$3^{-/-}$ mice may be linked to compromised host immunity in the total absence of endogenous galectin-3 in these mice.

During metastatic spread of cancer cells to distant organs through the circulation, these cells encounter different immune cell types of innate and adaptive immune compartment. In an immunocompetent host, these immune cells can effectively exert their anti-tumor effects to eradicate majority of the circulating cancer cell population. The heightened anti-tumor immune responses in Gal-$3^{+/-}$ mice might further explain the lowest incidence of B16F10 lung metastasis observed in these mice. However, in the scenario where the host immune system is not optimally performing or is dysregulated, major frequency of the tumor cells can survive and sustain in the circulation ultimately reaching their secondary target organ. The chances of high number of B16F10 melanoma cells that survive in the circulation, getting anatomically or mechanically trapped in the lungs of Gal-$3^{-/-}$ mice and giving rise to metastatic melanoma colonies would be very high. It would be interesting to explore the mechanisms employed by these tumor cells for lung homing in Gal-$3^{-/-}$ mice in the complete absence of endogenous galectin-3.

Functionally, galectin-3 is a complex molecule which exerts different effects on the cells depending on its subcellular localization. The secreted extracellular galectin-3

functions in an entirely different manner which is carbohydrate ligand dependent. The diversity of effects of galectin-3 seen on disease progression in large number of human cancer types is possibly a result of these differences in the localization of galectin-3 [65,129]. Our study demonstrates another aspect of endogenous host galectin-3, that of maintaining a functionally competent immune system in the host. We have comprehensively demonstrated that its absence may severely compromise host anti-tumor immunity and can adversely affect cancer progression in the host. Future galectin-3 targeted anti-cancer therapies would also need to take this aspect of galectin-3 function into account.

CHAPTER 8

SUMMARY AND CONCLUSION

Galectin-3 (Gal-3), a β-galactoside-binding mammalian lectin, is known to be involved in cancer progression and metastasis. However, there is an unmet need to identify the underlying mechanisms of cancer metastasis mediated by endogenous galectin-3 in the host. Galectin-3 is also known to be an important regulator of immune responses. However, the role of endogenous galectin-3 and mechanisms involved in the modulation of anti-tumor immune responses in the host remain unclear, demanding further in-depth investigation.

The present study was aimed at analyzing how expression of endogenous galectin-3 regulates host immunity and lung metastasis in B16F10 murine melanoma model using Gal-$3^{+/+}$, Gal-$3^{+/-}$ and Gal-$3^{-/-}$ mice genotypic groups. Detailed analysis of immune scenario in Gal-$3^{+/+}$, Gal-$3^{+/-}$ and Gal-$3^{-/-}$ mice with different endogenous galectin-3 expression levels revealed that their immune system has striking differences. Immunophenotyping analysis of freshly isolated splenocytes from Gal-$3^{+/+}$, Gal-$3^{+/-}$ and Gal-$3^{-/-}$ mice revealed that Gal-$3^{-/-}$ mice exhibited significantly decreased frequency of splenic NK ($CD3^{-}NK1.1^{+}$) cells as compared to Gal-$3^{+/+}$ mice. However, no significant differences were observed in the percentages of NKT ($CD3^{+}NK1.1^{+}$) cells, γδ T ($CD3^{+}\gamma\delta^{+}$) cells, macrophages ($CD14^{+}$), dendritic cells ($CD209^{+}$), helper ($CD3^{+}CD4^{+}$) and cytotoxic ($CD3^{+}CD8^{+}$) T cells as well as T_{reg} ($CD4^{+}CD25^{+}Foxp3^{+}$) in the splenocytes of Gal-$3^{+/+}$, Gal-$3^{+/-}$ and Gal-$3^{-/-}$ mice. No significant differences were noted in the intrathymic T cell lineage differentiation in Gal-$3^{+/+}$, Gal-$3^{+/-}$ and Gal-$3^{-/-}$ mice.

Upon *in vitro* stimulation using PMA + Ionomycin or anti-CD3/CD28 mAb, splenocytes of Gal-$3^{+/-}$ and Gal-$3^{-/-}$ mice showed increased T cell proliferation, but reduced T cell intracellular calcium flux and intracellular ROS generation than Gal-$3^{+/+}$ mice splenocytes. In splenic T cells ($CD3^{+}$) and helper T cell subset ($CD3^{+}CD4^{+}$), percentages of early

apoptotic (Annexin V^+PI^-) cells were found to be significantly higher in Gal-$3^{-/-}$ mice as compared to those in Gal-$3^{+/-}$ mice, whereas percentages of late apoptotic/necrotic (Annexin V^+PI^+) cells were remarkably lower in Gal-$3^{-/-}$ mice splenocytes than in Gal-$3^{+/+}$ and Gal-$3^{+/-}$ mice splenocytes. Further, Gal-$3^{-/-}$ mice exhibited marked reduction in the serum levels of Th1 (IL-2, IFN-γ, TNF), Th2 (IL-4, IL-6, IL-10) and Th17 (IL-17A) cytokines as studied by cytometric bead array using flow cytometry. Correlation analysis revealed dysregulation of the balance between pro-inflammatory and anti-inflammatory cytokines in the sera of Gal-$3^{-/-}$ mice. The imbalance in serum cytokine milieu may further contribute to the observed immune dysregulation in Gal-$3^{-/-}$ mice. By Kaplan-Meier survival curve analysis, it was observed that, the overall survival rate of Gal-$3^{+/-}$ mice group was significantly lower (P = 0.0232) than that of Gal-$3^{+/+}$ mice group. Interestingly, the median survival rates of Gal-$3^{+/+}$, Gal-$3^{+/-}$ and Gal-$3^{-/-}$ mice exhibited striking differences i.e. 854 days, 674 days and 575 days respectively, highlighting the importance of endogenous galectin-3 expression levels in the regulation of normal physiological functioning during the lifespan of the host.

B16F10 murine melanoma model was used to establish lung specific metastasis of B16F10 melanoma cells in Gal-$3^{+/+}$, Gal-$3^{+/-}$ and Gal-$3^{-/-}$ mice by experimental metastasis assay. On day 7 post intravenous injection of B16F10 cells in mice, no metastatic colonies were seen on mice lungs. On day 14, the numbers of lung metastatic colonies were almost equal in Gal-$3^{+/+}$ and Gal-$3^{-/-}$ mice and were found to be significantly lower in Gal-$3^{+/-}$ mice compared to Gal-$3^{+/+}$ and Gal-$3^{-/-}$ mice. On day 21, number of lung metastatic colonies exceeded the manually countable limit and the lungs were flooded with melanoma colonies in all the three groups of mice. Histopathological study of formalin fixed lung sections by hematoxylin-eosin staining provided further confirmatory evidence to support these results.

Immune responses were monitored during progression of melanoma lung metastasis in Gal-$3^{+/+}$, Gal-$3^{+/-}$ and Gal-$3^{-/-}$ mice i.e. on Day 7, Day 14 and Day 21 post intravenous B16F10 injection. On day 14, Gal-$3^{-/-}$ mice exhibited significantly decreased levels of splenic NK cells ($CD3^{-}NK1.1^{+}$) as compared to Gal-$3^{+/+}$ and Gal-$3^{+/-}$ mice. No significant differences were noted in the percentages of splenic NKT ($CD3^{+}NK1.1^{+}$) cells, γδ T ($CD3^{+}\gamma\delta^{+}$) cells, macrophages ($CD14^{+}$), dendritic cells ($CD209^{+}$), B cells ($B220^{+}$), helper ($CD3^{+}CD4^{+}$) and cytotoxic ($CD3^{+}CD8^{+}$) T cells as well as T_{reg} ($CD4^{+}CD25^{+}Foxp3^{+}$) in Gal-$3^{+/+}$, Gal-$3^{+/-}$ and Gal-$3^{-/-}$ mice on day 7, day 14 and day 21 under experimental metastatic assay conditions. Further, intrathymic T cell differentiation remained unaffected in Gal-$3^{+/+}$, Gal-$3^{+/-}$ and Gal-$3^{-/-}$ mice during progression of B16F10 lung metastasis. It was also observed that, frequencies of lung infiltrating leukocytes including T cells ($CD3^{+}$), B cells ($B220^{+}$), NK cells ($CD3^{-}NK1.1^{+}$), NKT cells ($CD3^{+}NK1.1^{+}$) and macrophages ($CD14^{+}$) were not significantly different between Gal-$3^{+/+}$, Gal-$3^{+/-}$ and Gal-$3^{-/-}$ mice groups on day 7, day 14 and day 21 of experimental metastatic assay conditions.

On day 7, day 14 and day 21, splenocytes of Gal-$3^{-/-}$ mice stimulated with PMA + Ionomycin and anti-CD3/CD28 mAbs showed significantly increased proliferative response, than Gal-$3^{+/+}$ and Gal-$3^{+/-}$ mice as studied by [^{3}H] Thymidine incorporation assay. Levels of intracellular Ca^{++} flux in stimulated splenocytes were found to decrease with progression of lung metastasis in Gal-$3^{+/+}$, Gal-$3^{+/-}$ and Gal-$3^{-/-}$ mice. In the B16F10 lung metastasis model, upon *in vitro* stimulation of splenocytes using PMA + Ionomycin or anti-CD3 mAb, Gal-$3^{+/-}$ and Gal-$3^{-/-}$ mice splenocytes showed decreased intracellular Ca^{++} flux compared to Gal-$3^{+/+}$ mice. On day 21, Gal-$3^{-/-}$ mice splenocytes exhibited significantly lower intracellular ROS generation compared to Gal-$3^{+/+}$ mice upon *in vitro* stimulation with PMA + Ionomycin or anti-CD3 mAb. Further, the relative pattern of serum

Th1, Th2 and Th17 cytokine concentrations in Gal-$3^{+/+}$, Gal-$3^{+/-}$ and Gal-$3^{-/-}$ mice changed gradually with the progression of lung metastasis. On Day 21, levels of pro-inflammatory cytokines IL-6 and IL-17A were found to be highest in Gal-$3^{-/-}$ mice sera amongst the three mice groups. However, it was observed that, survival rates of Gal-$3^{+/+}$, Gal-$3^{+/-}$ and Gal-$3^{-/-}$ mice bearing lung metastases did not differ significantly and mice from all the three genotypic groups died due to the common cause i.e. respiratory arrest owing to heavy burden of metastatic melanoma colonies flooding the lungs of Gal-$3^{+/+}$, Gal-$3^{+/-}$ and Gal-$3^{-/-}$ mice.

In the present investigation, striking differences were observed in the immune scenario of Gal-$3^{+/+}$, Gal-$3^{+/-}$ and Gal-$3^{-/-}$ mice under normal physiological conditions as well as during progression of B16F10 lung metastasis. It was therefore important to decipher the mechanisms involved in endogenous galectin-3 mediated regulation of anti-tumor immune responses in these mice. We analyzed whether the cytotoxic function of splenic NK cells correlated with their phenotype in Gal-$3^{+/+}$, Gal-$3^{+/-}$ and Gal-$3^{-/-}$ mice. Immunomagnetically purified splenic NK cells from Gal-$3^{+/-}$ and Gal-$3^{-/-}$ mice exhibited significantly lower NK cytotoxicity against YAC-1 tumor cells than splenic NK cells from Gal-$3^{+/+}$ mice, as studied by [^{51}Cr] Release Assay. On the other hand, purified and recombinant murine IL-2 activated splenic NK cells from Gal-$3^{+/-}$ mice exhibited higher cytotoxicity against B16F10 melanoma cells than those from Gal-$3^{+/+}$ and Gal-$3^{-/-}$ mice. Thus, endogenous galectin-3 expression levels appeared to be important determinants of anti-tumor cytolytic function of splenic NK cells in Gal-$3^{+/+}$, Gal-$3^{+/-}$ and Gal-$3^{-/-}$ mice.

IFN-γ is a multifunctional cytokine produced mainly by NK cells and activated T cells, that is known to exert anti-tumor immune responses against melanoma and various other cancers [37,329] In the present study, marked decrease in serum IFN-γ levels and splenic IFN-γR1 (IFN-γ Receptor 1) expressing T and NK cell percentages were observed in

Gal-3$^{-/-}$ mice. STAT1 mediated IFN-γ signaling pathway intermediates in stimulated mice splenocytes were studied by western blotting. Total STAT1 and activated phospho-STAT1(Tyr701) protein levels were found to be higher in recombinant IFN-γ stimulated splenocytes of Gal-3$^{+/-}$ mice compared to Gal-3$^{+/+}$ and Gal-3$^{-/-}$ mice. On the other hand, levels of SOCS1 and SOCS3 proteins, which are known to directly antagonize STAT1 activation by negative feedback mechanism, were found to be higher in Gal-3$^{-/-}$ mice splenocytes compared to those in Gal-3$^{+/+}$ and Gal-3$^{+/-}$ mice splenocytes; suggesting possible attenuation of STAT1 mediated IFN-γ signaling in Gal-3$^{-/-}$ mice.

In conclusion, the findings of the present thesis indicated that endogenous galectin-3 contributes to anti-tumor immune responses in the host. Absence of endogenous galectin-3 results in dysregulation of immune responses. These are reflected in decreased NK cell frequency and NK cytotoxicity, disturbed serum Th1, Th2, Th17 cytokines milieu, reduced serum IFN-γ levels, low frequency of IFN-γR1 expressing splenic T and NK cells and attenuation of STAT1 mediated IFN-γ signaling in Gal-3$^{-/-}$ mice. The enhanced lung metastasis of B16F10 observed in Gal-3$^{-/-}$ mice can be strongly attributed to the compromised anti-tumor immunity observed in these mice (Figure 48).

Galectin-3 is also expressed in many different human cancer cell types. Although high galectin-3 expression has been correlated with transformation and metastasis-related events, its downregulation has also been associated with malignancy and tumor progression [65,129]. For instance, the expression of galectin-3 is found to be upregulated in gastric, liver and thyroid cancers, while it is downregulated in prostate, head and neck cancers and uterine sarcoma when compared to normal tissues [137-140]. Numerous studies have reported that decreased expression of galectin-3 correlates with cancer progression,

metastatic spread and reduced survival and has been associated with a poorer prognosis in human breast, prostate, cervical, bladder, cholangiocarcinoma, colon and pancreatic cancers [19,130-136]. In this context, it would be important to investigate whether reduced galectin-3 expression levels in the tumor cells and in circulation lead to dysfunctional anti-tumor immunity in these cancer patients.

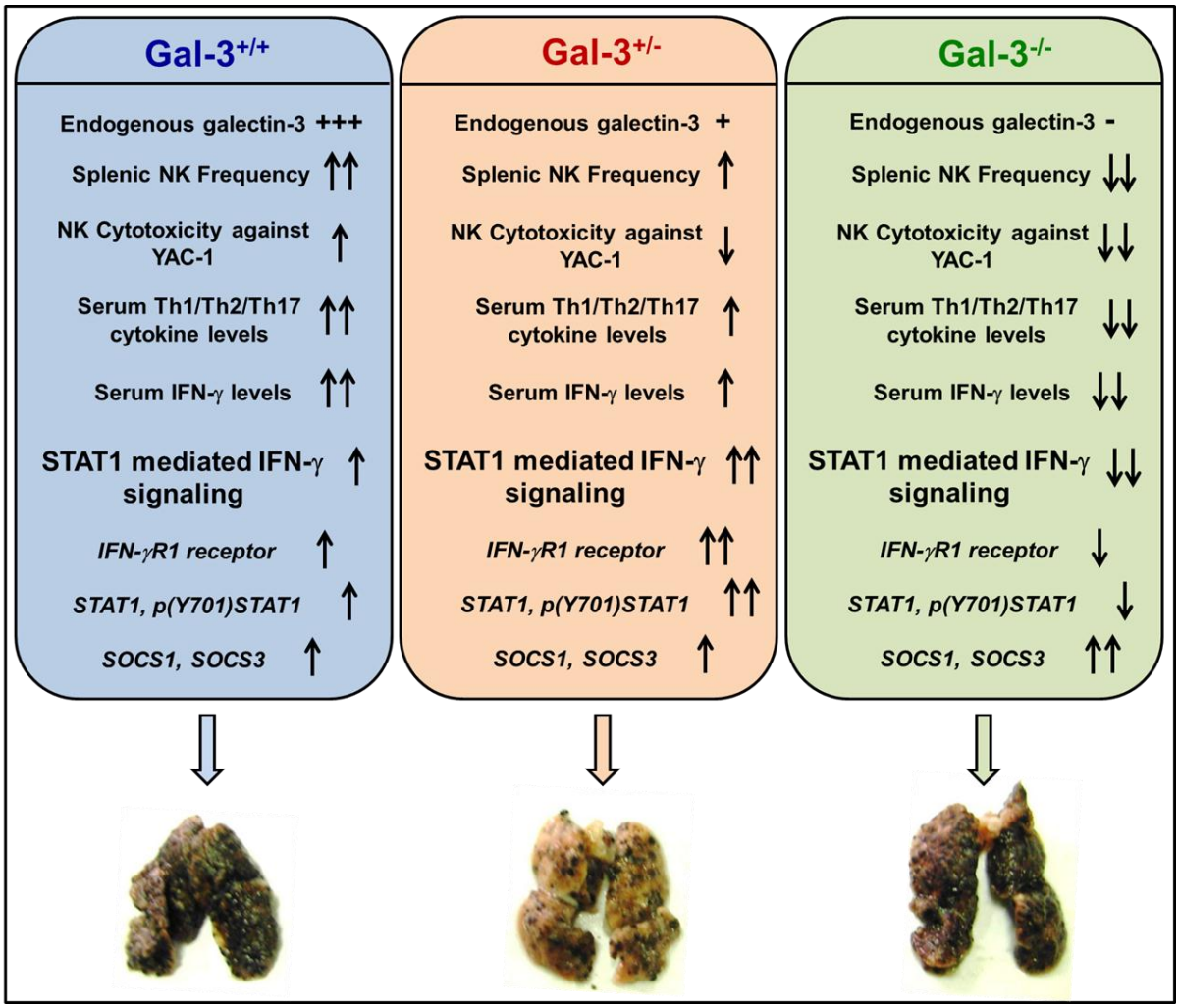

Figure 48: Role of endogenous galectin-3 in anti-tumor immune responses. The figure depicts the baseline immune scenario in Gal-$3^{+/+}$, Gal-$3^{+/-}$ and Gal-$3^{-/-}$ mice and provides explanation for the enhanced frequency of melanoma lung metastasis (B16F10 experimental metastasis assay) in Gal-$3^{-/-}$ mice due to compromised anti-tumor immune responses.

The apparently conflicting literature data highlight that the role of galectin-3 in cancer progression and metastasis is complex. Despite the multiple contradictory findings in experimental studies done using cancer cell lines and animal models as well as in the reported studies on human cancer specimen and sera samples of cancer patients, galectin-3 is considered a promising cancer biomarker and a potential therapeutic target in many different cancer types [12,16,18,220]. However, galectin-3 based anti-cancer therapies have not been successfully translated into clinics till date. A potential therapeutic approach to cancers with high galectin-3 expression is to use small molecule inhibitors of galectin-3 to enhance treatment response [341]. A non-randomized phase II pilot study of Modified Citrus Pectin (MCP) Pecta-Sol® (Econugenics Santa Rosa, CA) has investigated its tolerability and effect in 13 men with prostate cancer and biochemical prostate-specific antigen (PSA) failure after localized treatment, that is, radical prostatectomy, radiation or cryosurgery. This study suggested that MCP may lengthen the PSA doubling time in men with recurrent prostate cancer. However, the long-term impact that MCP will have on disease progression is not clear [342].

The present study adds a new dimension in understanding the complex role of endogenous host galectin-3 in the cancer metastasis process. The results emphasize that endogenous galectin-3 expression levels dictate the metastatic outcome through modulation of host immunity. Thus, while designing any galectin-3 targeted therapeutic strategies against cancer in the future, thorough understanding of host immune scenario is indispensable to ensure maximum efficacy of the anti-cancer therapies.

REFERENCES

[1] Houzelstein D, Goncalves IR, Fadden AJ, Sidhu SS, Cooper DN, Drickamer K, et al. Phylogenetic analysis of the vertebrate galectin family. Molecular biology and evolution 2004;21:1177-1187.
[2] Barondes SH, Castronovo V, Cooper DN, Cummings RD, Drickamer K, Feizi T, et al. Galectins: a family of animal beta-galactoside-binding lectins. Cell 1994;76:597-598.
[3] Moutsatsos IK, Wade M, Schindler M, Wang JL. Endogenous lectins from cultured cells: nuclear localization of carbohydrate-binding protein 35 in proliferating 3T3 fibroblasts. Proceedings of the National Academy of Sciences of the United States of America 1987;84:6452-6456.
[4] Perillo NL, Marcus ME, Baum LG. Galectins: versatile modulators of cell adhesion, cell proliferation, and cell death. Journal of molecular medicine 1998;76:402-412.
[5] Sato S, Hughes RC. Regulation of secretion and surface expression of Mac-2, a galactoside-binding protein of macrophages. The Journal of biological chemistry 1994;269:4424-4430.
[6] Califice S, Castronovo V, Bracke M, van den Brule F. Dual activities of galectin-3 in human prostate cancer: tumor suppression of nuclear galectin-3 vs tumor promotion of cytoplasmic galectin-3. Oncogene 2004;23:7527-7536.
[7] Dagher SF, Wang JL, Patterson RJ. Identification of galectin-3 as a factor in pre-mRNA splicing. Proceedings of the National Academy of Sciences of the United States of America 1995;92:1213-1217.
[8] Dumic J, Dabelic S, Flogel M. Galectin-3: an open-ended story. Biochimica et biophysica acta 2006;1760:616-635.
[9] Liu FT, Patterson RJ, Wang JL. Intracellular functions of galectins. Biochimica et biophysica acta 2002;1572:263-273.
[10] Liu FT. Regulatory roles of galectins in the immune response. International archives of allergy and immunology 2005;136:385-400.
[11] Nakahara S, Oka N, Raz A. On the role of galectin-3 in cancer apoptosis. Apoptosis : an international journal on programmed cell death 2005;10:267-275.
[12] Ochieng J, Furtak V, Lukyanov P. Extracellular functions of galectin-3. Glycoconjugate journal 2004;19:527-535.
[13] Wang JL, Gray RM, Haudek KC, Patterson RJ. Nucleocytoplasmic lectins. Biochimica et biophysica acta 2004;1673:75-93.
[14] Fortuna-Costa A, Gomes AM, Kozlowski EO, Stelling MP, Pavao MS. Extracellular galectin-3 in tumor progression and metastasis. Frontiers in oncology 2014;4:138.
[15] Funasaka T, Raz A, Nangia-Makker P. Galectin-3 in angiogenesis and metastasis. Glycobiology 2014;24:886-891.
[16] Liu FT, Rabinovich GA. Galectins as modulators of tumour progression. Nature reviews Cancer 2005;5:29-41.
[17] Newlaczyl AU, Yu LG. Galectin-3--a jack-of-all-trades in cancer. Cancer letters 2011;313:123-128.
[18] Radosavljevic G, Volarevic V, Jovanovic I, Milovanovic M, Pejnovic N, Arsenijevic N, et al. The roles of Galectin-3 in autoimmunity and tumor progression. Immunologic research 2012;52:100-110.

[19] Lotz MM, Andrews CW, Jr., Korzelius CA, Lee EC, Steele GD, Jr., Clarke A, et al. Decreased expression of Mac-2 (carbohydrate binding protein 35) and loss of its nuclear localization are associated with the neoplastic progression of colon carcinoma. Proceedings of the National Academy of Sciences of the United States of America 1993;90:3466-3470.

[20] Honjo Y, Nangia-Makker P, Inohara H, Raz A. Down-regulation of galectin-3 suppresses tumorigenicity of human breast carcinoma cells. Clinical cancer research : an official journal of the American Association for Cancer Research 2001;7:661-668.

[21] Yoshii T, Inohara H, Takenaka Y, Honjo Y, Akahani S, Nomura T, et al. Galectin-3 maintains the transformed phenotype of thyroid papillary carcinoma cells. International journal of oncology 2001;18:787-792.

[22] Almogren A, Abdullah J, Ghapure K, Ferguson K, Glinsky VV, Rittenhouse-Olson K. Anti-Thomsen-Friedenreich-Ag (anti-TF-Ag) potential for cancer therapy. Frontiers in bioscience 2012;4:840-863.

[23] Yu LG. The oncofetal Thomsen-Friedenreich carbohydrate antigen in cancer progression. Glycoconjugate journal 2007;24:411-420.

[24] Yu LG, Andrews N, Zhao Q, McKean D, Williams JF, Connor LJ, et al. Galectin-3 interaction with Thomsen-Friedenreich disaccharide on cancer-associated MUC1 causes increased cancer cell endothelial adhesion. The Journal of biological chemistry 2007;282:773-781.

[25] Zhao Q, Barclay M, Hilkens J, Guo X, Barrow H, Rhodes JM, et al. Interaction between circulating galectin-3 and cancer-associated MUC1 enhances tumour cell homotypic aggregation and prevents anoikis. Molecular cancer 2010;9:154.

[26] Srinivasan N, Bane SM, Ahire SD, Ingle AD, Kalraiya RD. Poly N-acetyllactosamine substitutions on N- and not O-oligosaccharides or Thomsen-Friedenreich antigen facilitate lung specific metastasis of melanoma cells via galectin-3. Glycoconjugate journal 2009;26:445-456.

[27] Agarwal AK, Gude RP, Kalraiya RD. Regulation of melanoma metastasis to lungs by cell surface Lysosome Associated Membrane Protein-1 (LAMP1) via galectin-3. Biochemical and biophysical research communications 2014;449:332-337.

[28] Dange MC, Agarwal AK, Kalraiya RD. Extracellular galectin-3 induces MMP9 expression by activating p38 MAPK pathway via lysosome-associated membrane protein-1 (LAMP1). Molecular and cellular biochemistry 2015;404:79-86.

[29] Agarwal AK, Srinivasan N, Godbole R, More SK, Budnar S, Gude RP, et al. Role of tumor cell surface lysosome-associated membrane protein-1 (LAMP1) and its associated carbohydrates in lung metastasis. Journal of cancer research and clinical oncology 2015;141:1563-1574.

[30] Dange MC, Srinivasan N, More SK, Bane SM, Upadhya A, Ingle AD, et al. Galectin-3 expressed on different lung compartments promotes organ specific metastasis by facilitating arrest, extravasation and organ colonization via high affinity ligands on melanoma cells. Clinical & experimental metastasis 2014;31:661-673.

[31] Krishnan V, Bane SM, Kawle PD, Naresh KN, Kalraiya RD. Altered melanoma cell surface glycosylation mediates organ specific adhesion and metastasis via lectin

receptors on the lung vascular endothelium. Clinical & experimental metastasis 2005;22:11-24.
[32] More SK, Srinivasan N, Budnar S, Bane SM, Upadhya A, Thorat RA, et al. N-glycans and metastasis in galectin-3 transgenic mice. Biochemical and biophysical research communications 2015;460:302-307.
[33] Comodo AN, Lacerda Bachi AL, Soares MF, Franco M, Castro Teixeira VdP. Galectin-3 expression favors metastasis in murine melanoma. Advances in Bioscience and Biotechnology 2013;04:55-62.
[34] Radosavljevic G, Jovanovic I, Majstorovic I, Mitrovic M, Lisnic VJ, Arsenijevic N, et al. Deletion of galectin-3 in the host attenuates metastasis of murine melanoma by modulating tumor adhesion and NK cell activity. Clinical & experimental metastasis 2011;28:451-462.
[35] Eude-Le Parco I, Gendronneau G, Dang T, Delacour D, Thijssen VL, Edelmann W, et al. Genetic assessment of the importance of galectin-3 in cancer initiation, progression, and dissemination in mice. Glycobiology 2009;19:68-75.
[36] Jia W, Kidoya H, Yamakawa D, Naito H, Takakura N. Galectin-3 accelerates M2 macrophage infiltration and angiogenesis in tumors. The American journal of pathology 2013;182:1821-1831.
[37] Dunn GP, Koebel CM, Schreiber RD. Interferons, immunity and cancer immunoediting. Nature reviews Immunology 2006;6:836-848.
[38] Kim R, Emi M, Tanabe K. Cancer immunoediting from immune surveillance to immune escape. Immunology 2007;121:1-14.
[39] Chen HY, Liu FT, Yang RY. Roles of galectin-3 in immune responses. Archivum immunologiae et therapiae experimentalis 2005;53:497-504.
[40] Pineda MA, Cuervo H, Fresno M, Soto M, Bonay P. Lack of Galectin-3 Prevents Cardiac Fibrosis and Effective Immune Responses in a Murine Model of Trypanosoma cruzi Infection. The Journal of infectious diseases 2015;212:1160-1171.
[41] Kouo T, Huang L, Pucsek AB, Cao M, Solt S, Armstrong T, et al. Galectin-3 Shapes Antitumor Immune Responses by Suppressing CD8+ T Cells via LAG-3 and Inhibiting Expansion of Plasmacytoid Dendritic Cells. Cancer immunology research 2015;3:412-423.
[42] Breuilh L, Vanhoutte F, Fontaine J, van Stijn CM, Tillie-Leblond I, Capron M, et al. Galectin-3 modulates immune and inflammatory responses during helminthic infection: impact of galectin-3 deficiency on the functions of dendritic cells. Infection and immunity 2007;75:5148-5157.
[43] Nieminen J, St-Pierre C, Sato S. Galectin-3 interacts with naive and primed neutrophils, inducing innate immune responses. Journal of leukocyte biology 2005;78:1127-1135.
[44] Sano H, Hsu DK, Yu L, Apgar JR, Kuwabara I, Yamanaka T, et al. Human galectin-3 is a novel chemoattractant for monocytes and macrophages. Journal of immunology 2000;165:2156-2164.
[45] Sato S, Ouellet N, Pelletier I, Simard M, Rancourt A, Bergeron MG. Role of galectin-3 as an adhesion molecule for neutrophil extravasation during streptococcal pneumonia. Journal of immunology 2002;168:1813-1822.

[46] Hsu DK, Chen HY, Liu FT. Galectin-3 regulates T-cell functions. Immunological reviews 2009;230:114-127.
[47] Yang RY, Hsu DK, Liu FT. Expression of galectin-3 modulates T-cell growth and apoptosis. Proceedings of the National Academy of Sciences of the United States of America 1996;93:6737-6742.
[48] Acosta-Rodriguez EV, Montes CL, Motran CC, Zuniga EI, Liu FT, Rabinovich GA, et al. Galectin-3 mediates IL-4-induced survival and differentiation of B cells: functional cross-talk and implications during Trypanosoma cruzi infection. Journal of immunology 2004;172:493-502.
[49] Rabinovich GA, Liu FT, Hirashima M, Anderson A. An emerging role for galectins in tuning the immune response: lessons from experimental models of inflammatory disease, autoimmunity and cancer. Scandinavian journal of immunology 2007;66:143-158.
[50] Henderson NC, Sethi T. The regulation of inflammation by galectin-3. Immunological reviews 2009;230:160-171.
[51] Hsu DK, Yang RY, Pan Z, Yu L, Salomon DR, Fung-Leung WP, et al. Targeted disruption of the galectin-3 gene results in attenuated peritoneal inflammatory responses. The American journal of pathology 2000;156:1073-1083.
[52] Ferraz LC, Bernardes ES, Oliveira AF, Ruas LP, Fermino ML, Soares SG, et al. Lack of galectin-3 alters the balance of innate immune cytokines and confers resistance to Rhodococcus equi infection. European journal of immunology 2008;38:2762-2775.
[53] Yang RY, Rabinovich GA, Liu FT. Galectins: structure, function and therapeutic potential. Expert reviews in molecular medicine 2008;10:e17.
[54] Advedissian T, Deshayes F, Poirier F, Grandjean C, Viguier M. [Galectins, a class of unconventional lectins]. Medecine sciences : M/S 2015;31:499-505.
[55] Liu FT, Yang RY, Saegusa J, Chen HY, Hsu DK. Galectins in regulation of apoptosis. Advances in experimental medicine and biology 2011;705:431-442.
[56] Ho MK, Springer TA. Mac-2, a novel 32,000 Mr mouse macrophage subpopulation-specific antigen defined by monoclonal antibodies. Journal of immunology 1982;128:1221-1228.
[57] Raimond J, Zimonjic DB, Mignon C, Mattei M, Popescu NC, Monsigny M, et al. Mapping of the galectin-3 gene (LGALS3) to human chromosome 14 at region 14q21-22. Mammalian genome : official journal of the International Mammalian Genome Society 1997;8:706-707.
[58] Hirabayashi J, Kasai K. The family of metazoan metal-independent beta-galactoside-binding lectins: structure, function and molecular evolution. Glycobiology 1993;3:297-304.
[59] Liu FT. S-type mammalian lectins in allergic inflammation. Immunology today 1993;14:486-490.
[60] Aubin JE, Liu F, Malaval L, Gupta AK. Osteoblast and chondroblast differentiation. Bone 1995;17:77S-83S.
[61] Rabinovich GA, Rubinstein N, Fainboim L. Unlocking the secrets of galectins: a challenge at the frontier of glyco-immunology. Journal of leukocyte biology 2002;71:741-752.

[62] Liu FT, Hsu DK. The role of galectin-3 in promotion of the inflammatory response. Drug news & perspectives 2007;20:455-460.
[63] van den Brule F, Califice S, Castronovo V. Expression of galectins in cancer: a critical review. Glycoconjugate journal 2004;19:537-542.
[64] Califice S, Castronovo V, Van Den Brule F. Galectin-3 and cancer (Review). International journal of oncology 2004;25:983-992.
[65] Song L, Tang JW, Owusu L, Sun MZ, Wu J, Zhang J. Galectin-3 in cancer. Clinica chimica acta; international journal of clinical chemistry 2014;431:185-191.
[66] Ahmed H, Bandyopadhyaya G. Examination of the regulation of galectin-3 expression in cancer. Methods in molecular biology 2015;1207:355-369.
[67] Wang L, Guo XL. Molecular regulation of galectin-3 expression and therapeutic implication in cancer progression. Biomedicine & pharmacotherapy = Biomedecine & pharmacotherapie 2016;78:165-171.
[68] Moutsatsos IK, Davis JM, Wang JL. Endogenous lectins from cultured cells: subcellular localization of carbohydrate-binding protein 35 in 3T3 fibroblasts. The Journal of cell biology 1986;102:477-483.
[69] Cowles EA, Moutsatsos IK, Wang JL, Anderson RL. Expression of carbohydrate binding protein 35 in human fibroblasts: comparisons between cells with different proliferative capacities. Experimental gerontology 1989;24:577-585.
[70] Hamann KK, Cowles EA, Wang JL, Anderson RL. Expression of carbohydrate binding protein 35 in human fibroblasts: variations in the levels of mRNA, protein, and isoelectric species as a function of replicative competence. Experimental cell research 1991;196:82-91.
[71] Dumic J, Lauc G, Hadzija M, Flogel M. Transfer to in vitro conditions influences expression and intracellular distribution of galectin-3 in murine peritoneal macrophages. Zeitschrift fur Naturforschung C, Journal of biosciences 2000;55:261-266.
[72] Sanjuan X, Fernandez PL, Castells A, Castronovo V, van den Brule F, Liu FT, et al. Differential expression of galectin 3 and galectin 1 in colorectal cancer progression. Gastroenterology 1997;113:1906-1915.
[73] Honjo Y, Inohara H, Akahani S, Yoshii T, Takenaka Y, Yoshida J, et al. Expression of cytoplasmic galectin-3 as a prognostic marker in tongue carcinoma. Clinical cancer research : an official journal of the American Association for Cancer Research 2000;6:4635-4640.
[74] van den Brule FA, Waltregny D, Liu FT, Castronovo V. Alteration of the cytoplasmic/nuclear expression pattern of galectin-3 correlates with prostate carcinoma progression. International journal of cancer Journal international du cancer 2000;89:361-367.
[75] Moisa A, Fritz P, Eck A, Wehner HD, Murdter T, Simon W, et al. Growth/adhesion-regulatory tissue lectin galectin-3: stromal presence but not cytoplasmic/nuclear expression in tumor cells as a negative prognostic factor in breast cancer. Anticancer research 2007;27:2131-2139.
[76] Weinberger PM, Adam BL, Gourin CG, Moretz WH, 3rd, Bollag RJ, Wang BY, et al. Association of nuclear, cytoplasmic expression of galectin-3 with beta-catenin/Wnt-

pathway activation in thyroid carcinoma. Archives of otolaryngology--head & neck surgery 2007;133:503-510.
[77] Puglisi F, Minisini AM, Barbone F, Intersimone D, Aprile G, Puppin C, et al. Galectin-3 expression in non-small cell lung carcinoma. Cancer letters 2004;212:233-239.
[78] Paron I, Scaloni A, Pines A, Bachi A, Liu FT, Puppin C, et al. Nuclear localization of Galectin-3 in transformed thyroid cells: a role in transcriptional regulation. Biochemical and biophysical research communications 2003;302:545-553.
[79] Berbis MA, Andre S, Canada FJ, Pipkorn R, Ippel H, Mayo KH, et al. Peptides derived from human galectin-3 N-terminal tail interact with its carbohydrate recognition domain in a phosphorylation-dependent manner. Biochemical and biophysical research communications 2014;443:126-131.
[80] Menon RP, Hughes RC. Determinants in the N-terminal domains of galectin-3 for secretion by a novel pathway circumventing the endoplasmic reticulum-Golgi complex. European journal of biochemistry / FEBS 1999;264:569-576.
[81] Nickel W. Unconventional secretory routes: direct protein export across the plasma membrane of mammalian cells. Traffic 2005;6:607-614.
[82] Nakahara S, Raz A. Regulation of cancer-related gene expression by galectin-3 and the molecular mechanism of its nuclear import pathway. Cancer metastasis reviews 2007;26:605-610.
[83] Akahani S, Nangia-Makker P, Inohara H, Kim HR, Raz A. Galectin-3: a novel antiapoptotic molecule with a functional BH1 (NWGR) domain of Bcl-2 family. Cancer research 1997;57:5272-5276.
[84] Nangia-Makker P, Nakahara S, Hogan V, Raz A. Galectin-3 in apoptosis, a novel therapeutic target. Journal of bioenergetics and biomembranes 2007;39:79-84.
[85] Matarrese P, Fusco O, Tinari N, Natoli C, Liu FT, Semeraro ML, et al. Galectin-3 overexpression protects from apoptosis by improving cell adhesion properties. International journal of cancer Journal international du cancer 2000;85:545-554.
[86] Kim HR, Lin HM, Biliran H, Raz A. Cell cycle arrest and inhibition of anoikis by galectin-3 in human breast epithelial cells. Cancer research 1999;59:4148-4154.
[87] Yoshii T, Fukumori T, Honjo Y, Inohara H, Kim HR, Raz A. Galectin-3 phosphorylation is required for its anti-apoptotic function and cell cycle arrest. The Journal of biological chemistry 2002;277:6852-6857.
[88] Delacour D, Koch A, Jacob R. The role of galectins in protein trafficking. Traffic 2009;10:1405-1413.
[89] Delacour D, Koch A, Ackermann W, Eude-Le Parco I, Elsasser HP, Poirier F, et al. Loss of galectin-3 impairs membrane polarisation of mouse enterocytes in vivo. Journal of cell science 2008;121:458-465.
[90] Koch A, Poirier F, Jacob R, Delacour D. Galectin-3, a novel centrosome-associated protein, required for epithelial morphogenesis. Molecular biology of the cell 2010;21:219-231.
[91] Argueso P, Guzman-Aranguez A, Mantelli F, Cao Z, Ricciuto J, Panjwani N. Association of cell surface mucins with galectin-3 contributes to the ocular surface epithelial barrier. The Journal of biological chemistry 2009;284:23037-23045.

[92] Nangia-Makker P, Balan V, Raz A. Regulation of tumor progression by extracellular galectin-3. Cancer microenvironment : official journal of the International Cancer Microenvironment Society 2008;1:43-51.
[93] Ochieng J, Leite-Browning ML, Warfield P. Regulation of cellular adhesion to extracellular matrix proteins by galectin-3. Biochemical and biophysical research communications 1998;246:788-791.
[94] D'Haene N, Sauvage S, Maris C, Adanja I, Le Mercier M, Decaestecker C, et al. VEGFR1 and VEGFR2 involvement in extracellular galectin-1- and galectin-3-induced angiogenesis. PloS one 2013;8:e67029.
[95] Subhash VV, Ling SS, Ho B. Extracellular galectin-3 counteracts adhesion and exhibits chemoattraction in Helicobacter pylori-infected gastric cancer cells. Microbiology 2016;162:1360-1366.
[96] Baptiste TA, James A, Saria M, Ochieng J. Mechano-transduction mediated secretion and uptake of galectin-3 in breast carcinoma cells: implications in the extracellular functions of the lectin. Experimental cell research 2007;313:652-664.
[97] Hsu DK, Liu FT. Regulation of cellular homeostasis by galectins. Glycoconjugate journal 2004;19:507-515.
[98] More SK, Chiplunkar SV, Kalraiya RD. Galectin-3-induced cell spreading and motility relies on distinct signaling mechanisms compared to fibronectin. Molecular and cellular biochemistry 2016;416:179-191.
[99] Inohara H, Raz A. Functional evidence that cell surface galectin-3 mediates homotypic cell adhesion. Cancer research 1995;55:3267-3271.
[100] Friedrichs J, Torkko JM, Helenius J, Teravainen TP, Fullekrug J, Muller DJ, et al. Contributions of galectin-3 and -9 to epithelial cell adhesion analyzed by single cell force spectroscopy. The Journal of biological chemistry 2007;282:29375-29383.
[101] Friedrichs J, Manninen A, Muller DJ, Helenius J. Galectin-3 regulates integrin alpha2beta1-mediated adhesion to collagen-I and -IV. The Journal of biological chemistry 2008;283:32264-32272.
[102] Hughes RC. Galectins as modulators of cell adhesion. Biochimie 2001;83:667-676.
[103] Kuwabara I, Sano H, Liu FT. Functions of galectins in cell adhesion and chemotaxis. Methods in enzymology 2003;363:532-552.
[104] Elola MT, Wolfenstein-Todel C, Troncoso MF, Vasta GR, Rabinovich GA. Galectins: matricellular glycan-binding proteins linking cell adhesion, migration, and survival. Cellular and molecular life sciences : CMLS 2007;64:1679-1700.
[105] Wan SY, Zhang TF, Ding Y. Galectin-3 enhances proliferation and angiogenesis of endothelial cells differentiated from bone marrow mesenchymal stem cells. Transplantation proceedings 2011;43:3933-3938.
[106] Yang E, Shim JS, Woo HJ, Kim KW, Kwon HJ. Aminopeptidase N/CD13 induces angiogenesis through interaction with a pro-angiogenic protein, galectin-3. Biochemical and biophysical research communications 2007;363:336-341.
[107] Nangia-Makker P, Honjo Y, Sarvis R, Akahani S, Hogan V, Pienta KJ, et al. Galectin-3 induces endothelial cell morphogenesis and angiogenesis. The American journal of pathology 2000;156:899-909.

[108] Machado CM, Andrade LN, Teixeira VR, Costa FF, Melo CM, dos Santos SN, et al. Galectin-3 disruption impaired tumoral angiogenesis by reducing VEGF secretion from TGFbeta1-induced macrophages. Cancer medicine 2014;3:201-214.
[109] Fukumori T, Takenaka Y, Yoshii T, Kim HR, Hogan V, Inohara H, et al. CD29 and CD7 mediate galectin-3-induced type II T-cell apoptosis. Cancer research 2003;63:8302-8311.
[110] Demetriou M, Granovsky M, Quaggin S, Dennis JW. Negative regulation of T-cell activation and autoimmunity by Mgat5 N-glycosylation. Nature 2001;409:733-739.
[111] Ahmad N, Gabius HJ, Andre S, Kaltner H, Sabesan S, Roy R, et al. Galectin-3 precipitates as a pentamer with synthetic multivalent carbohydrates and forms heterogeneous cross-linked complexes. The Journal of biological chemistry 2004;279:10841-10847.
[112] Dennis JW, Lau KS, Demetriou M, Nabi IR. Adaptive regulation at the cell surface by N-glycosylation. Traffic 2009;10:1569-1578.
[113] Xin M, Dong XW, Guo XL. Role of the interaction between galectin-3 and cell adhesion molecules in cancer metastasis. Biomedicine & pharmacotherapy = Biomedecine & pharmacotherapie 2015;69:179-185.
[114] Takenaka Y, Fukumori T, Raz A. Galectin-3 and metastasis. Glycoconjugate journal 2004;19:543-549.
[115] Zhao Q, Guo X, Nash GB, Stone PC, Hilkens J, Rhodes JM, et al. Circulating galectin-3 promotes metastasis by modifying MUC1 localization on cancer cell surface. Cancer research 2009;69:6799-6806.
[116] Nangia-Makker P, Honjo Y, Raz A. Galectin-3 binding and metastasis. Methods in molecular medicine 2001;58:149-157.
[117] Yu LG. Circulating galectin-3 in the bloodstream: An emerging promoter of cancer metastasis. World journal of gastrointestinal oncology 2010;2:177-180.
[118] Nangia-Makker P, Balan V, Raz A. Galectin-3 binding and metastasis. Methods in molecular biology 2012;878:251-266.
[119] Chen C, Duckworth CA, Zhao Q, Pritchard DM, Rhodes JM, Yu LG. Increased circulation of galectin-3 in cancer induces secretion of metastasis-promoting cytokines from blood vascular endothelium. Clinical cancer research : an official journal of the American Association for Cancer Research 2013;19:1693-1704.
[120] Ruvolo PP. Galectin 3 as a guardian of the tumor microenvironment. Biochimica et biophysica acta 2016;1863:427-437.
[121] Cardoso AC, Andrade LN, Bustos SO, Chammas R. Galectin-3 Determines Tumor Cell Adaptive Strategies in Stressed Tumor Microenvironments. Frontiers in oncology 2016;6:127.
[122] Peng W, Wang HY, Miyahara Y, Peng G, Wang RF. Tumor-associated galectin-3 modulates the function of tumor-reactive T cells. Cancer research 2008;68:7228-7236.
[123] Demotte N, Wieers G, Van Der Smissen P, Moser M, Schmidt C, Thielemans K, et al. A galectin-3 ligand corrects the impaired function of human CD4 and CD8 tumor-infiltrating lymphocytes and favors tumor rejection in mice. Cancer research 2010;70:7476-7488.

[124] Newton-Northup JR, Dickerson MT, Ma L, Besch-Williford CL, Deutscher SL. Inhibition of metastatic tumor formation in vivo by a bacteriophage display-derived galectin-3 targeting peptide. Clinical & experimental metastasis 2013;30:119-132.
[125] Shalom-Feuerstein R, Plowman SJ, Rotblat B, Ariotti N, Tian T, Hancock JF, et al. K-ras nanoclustering is subverted by overexpression of the scaffold protein galectin-3. Cancer research 2008;68:6608-6616.
[126] Levy R, Biran A, Poirier F, Raz A, Kloog Y. Galectin-3 mediates cross-talk between K-Ras and Let-7c tumor suppressor microRNA. PloS one 2011;6:e27490.
[127] Kadrofske MM, Openo KP, Wang JL. The human LGALS3 (galectin-3) gene: determination of the gene structure and functional characterization of the promoter. Archives of biochemistry and biophysics 1998;349:7-20.
[128] Ruebel KH, Jin L, Qian X, Scheithauer BW, Kovacs K, Nakamura N, et al. Effects of DNA methylation on galectin-3 expression in pituitary tumors. Cancer research 2005;65:1136-1140.
[129] Thijssen VL, Heusschen R, Caers J, Griffioen AW. Galectin expression in cancer diagnosis and prognosis: A systematic review. Biochimica et biophysica acta 2015;1855:235-247.
[130] Castronovo V, Van Den Brule FA, Jackers P, Clausse N, Liu FT, Gillet C, et al. Decreased expression of galectin-3 is associated with progression of human breast cancer. The Journal of pathology 1996;179:43-48.
[131] Pacis RA, Pilat MJ, Pienta KJ, Wojno K, Raz A, Hogan V, et al. Decreased galectin-3 expression in prostate cancer. The Prostate 2000;44:118-123.
[132] Merseburger AS, Kramer MW, Hennenlotter J, Simon P, Knapp J, Hartmann JT, et al. Involvement of decreased Galectin-3 expression in the pathogenesis and progression of prostate cancer. The Prostate 2008;68:72-77.
[133] Lee JW, Song SY, Choi JJ, Choi CH, Kim TJ, Kim J, et al. Decreased galectin-3 expression during the progression of cervical neoplasia. Journal of cancer research and clinical oncology 2006;132:241-247.
[134] Kramer MW, Kuczyk MA, Hennenlotter J, Serth J, Schilling D, Stenzl A, et al. Decreased expression of galectin-3 predicts tumour recurrence in pTa bladder cancer. Oncology reports 2008;20:1403-1408.
[135] Junking M, Wongkham C, Sripa B, Sawanyawisuth K, Araki N, Wongkham S. Decreased expression of galectin-3 is associated with metastatic potential of liver fluke-associated cholangiocarcinoma. European journal of cancer 2008;44:619-626.
[136] Shimamura T, Sakamoto M, Ino Y, Shimada K, Kosuge T, Sato Y, et al. Clinicopathological significance of galectin-3 expression in ductal adenocarcinoma of the pancreas. Clinical cancer research : an official journal of the American Association for Cancer Research 2002;8:2570-2575.
[137] Ahmed H, Cappello F, Rodolico V, Vasta GR. Evidence of heavy methylation in the galectin 3 promoter in early stages of prostate adenocarcinoma: development and validation of a methylated marker for early diagnosis of prostate cancer. Translational oncology 2009;2:146-156.

[138] Glinskii OV, Sud S, Mossine VV, Mawhinney TP, Anthony DC, Glinsky GV, et al. Inhibition of prostate cancer bone metastasis by synthetic TF antigen mimic/galectin-3 inhibitor lactulose-L-leucine. Neoplasia 2012;14:65-73.
[139] Ahmed H, Banerjee PP, Vasta GR. Differential expression of galectins in normal, benign and malignant prostate epithelial cells: silencing of galectin-3 expression in prostate cancer by its promoter methylation. Biochemical and biophysical research communications 2007;358:241-246.
[140] van den Brule FA, Buicu C, Berchuck A, Bast RC, Deprez M, Liu FT, et al. Expression of the 67-kD laminin receptor, galectin-1, and galectin-3 in advanced human uterine adenocarcinoma. Human pathology 1996;27:1185-1191.
[141] Prieto VG, Mourad-Zeidan AA, Melnikova V, Johnson MM, Lopez A, Diwan AH, et al. Galectin-3 expression is associated with tumor progression and pattern of sun exposure in melanoma. Clinical cancer research : an official journal of the American Association for Cancer Research 2006;12:6709-6715.
[142] Saussez S, Decaestecker C, Mahillon V, Cludts S, Capouillez A, Chevalier D, et al. Galectin-3 upregulation during tumor progression in head and neck cancer. The Laryngoscope 2008;118:1583-1590.
[143] Zubieta MR, Furman D, Barrio M, Bravo AI, Domenichini E, Mordoh J. Galectin-3 expression correlates with apoptosis of tumor-associated lymphocytes in human melanoma biopsies. The American journal of pathology 2006;168:1666-1675.
[144] Tas F, Bilgin E, Tastekin D, Erturk K, Duranyildiz D. Clinical Significance of Serum Galectin-3 Levels in Gastric Cancer Patients. Journal of gastrointestinal cancer 2016;47:182-186.
[145] Yilmaz E, Karsidag T, Tatar C, Tuzun S. Serum Galectin-3: diagnostic value for papillary thyroid carcinoma. Ulusal cerrahi dergisi 2015;31:192-196.
[146] Esmailiejah AA, Taheriazam A, Golbakhsh MR, Jamshidi M, Shakeri M, Yahaghi E, et al. Analysis of serum levels and tissue expression of galectin-1 and galectin-3 as noninvasive biomarkers in osteosarcoma patients. Tumour biology : the journal of the International Society for Oncodevelopmental Biology and Medicine 2015.
[147] Gendy HE, Madkour B, Abdelaty S, Essawy F, Khattab D, Hammam O, et al. Diagnostic and Prognostic Significance of Serum and Tissue Galectin 3 Expression in Patients with Carcinoma of the Bladder. Current urology 2014;7:185-190.
[148] Cheng D, Liang B, Li Y. Serum galectin-3 as a potential marker for gastric cancer. Medical science monitor : international medical journal of experimental and clinical research 2015;21:755-760.
[149] Ulu M, Alacacioglu A, Yuksel E, Pamukk BO, Bozkaya G, Ari A, et al. Prognostic significance of serum galectin-3 levels in patients with hepatocellular cancer and chronic viral hepatitis. Saudi journal of gastroenterology : official journal of the Saudi Gastroenterology Association 2015;21:47-50.
[150] Xue G, Liu J, Huang J, Zhang J, Zhang W, Wu J, et al. [Detection of galectin-3 in both serum and tissue for early diagnosis of thyroid carcinoma]. Nan fang yi ke da xue xue bao = Journal of Southern Medical University 2013;33:1027-1030.
[151] Barrow H, Rhodes JM, Yu LG. Simultaneous determination of serum galectin-3 and -4 levels detects metastases in colorectal cancer patients. Cellular oncology 2013;36:9-13.

[152] Xie L, Ni WK, Chen XD, Xiao MB, Chen BY, He S, et al. The expressions and clinical significances of tissue and serum galectin-3 in pancreatic carcinoma. Journal of cancer research and clinical oncology 2012;138:1035-1043.
[153] Fang QQ, Ni RZ, Xiao MB, Jiang F, Lu CH. [Serum and tissue expressions of galectin-3 in hepatocellular carcinoma and the clinical significances]. Zhonghua gan zang bing za zhi = Zhonghua ganzangbing zazhi = Chinese journal of hepatology 2011;19:527-531.
[154] Isic T, Savin S, Cvejic D, Marecko I, Tatic S, Havelka M, et al. Serum Cyfra 21.1 and galectin-3 protein levels in relation to immunohistochemical cytokeratin 19 and galectin-3 expression in patients with thyroid tumors. Journal of cancer research and clinical oncology 2010;136:1805-1812.
[155] Iacovazzi PA, Notarnicola M, Caruso MG, Guerra V, Frisullo S, Altomare DF, et al. Serum levels of galectin-3 and its ligand 90k/mac-2bp in colorectal cancer patients. Immunopharmacology and immunotoxicology 2010;32:160-164.
[156] Vereecken P, Awada A, Suciu S, Castro G, Morandini R, Litynska A, et al. Evaluation of the prognostic significance of serum galectin-3 in American Joint Committee on Cancer stage III and stage IV melanoma patients. Melanoma research 2009;19:316-320.
[157] Kim SJ, Lee SJ, Sung HJ, Choi IK, Choi CW, Kim BS, et al. Increased serum 90K and Galectin-3 expression are associated with advanced stage and a worse prognosis in diffuse large B-cell lymphomas. Acta haematologica 2008;120:211-216.
[158] Inohara H, Segawa T, Miyauchi A, Yoshii T, Nakahara S, Raz A, et al. Cytoplasmic and serum galectin-3 in diagnosis of thyroid malignancies. Biochemical and biophysical research communications 2008;376:605-610.
[159] Saussez S, Glinoer D, Chantrain G, Pattou F, Carnaille B, Andre S, et al. Serum galectin-1 and galectin-3 levels in benign and malignant nodular thyroid disease. Thyroid : official journal of the American Thyroid Association 2008;18:705-712.
[160] Sakaki M, Oka N, Nakanishi R, Yamaguchi K, Fukumori T, Kanayama HO. Serum level of galectin-3 in human bladder cancer. The journal of medical investigation : JMI 2008;55:127-132.
[161] Vereecken P, Heenen M. Serum galectin-3 in advanced melanoma patients: a hypothesis on a possible role in melanoma progression and inflammation. The Journal of international medical research 2006;34:119-120.
[162] Vereecken P, Zouaoui Boudjeltia K, Debray C, Awada A, Legssyer I, Sales F, et al. High serum galectin-3 in advanced melanoma: preliminary results. Clinical and experimental dermatology 2006;31:105-109.
[163] Rodriguez MC, Yegorova S, Pitteloud JP, Chavaroche AE, Andre S, Arda A, et al. Thermodynamic Switch in Binding of Adhesion/Growth Regulatory Human Galectin-3 to Tumor-Associated TF Antigen (CD176) and MUC1 Glycopeptides. Biochemistry 2015;54:4462-4474.
[164] Cvejic DS, Savin SB, Petrovic IM, Paunovic IR, Tatic SB, Havelka MJ. Galectin-3 expression in papillary thyroid carcinoma: relation to histomorphologic growth pattern, lymph node metastasis, extrathyroid invasion, and tumor size. Head & neck 2005;27:1049-1055.

[165] John CM, Leffler H, Kahl-Knutsson B, Svensson I, Jarvis GA. Truncated galectin-3 inhibits tumor growth and metastasis in orthotopic nude mouse model of human breast cancer. Clinical cancer research : an official journal of the American Association for Cancer Research 2003;9:2374-2383.
[166] Ellerhorst JA, Stephens LC, Nguyen T, Xu XC. Effects of galectin-3 expression on growth and tumorigenicity of the prostate cancer cell line LNCaP. The Prostate 2002;50:64-70.
[167] Ashery U, Yizhar O, Rotblat B, Elad-Sfadia G, Barkan B, Haklai R, et al. Spatiotemporal organization of Ras signaling: rasosomes and the galectin switch. Cellular and molecular neurobiology 2006;26:471-495.
[168] Shimura T, Takenaka Y, Tsutsumi S, Hogan V, Kikuchi A, Raz A. Galectin-3, a novel binding partner of beta-catenin. Cancer research 2004;64:6363-6367.
[169] Liu J, Cheng Y, He M, Yao S. Vascular endothelial growth factor C enhances cervical cancer cell invasiveness via upregulation of galectin-3 protein. Gynecological endocrinology : the official journal of the International Society of Gynecological Endocrinology 2014;30:461-465.
[170] Shetty P, Bargale A, Patil BR, Mohan R, Dinesh US, Vishwanatha JK, et al. Cell surface interaction of annexin A2 and galectin-3 modulates epidermal growth factor receptor signaling in Her-2 negative breast cancer cells. Molecular and cellular biochemistry 2016;411:221-233.
[171] Choi JH, Chun KH, Raz A, Lotan R. Inhibition of N-(4-hydroxyphenyl)retinamide-induced apoptosis in breast cancer cells by galectin-3. Cancer biology & therapy 2004;3:447-452.
[172] Shi Y, He B, Kuchenbecker KM, You L, Xu Z, Mikami I, et al. Inhibition of Wnt-2 and galectin-3 synergistically destabilizes beta-catenin and induces apoptosis in human colorectal cancer cells. International journal of cancer Journal international du cancer 2007;121:1175-1181.
[173] Glinsky VV, Kiriakova G, Glinskii OV, Mossine VV, Mawhinney TP, Turk JR, et al. Synthetic galectin-3 inhibitor increases metastatic cancer cell sensitivity to taxol-induced apoptosis in vitro and in vivo. Neoplasia 2009;11:901-909.
[174] Lin CI, Whang EE, Abramson MA, Donner DB, Bertagnolli MM, Moore FD, Jr., et al. Galectin-3 regulates apoptosis and doxorubicin chemoresistance in papillary thyroid cancer cells. Biochemical and biophysical research communications 2009;379:626-631.
[175] Lin CI, Whang EE, Donner DB, Jiang X, Price BD, Carothers AM, et al. Galectin-3 targeted therapy with a small molecule inhibitor activates apoptosis and enhances both chemosensitivity and radiosensitivity in papillary thyroid cancer. Molecular cancer research : MCR 2009;7:1655-1662.
[176] Li Y, Liu L, Niu Y, Feng J, Sun Y, Kong X, et al. Modified apple polysaccharide prevents against tumorigenesis in a mouse model of colitis-associated colon cancer: role of galectin-3 and apoptosis in cancer prevention. European journal of nutrition 2012;51:107-117.
[177] Guha P, Kaptan E, Bandyopadhyaya G, Kaczanowska S, Davila E, Thompson K, et al. Cod glycopeptide with picomolar affinity to galectin-3 suppresses T-cell apoptosis and

prostate cancer metastasis. Proceedings of the National Academy of Sciences of the United States of America 2013;110:5052-5057.

[178] Hossein G, Keshavarz M, Ahmadi S, Naderi N. Synergistic effects of PectaSol-C modified citrus pectin an inhibitor of Galectin-3 and paclitaxel on apoptosis of human SKOV-3 ovarian cancer cells. Asian Pacific journal of cancer prevention : APJCP 2013;14:7561-7568.

[179] Guha P, Bandyopadhyaya G, Polumuri SK, Chumsri S, Gade P, Kalvakolanu DV, et al. Nicotine promotes apoptosis resistance of breast cancer cells and enrichment of side population cells with cancer stem cell-like properties via a signaling cascade involving galectin-3, alpha9 nicotinic acetylcholine receptor and STAT3. Breast cancer research and treatment 2014;145:5-22.

[180] Liu L, Sakai T, Sano N, Fukui K. Nucling mediates apoptosis by inhibiting expression of galectin-3 through interference with nuclear factor kappaB signalling. The Biochemical journal 2004;380:31-41.

[181] Mazurek N, Sun YJ, Liu KF, Gilcrease MZ, Schober W, Nangia-Makker P, et al. Phosphorylated galectin-3 mediates tumor necrosis factor-related apoptosis-inducing ligand signaling by regulating phosphatase and tensin homologue deleted on chromosome 10 in human breast carcinoma cells. The Journal of biological chemistry 2007;282:21337-21348.

[182] Oka N, Nakahara S, Takenaka Y, Fukumori T, Hogan V, Kanayama HO, et al. Galectin-3 inhibits tumor necrosis factor-related apoptosis-inducing ligand-induced apoptosis by activating Akt in human bladder carcinoma cells. Cancer research 2005;65:7546-7553.

[183] Harazono Y, Kho DH, Balan V, Nakajima K, Zhang T, Hogan V, et al. Galectin-3 leads to attenuation of apoptosis through Bax heterodimerization in human thyroid carcinoma cells. Oncotarget 2014;5:9992-10001.

[184] Hu Z, Jiang X, Xu Y, Lu N, Wang W, Luo J, et al. Downregulation of galectin-3 by EGF mediates the apoptosis of HepG2 cells. Molecular and cellular biochemistry 2012;369:157-165.

[185] Suzuki O, Abe M. Cell surface N-glycosylation and sialylation regulate galectin-3-induced apoptosis in human diffuse large B cell lymphoma. Oncology reports 2008;19:743-748.

[186] Lin HM, Moon BK, Yu F, Kim HR. Galectin-3 mediates genistein-induced G(2)/M arrest and inhibits apoptosis. Carcinogenesis 2000;21:1941-1945.

[187] Cecchinelli B, Lavra L, Rinaldo C, Iacovelli S, Gurtner A, Gasbarri A, et al. Repression of the antiapoptotic molecule galectin-3 by homeodomain-interacting protein kinase 2-activated p53 is required for p53-induced apoptosis. Molecular and cellular biology 2006;26:4746-4757.

[188] Streetly MJ, Maharaj L, Joel S, Schey SA, Gribben JG, Cotter FE. GCS-100, a novel galectin-3 antagonist, modulates MCL-1, NOXA, and cell cycle to induce myeloma cell death. Blood 2010;115:3939-3948.

[189] O'Driscoll L, Linehan R, Liang YH, Joyce H, Oglesby I, Clynes M. Galectin-3 expression alters adhesion, motility and invasion in a lung cell line (DLKP), in vitro. Anticancer research 2002;22:3117-3125.

[190] Wang YG, Kim SJ, Baek JH, Lee HW, Jeong SY, Chun KH. Galectin-3 increases the motility of mouse melanoma cells by regulating matrix metalloproteinase-1 expression. Experimental & molecular medicine 2012;44:387-393.
[191] Shimura T, Takenaka Y, Fukumori T, Tsutsumi S, Okada K, Hogan V, et al. Implication of galectin-3 in Wnt signaling. Cancer research 2005;65:3535-3537.
[192] Mirandola L, Yu Y, Cannon MJ, Jenkins MR, Rahman RL, Nguyen DD, et al. Galectin-3 inhibition suppresses drug resistance, motility, invasion and angiogenic potential in ovarian cancer. Gynecologic oncology 2014;135:573-579.
[193] Le Marer N, Hughes RC. Effects of the carbohydrate-binding protein galectin-3 on the invasiveness of human breast carcinoma cells. Journal of cellular physiology 1996;168:51-58.
[194] Debray C, Vereecken P, Belot N, Teillard P, Brion JP, Pandolfo M, et al. Multifaceted role of galectin-3 on human glioblastoma cell motility. Biochemical and biophysical research communications 2004;325:1393-1398.
[195] Meng F, Joshi B, Nabi IR. Galectin-3 Overrides PTRF/Cavin-1 Reduction of PC3 Prostate Cancer Cell Migration. PloS one 2015;10:e0126056.
[196] Boscher C, Nabi IR. Galectin-3- and phospho-caveolin-1-dependent outside-in integrin signaling mediates the EGF motogenic response in mammary cancer cells. Molecular biology of the cell 2013;24:2134-2145.
[197] Shankar J, Wiseman SM, Meng F, Kasaian K, Strugnell S, Mofid A, et al. Coordinated expression of galectin-3 and caveolin-1 in thyroid cancer. The Journal of pathology 2012;228:56-66.
[198] Markowska AI, Liu FT, Panjwani N. Galectin-3 is an important mediator of VEGF- and bFGF-mediated angiogenic response. The Journal of experimental medicine 2010;207:1981-1993.
[199] Fukushi J, Makagiansar IT, Stallcup WB. NG2 proteoglycan promotes endothelial cell motility and angiogenesis via engagement of galectin-3 and alpha3beta1 integrin. Molecular biology of the cell 2004;15:3580-3590.
[200] Etulain J, Negrotto S, Tribulatti MV, Croci DO, Carabelli J, Campetella O, et al. Control of angiogenesis by galectins involves the release of platelet-derived proangiogenic factors. PloS one 2014;9:e96402.
[201] Elad-Sfadia G, Haklai R, Balan E, Kloog Y. Galectin-3 augments K-Ras activation and triggers a Ras signal that attenuates ERK but not phosphoinositide 3-kinase activity. The Journal of biological chemistry 2004;279:34922-34930.
[202] Shalom-Feuerstein R, Cooks T, Raz A, Kloog Y. Galectin-3 regulates a molecular switch from N-Ras to K-Ras usage in human breast carcinoma cells. Cancer research 2005;65:7292-7300.
[203] Song S, Ji B, Ramachandran V, Wang H, Hafley M, Logsdon C, et al. Overexpressed galectin-3 in pancreatic cancer induces cell proliferation and invasion by binding Ras and activating Ras signaling. PloS one 2012;7:e42699.
[204] Borges BE, Teixeira VR, Appel MH, Steclan CA, Rigo F, Filipak Neto F, et al. De novo galectin-3 expression influences the response of melanoma cells to isatin-Schiff base copper (II) complex-induced oxidative stimulus. Chemico-biological interactions 2013;206:37-46.

[205] Takenaka Y, Fukumori T, Yoshii T, Oka N, Inohara H, Kim HR, et al. Nuclear export of phosphorylated galectin-3 regulates its antiapoptotic activity in response to chemotherapeutic drugs. Molecular and cellular biology 2004;24:4395-4406.
[206] Gilmore TD. Introduction to NF-kappaB: players, pathways, perspectives. Oncogene 2006;25:6680-6684.
[207] Dumic J, Lauc G, Flogel M. Expression of galectin-3 in cells exposed to stress-roles of jun and NF-kappaB. Cellular physiology and biochemistry : international journal of experimental cellular physiology, biochemistry, and pharmacology 2000;10:149-158.
[208] Zeng Y, Danielson KG, Albert TJ, Shapiro IM, Risbud MV. HIF-1 alpha is a regulator of galectin-3 expression in the intervertebral disc. Journal of bone and mineral research : the official journal of the American Society for Bone and Mineral Research 2007;22:1851-1861.
[209] Ikemori RY, Machado CM, Furuzawa KM, Nonogaki S, Osinaga E, Umezawa K, et al. Galectin-3 up-regulation in hypoxic and nutrient deprived microenvironments promotes cell survival. PloS one 2014;9:e111592.
[210] Serizawa N, Tian J, Fukada H, Baghy K, Scott F, Chen X, et al. Galectin 3 regulates HCC cell invasion by RhoA and MLCK activation. Laboratory investigation; a journal of technical methods and pathology 2015;95:1145-1156.
[211] Sethi N, Kang Y. Notch signalling in cancer progression and bone metastasis. British journal of cancer 2011;105:1805-1810.
[212] Aithal MG, Rajeswari N. Role of Notch signalling pathway in cancer and its association with DNA methylation. Journal of genetics 2013;92:667-675.
[213] Acar A, Simoes BM, Clarke RB, Brennan K. A Role for Notch Signalling in Breast Cancer and Endocrine Resistance. Stem cells international 2016;2016:2498764.
[214] Yap LF, Lee D, Khairuddin A, Pairan MF, Puspita B, Siar CH, et al. The opposing roles of NOTCH signalling in head and neck cancer: a mini review. Oral diseases 2015;21:850-857.
[215] Marignol L, Rivera-Figueroa K, Lynch T, Hollywood D. Hypoxia, notch signalling, and prostate cancer. Nature reviews Urology 2013;10:405-413.
[216] Bolos V, Blanco M, Medina V, Aparicio G, Diaz-Prado S, Grande E. Notch signalling in cancer stem cells. Clinical & translational oncology : official publication of the Federation of Spanish Oncology Societies and of the National Cancer Institute of Mexico 2009;11:11-19.
[217] Nakajima K, Kho DH, Yanagawa T, Harazono Y, Gao X, Hogan V, et al. Galectin-3 inhibits osteoblast differentiation through notch signaling. Neoplasia 2014;16:939-949.
[218] Abdel-Magid AF. Inhibition of notch pathway signaling: a one compound mission to treat cancer. ACS medicinal chemistry letters 2013;4:373-374.
[219] Espinoza I, Miele L. Notch inhibitors for cancer treatment. Pharmacology & therapeutics 2013;139:95-110.
[220] Ahmed H, AlSadek DM. Galectin-3 as a Potential Target to Prevent Cancer Metastasis. Clinical Medicine Insights Oncology 2015;9:113-121.
[221] More SK, Srinivasan N, Budnar S, Bane SM, Upadhya A, Thorat RA, et al. N-glycans and metastasis in galectin-3 transgenic mice. Biochemical and biophysical research communications 2015;460:302-307.

[222] Nakajima K, Kho DH, Yanagawa T, Zimel M, Heath E, Hogan V, et al. Galectin-3 in bone tumor microenvironment: a beacon for individual skeletal metastasis management. Cancer metastasis reviews 2016;35:333-346.
[223] Demotte N, Stroobant V, Courtoy PJ, Van Der Smissen P, Colau D, Luescher IF, et al. Restoring the association of the T cell receptor with CD8 reverses anergy in human tumor-infiltrating lymphocytes. Immunity 2008;28:414-424.
[224] Wang Y, Nangia-Makker P, Tait L, Balan V, Hogan V, Pienta KJ, et al. Regulation of prostate cancer progression by galectin-3. The American journal of pathology 2009;174:1515-1523.
[225] Abdel-Aziz HO, Murai Y, Takasaki I, Tabuchi Y, Zheng HC, Nomoto K, et al. Targeted disruption of the galectin-3 gene results in decreased susceptibility to NNK-induced lung tumorigenesis: an oligonucleotide microarray study. Journal of cancer research and clinical oncology 2008;134:777-788.
[226] Cay T. Immunhistochemical expression of galectin-3 in cancer: a review of the literature. Turk patoloji dergisi 2012;28:1-10.
[227] Carver BS, Pandolfi PP. Mouse modeling in oncologic preclinical and translational research. Clinical cancer research : an official journal of the American Association for Cancer Research 2006;12:5305-5311.
[228] Benjamin CL, Melnikova VO, Ananthaswamy HN. Models and mechanisms in malignant melanoma. Molecular carcinogenesis 2007;46:671-678.
[229] Talmadge JE, Singh RK, Fidler IJ, Raz A. Murine models to evaluate novel and conventional therapeutic strategies for cancer. The American journal of pathology 2007;170:793-804.
[230] Bobek V, Kolostova K, Pinterova D, Kacprzak G, Adamiak J, Kolodziej J, et al. A clinically relevant, syngeneic model of spontaneous, highly metastatic B16 mouse melanoma. Anticancer research 2010;30:4799-4803.
[231] Overwijk WW, Restifo NP. B16 as a mouse model for human melanoma. Current protocols in immunology / edited by John E Coligan [et al] 2001;Chapter 20:Unit 20 21.
[232] Damsky WE, Jr., Bosenberg M. Mouse melanoma models and cell lines. Pigment cell & melanoma research 2010;23:853-859.
[233] Becker JC, Houben R, Schrama D, Voigt H, Ugurel S, Reisfeld RA. Mouse models for melanoma: a personal perspective. Experimental dermatology 2010;19:157-164.
[234] Gauvain KM, Garbow JR, Song SK, Hirbe AC, Weilbaecher K. MRI detection of early bone metastases in b16 mouse melanoma models. Clinical & experimental metastasis 2005;22:403-411.
[235] Klarquist JS, Janssen EM. Melanoma-infiltrating dendritic cells: Limitations and opportunities of mouse models. Oncoimmunology 2012;1:1584-1593.
[236] Tuting T. T cell immunotherapy for melanoma from bedside to bench to barn and back: how conceptual advances in experimental mouse models can be translated into clinical benefit for patients. Pigment cell & melanoma research 2013;26:441-456.
[237] Merlino G, Flaherty K, Acquavella N, Day CP, Aplin A, Holmen S, et al. Meeting report: The future of preclinical mouse models in melanoma treatment is now. Pigment cell & melanoma research 2013;26:E8-E14.

[238] Fidler IJ, Nicolson GL. Organ selectivity for implantation survival and growth of B16 melanoma variant tumor lines. Journal of the National Cancer Institute 1976;57:1199-1202.
[239] Hart IR, Fidler IJ. Role of organ selectivity in the determination of metastatic patterns of B16 melanoma. Cancer research 1980;40:2281-2287.
[240] Karlsen AE, Storling ZM, Sparre T, Larsen MR, Mahmood A, Storling J, et al. Immune-mediated beta-cell destruction in vitro and in vivo-A pivotal role for galectin-3. Biochemical and biophysical research communications 2006;344:406-415.
[241] Rabinovich GA, Toscano MA, Ilarregui JM, Rubinstein N. Shedding light on the immunomodulatory properties of galectins: novel regulators of innate and adaptive immune responses. Glycoconjugate journal 2004;19:565-573.
[242] Thiemann S, Baum LG. Galectins and Immune Responses-Just How Do They Do Those Things They Do? Annual review of immunology 2016;34:243-264.
[243] Than NG, Romero R, Goodman M, Weckle A, Xing J, Dong Z, et al. A primate subfamily of galectins expressed at the maternal-fetal interface that promote immune cell death. Proceedings of the National Academy of Sciences of the United States of America 2009;106:9731-9736.
[244] Timoshenko AV, Gorudko IV, Maslakova OV, Andre S, Kuwabara I, Liu FT, et al. Analysis of selected blood and immune cell responses to carbohydrate-dependent surface binding of proto- and chimera-type galectins. Molecular and cellular biochemistry 2003;250:139-149.
[245] Rabinovich GA, Rubinstein N. [Galectins: a novel family of proteins involved in the regulation of the immune response. Implications in immunopathological processes]. Medicina (B Aires) 2001;61:85-92.
[246] Vasta GR, Quesenberry M, Ahmed H, O'Leary N. C-type lectins and galectins mediate innate and adaptive immune functions: their roles in the complement activation pathway. Developmental and comparative immunology 1999;23:401-420.
[247] Chung AW, Sieling PA, Schenk M, Teles RM, Krutzik SR, Hsu DK, et al. Galectin-3 regulates the innate immune response of human monocytes. The Journal of infectious diseases 2013;207:947-956.
[248] Rotshenker S. The role of Galectin-3/MAC-2 in the activation of the innate-immune function of phagocytosis in microglia in injury and disease. Journal of molecular neuroscience : MN 2009;39:99-103.
[249] James RE, Hillis J, Adorjan I, Gration B, Mundim MV, Iqbal AJ, et al. Loss of galectin-3 decreases the number of immune cells in the subventricular zone and restores proliferation in a viral model of multiple sclerosis. Glia 2016;64:105-121.
[250] van den Berg TK, Honing H, Franke N, van Remoortere A, Schiphorst WE, Liu FT, et al. LacdiNAc-glycans constitute a parasite pattern for galectin-3-mediated immune recognition. Journal of immunology 2004;173:1902-1907.
[251] Chen C, Chi H, Sun BG, Sun L. The galectin-3-binding protein of Cynoglossus semilaevis is a secreted protein of the innate immune system that binds a wide range of bacteria and is involved in host phagocytosis. Developmental and comparative immunology 2013;39:399-408.

[252] Dumont P, Berton A, Nagy N, Sandras F, Tinton S, Demetter P, et al. Expression of galectin-3 in the tumor immune response in colon cancer. Laboratory investigation; a journal of technical methods and pathology 2008;88:896-906.
[253] Hsu DK, Hammes SR, Kuwabara I, Greene WC, Liu FT. Human T lymphotropic virus-I infection of human T lymphocytes induces expression of the beta-galactoside-binding lectin, galectin-3. The American journal of pathology 1996;148:1661-1670.
[254] Dong S, Hughes RC. Galectin-3 stimulates uptake of extracellular Ca2+ in human Jurkat T-cells. FEBS letters 1996;395:165-169.
[255] Stillman BN, Hsu DK, Pang M, Brewer CF, Johnson P, Liu FT, et al. Galectin-3 and galectin-1 bind distinct cell surface glycoprotein receptors to induce T cell death. Journal of immunology 2006;176:778-789.
[256] Joo HG, Goedegebuure PS, Sadanaga N, Nagoshi M, von Bernstorff W, Eberlein TJ. Expression and function of galectin-3, a beta-galactoside-binding protein in activated T lymphocytes. Journal of leukocyte biology 2001;69:555-564.
[257] Xue J, Gao X, Fu C, Cong Z, Jiang H, Wang W, et al. Regulation of galectin-3-induced apoptosis of Jurkat cells by both O-glycans and N-glycans on CD45. FEBS letters 2013;587:3986-3994.
[258] Stowell SR, Qian Y, Karmakar S, Koyama NS, Dias-Baruffi M, Leffler H, et al. Differential roles of galectin-1 and galectin-3 in regulating leukocyte viability and cytokine secretion. Journal of immunology 2008;180:3091-3102.
[259] Toscano MA, Bianco GA, Ilarregui JM, Croci DO, Correale J, Hernandez JD, et al. Differential glycosylation of TH1, TH2 and TH-17 effector cells selectively regulates susceptibility to cell death. Nature immunology 2007;8:825-834.
[260] Silva-Monteiro E, Reis Lorenzato L, Kenji Nihei O, Junqueira M, Rabinovich GA, Hsu DK, et al. Altered expression of galectin-3 induces cortical thymocyte depletion and premature exit of immature thymocytes during Trypanosoma cruzi infection. The American journal of pathology 2007;170:546-556.
[261] Chen HY, Fermin A, Vardhana S, Weng IC, Lo KF, Chang EY, et al. Galectin-3 negatively regulates TCR-mediated CD4+ T-cell activation at the immunological synapse. Proceedings of the National Academy of Sciences of the United States of America 2009;106:14496-14501.
[262] Hoyer KK, Pang M, Gui D, Shintaku IP, Kuwabara I, Liu FT, et al. An anti-apoptotic role for galectin-3 in diffuse large B-cell lymphomas. The American journal of pathology 2004;164:893-902.
[263] Colnot C, Ripoche MA, Milon G, Montagutelli X, Crocker PR, Poirier F. Maintenance of granulocyte numbers during acute peritonitis is defective in galectin-3-null mutant mice. Immunology 1998;94:290-296.
[264] MacKinnon AC, Farnworth SL, Hodkinson PS, Henderson NC, Atkinson KM, Leffler H, et al. Regulation of alternative macrophage activation by galectin-3. Journal of immunology 2008;180:2650-2658.
[265] Liu FT, Hsu DK, Zuberi RI, Kuwabara I, Chi EY, Henderson WR, Jr. Expression and function of galectin-3, a beta-galactoside-binding lectin, in human monocytes and macrophages. The American journal of pathology 1995;147:1016-1028.

[266] Jeng KC, Frigeri LG, Liu FT. An endogenous lectin, galectin-3 (epsilon BP/Mac-2), potentiates IL-1 production by human monocytes. Immunology letters 1994;42:113-116.
[267] Karlsson A, Christenson K, Matlak M, Bjorstad A, Brown KL, Telemo E, et al. Galectin-3 functions as an opsonin and enhances the macrophage clearance of apoptotic neutrophils. Glycobiology 2009;19:16-20.
[268] Jin R, Greenwald A, Peterson MD, Waddell TK. Human monocytes recognize porcine endothelium via the interaction of galectin 3 and alpha-GAL. Journal of immunology 2006;177:1289-1295.
[269] Li Y, Komai-Koma M, Gilchrist DS, Hsu DK, Liu FT, Springall T, et al. Galectin-3 is a negative regulator of lipopolysaccharide-mediated inflammation. Journal of immunology 2008;181:2781-2789.
[270] Bernardes ES, Silva NM, Ruas LP, Mineo JR, Loyola AM, Hsu DK, et al. Toxoplasma gondii infection reveals a novel regulatory role for galectin-3 in the interface of innate and adaptive immunity. The American journal of pathology 2006;168:1910-1920.
[271] Saegusa J, Hsu DK, Chen HY, Yu L, Fermin A, Fung MA, et al. Galectin-3 is critical for the development of the allergic inflammatory response in a mouse model of atopic dermatitis. The American journal of pathology 2009;174:922-931.
[272] Hsu DK, Chernyavsky AI, Chen HY, Yu L, Grando SA, Liu FT. Endogenous galectin-3 is localized in membrane lipid rafts and regulates migration of dendritic cells. The Journal of investigative dermatology 2009;129:573-583.
[273] Vray B, Camby I, Vercruysse V, Mijatovic T, Bovin NV, Ricciardi-Castagnoli P, et al. Up-regulation of galectin-3 and its ligands by Trypanosoma cruzi infection with modulation of adhesion and migration of murine dendritic cells. Glycobiology 2004;14:647-657.
[274] Yamaoka A, Kuwabara I, Frigeri LG, Liu FT. A human lectin, galectin-3 (epsilon bp/Mac-2), stimulates superoxide production by neutrophils. Journal of immunology 1995;154:3479-3487.
[275] Karlsson A, Follin P, Leffler H, Dahlgren C. Galectin-3 activates the NADPH-oxidase in exudated but not peripheral blood neutrophils. Blood 1998;91:3430-3438.
[276] Almkvist J, Faldt J, Dahlgren C, Leffler H, Karlsson A. Lipopolysaccharide-induced gelatinase granule mobilization primes neutrophils for activation by galectin-3 and formylmethionyl-Leu-Phe. Infection and immunity 2001;69:832-837.
[277] Farnworth SL, Henderson NC, Mackinnon AC, Atkinson KM, Wilkinson T, Dhaliwal K, et al. Galectin-3 reduces the severity of pneumococcal pneumonia by augmenting neutrophil function. The American journal of pathology 2008;172:395-405.
[278] Kuwabara I, Liu FT. Galectin-3 promotes adhesion of human neutrophils to laminin. Journal of immunology 1996;156:3939-3944.
[279] Fernandez GC, Ilarregui JM, Rubel CJ, Toscano MA, Gomez SA, Beigier Bompadre M, et al. Galectin-3 and soluble fibrinogen act in concert to modulate neutrophil activation and survival: involvement of alternative MAPK pathways. Glycobiology 2005;15:519-527.

[280] Frigeri LG, Zuberi RI, Liu FT. Epsilon BP, a beta-galactoside-binding animal lectin, recognizes IgE receptor (Fc epsilon RI) and activates mast cells. Biochemistry 1993;32:7644-7649.
[281] Zuberi RI, Frigeri LG, Liu FT. Activation of rat basophilic leukemia cells by epsilon BP, an IgE-binding endogenous lectin. Cellular immunology 1994;156:1-12.
[282] Suzuki Y, Inoue T, Yoshimaru T, Ra C. Galectin-3 but not galectin-1 induces mast cell death by oxidative stress and mitochondrial permeability transition. Biochimica et biophysica acta 2008;1783:924-934.
[283] Chen HY, Sharma BB, Yu L, Zuberi R, Weng IC, Kawakami Y, et al. Role of galectin-3 in mast cell functions: galectin-3-deficient mast cells exhibit impaired mediator release and defective JNK expression. Journal of immunology 2006;177:4991-4997.
[284] Cortegano I, del Pozo V, Cardaba B, de Andres B, Gallardo S, del Amo A, et al. Galectin-3 down-regulates IL-5 gene expression on different cell types. Journal of immunology 1998;161:385-389.
[285] Rao SP, Wang Z, Zuberi RI, Sikora L, Bahaie NS, Zuraw BL, et al. Galectin-3 functions as an adhesion molecule to support eosinophil rolling and adhesion under conditions of flow. Journal of immunology 2007;179:7800-7807.
[286] Zuberi RI, Hsu DK, Kalayci O, Chen HY, Sheldon HK, Yu L, et al. Critical role for galectin-3 in airway inflammation and bronchial hyperresponsiveness in a murine model of asthma. The American journal of pathology 2004;165:2045-2053.
[287] del Pozo V, Rojo M, Rubio ML, Cortegano I, Cardaba B, Gallardo S, et al. Gene therapy with galectin-3 inhibits bronchial obstruction and inflammation in antigen-challenged rats through interleukin-5 gene downregulation. American journal of respiratory and critical care medicine 2002;166:732-737.
[288] Lopez E, del Pozo V, Miguel T, Sastre B, Seoane C, Civantos E, et al. Inhibition of chronic airway inflammation and remodeling by galectin-3 gene therapy in a murine model. Journal of immunology 2006;176:1943-1950.
[289] Jiang HR, Al Rasebi Z, Mensah-Brown E, Shahin A, Xu D, Goodyear CS, et al. Galectin-3 deficiency reduces the severity of experimental autoimmune encephalomyelitis. Journal of immunology 2009;182:1167-1173.
[290] Pugliese G, Pricci F, Iacobini C, Leto G, Amadio L, Barsotti P, et al. Accelerated diabetic glomerulopathy in galectin-3/AGE receptor 3 knockout mice. FASEB journal : official publication of the Federation of American Societies for Experimental Biology 2001;15:2471-2479.
[291] Iacobini C, Menini S, Oddi G, Ricci C, Amadio L, Pricci F, et al. Galectin-3/AGE-receptor 3 knockout mice show accelerated AGE-induced glomerular injury: evidence for a protective role of galectin-3 as an AGE receptor. FASEB journal : official publication of the Federation of American Societies for Experimental Biology 2004;18:1773-1775.
[292] Iacobini C, Oddi G, Menini S, Amadio L, Ricci C, Di Pippo C, et al. Development of age-dependent glomerular lesions in galectin-3/AGE-receptor-3 knockout mice. American journal of physiology Renal physiology 2005;289:F611-621.
[293] Mensah-Brown EP, Al Rabesi Z, Shahin A, Al Shamsi M, Arsenijevic N, Hsu DK, et al. Targeted disruption of the galectin-3 gene results in decreased susceptibility to

multiple low dose streptozotocin-induced diabetes in mice. Clinical immunology 2009;130:83-88.
[294] Stitt AW, McGoldrick C, Rice-McCaldin A, McCance DR, Glenn JV, Hsu DK, et al. Impaired retinal angiogenesis in diabetes: role of advanced glycation end products and galectin-3. Diabetes 2005;54:785-794.
[295] Nachtigal M, Al-Assaad Z, Mayer EP, Kim K, Monsigny M. Galectin-3 expression in human atherosclerotic lesions. The American journal of pathology 1998;152:1199-1208.
[296] Nachtigal M, Ghaffar A, Mayer EP. Galectin-3 gene inactivation reduces atherosclerotic lesions and adventitial inflammation in ApoE-deficient mice. The American journal of pathology 2008;172:247-255.
[297] Nieminen J, St-Pierre C, Bhaumik P, Poirier F, Sato S. Role of galectin-3 in leukocyte recruitment in a murine model of lung infection by Streptococcus pneumoniae. Journal of immunology 2008;180:2466-2473.
[298] Ruas LP, Bernardes ES, Fermino ML, de Oliveira LL, Hsu DK, Liu FT, et al. Lack of galectin-3 drives response to Paracoccidioides brasiliensis toward a Th2-biased immunity. PloS one 2009;4:e4519.
[299] Kohatsu L, Hsu DK, Jegalian AG, Liu FT, Baum LG. Galectin-3 induces death of Candida species expressing specific beta-1,2-linked mannans. Journal of immunology 2006;177:4718-4726.
[300] Quah BJ, Warren HS, Parish CR. Monitoring lymphocyte proliferation in vitro and in vivo with the intracellular fluorescent dye carboxyfluorescein diacetate succinimidyl ester. Nature protocols 2007;2:2049-2056.
[301] Sakaguchi S, Yamaguchi T, Nomura T, Ono M. Regulatory T cells and immune tolerance. Cell 2008;133:775-787.
[302] Sakaguchi S. Naturally arising CD4+ regulatory t cells for immunologic self-tolerance and negative control of immune responses. Annual review of immunology 2004;22:531-562.
[303] Savino W. The thymus is a common target organ in infectious diseases. PLoS pathogens 2006;2:e62.
[304] Hsu DK, Yang RY, Saegusa J, Liu FT. Analysis of the intracellular role of galectins in cell growth and apoptosis. Methods in molecular biology 2015;1207:451-463.
[305] Ha TY. The role of regulatory T cells in cancer. Immune network 2009;9:209-235.
[306] Waldhauer I, Steinle A. NK cells and cancer immunosurveillance. Oncogene 2008;27:5932-5943.
[307] Zamai L, Ponti C, Mirandola P, Gobbi G, Papa S, Galeotti L, et al. NK cells and cancer. Journal of immunology 2007;178:4011-4016.
[308] Pahl J, Cerwenka A. Tricking the balance: NK cells in anti-cancer immunity. Immunobiology 2015.
[309] Kakuta S, Tagawa Y, Shibata S, Nanno M, Iwakura Y. Inhibition of B16 melanoma experimental metastasis by interferon-gamma through direct inhibition of cell proliferation and activation of antitumour host mechanisms. Immunology 2002;105:92-100.

[310] Schroder K, Hertzog PJ, Ravasi T, Hume DA. Interferon-gamma: an overview of signals, mechanisms and functions. Journal of leukocyte biology 2004;75:163-189.
[311] Larkin J, 3rd, Ahmed CM, Wilson TD, Johnson HM. Regulation of interferon gamma signaling by suppressors of cytokine signaling and regulatory T cells. Frontiers in immunology 2013;4:469.
[312] Schwarz EC, Kummerow C, Wenning AS, Wagner K, Sappok A, Waggershauser K, et al. Calcium dependence of T cell proliferation following focal stimulation. European journal of immunology 2007;37:2723-2733.
[313] Clapham DE. Calcium signaling. Cell 2007;131:1047-1058.
[314] Feske S. Calcium signalling in lymphocyte activation and disease. Nature reviews Immunology 2007;7:690-702.
[315] Donnadieu E, Bismuth G, Trautmann A. Calcium fluxes in T lymphocytes. The Journal of biological chemistry 1992;267:25864-25872.
[316] Fracchia KM, Pai CY, Walsh CM. Modulation of T Cell Metabolism and Function through Calcium Signaling. Frontiers in immunology 2013;4:324.
[317] Lewis RS. Calcium signaling mechanisms in T lymphocytes. Annual review of immunology 2001;19:497-521.
[318] Freedman BD. Mechanisms of calcium signaling and function in lymphocytes. Critical reviews in immunology 2006;26:97-111.
[319] Schieber M, Chandel NS. ROS function in redox signaling and oxidative stress. Current biology : CB 2014;24:R453-462.
[320] Yang Y, Bazhin AV, Werner J, Karakhanova S. Reactive oxygen species in the immune system. International reviews of immunology 2013;32:249-270.
[321] Kohchi C, Inagawa H, Nishizawa T, Soma G. ROS and innate immunity. Anticancer research 2009;29:817-821.
[322] Humphries MJ, Matsumoto K, White SL, Molyneux RJ, Olden K. Augmentation of murine natural killer cell activity by swainsonine, a new antimetastatic immunomodulator. Cancer research 1988;48:1410-1415.
[323] Rabinovich GA, Rubinstein N, Toscano MA. Role of galectins in inflammatory and immunomodulatory processes. Biochimica et biophysica acta 2002;1572:274-284.
[324] Forsman H, Islander U, Andreasson E, Andersson A, Onnheim K, Karlstrom A, et al. Galectin 3 aggravates joint inflammation and destruction in antigen-induced arthritis. Arthritis and rheumatism 2011;63:445-454.
[325] Jawhara S, Thuru X, Standaert-Vitse A, Jouault T, Mordon S, Sendid B, et al. Colonization of mice by Candida albicans is promoted by chemically induced colitis and augments inflammatory responses through galectin-3. The Journal of infectious diseases 2008;197:972-980.
[326] Fermin Lee A, Chen HY, Wan L, Wu SY, Yu JS, Huang AC, et al. Galectin-3 modulates Th17 responses by regulating dendritic cell cytokines. The American journal of pathology 2013;183:1209-1222.
[327] Volarevic V, Markovic BS, Bojic S, Stojanovic M, Nilsson U, Leffler H, et al. Gal-3 regulates the capacity of dendritic cells to promote NKT-cell-induced liver injury. European journal of immunology 2015;45:531-543.

[328] Wu SY, Yu JS, Liu FT, Miaw SC, Wu-Hsieh BA. Galectin-3 negatively regulates dendritic cell production of IL-23/IL-17-axis cytokines in infection by Histoplasma capsulatum. Journal of immunology 2013;190:3427-3437.
[329] Ikeda H, Old LJ, Schreiber RD. The roles of IFN gamma in protection against tumor development and cancer immunoediting. Cytokine & growth factor reviews 2002;13:95-109.
[330] Dighe AS, Richards E, Old LJ, Schreiber RD. Enhanced in vivo growth and resistance to rejection of tumor cells expressing dominant negative IFN gamma receptors. Immunity 1994;1:447-456.
[331] Mitra-Kaushik S, Harding J, Hess J, Schreiber R, Ratner L. Enhanced tumorigenesis in HTLV-1 tax-transgenic mice deficient in interferon-gamma. Blood 2004;104:3305-3311.
[332] Xu Z, Hurchla MA, Deng H, Uluckan O, Bu F, Berdy A, et al. Interferon-gamma targets cancer cells and osteoclasts to prevent tumor-associated bone loss and bone metastases. The Journal of biological chemistry 2009;284:4658-4666.
[333] Kaplan DH, Shankaran V, Dighe AS, Stockert E, Aguet M, Old LJ, et al. Demonstration of an interferon gamma-dependent tumor surveillance system in immunocompetent mice. Proceedings of the National Academy of Sciences of the United States of America 1998;95:7556-7561.
[334] Shankaran V, Ikeda H, Bruce AT, White JM, Swanson PE, Old LJ, et al. IFNgamma and lymphocytes prevent primary tumour development and shape tumour immunogenicity. Nature 2001;410:1107-1111.
[335] Alexander WS, Starr R, Fenner JE, Scott CL, Handman E, Sprigg NS, et al. SOCS1 is a critical inhibitor of interferon gamma signaling and prevents the potentially fatal neonatal actions of this cytokine. Cell 1999;98:597-608.
[336] Song MM, Shuai K. The suppressor of cytokine signaling (SOCS) 1 and SOCS3 but not SOCS2 proteins inhibit interferon-mediated antiviral and antiproliferative activities. The Journal of biological chemistry 1998;273:35056-35062.
[337] Endo TA, Masuhara M, Yokouchi M, Suzuki R, Sakamoto H, Mitsui K, et al. A new protein containing an SH2 domain that inhibits JAK kinases. Nature 1997;387:921-924.
[338] Nicholson SE, Willson TA, Farley A, Starr R, Zhang JG, Baca M, et al. Mutational analyses of the SOCS proteins suggest a dual domain requirement but distinct mechanisms for inhibition of LIF and IL-6 signal transduction. The EMBO journal 1999;18:375-385.
[339] Lopez E, Zafra MP, Sastre B, Gamez C, Lahoz C, del Pozo V. Gene expression profiling in lungs of chronic asthmatic mice treated with galectin-3: downregulation of inflammatory and regulatory genes. Mediators of inflammation 2011;2011:823279.
[340] Lalancette-Hebert M, Swarup V, Beaulieu JM, Bohacek I, Abdelhamid E, Weng YC, et al. Galectin-3 is required for resident microglia activation and proliferation in response to ischemic injury. The Journal of neuroscience : the official journal of the Society for Neuroscience 2012;32:10383-10395.
[341] Idikio HA. Galectin-3 and Beclin1/Atg6 genes in human cancers: using cDNA tissue panel, qRT-PCR, and logistic regression model to identify cancer cell biomarkers. PloS one 2011;6:e26150.

[342] Guess BW, Scholz MC, Strum SB, Lam RY, Johnson HJ, Jennrich RI. Modified citrus pectin (MCP) increases the prostate-specific antigen doubling time in men with prostate cancer: a phase II pilot study. Prostate cancer and prostatic diseases 2003;6:301-304.

PUBLICATION

Molecular Immunology 68 (2015) 300–311

Contents lists available at ScienceDirect

Molecular Immunology

journal homepage: www.elsevier.com/locate/molimm

Endogenous galectin-3 expression levels modulate immune responses in galectin-3 transgenic mice

Aparna D. Chaudhari[a], Rajiv P. Gude[b], Rajiv D. Kalraiya[b], Shubhada V. Chiplunkar[a,*]

[a] Chiplunkar Laboratory, Advanced Centre for Treatment, Research and Education in Cancer (ACTREC), Tata Memorial Centre, Sector 22, Kharghar, Navi Mumbai 410210, Maharashtra, India
[b] Advanced Centre for Treatment, Research and Education in Cancer (ACTREC), Tata Memorial Centre, Sector 22, Kharghar, Navi Mumbai 410210, Maharashtra, India

ARTICLE INFO

Article history:
Received 27 April 2015
Received in revised form
13 September 2015
Accepted 22 September 2015

Keywords:
Galectin-3
Immune dysregulation
NK cytotoxicity
B16F10 melanoma
Lung metastasis

ABSTRACT

Galectin-3 (Gal-3), a β-galactoside-binding mammalian lectin, is involved in cancer progression and metastasis. However, there is an unmet need to identify the underlying mechanisms of cancer metastasis mediated by endogenous host galectin-3. Galectin-3 is also known to be an important regulator of immune responses. The present study was aimed at analysing how expression of endogenous galectin-3 regulates host immunity and lung metastasis in B16F10 murine melanoma model. Transgenic Gal-3$^{+/-}$ (hemizygous) and Gal-3$^{-/-}$ (null) mice exhibited decreased levels of Natural Killer (NK) cells and lower NK mediated cytotoxicity against YAC-1 tumor targets, compared to Gal-3$^{+/+}$ (wild-type) mice. On stimulation, Gal-3$^{+/-}$ and Gal-3$^{-/-}$ mice splenocytes showed increased T cell proliferation than Gal-3$^{+/+}$ mice. Intracellular calcium flux was found to be lower in activated T cells of Gal-3$^{-/-}$ mice as compared to T cells from Gal-3$^{+/+}$ and Gal-3$^{+/-}$ mice. In Gal-3$^{-/-}$ mice, serum Th1, Th2 and Th17 cytokine levels were found to be lowest, exhibiting dysregulation of pro-inflammatory and anti-inflammatory cytokines balance. Marked decrease in serum IFN-γ levels and splenic IFN-γR1 (IFN-γ Receptor 1) expressing T and NK cell percentages were observed in Gal-3$^{-/-}$ mice. On recombinant IFN-γ treatment of splenocytes *in vitro*, Suppressor of Cytokine Signaling (SOCS) 1 and SOCS3 protein expression was higher in Gal-3$^{-/-}$ mice compared to that in Gal-3$^{+/+}$ and Gal-3$^{+/-}$ mice; suggesting possible attenuation of Signal Transducer and Activator of Transcription (STAT) 1 mediated IFN-γ signaling in Gal-3$^{-/-}$ mice. The ability of B16F10 melanoma cells to form metastatic colonies in the lungs of Gal-3$^{+/+}$ and Gal-3$^{-/-}$ mice remained comparable, whereas it was found to be reduced in Gal-3$^{+/-}$ mice. Our data indicates that complete absence of endogenous host galectin-3 facilitates lung metastasis of B16F10 cells in mice, which may be contributed by dysregulated immune responses resulting from decreased NK cytotoxicity, disturbed serum Th1, Th2, Th17 cytokine milieu, reduced serum IFN-γ levels and attenuation of splenic STAT1 mediated IFN-γ signalling in Gal-3$^{-/-}$ mice.

1. Introduction

Galectin-3 is a unique chimera-type member of the β-galactoside-binding mammalian galectin family. It is a 31 kDa protein composed of an N-terminal domain, a repetitive collagen-like sequence rich in glycine, proline and tyrosine and a C-terminal carbohydrate recognition domain (CRD) (Houzelstein et al., 2004). Galectin-3 can be found within the nucleus, in the cytoplasm, on the cell surface and in the extracellular compartment, depending on the cell type and the proliferative status (Moutsatsos et al., 1987; Perillo et al., 1998; Sato and Hughes, 1994). Thus, it is a ubiquitously expressed molecule with diverse physiological functions based on its subcellular and extracellular localization. Galectin-3 is involved in various biological processes such as maintenance of cellular homeostasis, organogenesis, immune responses, angiogenesis, tumor invasion and metastasis (Califice et al., 2004; Dagher et al., 1995; Dumic et al., 2006; Liu, 2005; Liu et al., 2002; Nakahara et al., 2005; Ochieng et al., 2004; Wang et al., 2004).

Abbreviations: Gal-3, galectin-3; *Lgals3*, lectin galactoside-binding soluble 3; NK, natural killer; Th, T helper; T_{reg}, regulatory T cells; PMA, phorbol 12-myristate 13-acetate; Iono, ionomycin; mAb, monoclonal antibody; FBS, fetal bovine serum; PBS, phosphate buffered saline; FACS, fluorescence-activated cell sorting; CFSE, carboxyfluorescein succinimidyl ester; STAT, signal transducer and activator of transcription; SOCS, suppressor of cytokine signaling.

* Corresponding author.
E-mail address: schiplunkar@actrec.gov.in (S.V. Chiplunkar).

http://dx.doi.org/10.1016/j.molimm.2015.09.015
0161-5890/

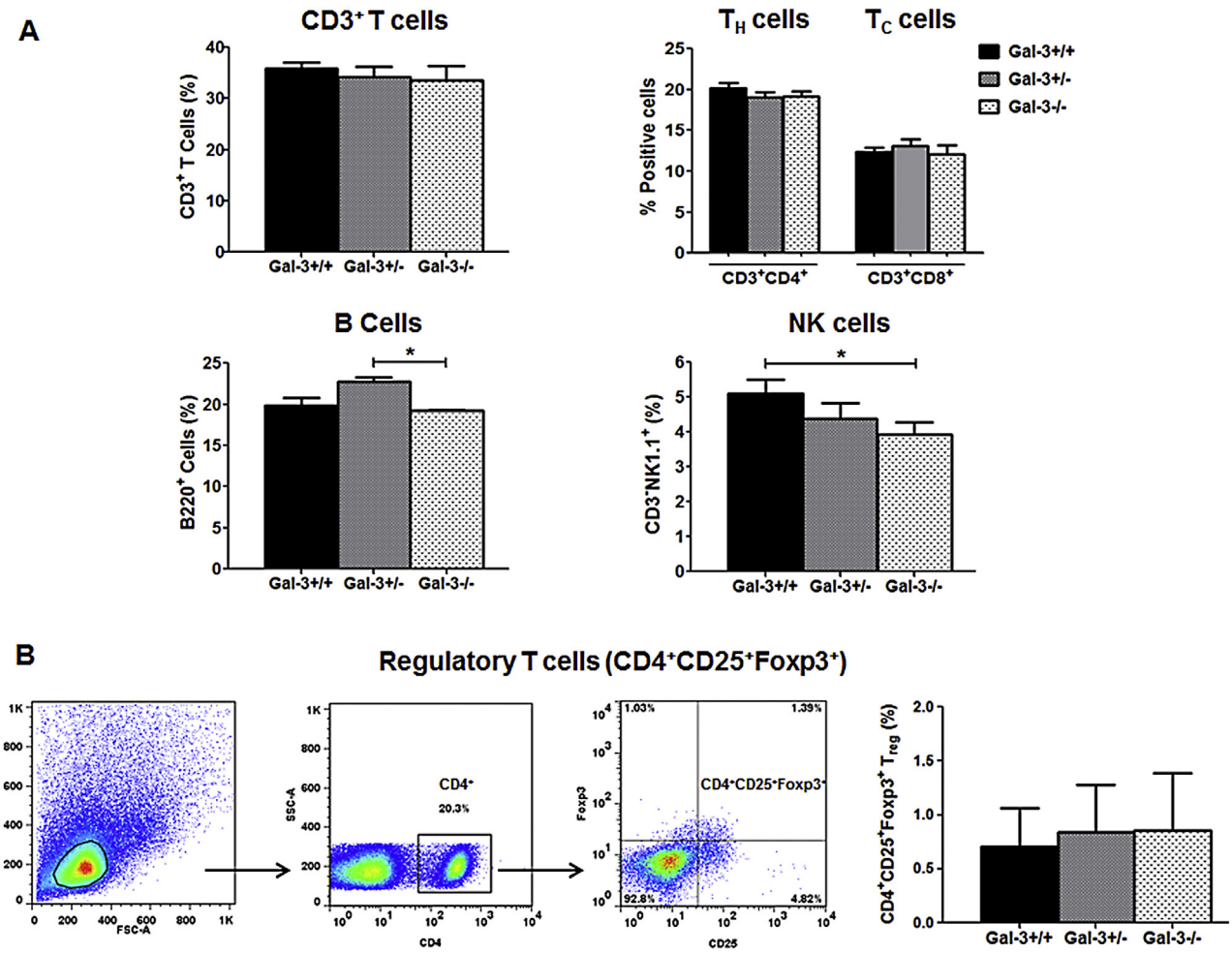

Fig. 1. Immune cell subsets in Gal-3$^{+/+}$, Gal-3$^{+/-}$ and Gal-3$^{-/-}$ mice. Single cell suspensions of spleen cells were prepared from Gal-3$^{+/+}$, Gal-3$^{+/-}$ and Gal-3$^{-/-}$ mice. The cells were fixed, subjected to surface or intracellular antibody staining and analyzed by multicolor flow cytometry. (A) Frequencies of T cells (CD3$^+$), helper T cells (T_H, CD3$^+$CD4$^+$), cytotoxic T cells (T_C, CD3$^+$CD8$^+$), B cells (B220$^+$) and NK cells (CD3$^-$NK1.1$^+$) in mice splenocytes. (B) Gating strategy and percentages of CD4$^+$CD25$^+$Foxp3$^+$ regulatory T cells in mice splenocytes. The graphs represent consolidated data of 5 independent experiments. $^*P < 0.05$.

Involvement of galectin-3 in various steps of cancer progression and metastasis has been extensively documented (Fortuna-Costa et al., 2014; Funasaka et al., 2014; Liu and Rabinovich, 2005; Newlaczyl and Yu, 2011; Radosavljevic et al., 2012). Most studies have demonstrated the effect of galectin-3 produced either by the tumor cells themselves or that of the endogenous host galectin-3 on the properties of tumor cells. In the first case depending on the subcellular localization, variety of effects on the tumor cell properties have been demonstrated (Califice et al., 2004; Fortuna-Costa et al., 2014; Liu et al., 2002; Liu and Rabinovich, 2005; Lotz et al., 1993; Nakahara et al., 2005). Using genetic manipulation techniques, effect of ectopic expression or complete knockdown of galectin-3 in cancer cell lines has been assessed through *in vitro* and *in vivo* approaches (Honjo et al., 2001; Yoshii et al., 2001). The effects of host galectin-3 on the tumor cells are exerted via tumor cell surface carbohydrates associated with cancer progression, like TF-antigens on mucinous oligosaccharides (Almogren et al., 2012; Yu, 2007; Yu et al., 2007; Zhao et al., 2010) or poly *N*-acetyl lactosamine substituted *N*-oligosaccharides (Agarwal et al., 2014; Agarwal et al., 2015; Dange et al., 2015; Dange et al., 2014; Srinivasan et al., 2009). However, how the levels of expression of endogenous galectin-3 in the host influence tumor growth and metastasis remains poorly understood till date.

Galectin-3 has been found to be expressed in highest amounts on majority of the tissue compartments of lung and constitutively on lung vascular endothelium in mice (Dange et al., 2014; Krishnan et al., 2005). Previous studies using B16F10 murine melanoma model have shown that, interactions between galectin-3 on the mice lung endothelium and its high affinity ligand poly-*N*-acetyl lactosamine (polyLacNAc) on β1,6 branched *N*-oligosaccharides present on B16F10 melanoma cells facilitates B16F10 colonization in the lungs of the mice (Dange et al., 2014; More et al., 2015; Srinivasan et al., 2009). The studies done in transgenic *Lgals3* mice that are wild type or null for galectin-3 expression have reported contradictory research findings related to primary tumor growth as well as metastatic frequency. A study using C57BL/6 wild-type and galectin-3-null mice has shown that primary subcutaneous B16F10 melanoma tumor growth did not differ between these two groups. However, the number of lung metastatic colonies in wild-type mice was significantly increased in comparison to that observed in galectin-3-null mice (Comodo et al., 2013). Another group has reported that deletion of galectin-3 in the host attenuates lung metastasis of B16F1 malignant melanoma by modulating tumor adhesion and NK cell activity. This study has focused on B16F1 cells, a variant of B16 melanoma possessing lower metastatic potential than B16F10 cells (Radosavljevic et al., 2011). Conversely, it has also been shown that in Gal-3$^{-/-}$ mice, both *Apc* intestinal tumors and *PyMT* mammary gland tumors appear at the same frequency as in Gal-3$^{+/+}$ animals. Further, galectin-3 deletion did not influence the frequency of dissemination of *PyMT* tumors to lungs. Thus, there

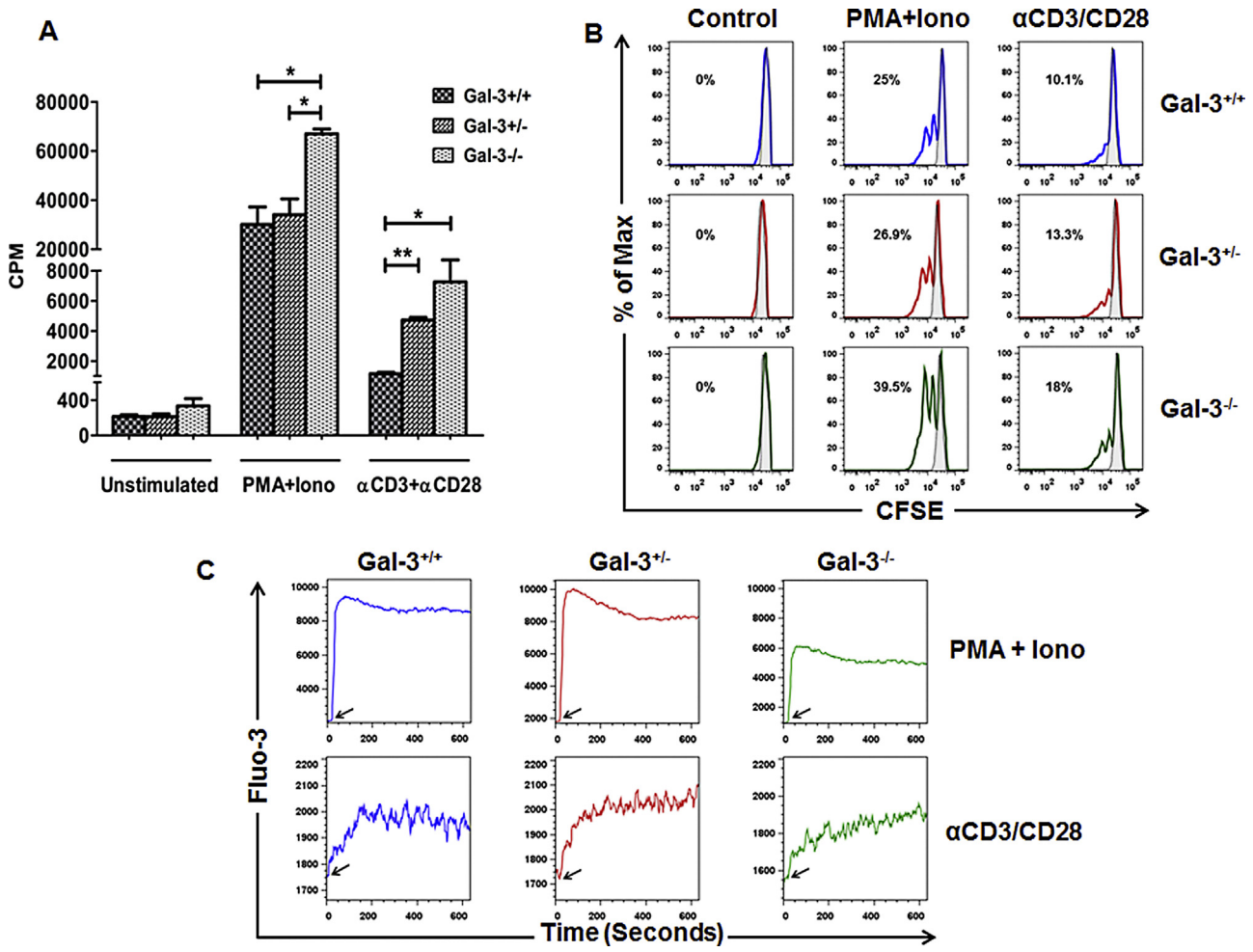

Fig. 2. Proliferative responses and intracellular calcium flux in lymphocytes of Gal-3$^{+/+}$, Gal-3$^{+/-}$ and Gal-3$^{-/-}$ mice upon stimulation with PMA + Ionomycin and anti-CD3/CD28 mAbs. (A) Proliferative responses as measured by [^{3}H] thymidine incorporation assay. Freshly isolated splenocytes (1.5×10^5 cells/200 μl medium/well) of Gal-3$^{+/+}$, Gal-3$^{+/-}$ and Gal-3$^{-/-}$ mice were stimulated with either PMA + Ionomycin (50 ng each) or plate bound anti-CD3 mAb (0.25 μg) + soluble anti-CD28 mAb (0.25 μg) in 96-well microtiter plate for 72 h. Unstimulated splenocytes were used as control. The graph represents consolidated data of 5 independent assays as radioactive counts per minute (CPM). Each set in the assay was performed in triplicate wells. (B) Proliferative responses of purified splenic T cells as assessed by CFSE staining assay. Immunomagnetically purified T cells of Gal-3$^{+/+}$, Gal-3$^{+/-}$ and Gal-3$^{-/-}$ mice were subjected to CFSE staining. After staining, T cells (1.5×10^5 cells/100 μl medium/well) were stimulated *in vitro* with either PMA + Ionomycin (50 ng each; middle panel) or plate bound anti-CD3 mAb + soluble anti-CD28 mAb (0.25 μg each; right panel) in 96-well microtiter plates for 3 days. Unstimulated T cells served as control (left panel). On day 3, cells were harvested from the culture wells and were analyzed by flow cytometry. Each histogram represents CFSE fluorescence intensity of purified T lymphocyte population. A fraction of CFSE labeled T cells were treated with mitomycin C (50 μg/ml) to block the cell proliferation and cultured under the conditions mentioned above to serve as non-proliferating control for each group (Gray filled histogram in each graph). The numbers in each histogram plot represent percentages of divided cell population in each group. The histogram graphs show representative data of 3 independent assays. Each set in the assay was performed in triplicate wells. (C) Intracellular calcium flux in purified T cells upon *in vitro* stimulation. Immunomagnetically purified splenic T cells of Gal-3$^{+/+}$, Gal-3$^{+/-}$ and Gal-3$^{-/-}$ mice were stained with calcium indicator dye Fluo-3-AM. The baseline fluorescence intensity of T cells was measured by flow cytometry for 30 s. The T cells were stimulated with either PMA (100 ng) + Ionomycin (500 ng) (top panel) or soluble anti-CD3 + anti-CD28 mAbs (10 μg each; bottom panel) and the changes in the Fluo-3 fluorescence intensity were then quantitated over a period of up to 10 min by flow cytometry. The histograms show representative data of 3 independent experiments. Arrows indicate the time points of addition of stimulants. $^*P < 0.05$, $^{**}P < 0.01$.

was no detectable effect of the absence of galectin-3 on tumor formation as well as metastasis in mice (Eude-Le Parco et al., 2009). On the other hand, a recent study has used B16 mouse melanoma and LLC mouse lung cancer cells for the allograft model using wild type (Gal-3$^{+/+}$) and Gal-3-deficient (Gal-3$^{-/-}$) mice as hosts. Their findings showed enhancement of primary solid tumor growth in Gal3$^{-/-}$ mice compared with Gal-3$^{+/+}$ mice in both B16 and LLC tumors. However, the incidence of pulmonary metastases of B16 melanoma in these two mice groups was not reported in this study (Jia et al., 2013). Interestingly, it was recently documented that the number and size of metastatic B16F10 melanoma colonies formed in lungs of Gal-3$^{-/-}$ mice was very similar to that seen in Gal-3$^{+/+}$ mice. Gal-3$^{+/-}$ mice that showed reduced expression of galectin-3 on the lungs showed proportionate decrease in the number of metastatic melanoma colonies (More et al., 2015). To resolve the ambiguity in the reported findings, it is important to unveil the possible underlying mechanisms in endogenous galectin-3 mediated regulation of tumorigenic and metastatic events in the host.

Role of immune system in the modulation of tumor progression and metastasis has been widely reported (Dunn et al., 2006; Kim et al., 2007). According to the cancer immunoediting theory, an optimally functioning immune system plays a pivotal role in either elimination or maintenance of metastatic tumor cells in dormancy over a prolonged time period (Kim et al., 2007). Galectin-3 is expressed in many cells subsets of immune system, including monocytes/macrophages, dendritic cells, eosinophils, neutrophils, mast cells, uterine NK cells, activated T and B cells. Accumulating evidence suggests the importance of galectin-3 in functionally regulating the host immune response (Breuilh et al., 2007; Chen et al., 2005; Kouo et al., 2015; Liu, 2005; Nieminen et al., 2005; Pineda

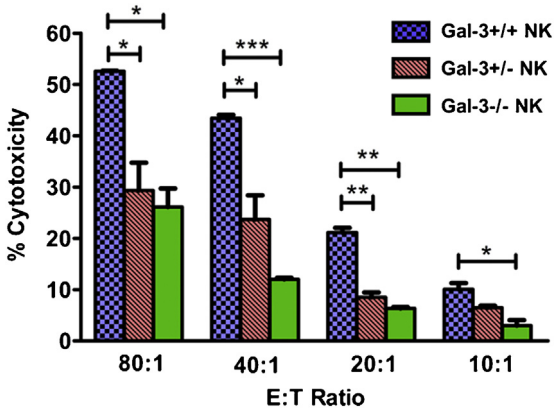

Fig. 3. Ability of splenic NK cells from Gal-$3^{+/+}$, Gal-$3^{+/-}$ and Gal-$3^{-/-}$ mice to kill YAC-1 tumor targets. NK cells ($CD3^{-}NK1.1^{+}$) were purified from freshly isolated splenocytes of Gal-$3^{+/+}$, Gal-$3^{+/-}$ and Gal-$3^{-/-}$ mice by immunomagnetic purification. NK cells were co-cultured with [^{51}Cr] labeled YAC-1 tumor targets at the indicated Effector: Target ratios in a standard 4-h [^{51}Cr] release assay. The graph represents percentage (%) cytotoxicity calculated as described (Section 2.8). Data shows mean ± SE of % cytotoxicity of triplicate wells of a representative experiment. The cytotoxicity assay was performed 3 times using purified splenic NK cells from mice. $^{*}P < 0.05$, $^{**}P < 0.01$, $^{***}P < 0.001$.

et al., 2015). For instance, galectin-3 is known to be a chemoattractant for monocytes and macrophages (Sano et al., 2000), while its expression in neutrophils plays an important role in adhesion and extravasation (Sato et al., 2002). Galectin-3 also modulates growth and apoptosis of T cells (Hsu et al., 2009; Yang et al., 1996), as well as survival of memory B cells (Acosta-Rodriguez et al., 2004). However, the role of endogenous galectin-3 in the modulation of tumor-specific immunity in the host and the mechanisms involved therein need to be further investigated.

Based on the above studies, we hypothesized that endogenous galectin-3 regulates host immune response in mice thereby modulating lung metastasis of B16F10 murine melanoma cells. To test this hypothesis, we analyzed how different levels of expression of endogenous galectin-3 in the host regulate immune responses and what are the mechanisms involved. *Lgals3* transgenic mice of C57BL/6 background strain, including Gal-$3^{+/+}$ (Wild-type), Gal-$3^{+/-}$ (Hemizygous) and Gal-$3^{-/-}$ (Knockout) genotypes were used and their immune status was thoroughly investigated. This to our knowledge is the first comprehensive experimental study done for the detailed analysis of host immunity and regulatory mechanisms orchestrated by endogenous galectin-3 expression levels in the murine model system. The findings provide strong links to understand the crosstalk between galectin-3, immune system and cancer metastasis for designing efficient therapeutic strategies against cancer.

2. Materials and methods

2.1. Mice

6–8 Weeks old female *Lgals3* transgenic mice (C57BL/6 background strain) of 3 genotype groups: Gal-$3^{+/+}$ (Wild type), Gal-$3^{+/-}$ (Hemizygous) and Gal-$3^{-/-}$ (Knockout) were used for the study. Galectin-3 knockout mice generated by targeted disruption of the galectin-3 gene (Hsu et al., 2000) were procured from Prof. F.T. Liu, University of California, Davis, California, USA. Initially, two pairs of male and female transgenic *Lgals3* mice i.e. hemizygous (Gal-$3^{+/-}$) and null (Gal-$3^{-/-}$) were purchased. The wild type (Gal-$3^{+/+}$) littermates were obtained by breeding the hemizygous pair. Genotyping of *Lgals3* transgenic mice to determine their galectin-3 status was done by PCR as described earlier (More et al., 2015). All the animals were propagated and maintained in pathogen-free environments in the Laboratory Animal Facility, ACTREC-Tata Memorial Centre. Standard laboratory diet and filtered water were available *ad libitum*. All animal experiments were done as per the guidelines of Institutional Animal Ethics Committee, ACTREC-Tata Memorial Centre.

2.2. Cell lines and reagents

YAC-1 Murine T cell Lymphoma cell line was obtained from National Centre for Cell Sciences (NCCS, Pune, India). YAC-1 cells were cultured in RPMI 1640 medium (Gibco, Invitrogen) supplemented with 10% Fetal Bovine Serum (Gibco, Invitrogen), 2 mM L-Glutamine and antibiotics. B16F10 Murine melanoma cell line was obtained from National Centre for Cell Sciences (NCCS, Pune, India). B16F10 cells were cultured in Dulbecco's Modified Eagle Medium (DMEM, Gibco, Invitrogen) supplemented with 10% Fetal Bovine Serum (Gibco, Invitrogen), 2 mM L-Glutamine and antibiotics (Penicillin, Streptomycin, gentamycin, mycostatin). The cell lines were maintained at 37 °C in humidified CO_2 incubator containing 5% CO_2 and 95% air for up to 4–5 passages. Recombinant murine Interferon-γ (IFN-γ) was purchased from Peprotech (Rock Hill, NJ).

2.3. Isolation of splenocytes from mice

Mice were sacrificed under deep anesthesia and spleens were collected. Spleens were gently minced and single cell suspension of splenocytes was prepared in plain RPMI 1640 medium. The cells were pelleted by centrifugation and treated with 1X RBC lysis buffer (eBioscience) to lyse erythrocytes. The lysed erythrocytes were removed by washing twice with plain RPMI 1640 at 1000 rpm for 10 min each. The splenocytes were suspended in complete RPMI 1640 medium (RPMI 1640 medium supplemented with 10% Fetal Bovine Serum, 2 mM L-Glutamine and antibiotics). Splenocytes count was calculated using hemocytometer by trypan blue dye exclusion method. The cells were aliquoted as per the experimental requirements and used further for all the cell based assays.

2.4. Flow cytometric analysis of immune cell subsets

Freshly isolated mice splenocytes were rinsed with 1X PBS and cold-fixed in 1% paraformaldehyde in PBS for 15 min at 4 °C. The fixed cells were washed with PBS and suspended in cold FACS buffer (1X PBS containing 1% FBS and 0.02% sodium azide) at the concentration of 1×10^6 cells/50 μl buffer in each tube. For surface markers analysis by multicolor immunophenotyping, the non-permeabilized cells were stained with fluorochrome-conjugated anti-mouse antibodies: CD3 Alexa Fluor 647, CD4 PE-CF594, CD8 Pacific blue, NK1.1 PerCP-Cy5.5, B220 PE-Cy7, CD14 FITC (BD Biosciences, San Diego, CA) and CD119 PE (eBioscience) for 45 min at 4 °C. For intracellular staining, fixed cells were washed with PBS and permeabilized for 15 min at room temperature in saponin buffer (FACS buffer with 0.1% saponin). Permeabilized cells were washed with saponin buffer and suspended in FACS buffer at the concentration of 1×10^6 cells/50 μl buffer in each tube. These cells were stained with fluorochrome-conjugated anti-mouse antibodies: CD4 PE, CD25 FITC and Foxp3 Alexa Fluor 647 for 30 min at room temperature. Appropriate isotype controls were used in all experiments. After the incubation period, the cells were washed by centrifugation using FACS buffer, pellet was suspended in 300 μl FACS buffer and cells were acquired using flow cytometer (FACS-Aria; BD Biosciences). Results were analyzed by FlowJo software (Tree Star, Ashland, OR).

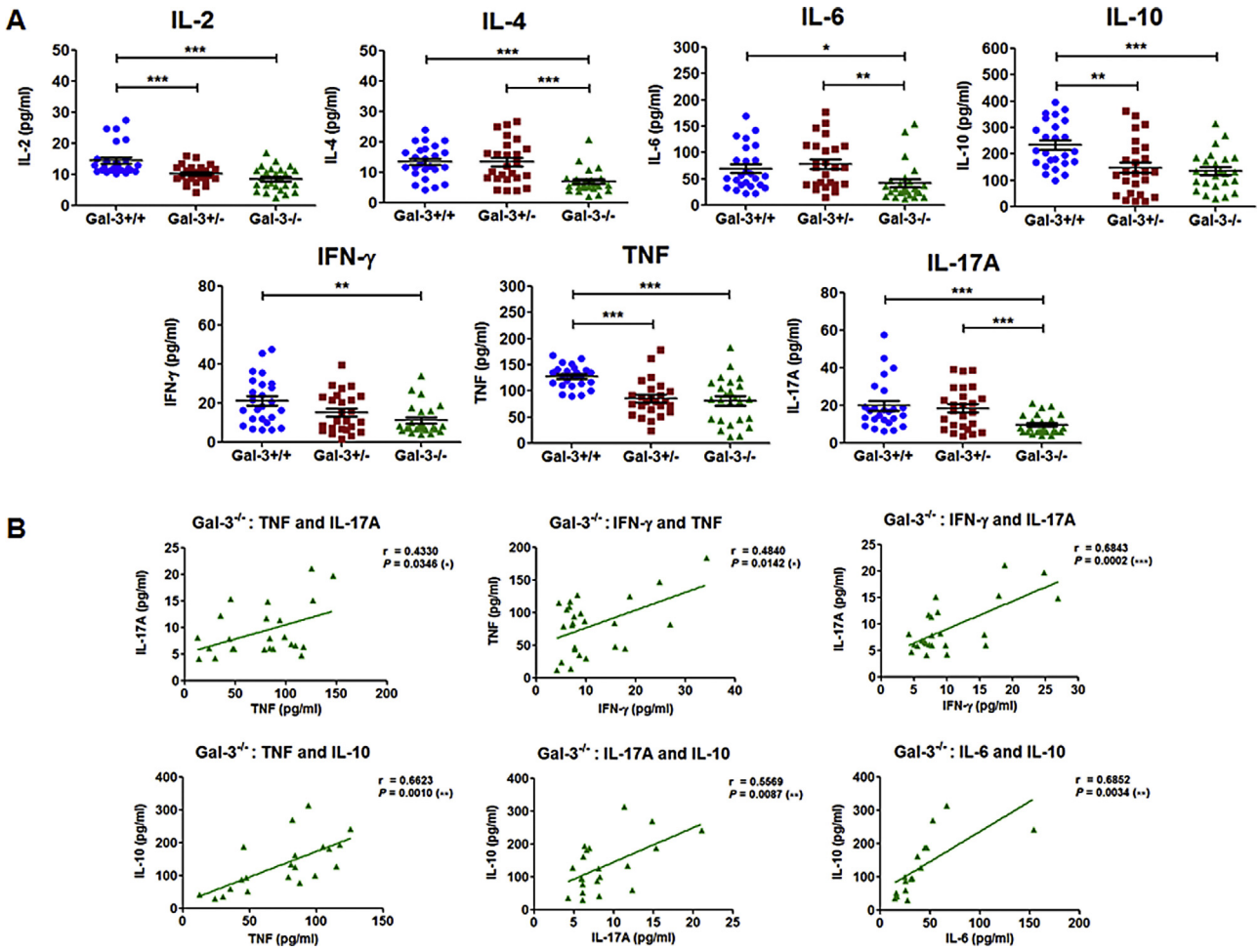

Fig. 4. Serum Th1/Th2/Th17 cytokine profile in Gal-3$^{+/+}$, Gal-3$^{+/-}$ and Gal-3$^{-/-}$ mice. Blood was collected from Gal-3$^{+/+}$, Gal-3$^{+/-}$ and Gal-3$^{-/-}$ mice before sacrifice by retro-orbital puncture and serum was separated by centrifugation. Serum cytokine profile was assessed by Th1/Th2/Th17Cytometric Bead Array using flow cytometry. (A) Concentrations of Th1 (IL-2, IFN-γ, TNF), Th2 (IL-4, IL-6, IL-10) and Th17 (IL-17A) cytokines in mice sera. Each dot in the dot plot represents serum cytokine concentration (pg/ml) of one mouse from the corresponding group ($n = 25$ mice per group). $^{*}P < 0.05$, $^{**}P < 0.01$, $^{***}P < 0.001$. (B) Correlation analysis of levels (pg/ml) of pro-inflammatory cytokines including IFN-γ, TNF and IL-17A with each other in Gal-3$^{-/-}$ mice sera (upper panel). Correlations of IL-6, TNF and IL-17A levels (pg/ml) independently with IL-10 levels (pg/ml) in Gal-3$^{-/-}$ mice sera (lower panel). Pearson's correlation coefficients (r) and P values indicating significance of correlation between the groups are mentioned next to each correlation graph. $^{*}P < 0.05$, $^{**}P < 0.01$, $^{***}P < 0.001$.

2.5. Lymphocyte proliferation by [^{3}H] thymidine incorporation assay

Proliferation of splenocytes was determined by the [^{3}H] thymidine incorporation assay. Freshly isolated splenocytes were cultured at a density of 1.5×10^5 cells/200 μl complete RPMI medium/well in 96 well microtiter plates. The cells were stimulated with either PMA (50 ng, Sigma–Aldrich, St. Louis, MO, USA) + ionomycin (50 ng, Sigma–Aldrich, St. Louis, MO, USA); or plate bound anti-CD3 mAb (0.25 μg; BD Biosciences) + soluble anti-CD28 mAb (0.25 μg; BD Biosciences) for 72 h. Unstimulated splenocytes in complete medium were used as controls. Cells were incubated at 37 °C in humidified CO_2 incubator containing 5% CO_2 and 95% air. [^{3}H] thymidine (0.5 μCi/10 μl/well; Board of Radiation and Isotope Technology, Mumbai, India) was added during the last 18 h of the assay. After the incubation period, the cells were harvested and the radioactivity incorporated into DNA was measured as β emission using a liquid scintillation counter (Packard TRI-CARB 2100 TR counters; Downers Grove, IL, USA). Data were expressed as counts per minute (CPM).

2.6. T cell proliferation by CFSE assay

To study the proliferation of splenic T cell population from mice, CFSE proliferation assay was performed. T cells were immunomagnetically purified from freshly isolated mice splenocyte suspension by negative selection using Mouse Pan T cell isolation kit (Miltenyi Biotec, Bergisch Gladbach, Germany) as per the manufacturer's instructions. Purity of the T cells was checked using anti-mouse CD3 antibody and was found to be ~95% (CD3$^+$) for each isolation. Purified T cells were stained with CFSE dye as described earlier (Quah et al., 2007). Briefly, 15×10^6 T cells were thoroughly suspended in 1 ml of 1X PBS containing 5% (v/v) FBS in a fresh tube. The tube was laid horizontally and 110 μl of PBS was added to the non-wetted portion of the plastic at the top of the tube. 1.1 μl of the 5 mM stock of CFSE (Invitrogen) was added to PBS, tube is capped, quickly inverted several times and vortexed. After thorough mixing, cells were incubated for 5 min at room temperature. Cells were washed thrice with PBS containing 5% (v/v) FCS by centrifugation at 1000 rpm for 5 min at room temperature to remove excess dye. CFSE labeled T cells (1.5×10^5 cells/100 μl complete RPMI/well) were stimulated with either PMA + Ionomycin (50 ng

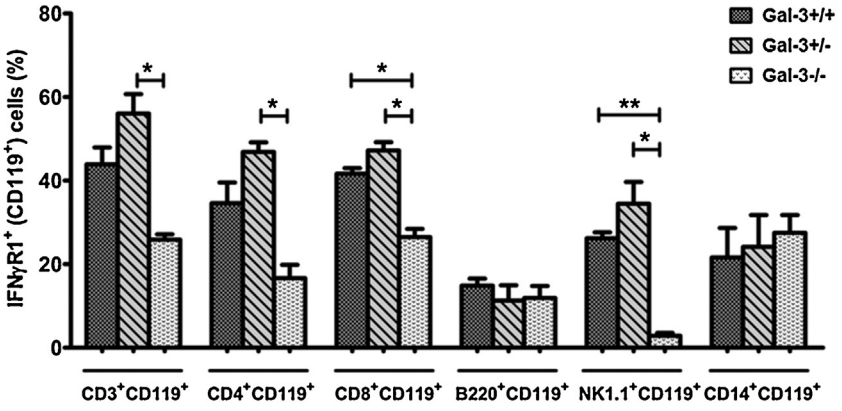

Fig. 5. IFN-γR1 (CD119) expressing splenocyte subsets. Freshly isolated splenocytes of Gal-$3^{+/+}$, Gal-$3^{+/-}$ and Gal-$3^{-/-}$ mice were fixed and stained using fluorochrome conjugated antibodies against CD3, CD4, CD8, B220, NK1.1, CD14 and CD119 by multicolor immunophenotyping. The percentages of $CD119^+$ cells amongst each splenocyte subset were analyzed by flow cytometry. The graph shows consolidated data of 3 independent experiments. $^*P < 0.05$, $^{**}P < 0.01$.

each) or plate bound anti-CD3 mAb (0.25 μg) + soluble anti-CD28 mAb (0.25 μg) in 96-well microtiter plates for 3 days. A fraction of CFSE labeled T cells were treated with mitomycin C (50 μg/ml) for 30 min at 37 °C in CO_2 incubator to block the cell proliferation, washed and cultured in the presence or absence of stimulants mentioned above to serve as non-proliferating control for each group. On day 3, cells were harvested from the culture wells and CFSE fluorescence intensity of splenic T cell population was measured by flow cytometer (FACSAria; BD Biosciences). Results were analyzed using FlowJo software (Tree Star, Ashland, OR).

2.7. Intracellular calcium flux measurement

Immunomagnetically purified splenic T cells (1×10^6 cells/ml PBS) were loaded with 5 μM Fluo-3-AM (Sigma–Aldrich, St. Louis, MO, USA) for 30 min at 37 °C in CO_2 incubator. Cells were washed with 1X PBS to remove excess dye, suspended in 1 ml calcium estimation buffer (137 mM NaCl, 5 mM KCl, 1 mM Na_2HPO_4, 5 mM Glucose, 0.5 mM $MgCl_2$, 10 mM HEPES, 1 mM $CaCl_2$, 1 g/L BSA) and acquired on the flow cytometer (FACSAria, BD Biosciences) for 30 s to determine the baseline Fluo-3 fluorescence intensity in unstimulated cells. PMA (100 ng) + Ionomycin (500 ng) or soluble anti-CD3 + anti-CD28 mAbs (10 μg each) were then added as stimulants and Fluo-3 fluorescence intensity was measured immediately for up to 10 min in a continuous manner. Changes in Fluo-3 intensity were analyzed by FlowJo software (Tree Star, Ashland, OR).

2.8. ^{51}Chromium release cytotoxicity assay

[^{51}Cr] release assay was used to measure the cytotoxicity of splenic NK cells against murine T cell lymphoma cell line (YAC-1) as target cells. NK cells were immunomagnetically purified from mice splenocytes by negative selection using NK cell isolation kit (Miltenyi Biotec, Bergisch Gladbach, Germany) as per the manufacturer's instructions. Purity of the NK cells was checked using antibodies against anti-mouse CD3 and NK1.1 and was found to be >90% ($CD3^-NK1.1^+$) for each isolation. YAC-1 cells were labeled with 50 μCi [^{51}Cr] for 90 min at 37 °C in CO_2 incubator. Labeled target cells were washed in plain RPMI 1640 medium and were incubated with effector NK cells at different Effector to Target (E:T) ratios including 80:1, 40:1, 20:1 and 10:1 at 37 °C in 5% CO_2 for 4 h. After incubation, plates were centrifuged, 100 μl supernatants were collected from each well and radioactive chromium release was measured as counts per minute (CPM) using 1470 Wallac automated gamma counter (PerkinElmer, Downers Grove, IL). Spontaneous release was determined by incubating the target cells with medium alone, and maximum release was determined by incubating target cells with 10% Triton X-100. The percent specific lysis (%cytotoxicity) was calculated as: [(experimental release—spontaneous release)/(maximum release—spontaneous release)] × 100.

2.9. Cytometric bead array

Blood was collected from mice before sacrifice by retro-orbital puncture and serum was separated by centrifugation. Sera samples were stored at −80 °C until used. Serum cytokine profiles including IL-2, IL-4, IL-6, IFN-γ, TNF, IL-17A, IL-10 cytokine levels in mice were assessed by Th1/Th2/Th17Cytometric Bead Array kit (BD Biosciences) as per manufacturer's instructions. Samples were acquired on flow cytometer (FACSAria, BD Biosciences) and data were analyzed using FCAP Array software (BD Biosciences).

2.10. Western blotting

STAT1 mediated IFN-γ signaling pathway intermediates in stimulated mice splenocytes were studied by western blotting. Freshly isolated splenocytes of mice (2.5×10^6 cells/ml complete RPMI 1640/well) were stimulated *in vitro* using recombinant murine IFN-γ (Peprotech, Rock Hill, NJ) at two different concentrations (1 and 10 ng/ml) in 24-well microtiter plates for 30 min or 12 h. Unstimulated cells cultured in medium alone were used as controls. The cells were harvested at the desired time points, washed with 1X PBS and whole-cell lysates (10×10^6 cells) were prepared in SDS sample buffer (62.5 mM Tris–HCl, 2% w/v SDS, 10% glycerol, 50 mM DTT, and 0.1% bromophenol blue, pH 6.8). Lysates were sonicated to reduce sample viscosity, denatured by boiling, and then cooled on ice. Samples were resolved on 10% SDS-PAGE gels, transferred onto Hybond-ECL nitrocellulose membrane (Amersham Pharmacia Biotech, Piscataway, NJ). The membranes were blocked and primary Abs to total STAT-1, phospho-STAT1(Tyr701), SOCS-1, SOCS-3 (Cell Signaling Technology) and β-actin (Sigma–Aldrich) were added at 1:1000 dilution followed by overnight incubation at 4 °C. Appropriate secondary antibodies including GAR-HRPO (Sigma–Aldrich) for total STAT-1, phospho-STAT1(Tyr701), SOCS-1, SOCS-3 and GAM-HRPO (Sigma–Aldrich) for β-actin were used at a dilution of 1:1000 at room temperature for 2 h. The blots were washed and developed with ECL plus Western blot detection system (GE Healthcare). Densitometric analysis of western blots was done using ImageJ software.

2.11. Experimental metastasis assay

To establish experimental metastasis, B16F10 murine melanoma cells were intravenously injected at the concentration of 1×10^5 cells/100 μl plain DMEM/mouse in the lateral tail vein of mice. On day 14 post intravenous B16F10 injection, mice were sacrificed and lungs were collected by dissection. The melanoma colonies on each mouse lung were counted using a dissecting microscope. The lungs were fixed using 10% neutral buffered formalin. Paraffin embedded 5 μm thin sections of formalin fixed lungs were stained by hematoxylin and eosin for histopathological analysis of melanoma colonies in the lungs. The H&E stained lung sections were observed under upright microscope and images were captured at 5× magnification.

2.12. Statistical analysis

Statistical analyses were performed using GraphPad Prism Software version 5.0 (La Jolla, USA). Student's *t* test was used to determine the statistical significance. Results are represented as Mean ± SE. A value of $P < 0.05$ was considered statistically significant.

3. Results

3.1. Immune cell subsets in Gal-3$^{+/+}$, Gal-3$^{+/-}$ and Gal-3$^{-/-}$ mice

The comparison of the levels of galectin-3 protein expression in the lungs of *Lgals3* transgenic mice by western blotting has been reported in our recently published study (More et al., 2015). Gal-3$^{+/+}$ mice showed the expression of galectin-3 protein, while there is complete absence of galectin-3 in Gal-3$^{-/-}$ mice. Gal-3$^{+/-}$ mice showed marked reduction in the galectin-3 protein levels in lung tissue extract as compared to that of Gal-3$^{+/+}$ mice, due to the presence of one mutated *Lgals3* allele (More et al., 2015). These results confirmed that endogenous galectin-3 protein expression levels correlated well with the *Lgals3* gene dosage in Gal-3$^{+/+}$, Gal-3$^{+/-}$ and Gal-3$^{-/-}$ mice.

To assess whether reduction or total absence of galectin-3 levels in host affects the frequency of major immune cell subtypes, we performed immunophenotyping of splenocytes isolated from Gal-3$^{+/+}$, Gal-3$^{+/-}$ and Gal-3$^{-/-}$ mice. Lymphocytes were gated based on their forward and side scatter characteristics by flow cytometric analysis. In the innate immune compartment, percentages of splenic NK ($CD3^-NK1.1^+$) cells were found to be significantly lower in Gal-3$^{-/-}$ mice compared to Gal-3$^{+/+}$ mice. The percentages of splenic NK cells correlated with the *Lgals3* gene dosage in Gal-3$^{+/+}$, Gal-3$^{+/-}$ and Gal-3$^{-/-}$ mice (Fig. 1A). To study the key players of adaptive immune response, we checked the levels of total $CD3^+$ T cells, helper T cells (T_H, $CD3^+CD4^+$), cytotoxic T cells (T_C, $CD3^+CD8^+$) and B cells ($B220^+$). Significant differences were not observed in the percentages of total $CD3^+$ T cells, helper T cells (T_H, $CD3^+CD4^+$) and cytotoxic T cells (T_C, $CD3^+CD8^+$) in the three groups of mice. Higher levels of splenic B cells ($B220^+$) were found in Gal-3$^{+/-}$ mice than in Gal-3$^{-/-}$ mice (Fig. 1A). We also compared the splenic regulatory T cell (T_{reg}) populations in the three strains of mice. No significant differences were observed in the percentages of $CD4^+CD25^+Foxp3^+$ T_{reg} in splenocytes of Gal-3$^{+/+}$, Gal-3$^{+/-}$ and Gal-3$^{-/-}$ mice (Fig. 1B).

3.2. Proliferative responses and intracellular calcium flux in lymphocytes from Gal-3$^{+/+}$, Gal-3$^{+/-}$ and Gal-3$^{-/-}$ mice upon in vitro stimulation

In order to study whether functional immune responses differ with galectin-3 expression levels in the host, we checked the ability of splenocytes isolated from Gal-3$^{+/+}$, Gal-3$^{+/-}$ and Gal-3$^{-/-}$ mice to respond to stimulants *in vitro*. The proliferative response of splenocytes on stimulation was compared between the three groups of mice using [^{3}H] thymidine incorporation assay. On stimulation with PMA + Ionomycin, Gal-3$^{-/-}$ mice splenocytes showed remarkably higher proliferation as compared to that of Gal-3$^{+/+}$ and Gal-3$^{+/-}$ mice. On stimulation using plate-bound anti-CD3 mAb + soluble anti-CD28 mAb, proliferation of Gal-3$^{+/-}$ and Gal-3$^{-/-}$ splenocytes was found to be significantly increased than that of Gal-3$^{+/+}$ splenocytes (Fig. 2A). Simultaneously, T cells were purified from total splenocytes and their proliferation in response to stimulants was monitored using CFSE assay. It was confirmed that, purified splenic T cells of Gal-3$^{+/-}$ and Gal-3$^{-/-}$ mice exhibited higher proliferative response to stimulants (PMA + Ionomycin and anti-CD3/CD28 mAbs) than that observed in T cells from Gal-3$^{+/+}$ mice, on day 3 post stimulation (Fig. 2B).

Calcium ions (Ca^{++}) act as important secondary messengers in T cell activation and signaling cascade leading to various T cell responses. We analyzed the flux of intracellular Ca^{++} ions produced after stimulation of Fluo-3-AM labeled purified T cells *in vitro*. Fluo-3 is a calcium indicator dye widely used to probe the levels of cytosolic Ca^{++} ions produced on stimulation of cells. T cells isolated from Gal-3$^{-/-}$ mice were found to produce lower levels of intracellular Ca^{++} flux compared to T cells from Gal-3$^{+/+}$ and Gal-3$^{+/-}$ mice, in response to stimulation with PMA + Ionomycin and soluble anti-CD3/CD28 mAbs *in vitro*. It was also observed that, the baseline Ca^{++} levels in T cells of Gal-3$^{-/-}$ mice were lower than those in Gal-3$^{+/+}$ and Gal-3$^{+/-}$ mice (Fig. 2C).

3.3. Comparison of NK cell cytotoxicity in Gal-3$^{+/+}$, Gal-3$^{+/-}$ and Gal-3$^{-/-}$ mice

NK cells are the key players of innate immune responses, providing first line of defense against transformed and tumorigenic cells. We found reduced splenic NK cell population in Gal-3$^{-/-}$ mice than in Gal-3$^{+/+}$ mice (Fig. 1A). It was therefore interesting to analyze whether the cytotoxic function of splenic NK cells correlated with their phenotype in Gal-3$^{+/+}$, Gal-3$^{+/-}$ and Gal-3$^{-/-}$ mice.

YAC-1 mouse T lymphoma cells have been used as classical tumor targets of NK cells in murine system in numerous studies because of their NK sensitive nature. In our study, we found that freshly isolated NK cells ($CD3^-NK1.1^+$) from Gal-3$^{+/-}$ and Gal-3$^{-/-}$ mice exhibited significantly decreased cytotoxicity against YAC-1 tumor cells, as compared to that of Gal-3$^{+/+}$ mice at all the E:T ratios tested (Fig. 3). Thus, galectin-3 expression levels in these mice appear to be important determinants of anti-tumor cytolytic function of NK cells.

3.4. Serum cytokine profile in Gal-3$^{+/+}$, Gal-3$^{+/-}$ and Gal-3$^{-/-}$ mice

Cytokines are the important modulators of balance between humoral and cell based immune responses in normal physiological processes as well as during pathological conditions; including infection, inflammation and cancer. It was important to explore the serum cytokine profile in the three groups of mice with different endogenous galectin-3 expression levels.

The levels of Th1 (IL-2, IFN-γ, TNF), Th2 (IL-4, IL-6, IL-10) and Th17 (IL-17A) cytokines were measured in the sera of Gal-3$^{+/+}$, Gal-3$^{+/-}$ and Gal-3$^{-/-}$ mice by cytometric bead array using flow cytometry. It was found that, Gal-3$^{+/-}$ and Gal-3$^{-/-}$ mice showed reduced serum cytokine levels as compared to Gal-3$^{+/+}$ mice. The Th1, Th2 and Th17 cytokine levels were found to be affected the most in the total absence of endogenous galectin-3. Sera of Gal-3$^{-/-}$ mice showed marked reduction in all cytokine levels. It was interesting to note that, serum levels of IL-2 and IFN-γ showed a trend that correlated with endogenous galectin-3 expression levels in

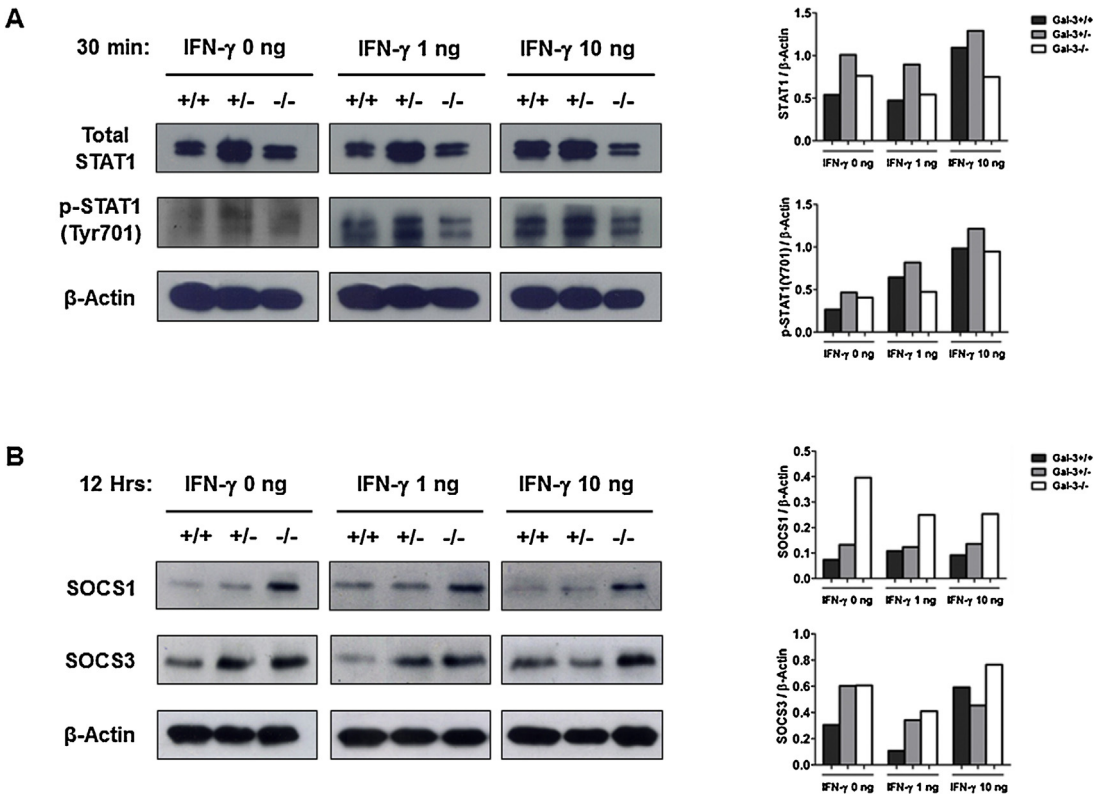

Fig. 6. STAT1 mediated IFN-γ signaling in Gal-$3^{+/+}$, Gal-$3^{+/-}$ and Gal-$3^{-/-}$ mice splenocytes. (A) IFN-γ induced STAT1 signaling in mice splenocytes. Freshly isolated splenocytes of Gal-$3^{+/+}$, Gal-$3^{+/-}$ and Gal-$3^{-/-}$ mice (2.5×10^6 cells/ml complete medium/well) were stimulated *in vitro* using recombinant murine IFN-γ (1 and 10 ng/ml) in 24-well microtiter plates for 30 min. Unstimulated cells cultured in medium alone were used as controls (IFN-γ 0 ng/ml). The cells were then harvested, lysed and equal amounts of lysates were analyzed by western blotting to detect protein levels of total STAT1 (STAT1α: 91 kDa and STAT1β: 84 kDa) and phospho-STAT1(Tyr701). β-actin (42 kDa) served as loading control. The blots are representative of 3 independent experiments (Left panel). Densitometry results are indicated as ratios of optical densities for STAT1 or phospho-STAT1(Tyr701) protein bands relative to loading control i.e. β-Actin band for the representative blots (Right panel). (B) Suppressors of IFN-γ signaling pathway in mice splenocytes. Freshly isolated splenocytes of Gal-$3^{+/+}$, Gal-$3^{+/-}$ and Gal-$3^{-/-}$ mice (2.5×10^6 cells/ml complete medium/well) were stimulated using recombinant murine IFN-γ (1 and 10 ng/ml) in 24-well plates for 12 h. Unstimulated cells cultured in medium alone were used as controls (IFN-γ 0 ng/ml). The cells were then harvested, lysed and equal amounts of lysates were analyzed by western blotting to detect protein levels of SOCS-1 (23 kDa) and SOCS-3 (26 kDa). β-actin (42 kDa) served as loading control. The blots are representative of 3 independent experiments (Left panel). Densitometry results are indicated as ratios of optical densities for SOCS1 or SOCS3 protein bands relative to loading control i.e. β-Actin band for the representative blots (Right panel).

Gal-$3^{+/+}$, Gal-$3^{+/-}$ and Gal-$3^{-/-}$ mice (Fig. 4A). However, correlation analysis revealed that, there was no significant correlation between serum IL-2 and IFN-γ levels in all the three groups of mice (data not shown). The levels of pro-inflammatory cytokines TNF, IFN-γ and IL-17A had significantly strong positive correlations with each other exclusively in Gal-$3^{-/-}$ mice sera. Interestingly, concentrations of pro-inflammatory cytokines IL-6, TNF and IL-17A correlated positively with anti-inflammatory cytokine IL-10 and these correlations were significant only in Gal-$3^{-/-}$ mice sera (Fig. 4B). All these correlations were not observed in the sera of Gal-$3^{+/+}$ and Gal-$3^{+/-}$ mice (Data not shown). These findings indicate that, in the complete absence of endogenous host galectin-3, the serum cytokine milieu may be disturbed, exhibiting dysregulation of the balance between pro-inflammatory and anti-inflammatory cytokines.

3.5. *STAT1 mediated IFN-γ signaling in Gal-$3^{+/+}$, Gal-$3^{+/-}$ and Gal-$3^{-/-}$ mice*

IFN-γ is a multi-functional cytokine produced by NK cells and activated T cells in host. IFN-γ exerts its effects on cells by binding to IFN-γ Receptor (IFN-γR) on the cell surface and signal transduction through STAT1 mediated pathway. We quantitated the expression of ligand binding chain of IFN-γ Receptor i.e. IFN-γR1 (CD119) on T cell subsets, B cells, NK cells and macrophages in mice splenocytes. Percentages of IFN-γR1 receptor expressing splenic T cell subsets and NK cells were found to be higher in Gal-$3^{+/-}$ mice and lower in Gal-$3^{-/-}$ mice as compared to Gal-$3^{+/+}$ mice. No significant differences were observed in the percentages of B cells and macrophages expressing IFN-γR1 (Fig. 5).

To understand whether the differences in the splenic IFN-γR1 expression affect the subsequent STAT1 mediated signal transduction, we examined levels of total STAT1 and activated phospho-STAT1(Tyr701) proteins in IFN-γ stimulated splenocytes of Gal-$3^{+/+}$, Gal-$3^{+/-}$ and Gal-$3^{-/-}$ mice by western blotting. On stimulation of splenocytes with recombinant murine IFN-γ (1 and 10 ng/ml) for 30 min, total STAT1 and activated phospho-STAT1(Tyr701) protein levels were found to be higher in Gal-$3^{+/-}$ mice splenocytes compared to Gal-$3^{+/+}$ and Gal-$3^{-/-}$ mice splenocytes (Fig. 6A). On the other hand, when splenocytes were stimulated using recombinant murine IFN-γ (1 and 10 ng/ml) for 12 h, levels of suppressors of cytokine signaling including SOCS1 and SOCS3 proteins were remarkably higher in Gal-$3^{-/-}$ mice as compared to Gal-$3^{+/+}$ and Gal-$3^{+/-}$ mice splenocytes (Fig. 6B). Together, these findings suggest possible attenuation of STAT1 mediated IFN-γ signaling in the splenocytes of Gal-$3^{-/-}$ mice.

4. Discussion

Galectin-3 plays important roles in the immune responses through regulating the homeostasis and functions of the immune cells (Chen et al., 2005; Dumic et al., 2006; Liu, 2005). The immunomodulatory functions of galectin-3 have been majorly

studied using recombinant galectin-3. Whether endogenous host galectin-3 also exerts these activities is not well investigated. A number of intracellular functions of galectin-3 have been revealed by using gene transfection or antisense oligonucleotide approaches to influence expression of galectin-3 protein in the cell (Liu et al., 2002). Because of the inherent limitations of these approaches, the immunoregulatory functions of galectin-3 have been confirmed by other experimental strategies, such as the use of immune cells from Gal-3$^{-/-}$ mice or by knocking down the *Lgals3* gene expression by siRNA (Dumic et al., 2006; Rabinovich et al., 2007). Scanty literature demonstrating the role of galectin-3 in immune regulation *in vivo* using Gal-3$^{-/-}$ mice is available (Breuilh et al., 2007; Chen et al., 2005; Dumic et al., 2006; Ferraz et al., 2008; Henderson and Sethi, 2009; Hsu et al., 2000; Jia et al., 2013; Kouo et al., 2015; Pineda et al., 2015; Rabinovich et al., 2007; Radosavljevic et al., 2011). However, the underlying mechanisms in endogenous galectin-3 mediated modulation of host immunity remain poorly understood till date.

In the present investigation, we performed comparative analysis of the immune scenario with respect to different levels of endogenous galectin-3 in Gal-3$^{+/+}$, Gal-3$^{+/-}$ and Gal-3$^{-/-}$ mice. We observed two broad categories of immune responses: (a) Immune responses that correlated with levels of endogenous galectin-3 expression and clearly showed *Lgals3* gene dosage effects in mice (b) No *Lgals3* gene dosage effects were observed in immune responses with respect to levels of endogenous galectin-3 expression in mice.

Higher splenic T cell proliferative response was exhibited by Gal-3$^{+/-}$ and Gal-3$^{-/-}$ mice as compared to Gal-3$^{+/+}$ mice on *in vitro* stimulation with PMA + Ionomycin and anti-CD3/CD28 mAbs. This response showed *Lgals3* gene dosage effects, albeit with an inverse correlation to galectin-3 expression levels. Galectin-3 is absent in resting CD4^{+} and CD8^{+} T cells. It is inducible by various stimuli such as viral trans-activating factors, TCR ligation, calcium ionophores etc. (Hsu et al., 2009). Extracellular galectin-3 is known to form multivalent lattices with glycoproteins of TCR and restrains lateral mobility of TCR complex necessary for clustering, thereby Inhibiting TCR mediated signal transduction and activation of T cells (Demetriou et al., 2001). The enhancement of T cell proliferative response observed in Gal-3$^{+/-}$ and Gal-3$^{-/-}$ mice might be possibly due to abrogation of inhibitory effects of galectin-3 on TCR signaling.

Calcium is an important secondary messenger involved in the regulation of many signaling pathways in a multitude of different biological processes. Stimulation of T cells with soluble antibodies to the CD3/T-cell receptor complex causes rapid increases in the intracellular concentration of calcium, which plays a crucial role during the activation of T cells. In the present study, reduced intracellular Ca^{++} flux observed in PMA + Ionomycin or soluble anti-CD3/CD28 mAbs stimulated T cells of Gal-3$^{-/-}$ mice as compared to those of Gal-3$^{+/+}$ and Gal-3$^{+/-}$ mice, highlights the importance of endogenous galectin-3 expression in the regulation of T cell calcium signaling in the host. The increased T cell proliferation with reduced intracellular Ca^{++} flux observed in stimulated T cells of Gal-3$^{-/-}$ mice indicates possible impairment of functional T cell responses in the absence of endogenous galectin-3 expression in these mice.

NK cells are crucial players in host anti-tumor immune responses mediated by their cytolytic activities and IFN-γ production. In the present study, immunophenotyping results indicated differences in the levels of splenic NK cells (CD3^{-}NK1.1^{+}) in *Lgals3* gene dosage dependent manner in Gal-3$^{+/+}$, Gal-3$^{+/-}$ and Gal-3$^{-/-}$ mice. Marked decrease in splenic NK-mediated cytotoxicity against YAC-1 murine T lymphoma cells was observed in Gal-3$^{+/-}$ and Gal-3$^{-/-}$ mice compared to Gal-3$^{+/+}$ mice, exhibiting *Lgals3* gene dosage effect. It has been previously demonstrated that, treatment of B16F10 murine melanoma cells with swainsonine, an *N*-glycosylation inhibitor, inhibits their lung metastasis in syngeneic C57BL/6 mice by prevention of *N*-glycosylation in these cells (Srinivasan et al., 2009). Earlier study has reported that, systemic administration of swainsonine to C57BL/6 mice also results in inhibition of metastasis of untreated B16F10 cells. In contrast, the inhibitory activity of swainsonine was completely abrogated when assays were performed in mice depleted of their natural killer (NK) cell activity either experimentally (C57BL/6 mice treated with anti-asialo-GM1 antibody or cyclophosphamide) or as a result of genetic mutation (homozygous C57BL/6$^{bg/bg}$ beige mice) (Humphries et al., 1988). This indicates that, the impaired ability of NK cells to kill the tumor targets might be an important predisposing factor facilitating enhanced tumorigenesis and metastasis in Gal-3$^{-/-}$ mice. This finding is further supported in Gal-3$^{+/-}$ mice as we observed increased NK cytotoxicity and reduced pulmonary melanoma metastases in these mice as compared to Gal-3$^{-/-}$ mice.

The studies of the functional role of galectin-3 using Gal-3$^{-/-}$ mice have also revealed the protein's ability to regulate Th1/Th2 polarization under various pathological conditions (Bernardes et al., 2006; Ferraz et al., 2008; Zuberi et al., 2004). It has been reported that, galectin-3 suppresses the production of IL-12 in dendritic cells, which is the major cytokine that drives the Th1 response (Bernardes et al., 2006). Several *in vitro* and *in vivo* studies suggest that, galectin-3 may modulate inflammatory responses through its functions on cell activation, cell migration or inhibition of apoptosis thus prolonging the survival of inflammatory cells (Rabinovich et al., 2002). The emerging data from studies of Gal-3$^{-/-}$ mice support the role of galectin-3 in the promotion of inflammatory responses (Chen et al., 2005; Henderson and Sethi, 2009; Hsu et al., 2000; Zuberi et al., 2004). In our study, the production of Th1, Th2 and Th17 cytokines was found to be hampered in Gal-3$^{+/-}$ and Gal-3$^{-/-}$ mice sera, with serum IL-2 and IFN-γ levels demonstrating *Lgals3* gene dosage effect. Correlation analysis of different serum cytokine levels indicated that, the cytokine milieu was disturbed in Gal-3$^{-/-}$ mice, with dysregulation of pro-inflammatory and anti-inflammmatory cytokine balance. The balance between pro-inflammatory and anti-inflammatory signaling is critical to maintain the immune homeostasis under normal physiological conditions. In Gal-3$^{-/-}$ mice, the immune homeostasis appeared to be disturbed, which may contribute to the observed immune dysregulation in these mice.

IFN-γ is a multifunctional cytokine produced mainly by NK cells and activated T cells. IFN-γ is a key cytokine exerting anti-tumor immunity against melanoma and various other cancers (Dunn et al., 2006; Ikeda et al., 2002). It has been found to have direct anti-proliferative and pro-apoptotic effects on tumor cells in animal models (Dighe et al., 1994; Kakuta et al., 2002; Kaplan et al., 1998; Mitra-Kaushik et al., 2004; Shankaran et al., 2001; Xu et al., 2009). IFN-γ prevents B16 experimental metastasis by directly inhibiting cell growth (Kakuta et al., 2002). Another study reported that, HTLV-1-Tax$^{+/+}$ IFNγ$^{-/-}$ mice develop increased numbers of soft tissue tumors with enhanced tumor-associated angiogenesis and up-regulation of vascular endothelial growth factor expression (Mitra-Kaushik et al., 2004).

In the present study, serum IFN-γ levels as well as splenic IFN-γR1 (CD119) expressing T and NK cell frequencies were found to be significantly reduced in Gal-3$^{-/-}$ mice as compared to Gal-3$^{+/+}$ mice. Interestingly, percentages of IFN-γR1 (CD119) expressing T and NK cells were highest in Gal-3$^{+/-}$ mice splenocytes amongst the three groups of mice. IFN-γ exerts its effects by binding to IFN-γ receptor on the cell surface which is followed by STAT1 mediated signaling pathway. On stimulation of splenocytes using recombinant IFN-γ, activated phospho-STAT1(Tyr701) protein levels were found to be higher in Gal-3$^{+/-}$ mice than in Gal-3$^{+/+}$ and Gal-3$^{-/-}$ mice, which correlated with the highest frequency of IFN-γR1 expressing splenic T and NK cells in Gal-3$^{+/-}$ mice. On the other hand, IFN-γ stimulated Gal-3$^{-/-}$ mice splenocytes exhibited high-

est intracellular expression of SOCS1 and SOCS3 proteins, which are known to directly antagonize STAT1 activation by negative feedback mechanism (Alexander et al., 1999; Song and Shuai, 1998). Thus, complete absence of endogenous host galectin-3 appeared to contribute in the attenuation of STAT1 mediated IFN-γ signaling in Gal-3$^{-/-}$ mice splenocytes.

SOCS1 and SOCS3 proteins can both inhibit JAK phosphorylation of STAT, thus creating a negative feedback loop that attenuates cytokine signal transduction, although the mechanisms by which they act appear to differ. Whereas SOCS1 functions by binding directly to JAK proteins, SOCS3 inhibits signaling by binding to phosphorylated tyrosine sites on the cytoplasmic domain of the receptor (Endo et al., 1997; Nicholson et al., 1999). In addition, SOCS1 is known to exhibit a much stronger inhibitory activity toward the activation of STAT1 than did SOCS3 (Song and Shuai, 1998). The literature data indicate that induction of SOCS1 and SOCS3 proteins in host cells upon IFN-γ stimulation is a result of a complex interplay between several different factors; including cell type, concentration of exogenous IFN-γ used for stimulation, levels of other cytokines present in the cellular environment, expression of cytokine receptors, relative abundance and activation level of IFN-γ/STAT1 and IL-6,IL-10 /STAT3 signaling in cells and galectin-3 expression levels in host. In the present study, due to striking reduction in IFN-γR1 expression observed in Gal-3$^{-/-}$ mice, stimulation of murine splenocytes with increasing doses of exogenous IFN-γ might not lead to a gradual and sustained increase in SOCS1 production in IFN-γ dose dependent manner in Gal-3$^{-/-}$ mice, as expected. Further, galectin-3 being an important regulator of SOCS1 and SOCS3 expression in host (Lalancette-Hebert et al., 2012; Lopez et al., 2011), this regulatory mechanism appears to be impaired in Gal-3$^{+/-}$ and Gal-3$^{-/-}$ mice, leading to abrupt decrease in splenic SOCS1 and SOCS3 levels upon stimulation with increasing doses of recombinant murine IFN-γ *in vitro*.

In the present investigation, detailed analysis of immune scenario in mice with different endogenous galectin-3 expression levels revealed that their immune system has striking differences. Endogenous host galectin-3 appeared to exhibit its immunomodulatory effects in *Lgals3* gene dosage dependent manner, as seen in terms of splenic NK cell frequency, NK mediated cytotoxicity, serum IL-2 and IFN-γ levels (Direct correlation with endogenous galectin-3 expression levels) as well as T cell proliferative response (Inverse correlation with endogenous galectin-3 expression levels) in Gal-3$^{+/+}$, Gal-3$^{+/-}$ and Gal-3$^{-/-}$ mice. On the other hand, in Gal-3$^{+/-}$ mice, endogenous galectin-3 exerts paradoxical effects that are independent of *Lgals3* gene dosage. Gal-3$^{+/-}$ mice demonstrated highest percentages of IFN-γR1 expressing splenic T cells and NK cells, elevated total STAT1 and activated phospho-STAT1(Tyr701) protein levels amongst the three mice groups. The possible mechanisms underlying such a paradoxical immunoregulatory role of endogenous host galectin-3 in the Gal-3$^{+/-}$ mice warrants further investigation.

We assessed whether incidence of organ specific metastasis of tumor cells was affected in Gal-3$^{+/+}$, Gal-3$^{+/-}$ and Gal-3$^{-/-}$ mice. B16F10 murine melanoma model was used to establish lung specific metastasis of B16F10 melanoma cells in Gal-3$^{+/+}$, Gal-3$^{+/-}$ and Gal-3$^{-/-}$ mice by experimental metastasis assay. On day 14 post lateral tail vein injection of B16F10 cells (1×10^5 cells per mouse), it was observed that frequency of B16F10 pulmonary metastasis was not significantly different between Gal-3$^{+/+}$ and Gal-3$^{-/-}$ mice groups. However, in Gal-3$^{+/-}$ mice, the number of metastatic melanoma colonies present on the lungs was significantly lower than in Gal-3$^{+/+}$ and Gal-3$^{-/-}$ mice (Supplementary Fig. S1A and S1B). Histopathology of lung sections provided further confirmatory evidence to support our observation (Supplementary Fig. S1C). These results were in accordance with our recently published study done with Gal-3$^{+/+}$, Gal-3$^{+/-}$ and Gal-3$^{-/-}$ mice to study lung metastasis of B16F10 cells by experimental metastasis assay (More et al., 2015).

Experimental metastasis assay using well characterized B16 murine melanoma model for lung specific metastasis in Gal-3$^{+/+}$, Gal-3$^{+/-}$ and Gal-3$^{-/-}$ mice confirmed that apart from promoting interaction with cells in the lungs, galectin-3 by other mechanisms as well, has a major role in dictating the metastatic outcome. Although, the functional redundancy by other galectins and the role of polyLacNAc on *N*-glycans has been ruled out in Gal-3$^{-/-}$ mice (More et al., 2015), the enhanced lung metastasis in these mice is clearly due to compromised host immunity in the absence of endogenous galectin-3.

During metastatic spread of cancer cells to distant organs through the circulation, these cells encounter different cell types of innate and adaptive immune compartment. In an immunocompetent host, these immune cells can effectively exert their anti-tumor effects to eradicate majority of the circulating cancer cell population. The heightened anti-tumor immune responses in Gal-3$^{+/-}$ mice might further explain the lowest incidence of B16F10 lung metastasis observed in these mice. However, in the scenario where the host immune system is not optimally performing or is dysfunctional, major frequency of the tumor cells can survive and sustain in the circulation ultimately reaching their secondary target organ. The chances of high number of circulating B16F10 melanoma cells getting anatomically or mechanically trapped in the lungs of Gal-3$^{-/-}$ mice and giving rise to metastatic melanoma colonies would be very high. It would be interesting to explore the mechanisms employed by these tumor cells for lung homing in Gal-3$^{-/-}$ mice in the absence of endogenous galectin-3.

Functionally, galectin-3 is a complex molecule which exerts different effects on the cells depending on its subcellular localization. The secreted galectin-3 functions in an entirely different manner which is carbohydrate ligand dependent. The diversity of effects of galectin-3 seen on disease progression in large number of human cancer types is possibly a result of these differences in the localization of galectin-3 (Song et al., 2014; Thijssen et al., 2015). Our study demonstrates another aspect of endogenous host galectin-3, that of maintaining a functionally competent immune system in the host. We have comprehensively demonstrated that its absence may severely compromise host anti-tumor immunity and can adversely affect cancer progression. Future galectin-3 targeted anti-cancer therapies would also need to take this aspect of galectin-3 function into account.

5. Conclusion

The present investigation indicates that, anti-tumor immunity orchestrated by levels of endogenous host galectin-3 expression plays an important role in modulating the incidence of organ specific metastasis as studied in the B16F10 murine melanoma model. The dysregulation of immune responses observed in Gal-3$^{-/-}$ mice, in terms of decreased NK cytotoxicity, disturbed serum Th1, Th2, Th17 cytokines milieu, reduced serum IFN-γ levels, lower frequency of IFN-γR1 expressing splenic T and NK cells and attenuation of STAT1 mediated IFN-γ signaling, lends support to the high incidence of lung metastasis observed in these mice. This study opens new exciting avenues in understanding the complex role of endogenous host galectin-3 in cancer metastasis process. The results collectively explain that endogenous galectin-3 exerts its effects through modulation of host immunity. Thus, thorough understanding of host immune scenario is indispensable while designing galectin-3 targeted therapeutic strategies against cancer.

Conflict of interest

The authors declare no conflicts of interest.

Acknowledgments

We thank Prof. Fu Tong Liu (University of California at Davis, USA) for providing galectin-3 knock-out (Gal-3$^{-/-}$) mice via Consortium for Functional Glycomics, USA to Dr. R.D. Kalraiya. We acknowledge the technical help from Mr. Suresh Dakave for the animal handling experiments. We acknowledge research fellowship to A. D. Chaudhari from Department of Atomic Energy—Tata Memorial Centre (DAE-TMC).

Appendix A. Supplementary data

Supplementary data associated with this article can be found, in the online version, at http://dx.doi.org/10.1016/j.molimm.2015.09.015.

References

Acosta-Rodriguez, E.V., Montes, C.L., Motran, C.C., Zuniga, E.I., Liu, F.T., Rabinovich, G.A., Gruppi, A., 2004. Galectin-3 mediates IL-4-induced survival and differentiation of B cells: functional cross-talk and implications during Trypanosoma cruzi infection. J. Immunol. 172, 493–502.

Agarwal, A.K., Gude, R.P., Kalraiya, R.D., 2014. Regulation of melanoma metastasis to lungs by cell surface Lysosome Associated Membrane Protein-1 (LAMP1) via galectin-3. Biochem. Biophys. Res. Commun. 449, 332–337.

Agarwal, A.K., Srinivasan, N., Godbole, R., More, S.K., Budnar, S., Gude, R.P., Kalraiya, R.D., 2015. Role of tumor cell surface lysosome-associated membrane protein-1 (LAMP1) and its associated carbohydrates in lung metastasis. J. Cancer Res. Clin. Oncol.

Alexander, W.S., Starr, R., Fenner, J.E., Scott, C.L., Handman, E., Sprigg, N.S., Corbin, J.E., Cornish, A.L., Darwiche, R., Owczarek, C.M., Kay, T.W., Nicola, N.A., Hertzog, P.J., Metcalf, D., Hilton, D.J., 1999. SOCS1 is a critical inhibitor of interferon gamma signaling and prevents the potentially fatal neonatal actions of this cytokine. Cell 98, 597–608.

Almogren, A., Abdullah, J., Ghapure, K., Ferguson, K., Glinsky, V.V., Rittenhouse-Olson, K., 2012. Anti-Thomsen-Friedenreich-Ag (anti-TF-Ag) potential for cancer therapy. Front Biosci. (Schol Ed) 4, 840–863.

Bernardes, E.S., Silva, N.M., Ruas, L.P., Mineo, J.R., Loyola, A.M., Hsu, D.K., Liu, F.T., Chammas, R., Roque-Barreira, M.C., 2006. Toxoplasma gondii infection reveals a novel regulatory role for galectin-3 in the interface of innate and adaptive immunity. Am. J. Pathol. 168, 1910–1920.

Breuilh, L., Vanhoutte, F., Fontaine, J., van Stijn, C.M., Tillie-Leblond, I., Capron, M., Faveeuw, C., Jouault, T., van Die, I., Gosset, P., Trottein, F., 2007. Galectin-3 modulates immune and inflammatory responses during helminthic infection: impact of galectin-3 deficiency on the functions of dendritic cells. Infect. Immun. 75, 5148–5157.

Califice, S., Castronovo, V., Bracke, M., van den Brule, F., 2004. Dual activities of galectin-3 in human prostate cancer: tumor suppression of nuclear galectin-3 vs tumor promotion of cytoplasmic galectin-3. Oncogene 23, 7527–7536.

Chen, H.Y., Liu, F.T., Yang, R.Y., 2005. Roles of galectin-3 in immune responses. Arch. Immunol. Ther. Exp. (Warsz) 53, 497–504.

Comodo, A.N., Lacerda Bachi, A.L., Soares, M.F., Franco, M., Castro Teixeira, V.d.P., 2013. Galectin-3 expression favors metastasis in murine melanoma. Adv. Biosci. Biotechnol. 04, 55–62.

Dagher, S.F., Wang, J.L., Patterson, R.J., 1995. Identification of galectin-3 as a factor in pre-mRNA splicing. Proc. Natl. Acad. Sci. U. S. A. 92, 1213–1217.

Dange, M.C., Agarwal, A.K., Kalraiya, R.D., 2015. Extracellular galectin-3 induces MMP9 expression by activating p38 MAPK pathway via lysosome-associated membrane protein-1 (LAMP1). Mol. Cell. Biochem.

Dange, M.C., Srinivasan, N., More, S.K., Bane, S.M., Upadhya, A., Ingle, A.D., Gude, R.P., Mukhopadhyaya, R., Kalraiya, R.D., 2014. Galectin-3 expressed on different lung compartments promotes organ specific metastasis by facilitating arrest, extravasation and organ colonization via high affinity ligands on melanoma cells. Clin. Exp. Metastasis 31, 661–673.

Demetriou, M., Granovsky, M., Quaggin, S., Dennis, J.W., 2001. Negative regulation of T-cell activation and autoimmunity by Mgat5 *N*-glycosylation. Nature 409, 733–739.

Dighe, A.S., Richards, E., Old, L.J., Schreiber, R.D., 1994. Enhanced in vivo growth and resistance to rejection of tumor cells expressing dominant negative IFN gamma receptors. Immunity 1, 447–456.

Dumic, J., Dabelic, S., Flogel, M., 2006. Galectin-3: an open-ended story. Biochim. Biophys. Acta 1760, 616–635.

Dunn, G.P., Koebel, C.M., Schreiber, R.D., 2006. Interferons, immunity and cancer immunoediting. Nat. Rev. Immunol. 6, 836–848.

Endo, T.A., Masuhara, M., Yokouchi, M., Suzuki, R., Sakamoto, H., Mitsui, K., Matsumoto, A., Tanimura, S., Ohtsubo, M., Misawa, H., Miyazaki, T., Leonor, N., Taniguchi, T., Fujita, T., Kanakura, Y., Komiya, S., Yoshimura, A., 1997. A new protein containing an SH2 domain that inhibits JAK kinases. Nature 387, 921–924.

Eude-Le Parco, I., Gendronneau, G., Dang, T., Delacour, D., Thijssen, V.L., Edelmann, W., Peuchmaur, M., Poirier, F., 2009. Genetic assessment of the importance of galectin-3 in cancer initiation, progression, and dissemination in mice. Glycobiology 19, 68–75.

Ferraz, L.C., Bernardes, E.S., Oliveira, A.F., Ruas, L.P., Fermino, M.L., Soares, S.G., Loyola, A.M., Oliver, C., Jamur, M.C., Hsu, D.K., Liu, F.T., Chammas, R., Roque-Barreira, M.C., 2008. Lack of galectin-3 alters the balance of innate immune cytokines and confers resistance to Rhodococcus equi infection. Eur. J. Immunol. 38, 2762–2775.

Fortuna-Costa, A., Gomes, A.M., Kozlowski, E.O., Stelling, M.P., Pavao, M.S., 2014. Extracellular galectin-3 in tumor progression and metastasis. Front. Oncol. 4 (138).

Funasaka, T., Raz, A., Nangia-Makker, P., 2014. Galectin-3 in angiogenesis and metastasis. Glycobiology 24, 886–891.

Henderson, N.C., Sethi, T., 2009. The regulation of inflammation by galectin-3. Immunol. Rev. 230, 160–171.

Honjo, Y., Nangia-Makker, P., Inohara, H., Raz, A., 2001. Down-regulation of galectin-3 suppresses tumorigenicity of human breast carcinoma cells. Clin. Cancer Res. 7, 661–668.

Houzelstein, D., Goncalves, I.R., Fadden, A.J., Sidhu, S.S., Cooper, D.N., Drickamer, K., Leffler, H., Poirier, F., 2004. Phylogenetic analysis of the vertebrate galectin family. Mol. Biol. Evol. 21, 1177–1187.

Hsu, D.K., Chen, H.Y., Liu, F.T., 2009. Galectin-3 regulates T-cell functions. Immunol. Rev. 230, 114–127.

Hsu, D.K., Yang, R.Y., Pan, Z., Yu, L., Salomon, D.R., Fung-Leung, W.P., Liu, F.T., 2000. Targeted disruption of the galectin-3 gene results in attenuated peritoneal inflammatory responses. Am. J. Pathol. 156, 1073–1083.

Humphries, M.J., Matsumoto, K., White, S.L., Molyneux, R.J., Olden, K., 1988. Augmentation of murine natural killer cell activity by swainsonine, a new antimetastatic immunomodulator. Cancer Res. 48, 1410–1415.

Ikeda, H., Old, L.J., Schreiber, R.D., 2002. The roles of IFN gamma in protection against tumor development and cancer immunoediting. Cytokine Growth Factor Rev. 13, 95–109.

Jia, W., Kidoya, H., Yamakawa, D., Naito, H., Takakura, N., 2013. Galectin-3 accelerates M2 macrophage infiltration and angiogenesis in tumors. Am. J. Pathol. 182, 1821–1831.

Kakuta, S., Tagawa, Y., Shibata, S., Nanno, M., Iwakura, Y., 2002. Inhibition of B16 melanoma experimental metastasis by interferon-gamma through direct inhibition of cell proliferation and activation of antitumour host mechanisms. Immunology 105, 92–100.

Kaplan, D.H., Shankaran, V., Dighe, A.S., Stockert, E., Aguet, M., Old, L.J., Schreiber, R.D., 1998. Demonstration of an interferon gamma-dependent tumor surveillance system in immunocompetent mice. Proc. Natl. Acad. Sci. U. S. A. 95, 7556–7561.

Kim, R., Emi, M., Tanabe, K., 2007. Cancer immunoediting from immune surveillance to immune escape. Immunology 121, 1–14.

Kouo, T., Huang, L., Pucsek, A.B., Cao, M., Solt, S., Armstrong, T., Jaffee, E., 2015. Galectin-3 Shapes Antitumor Immune Responses by Suppressing CD8+ T Cells via LAG-3 and Inhibiting Expansion of Plasmacytoid Dendritic Cells. Cancer Immunol. Res. 3, 412–423.

Krishnan, V., Bane, S.M., Kawle, P.D., Naresh, K.N., Kalraiya, R.D., 2005. Altered melanoma cell surface glycosylation mediates organ specific adhesion and metastasis via lectin receptors on the lung vascular endothelium. Clin. Exp. Metastasis 22, 11–24.

Lalancette-Hebert, M., Swarup, V., Beaulieu, J.M., Bohacek, I., Abdelhamid, E., Weng, Y.C., Sato, S., Kriz, J., 2012. Galectin-3 is required for resident microglia activation and proliferation in response to ischemic injury. J. Neurosci. 32, 10383–10395.

Liu, F.T., 2005. Regulatory roles of galectins in the immune response. Int. Arch. Allergy Immunol. 136, 385–400.

Liu, F.T., Patterson, R.J., Wang, J.L., 2002. Intracellular functions of galectins. Biochim. Biophys. Acta 1572, 263–273.

Liu, F.T., Rabinovich, G.A., 2005. Galectins as modulators of tumour progression. Nat. Rev. Cancer 5, 29–41.

Lopez, E., Zafra, M.P., Sastre, B., Gamez, C., Lahoz, C., del Pozo, V., 2011. Gene expression profiling in lungs of chronic asthmatic mice treated with galectin-3: downregulation of inflammatory and regulatory genes. Mediators Inflamm. 2011 (823279).

Lotz, M.M., Andrews Jr., C.W., Korzelius, C.A., Lee, E.C., Steele Jr., G.D., Clarke, A., Mercurio, A.M., 1993. Decreased expression of Mac-2 (carbohydrate binding protein 35) and loss of its nuclear localization are associated with the neoplastic progression of colon carcinoma. Proc Natl Acad Sci U S A 90, 3466–3470.

Mitra-Kaushik, S., Harding, J., Hess, J., Schreiber, R., Ratner, L., 2004. Enhanced tumorigenesis in HTLV-1 tax-transgenic mice deficient in interferon-gamma. Blood 104, 3305–3311.

More, S.K., Srinivasan, N., Budnar, S., Bane, S.M., Upadhya, A., Thorat, R.A., Ingle, A.D., Chiplunkar, S.V., Kalraiya, R.D., 2015. N-glycans and metastasis in galectin-3 transgenic mice. Biochem. Biophys. Res. Commun. 460, 302–307.

Moutsatsos, I.K., Wade, M., Schindler, M., Wang, J.L., 1987. Endogenous lectins from cultured cells: nuclear localization of carbohydrate-binding protein 35 in proliferating 3T3 fibroblasts. Proc. Natl. Acad. Sci. U. S. A. 84, 6452–6456.

Nakahara, S., Oka, N., Raz, A., 2005. On the role of galectin-3 in cancer apoptosis. Apoptosis 10, 267–275.

Newlaczyl, A.U., Yu, L.G., 2011. Galectin-3–a jack-of-all-trades in cancer. Cancer Lett. 313, 123–128.

Nicholson, S.E., Willson, T.A., Farley, A., Starr, R., Zhang, J.G., Baca, M., Alexander, W.S., Metcalf, D., Hilton, D.J., Nicola, N.A., 1999. Mutational analyses of the SOCS proteins suggest a dual domain requirement but distinct mechanisms for inhibition of LIF and IL-6 signal transduction. EMBO J. 18, 375–385.
Nieminen, J., St-Pierre, C., Sato, S., 2005. Galectin-3 interacts with naive and primed neutrophils, inducing innate immune responses. J. Leukoc. Biol. 78, 1127–1135.
Ochieng, J., Furtak, V., Lukyanov, P., 2004. Extracellular functions of galectin-3. Glycoconj J. 19, 527–535.
Perillo, N.L., Marcus, M.E., Baum, L.G., 1998. Galectins: versatile modulators of cell adhesion, cell proliferation, and cell death. J. Mol. Med. (Berl.) 76, 402–412.
Pineda, M.A., Cuervo, H., Fresno, M., Soto, M., Bonay, P., 2015. Lack of galectin-3 prevents cardiac fibrosis and effective immune responses in a murine model of Trypanosoma cruzi infection. J. Infect. Dis.
Quah, B.J., Warren, H.S., Parish, C.R., 2007. Monitoring lymphocyte proliferation *in vitro* and *in vivo* with the intracellular fluorescent dye carboxyfluorescein diacetate succinimidyl ester. Nat. Protoc. 2, 2049–2056.
Rabinovich, G.A., Liu, F.T., Hirashima, M., Anderson, A., 2007. An emerging role for galectins in tuning the immune response: lessons from experimental models of inflammatory disease, autoimmunity and cancer. Scand. J. Immunol. 66, 143–158.
Rabinovich, G.A., Rubinstein, N., Toscano, M.A., 2002. Role of galectins in inflammatory and immunomodulatory processes. Biochim. Biophys. Acta 1572, 274–284.
Radosavljevic, G., Jovanovic, I., Majstorovic, I., Mitrovic, M., Lisnic, V.J., Arsenijevic, N., Jonjic, S., Lukic, M.L., 2011. Deletion of galectin-3 in the host attenuates metastasis of murine melanoma by modulating tumor adhesion and NK cell activity. Clin. Exp. Metastasis 28, 451–462.
Radosavljevic, G., Volarevic, V., Jovanovic, I., Milovanovic, M., Pejnovic, N., Arsenijevic, N., Hsu, D.K., Lukic, M.L., 2012. The roles of Galectin-3 in autoimmunity and tumor progression. Immunol. Res. 52, 100–110.
Sano, H., Hsu, D.K., Yu, L., Apgar, J.R., Kuwabara, I., Yamanaka, T., Hirashima, M., Liu, F.T., 2000. Human galectin-3 is a novel chemoattractant for monocytes and macrophages. J. Immunol. 165, 2156–2164.
Sato, S., Hughes, R.C., 1994. Regulation of secretion and surface expression of Mac-2, a galactoside-binding protein of macrophages. J. Biol. Chem. 269, 4424–4430.
Sato, S., Ouellet, N., Pelletier, I., Simard, M., Rancourt, A., Bergeron, M.G., 2002. Role of galectin-3 as an adhesion molecule for neutrophil extravasation during streptococcal pneumonia. J. Immunol. 168, 1813–1822.
Shankaran, V., Ikeda, H., Bruce, A.T., White, J.M., Swanson, P.E., Old, L.J., Schreiber, R.D., 2001. IFNgamma and lymphocytes prevent primary tumour development and shape tumour immunogenicity. Nature 410, 1107–1111.
Song, L., Tang, J.W., Owusu, L., Sun, M.Z., Wu, J., Zhang, J., 2014. Galectin-3 in cancer. Clin. Chim. Acta 431, 185–191.
Song, M.M., Shuai, K., 1998. The suppressor of cytokine signaling (SOCS) 1 and SOCS3 but not SOCS2 proteins inhibit interferon-mediated antiviral and antiproliferative activities. J. Biol. Chem. 273, 35056–35062.
Srinivasan, N., Bane, S.M., Ahire, S.D., Ingle, A.D., Kalraiya, R.D., 2009. Poly N-acetyllactosamine substitutions on *N*- and not *O*-oligosaccharides or Thomsen–Friedenreich antigen facilitate lung specific metastasis of melanoma cells via galectin-3. Glycoconj. J. 26, 445–456.
Thijssen, V.L., Heusschen, R., Caers, J., Griffioen, A.W., 2015. Galectin expression in cancer diagnosis and prognosis: a systematic review. Biochim. Biophys. Acta 1855, 235–247.
Wang, J.L., Gray, R.M., Haudek, K.C., Patterson, R.J., 2004. Nucleocytoplasmic lectins. Biochim. Biophys. Acta 1673, 75–93.
Xu, Z., Hurchla, M.A., Deng, H., Uluckan, O., Bu, F., Berdy, A., Eagleton, M.C., Heller, E.A., Floyd, D.H., Dirksen, W.P., Shu, S., Tanaka, Y., Fernandez, S.A., Rosol, T.J., Weilbaecher, K.N., 2009. Interferon-gamma targets cancer cells and osteoclasts to prevent tumor-associated bone loss and bone metastases. J. Biol. Chem. 284, 4658–4666.
Yang, R.Y., Hsu, D.K., Liu, F.T., 1996. Expression of galectin-3 modulates T-cell growth and apoptosis. Proc. Natl. Acad. Sci. U. S. A. 93, 6737–6742.
Yoshii, T., Inohara, H., Takenaka, Y., Honjo, Y., Akahani, S., Nomura, T., Raz, A., Kubo, T., 2001. Galectin-3 maintains the transformed phenotype of thyroid papillary carcinoma cells. Int. J. Oncol. 18, 787–792.
Yu, L.G., 2007. The oncofetal Thomsen–Friedenreich carbohydrate antigen in cancer progression. Glycoconj. J. 24, 411–420.
Yu, L.G., Andrews, N., Zhao, Q., McKean, D., Williams, J.F., Connor, L.J., Gerasimenko, O.V., Hilkens, J., Hirabayashi, J., Kasai, K., Rhodes, J.M., 2007. Galectin-3 interaction with Thomsen–Friedenreich disaccharide on cancer-associated MUC1 causes increased cancer cell endothelial adhesion. J. Biol. Chem. 282, 773–781.
Zhao, Q., Barclay, M., Hilkens, J., Guo, X., Barrow, H., Rhodes, J.M., Yu, L.G., 2010. Interaction between circulating galectin-3 and cancer-associated MUC1 enhances tumour cell homotypic aggregation and prevents anoikis. Mol. Cancer 9, 154.
Zuberi, R.I., Hsu, D.K., Kalayci, O., Chen, H.Y., Sheldon, H.K., Yu, L., Apgar, J.R., Kawakami, T., Lilly, C.M., Liu, F.T., 2004. Critical role for galectin-3 in airway inflammation and bronchial hyperresponsiveness in a murine model of asthma. Am. J. Pathol. 165, 2045–2053.